

IHDP/Future Earth-Integrated Risk Governance Project Series

Peijun Shi *Editor*

Natural Disasters in China

 BNUP

 Springer

IHDP/Future Earth-Integrated Risk Governance Project Series

Series editors

Carlo Jaeger, Potsdam, Germany

Peijun Shi, Beijing Normal University, Beijing, China

About this Series

This book series, entitled “IHDP/Future Earth—Integrated Risk Governance Project Series” for the International Human Dimensions Programme on Global Environmental Change—Integrated Risk Governance Project (IHDP/Future Earth—IRG Project), is intended to present in monograph form the most recent scientific achievements in the identification, evaluation and management of emerging global large-scale risks. Future Earth is a flagship initiative of the Science and Technology Alliance for Global Sustainability. It aims to provide critical knowledge required for societies to understand and address challenges posed by global environmental change (GEC) and to seize opportunities for transitions to global sustainability. Future Earth identifies three research themes, i.e., Dynamic Planet, Global Development and Transition toward Sustainability in its plan and adopts a new approach of “Co-designing and co-producing” to incorporate GEC researchers with stakeholders in governments, industry and business, international or intergovernmental organizations, and civil society.

Books published in this series are mainly collected research works on theories, methods, models and modeling, and case analyses conducted by scientists from various disciplines and practitioners from various sectors under the IHDP/Future Earth—IRG Project. It includes the IRG Project Science Plan, research on social-ecological system responses, “Entry and Exit Transition” mechanisms, models and modeling, early warning systems, understanding regional dynamics of vulnerability, as well as case comparison studies of large-scale disasters and paradigms for integrated risk governance around the world. This book series, therefore, will be of interest not only to researchers, educators and students working in this field but also to policy-makers and decision-makers in government, industry and civil society around the world.

The series will be contributed by the international research teams working on the six scientific themes identified by the IHDP/Future Earth—IRG Project Science Plan, i.e., Social-Ecological Systems, Entry and Exit Transitions, Early Warning Systems, Models and Modeling, Comparative Case Studies, and Governance and Paradigms, and by six regional offices of the IRG Project around the world.

More information about this series at <http://www.springer.com/series/13536>

Peijun Shi
Editor

Natural Disasters in China

 BNUP

 Springer

Editor
Peijun Shi
Beijing Normal University
Beijing
China

ISSN 2363-4979 ISSN 2363-4987 (electronic)
IHDP/Future Earth-Integrated Risk Governance Project Series
ISBN 978-3-662-50268-6 ISBN 978-3-662-50270-9 (eBook)
DOI 10.1007/978-3-662-50270-9

Jointly published with Beijing Normal University Press
ISBN: 978-7-303-20273-7 Beijing Normal University Press

Library of Congress Control Number: 2016939359

© Beijing Normal University Press and Springer-Verlag Berlin Heidelberg 2016

This work is subject to copyright. All rights are reserved by the Publishers, whether the whole or part of the material is concerned, specifically the rights of translation, reprinting, reuse of illustrations, recitation, broadcasting, reproduction on microfilms or in any other physical way, and transmission or information storage and retrieval, electronic adaptation, computer software, or by similar or dissimilar methodology now known or hereafter developed.

The use of general descriptive names, registered names, trademarks, service marks, etc. in this publication does not imply, even in the absence of a specific statement, that such names are exempt from the relevant protective laws and regulations and therefore free for general use.

The publishers, the authors and the editors are safe to assume that the advice and information in this book are believed to be true and accurate at the date of publication. Neither the publishers nor the authors or the editors give a warranty, express or implied, with respect to the material contained herein or for any errors or omissions that may have been made.

Printed on acid-free paper

This Springer imprint is published by Springer Nature
The registered company is Springer-Verlag GmbH Berlin Heidelberg

Preface

Catastrophes that are beyond the coping capability of current social-ecological systems are occurring at an increasing pace in recent years. Examples are the devastating Hurricane Katrina occurred in the United States in 2005, the extreme low-temperature freezing rain and snow disaster in southern China in 2008, the Wenchuan Earthquake in Sichuan, China in 2008, and the Great Eastern Japan Earthquake and Tsunami in 2011. These catastrophes brought great challenges to existing disaster planning, response, and management, as well as to post-disaster reconstruction efforts. As a result, questions such as how to reduce disaster risks and cope with catastrophes more effectively have caught widespread attention of scientific communities, governments, and societies both at home and abroad.

In order to strengthen the innovation capability of scientific disciplines, the Chinese government, through the Ministry of Education (MOE) and the State Administration of Foreign Experts Affairs (SAFEA), organized and implemented the Expertise-Introduction Project for Disciplinary Innovation of Universities (the “111 Project”) that aims at building capacities of Chinese higher education institutions and facilitating their transformation into world-class universities. The project’s overall goal is to develop about 100 world-class research and education bases for introducing talents of various disciplines through building high-level research teams formed by some 1,000 leading overseas scholars and researchers introduced from the world’s top 100 universities and key research groups of research institutions, and is based on the platforms of national, provincial, and ministerial level key scientific research bases. It focuses on cutting-edge research areas internationally and national key disciplinary development goals, and prioritizes disciplines in universities that have a leading position internationally or disciplines that are priority support areas in national plans. The Hazard and Risk Science Base (HRSB) at Beijing Normal University is one of the projects under the “111 Project.”

In the third batch of the “111 Project,” the Hazard and Risk Science Base of Beijing Normal University was approved officially at the end of 2007 and implemented from the beginning of 2008, with an execution period between 2008 and

2012. Peijun Shi and Roger Kaspersen were appointed as the chief professors for the project. The project involved a large number of renowned scientists in the disaster risk field worldwide, including David Alexander, Joanne Bayer, Colin Green, Guoyi Han, Saburo Ikeda, Carlo Jaeger, Gordon McGranahan, Dennis Ojima, Norio Okada, Nick Pidgeon, Bonnie Ram, Andreas Rechkemmer, Ortwin Renn, Charles Scawthorn, Paul Slovic, Hirokazu Tatano, Kathleen Tierney, Brain Walker, and Qian Ye. Wenjie Dong, Yuan Jiang, Ning Li, Lianyou Liu, Jing'ai Wang, Weihua Fang, Wei Xu, Ying Li, Juan Du, Ming Wang, Saini Yang, Tao Ye, Deyong Yu, Yaojie Yue, and Zhao Zhang also participated in this project. In September 2012, the second 5-year phase of the project (2013–2017) was also approved. We completed this compiled volume, *Natural Disasters in China*, under the scientific framework developed through discussions and field research and investigations jointly performed by Chinese and invited international experts, based on a systematic review of existing research on natural disaster risks by Chinese experts, under the support of this project.

In the course of project implementation, we mainly carried out the following three activities:

First, we organized the Summer Institute for Advanced Study of Disaster and Risk for 5 years, and selected Ph.D. candidates, postdoctoral researchers, and other young scholars who are engaged in the research of disaster risks both in China and internationally to participate. Together with internationally renowned scholars in this field, the summer institute participants discussed the cutting-edge research areas in the field of disaster and risk study, essentials of the discipline, and major theoretical and practical issues in integrated disaster risk governance. The summer institute over 5 years has recruited more than 60 young international scholars and 120 young scholars in China, which helped develop the capacity of young scholars in conducting disaster risk research.

Second, five annual international seminars on the integrated disaster risk governance in China were held in Beijing, and three short field research and investigations were conducted during the project period. These activities aimed at thoroughly understanding the status of integrated disaster risk research and systematically reviewing the achievements obtained from such research in China, understanding the spatiotemporal trends of disaster risks in the process of rapid economic growth, and introducing the Chinese experiences in and lessons learned from integrated disaster risk governance to the colleagues from other countries. The short field research and investigations in different years focused on integrated approaches for combating drought and sandstorms in Ordos, Inner Mongolian Autonomous Region and Yulin, Shaanxi Province; integrated approaches for mitigating flood risks in the Dongting Lake area, Hunan Province and the area along the Yangtze River main stream in Hubei Province; and integrated approaches for mitigating risks of typhoon and rainstorm in Shenzhen, Guangdong Province. Based on these, we compiled the book *Integrated Risk Governance: Science Plan and Case Studies of Large-scale Disasters* and the *World Atlas of Natural Disaster Risk*. These works contribute to improving the research of integrated natural disaster risk governance and enriching the academic resources for education and

scientific research. *Integrated Risk Governance* and *World Atlas of Natural Disaster Risk*, are also part of the book series of the International Human Dimension Programme on Global Environmental Change/Future Earth—Integrated Risk Governance Project (IHDP/FE-IRG) Core Science Program.

Third, we developed a close cooperation with the IHDP/FE-IRG Core Science Program Committee in the field of integrated risk governance research. A number of “111 Project” experts are also members of the IHDP/FE-IRG Core Science Program Committee. In order to improve the IHDP/FE-IRG Core Science Program, we conducted in-depth academic research—an important topic of discussion in the “111 Project” annual meeting was the design of the IHDP/FE-IRG Core Science Program. Based on the English edition of the journal *Disaster Reduction in China*, the “111 Project” and IHDP/FE-IRG Core Science Program co-founded the *International Journal of Disaster Risk Science (IJDRS)*. By 2015, the *IJDRS* has published six volumes. It creates a global network for academic exchange for promoting the development of disaster risk science.

Compiling this book is not only an important part of the effort of the “111 Project” on producing academic resources of disaster risk science, but also a key component of the “111 Project” participation in the IHDP/FE-IRG Core Science Program. It facilitates the understanding of the essence of social-ecological systems that are the central concern of the IHDP/FE-IRG Core Science Program, improving the “transition in and transition out” theory and models of integrated risk assessment, developing disaster risk early-warning systems, conducting comparative study of catastrophic disaster responses among different countries, and establishing integrated risk governance paradigms.

In order to achieve the goal of this book, we attempt to introduce the spatiotemporal patterns, formation mechanisms and processes, vulnerability, risk levels, and disaster reduction strategies of major natural disasters in China from the perspective of science. Furthermore, we seek to summarize integrated disaster risk governance in China, especially the experiences and lessons learned from disaster reduction and prevention. From the global perspective, we attempt to learn from achievements of integrated disaster risk governance in other countries and regions, to propose strategies for integrated disaster risk governance in China.

We carried out a systematic study of major natural disasters and disaster risks in China based on our understanding of the development of international disaster risk research and the structure and function of “regional disaster systems.” The scientific framework of this book was formed through a series of discussions after carefully evaluating a number of research outputs of Chinese colleagues, including *Atlas of Natural Disasters of China*, *Atlas of Natural Disaster System of China*, *Spatiotemporal Patterns of Natural Disasters of China*, *Atlas of Natural Disaster Risks of China*, among others. This framework includes two parts.

Part one is “Natural Disaster System of China” (Chap. “**Natural Disaster System in China**” of this book). In a nutshell overview, it introduces China’s disaster-formative environment, that is, the human-environmental system in which natural disasters occur; natural hazards; exposure units; natural disaster situation; and natural disaster risks.

Part two is “China’s Major Natural Disasters” (Chaps. “[Earthquake Disasters in China](#)”—“[Storm Surges in China](#)” of this book). It covers the spatiotemporal patterns and formation processes of earthquakes, landslides and debris flows, typhoons, floods, droughts, snowstorms, frost and hails, sandstorms, storm surges, and other natural hazards in China; disaster situations; vulnerability and risks; risk governance; and typical cases of coping with catastrophic disasters.

In the book, we summarize the characteristics of China’s natural disaster system, reveal natural disaster formation mechanisms and processes, quantify natural disaster situation and vulnerability, evaluate natural disaster risk levels, summarize the key strategies of integrated natural disaster risk governance (especially the institution, mechanism, and legal system of integrated disaster prevention and reduction), analyze catastrophic natural disaster response models, and propose integrated natural disaster risk governance strategies in China.

We are generously supported and assisted by many institutions and individuals during the compilation of this book. The State Administration of Foreign Experts Affairs and Ministry of Education of China provided precious financial support for the “111 Project” (B08008). The Department of International Cooperation and Department of Social Development of the Ministry of Science and Technology of China, Geoscience Department of National Natural Science Foundation of China, and Beijing Normal University also supported the compilation of the book through scientific research projects. We are truly grateful for these supports.

Special thanks to Prof. Roger Kasperson, the leading master scholar of the “111 Project,” and Prof. Guoyi Han, the international coordinator, for their advice and various support in finishing the book. Professor Carlo Jaeger, Kathleen Tierney, Gordon McGranahan, Saburo Ikeda, Norio Okada, Colin Green, Charles Scawthorn, and Yanhua Liu provided direct support and guidance in structuring and compiling this book. Walter J. Ammann, Dahe Qin, Guanhua Xu, Xiaowen Li, Hiroyuki Kameda, Huadong Guo, Changqing Song, and Shuying Leng, as well as Shangyu Gao and Mingchuan Yang offered their assistance in various capacities; and we sincerely thank all of them.

Special thanks to Dr. Wei Xu, who worked closely with the authors of each chapter to improve the scientific content and the presentation of the chapters. Dr. Ying Li edited this book, provided many critical comments that helped improve the quality of the book and the English language.

International organizations including International Risk Governance Council (IRGC), Organisation for Economic Co-operation and Development (OECD), Global Risk Forum (GRF) Davos, and the IDRiM Society closely follow and support the execution of the “111 Project” and IHDP/FE-IRG Project. We deeply appreciate their cooperation.

This book—*Natural Disasters in China*—is published under the support of the “111 Project” (B08008), the Foundation for Innovative Research Groups of the National Natural Science Foundation of China (41321001), the International Cooperation Projects of the Ministry of Science and Technology of China (2008DFA20640, 2010DFB20880), the National (Regional) Cooperation Project of National Natural Science Foundation of China (40821140354), and the National

Basic Research Program of China (2012CB955404), as well as Springer, Science Press of China, and the Beijing Normal University Publishing Group. We express sincere thanks for their support.

Peijun Shi
State Key Laboratory of Earth Surface Processes and Resource Ecology
Key Laboratory of Environmental Change and Natural Disasters, MOE
Academy of Disaster Reduction and Emergency Management
MOCA and MOE, Beijing Normal University

Contents

Natural Disaster System in China	1
Peijun Shi, Wei Xu and Jing'ai Wang	
Earthquake Disasters in China	37
Wei Xu, Jifu Liu, Guodong Xu, Ying Wang, Lianyou Liu and Peijun Shi	
Landslide and Debris Flow Disasters in China	73
Yongqiu Wu, Xilin Liu, Jing'ai Wang, Lianyou Liu and Peijun Shi	
Typhoon Disasters in China	103
Weihua Fang, Xingchun Zhong and Xianwu Shi	
Floods in China	133
Juan Du, Feng Kong, Shiqiang Du, Ning Li, Ying Li and Peijun Shi	
Droughts in China	161
Tao Ye, Huicong Jia, Yongdeng Lei, Peijun Shi and Jing'ai Wang	
Snow, Frost, and Hail Disasters in China	187
Jing'ai Wang, Yaojie Yue, Jingtao Zhao, Yuan Bai, Lili Lv, Peijun Shi and Wenjie Dong	
Blown Sand Disasters in China	239
Lianyou Liu, Yanli Lyu, Wei Xu, Jing'ai Wang and Peijun Shi	
Storm Surge Disasters in China	273
Weihua Fang, Fujiang Yu, Jianxi Dong and Xianwu Shi	

Natural Disaster System in China

Peijun Shi, Wei Xu and Jing'ai Wang

Abstract Due to the complicated geological and climatic conditions, China is one of the countries in the world that are most frequently and severely affected by natural hazards, and an increasing trend of disaster losses has been observed over the past decades. This chapter systematically examines the natural disaster system of China. The environmental conditions that are inductive to the occurrence of natural hazards, including the lithosphere, atmosphere, hydrosphere, and biosphere are first discussed. Then, the types, intensity, and spatiotemporal patterns of major natural hazards in China are presented. After that, characteristics of the main exposure units, including population, urban settlements, transportation system, economy, and land use are discussed. The temporal trends and spatial characteristics of disaster losses including casualty, collapsed buildings, losses in agricultural production, and directly economic losses, are then systematically presented. Finally, natural disaster risks in China are analyzed.

Keywords Natural hazard · Exposure unit · Human-environmental condition · Natural disaster · China

Disaster system, a dynamic system on the earth's surface with complex characteristics, is composed of natural hazards, exposure units, disaster-formative environment, and disaster losses. It is a type of social-ecological system and also an important part of the earth's surface system. Since hazards can be classified into three types by origin—natural, natural-human (environmental or ecological), and

P. Shi (✉)

State Key Laboratory of Earth Surface Processes and Resource Ecology,
Beijing Normal University, Beijing 100875, China
e-mail: spj@bnu.edu.cn

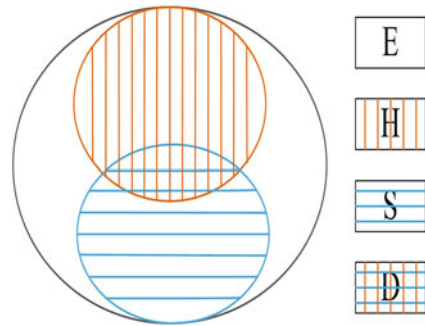
W. Xu

Key Laboratory of Environmental Change and Natural Disasters
of Ministry of Education, Beijing Normal University, Beijing 100875, China

J. Wang

School of Geography, Beijing Normal University, Beijing 100875, China

Fig. 1 Disaster system
(Source Shi 1991)



human, a disaster system can also be classified into three subsystems—natural system, environmental system, and human system. Disaster losses are the consequence of the interactions of hazard, exposure units, and the human-environmental system in which disasters occur (Shi 1991). Figure 1 illustrates the natural disaster system. Each of its components is discussed as follows:

Disaster-formative environment (E): In a broad sense, a disaster-formative environment includes natural environment and human environment—as a human-environmental system. Natural environment can be divided into atmosphere, hydrosphere, lithosphere, and biosphere and human environment can be classified as anthroposphere and technosphere. The natural environmental conditions that are inductive to the occurrence of natural hazards have characteristics such as zonality or non-zonality, variability, sudden change, gradual change, and tendency.

Hazard (H): A hazard system includes natural, human activity-induced, and environmental hazards. Hazards can be classified into sudden onset and slow onset types.

Exposure units (S): Exposure units are humans and lifeline systems, various buildings and production systems, as well as all types of natural resources. Except humans, exposure units can also be divided into fixed assets and movable assets.

Disaster losses (D): Disaster losses include personal injury and deaths, psychological impacts, direct and indirect economic losses, damage to buildings, and damage of ecological environment and resources.

Based on the above theory of disaster system, this chapter first briefly summarizes the natural environmental conditions that are inductive to the occurrence of natural hazards in China. It then introduces the types, intensity, and spatiotemporal patterns of major natural hazards in China; describes the characteristics of exposure units including population, urban settlements, transportation system, economy, and land use; examines the spatial characteristics of disaster losses including casualties, direct economic losses, and collapsed buildings; and systematically depicts the risk and risk regionalization of natural disasters in China with the aim of providing important references for understanding the spatiotemporal dynamics of natural disasters and reducing disaster risks (Shi 1991, 1996, 2002, 2005, 2009).

The work of this chapter was mainly funded by the projects of the National Key Technology R&D Program and National Natural Science Foundation of China, and supported by State Key Laboratory of Earth Surface Processes and Resource Ecology of Beijing Normal University; Key Laboratory of Environmental Change and Natural Disasters, Ministry of Education of China, Beijing Normal University; and Key Laboratory of Regional Geography of Beijing Normal University. Some of the research results have been published in the *Atlas of Natural Disasters of China* (Chinese and English editions) (Zhang and Liu 1992), *Atlas of Natural Disaster System of China* (Chinese-English edition) (Shi 2003), *Spatiotemporal Patterns of Natural Disasters of China* (Wang et al. 2006), and *Atlas of Natural Disaster Risks of China* (Chinese-English edition) (Shi 2011).

1 Disaster-Formative Environment

Disaster-formative environment, which includes the natural and human environments, is an important component of a regional disaster system (Shi 1996; Zhang and Liu 1992; Wang et al. 2006). Natural environmental conditions that are inductive to the occurrence of hazards are often the root cause of disasters. Instability of the regional natural environment conditions offers possibility for the occurrence and development of extreme natural events and natural disasters. This natural environment covers four spheres—the lithosphere, the atmosphere, the hydrosphere, and the biosphere (Shi 2003). The regional characteristics of natural hazard-inducing environmental conditions in China deeply affect the spatiotemporal distribution of natural disasters (Shi 2011).

1.1 Lithosphere

Natural hazard-inducing factors in the lithosphere include geological structures, topographical and geomorphic types, rock and soil types, and so on. Activity of the lithosphere is not only a major reason for the occurrence of earthquakes, landslides, debris flows, and other geological disasters, but also an important factor affecting the magnitude or intensity of such hazards. The natural hazard-inducing factors of the lithosphere in China have the following characteristics (Wang et al. 2006; Zhang and Liu 1992).

Active tectonic movement: The Chinese mainland, located at the southeast of the Eurasian Plate, is a region with complicated geological structures. It adjoins the Pacific Plate and its subduction zone in the east, borders the collision orogenic belt of the Indian Plate and the Eurasian Plate in the south, and is located in the special zone where three major plates—the Eurasian Plate, the Indian Plate, and the Pacific Plate intersect. Many active tectonic zones develop at the connection parts between these plates. In addition, development of small-scale ancient continental blocks in

Chinese mainland is especially clear, forming a series of latitudinal zones such as the Qinling–Kunlun Mountains and Tianshan–Yin Mountains, some south–north tectonic zones in Sichuan and Yunnan Provinces, as well as other northeast and northwest tectonic zones. Terrestrial stress continuously accumulates and releases along these tectonic zones, causing frequent earthquakes. Areas with active tectonic movements such as extrusion, subsidence, and uplifting are places where earthquakes and other geological hazards frequently occur.

Staircase-like topography: The topography in China is higher in the west and lower in the east, showing a three-step staircase shape, which is the basic structure of the landform in China (Fig. 2). The staircase-like topography, great undulation of land surface, and intense fluvial erosion causes the formation of steep slopes that makes the corresponding areas prone to landslides and debris flows. The transitional zones between the first topographical step in southwestern China and the second in central and northwestern China and between the second topographical step and the third in eastern China, as well as the southwestern region of the country, are areas with the most serious geological hazards. Many major rivers originate from mountainous areas on the first and second topographical steps and flow from the west to the east. Meanwhile, rain belt in China stretches roughly in the east–west direction and advances from the south to the north or vice versa in the rainy seasons, which is largely parallel to the main streams of major rivers. Therefore, when the rain belt moves to or stagnates in a certain region, substantial

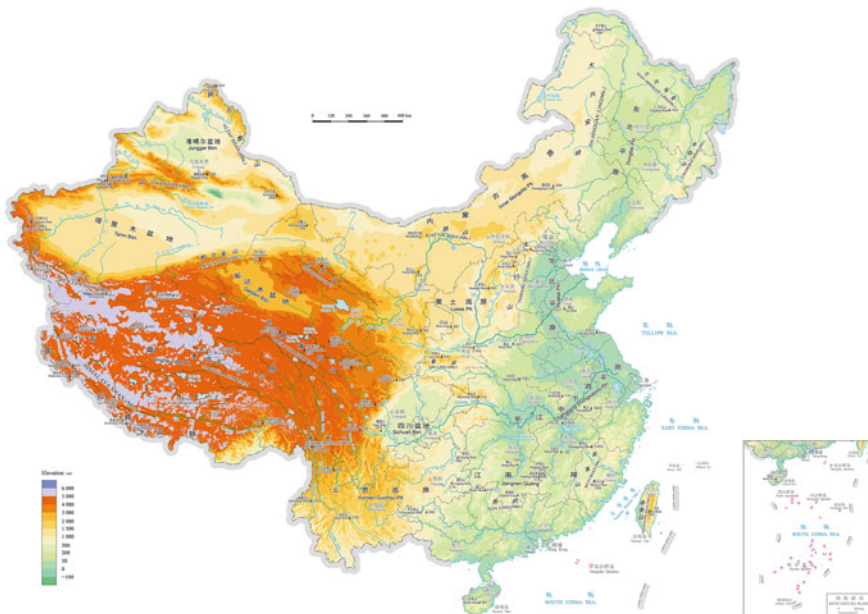


Fig. 2 Topography of China (Source Shi 2011, p. 6–7)

amount of rainfall may occur at the upper, middle, and lower reaches of a river simultaneously, causing flood in the whole drainage areas.

Basic geomorphic types of China include mountains, plateaus, hills, plains, and basins, with mountains and hills accounting for 59 % of the total areas nationwide. Most of the mountains and dissected plateaus feature complicated geological structure, great topographical relief, fractured rock mass on the surface, infertile soil layer, and low vegetation cover as a result of human activities, which makes natural hazards such as landslides, debris flows, water loss and soil erosion, and flash floods to easily occur. In addition, the terrain of the vast plain areas in eastern China is flat; therefore water logging may occur in large areas in the face of spatially extensive strong rainfall of long duration, even causing vast areas being flooded.

1.2 Atmosphere

Atmospheric condition affects the spatiotemporal differentiation of meteorological factors such as temperature and precipitation. Unstable atmospheric circulation or weather system leads to extreme weather and triggers tropical cyclones, cold waves, rainstorms, droughts, heat waves, and other meteorological hazards. Characteristics of natural hazard-inducing conditions of the atmosphere in China are discussed as follows (Wang et al. 2006; Zhang and Liu 1992).

Prominent monsoon climate: Located at the border of the largest continent and the largest ocean, China has prominent monsoon climate. Affected by the monsoon climate, the prevailing wind directions in the winter and the summer have remarkable variations. With the advance and retreat of the monsoon, precipitation shows clear seasonal variation, resulting in frequent rainstorms, floods, and water logging in the summer, and gales, snow, and cold waves in the winter. The occurrence of typhoon also has close connection with summer monsoon. After the subtropical anticyclone (the strong southward airflow at the north side of this is the summer monsoon) advances northward in the early and mid-July, tropical cyclone, induced by airflow from the east at the south edge of the subtropical anticyclone, will advance westward or northwestward and land at the east coast of China. Gales, floods, water logging, and storm surges are often caused by typhoon in the coastal areas. Cold and warm air masses or mountain ridges prevent typhoon from pressing forward, causing strong rainstorms. Stagnation and repeated passing of typhoons is the key reason for the aggravation of flooding and water logging.

Complicated weather systems with great variations: Affected by the continental climate, inland regions in Northwest China is dry year round and the seasonal difference in temperature is large, thus, high temperature and heat waves in the summer and low temperature and cold waves in the winter are prevalent. China, with its vast land area that crosses several climatic regions, is located in an area between the subtropical anticyclone and polar high, the westerlies and the monsoon region, and the continental climate and maritime climate; and characteristics of the land surface vary greatly. Therefore it has complicated and diversified weather

systems and poor stability of weather, resulting in high frequency and wide influence of meteorological hazards such as droughts, floods, low temperature, typhoon, and hailstorm.

1.3 Hydrosphere

Stability of the natural hazard-inducing factors of the hydrosphere (oceans, rivers, lakes, reservoirs, and so on) is closely related to floods, water logging, droughts, storm surges, and other related hazards. Natural hazard-inducing conditions of the hydrosphere in China have two main characteristics—the uneven spatiotemporal distribution of stream runoff, and uneven distribution of water resources. Affected by the uneven spatiotemporal distribution of rainfall, on the one hand water resources in China have large interannual and annual variations. Surface water flows vary seasonally and between different years. Uneven temporal distribution of stream runoff causes frequent droughts, floods, and water logging in China; on the other hand, stream runoff is in line with the spatial distribution of rainfall—it gradually declines from the southeast coastal areas to the northwest inland areas, resulting in serious droughts in Northwest China that lead to dust storms and desertification. In Northeast China, North China, Southwest China, and Central China, although precipitation and surface runoff is much higher, their temporal distribution is again uneven. Therefore not only droughts are frequent in these areas, but also serious floods are present. Variation of ocean circulation system is deeply affected by weather and climatic systems. Once variation occurs in the weather and climatic systems at a large scale, it may cause changes in ocean circulation and lead to a series of hazards (Wang et al. 2006; Zhang and Liu 1992; Shi 2003).

1.4 Biosphere

Biosphere interacts with other spheres and may change their conditions, causing natural disasters. On the other hand, biosphere is the largest ecosystem on earth, within which harmful organisms may propagate in large scales, leading to plant diseases, pests, and rodent damages. Ecosystems in China are diversified, and habitat conditions are fairly complicated. Together with climatic conditions, hazard-inducing factors in the ecosystem create favorable conditions for the occurrence of plant diseases and pests. Furthermore, with the rapid development of the Chinese economy, ecological environment is sometimes seriously damaged, increasing the instability of ecosystems. Impacted by the development of farming and animal husbandry, vegetation cover in the southwest and northwest has greatly declined, which aggravates the situation of landslide and debris flow in southwestern China and drought in northwestern China. Damage of the ecological

environment and decreased vegetation cover greatly accelerate the development of environmental hazards such as water loss and soil erosion, desertification, deterioration of grassland conditions, salinization, and the intrusion of invasive species, among others (Wang et al. 2006; Zhang and Liu 1992).

2 Natural Hazards

2.1 Diversity of Natural Hazards

There exist various schemes for the classification of natural hazards in China. Table 1 presents three classifications, where natural hazards are divided into 24, 26, and 30 types respectively. Compared with major natural hazards in the world, China has all except volcanic eruption. Great variety of natural hazards is one of the most distinctive features of natural disasters in China (Wang et al. 2006).

2.2 Characteristics of Natural Hazards

Multiplicity, spatial extensiveness, and intensity are important features of all natural hazards in a region. From the perspective of regional analysis, the characterization of multiplicity of regional natural hazards can use the same method as analyzing plant sampling data in vegetation research, which is, calculating diversity that reflects the concentration of hazards. Calculation of regional multiple-cropping index in land use research can be adapted and applied to create a coverage area index for characterizing the spatial extensiveness of natural hazards in the region. In order to represent the overall intensity of regional natural hazards, we scale each individual hazard into relative intensity, then calculate the weighted sum based on the proportion of the area affected by each hazard over a certain time period in the region, which can approximately represent the overall relative intensity of natural hazards in the region.

Diversity (H_D): Diversity reflects the concentration of natural hazards in a certain region. The calculation formula is as follows:

$$H_D = n/N \quad (1)$$

where, H_D is the diversity of natural hazards in a specific area (%), n is the total number of hazards in the area, and N is the total number of hazards in the country. In the analysis conducted by Wang and colleagues that is presented in the next section, the spatial unit is county, and the total number of hazards is 107 (see Wang et al. 2006).

Table 1 Classification of major natural hazards in China

Subclass	Natural hazards	Data source
Seismic hazards	Earthquake	Research Team for the Major Natural Disaster of National Science and Technology Commission (1994)
Climatic hazards	Drought, flood, typhoon, hurricane, tornado, cold wave	
Oceanic hazards	Tsunami, storm surge, swell, sea ice, red tide	
Hydrological hazards	Flood	
Geological hazards	Rockfall, landslide, debris flow, ground fissure	
Biohazards for crops	Plant disease, insect pest, weed damage	
Forest hazards	Plant disease, insect pest, rodent damage, fire	
Hazards in the atmosphere	Drought, typhoon, rainstorm, hailstorm, low temperature, frost, ice and snow, dry hot wind	Wang et al. (1994) (revised version)
Hazards in the hydrosphere	Flood, water logging, storm surge, ocean wave, sea ice	
Hazards in biosphere	Crop disease, crop pests, forest disease, forest pests, rodent damage, poisonous weeds, red tide	
Hazards in lithosphere	Earthquake, landslide, debris flow, blown sand, ground fissure	
Atmosphere	Drought, typhoon, rainstorm, hailstorm, low temperature, frost, ice and snow, sandstorm, dry hot wind	
Hydrosphere	Flood, water logging, storm surge, ocean wave	
Lithosphere	Landslide, debris flow, subsidence, blown sand, earthquake	
Biosphere	Crop disease, crop pests, disease and insect pests of forest, rodent damage, poisonous weeds, red tide	
Geosphere	Soil erosion, desertification, salinization, frozen earth, endemic disease, environmental pollution	

Relative intensity (H_i): Potential damage or devastation caused by a natural hazard in relative terms represents the relative strength of the hazard. This relative intensity is not positively correlation with disaster losses, but is a condition of regional disaster losses. The calculation formula of relative intensity is as follows:

$$H_i = \sum_{i=1}^n P_i \cdot S_i \quad (i = 1, 2, \dots, n) \tag{2}$$

where, H_i is the relative intensity of natural hazards in a county, P_i is the relative intensity of hazard i , and S_i is the areal ratio of hazard i , valued from 0.01 to 1.0 (from 1 to 100 % coverage).

Coverage area index (H_C): Coverage area index is the percentage of areas affected by natural hazards in a county. Calculation formula of the index is as follows:

$$H_C = \sum_{i=1}^n S_i \quad (i = 1, 2, \dots, n) \tag{3}$$

where, S_i is the percentage of areas affected by hazard i in the county.

Composite hazard index (H): The sum of the above three index values divided by the maximum values of the corresponding indexes is the composite hazard index (H).

$$H = H_D / \max(H_D) + H_i / \max(H_i) + H_C / \max(H_C) \tag{4}$$

where, H_D is the diversity of natural hazards in a county, H_i is the relative intensity of all hazards, H_C is the coverage area index of these hazards, and $\max()$ is the maximum value of the indexes.

2.3 Regional Differentiation of Natural Hazards

The natural hazards in China are discussed based on Figs. 3, 4, and 5 (Shi 2003; Wang et al. 2006). The spatial unit of mapping and analysis in this study is county.

Regional differentiation of diversity of natural hazards: The high diversity of natural hazards in China is eight times that of the low diversity. Diversity values range from 0.01 to 0.30. Figure 3 indicates a distinct spatial clustering feature of natural hazards in China. Overall, the high diversity area extends to northeastern, northwestern, and southeast coastal regions with North China at the center. Around 90 % of the districts and counties with $H_D > 20$ % is located in the middle latitude area between 25° N–45° N. In Southwest China where the H_D values are relatively low, this value increases in the transitional areas between high lands and lower lands. It can be concluded that, natural hazards are relatively concentrated in transitional zones of the natural environment such as in the middle latitude; between land and ocean, highland and lowland, farming and pastoral areas in the semi-arid climatic zone, and so forth. Intersections of several transitional zones form high H_D centers. North China is precisely in such position and therefore it is the most concentrated region of natural hazards in China; it is also an important part of the

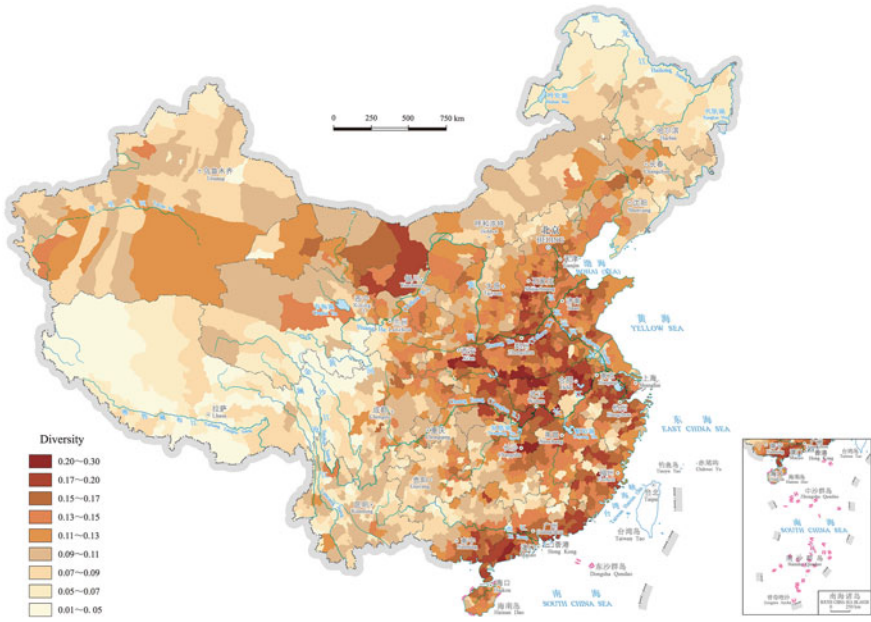


Fig. 3 Diversity of natural hazards in China (Source Shi 2011, p. 22)

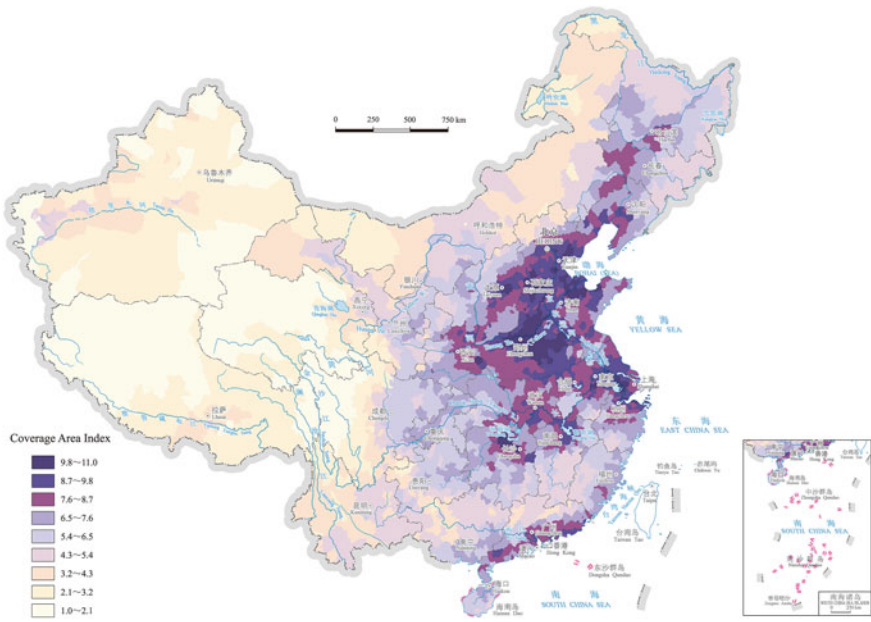


Fig. 4 Coverage area index of natural hazards in China (Source Shi 2011, p. 23)

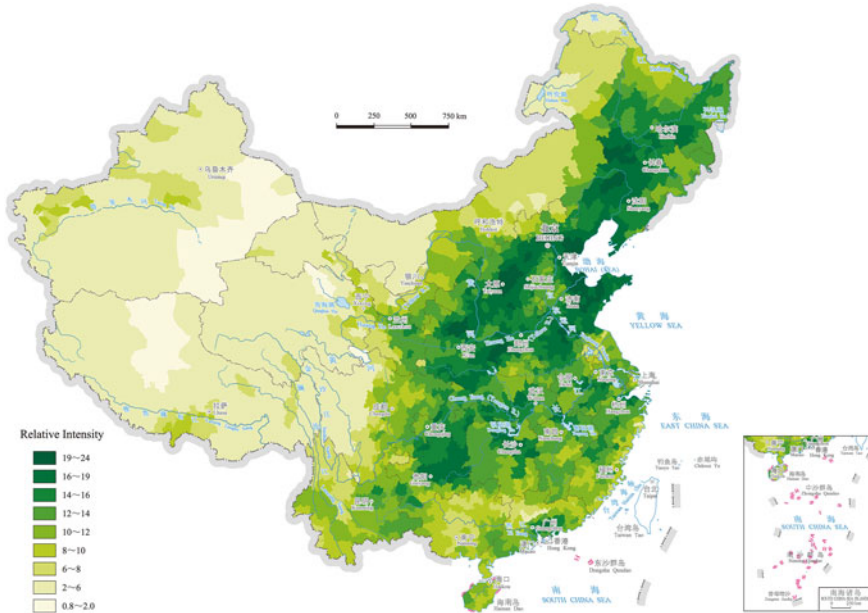


Fig. 5 Relative intensity of natural hazards in China (Source Shi 2011, p. 22)

Pacific Rim and middle latitude multiple hazards zone. Analyzing natural hazards based on the gradient of change of regional environment is of significant value.

Regional differentiation of coverage area index of natural hazards:

Difference between high and low coverage area index of natural hazards in China is great, ranging from 1.0 to 11.0. Figure 4 indicates a distinct regional differentiation. Overall, H_C values in the trapezoid-like region linking Qiqihar, Harbin, Tianshui, and Hangzhou are generally higher than 0.08, making the region high in H_C . Within the region of high H_C , H_C values of Northeast Plain and North China Plain are above 6.5. The high-value center of H_C (higher than 8.7) is in the shape of a reversed “Y”, extending from Qiqihar—Tongliao—Beijing—Taiyuan—Baoji to Tianshui, and from southern Hebei Province to Hangzhou along the Grand Canal. Regions of low H_C center around northern Tibetan Plateau and H_C value increases outward. To the south of the Yangtze River, there are two regions with high H_C —one in the southeast coastal area and the other in Yunnan, Guizhou, and Sichuan Provinces in the southwest. H_C values are generally positively correlated with H_D . Comparing Figs. 3 and 4, consistency of the spatial distribution of these two sets of values is very clear. The correlation is most clear in North China. Moreover, H_C is related to the distribution pattern of natural hazards. Regions affected by natural hazards that are spatially extensive, including hazards in the atmosphere, hydrosphere, and biosphere, have relatively high H_C values. The above-mentioned North China Plain, Northeast Plain, and Loess Plateau regions

with high H_C all belong to the concentrated regions of climatic hazards, flooding, water logging, and biological hazards, and are affected widely by such hazards.

Regional differentiation of relative intensity of natural hazards: H_i values of most areas in China are between 6 and 20.0. Figure 5 shows that regions with H_i value above 19.0 are sparsely distributed. Regions of high relative hazards intensity (H_i higher than 16.0) form a concentrated zone from North China to Southwest China. To the southeast of this zone another area of high hazards intensity is found in Hunan and Jiangxi Provinces. The vast central and northern Qinghai–Tibet Plateau and northwestern inland areas are regions with low relative hazards intensity. The regional differentiation of relative intensity of natural hazards is closely related to the regional distribution of several types of major disaster-inducing factors. First, the seismotectonic zones in China, that is, the Pacific Rim active tectonic zone and Himalayan active tectonic zone, correspond to areas of high relative intensity of hazards. Areas where magnitude 8.0 and above earthquake occurred often become the center of high relative hazards intensity, such as West China and Tangshan. Second, concentrated areas of rainstorms in China also overlap with areas of high relative hazards intensity. For example, typhoon and rainstorm belts in the coastal areas; rainstorm belts of the mountainous areas of northern Hebei Province–Taihang Mountain–Dabie Mountain, western Sichuan and western Hunan are such areas. Third, areas with frequent occurrence of floods and water logging are all areas with high relative intensity of hazards, such as Liao River Plain, North China Plain, especially northern Jiangsu Plain and the Yangtze River–Han River–Dongting Lake Plain. Fourth, concentrated areas of debris flows and landslides are mainly located at the second topographical step of China to the east of the Qinghai–Tibet Plateau, and most of the areas have high relative intensity of hazards. Relative intensity of combined regional natural hazards is controlled by several types of major natural hazards. Interactions between these high intensity hazards makes the regional differentiation of relative intensity of natural hazards in China complicated, and the spatial coverage of high relative hazards intensity areas expanded. At least one leading hazard can be found in each area with high relative hazards intensity.

Regional differentiation of the relationship between diversity, relative intensity, and coverage area index of natural hazards: The relationship between diversity, relative intensity, and coverage area index of natural hazards varies in different areas. Figure 6 indicates that the composite index of hazards concentration, intensity, and spatial extensiveness has the highest value in North China, where various types of natural disasters are both frequent and severe. Coastal areas have the second highest values of integrated hazard index, forming an area of multiple, frequent, and severe disasters. The third area with high integrated hazard index values is the transitional zone between agriculture and animal husbandry in northern China, the desert-steppe area, and western Sichuan, Yunnan, western Guizhou, and southeastern Tibet in southwestern China. Northern Tibet is an area with the lowest H values. The above is the basic pattern of regional differentiation of natural hazard in mainland China.

East–west differentiation and north–south differentiation of natural hazard is manifested at different levels. In terms of east–west differentiation, the values of

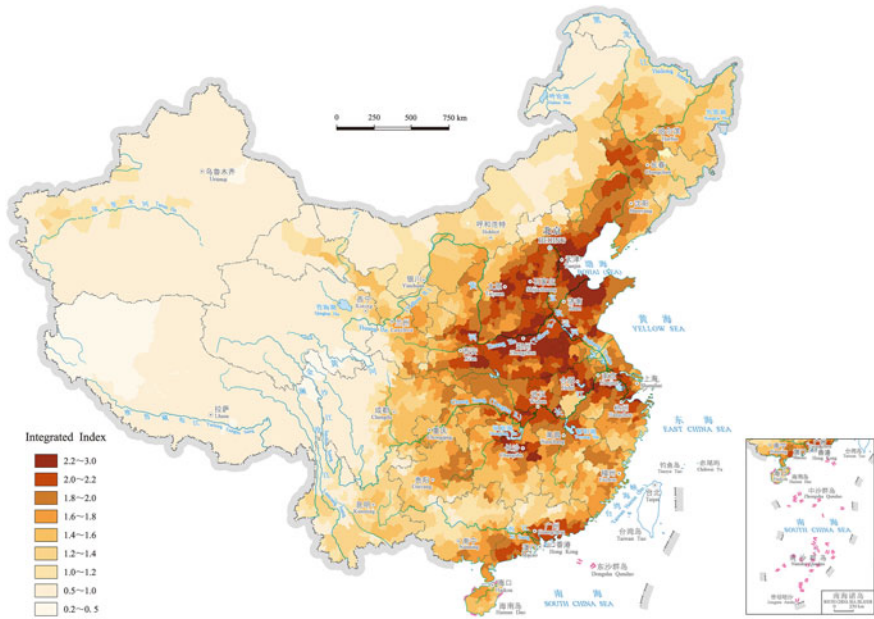


Fig. 6 Regional differentiation of integrated index of natural hazards in China (Source Shi 2011, p. 23)

diversity, relative intensity, and coverage area index of natural hazards in eastern areas are all higher than that in western areas, among which, North China in the eastern area is the center of high integrated hazard index values and northern Tibet in the western area is the center of low index values. From north to south, values of diversity, relative intensity, and coverage area index are higher between 25° N–45° N in the east, and the area between 30° N–40° N has the highest values in all three aspects. North–south differentiation in western China is much more complex—it is remarkably affected by topography. Meanwhile, there is a general lack of data for hazard intensity and coverage. The neighboring area of Tibet, Qinghai, and Xinjiang, that is, HOh Xil, has the lowest values of diversity, coverage area index, and relative intensity of natural hazards in the country.

Regional differentiation of natural hazards is closely related to the natural hazard-inducing conditions of the environment. The sensitive areas of environmental change are generally areas with high values of diversity, relative intensity, and coverage area index of natural hazards, or areas with multiple or severe disasters. However, there is a small number of areas where the natural environment is fragile but both the diversity and relative intensity of hazards are fairly low. For example, eastern Guizhou is one such area. The diversity and relative intensity of natural hazards are not necessarily high in areas with severe natural environmental conditions—the vast western China area is an example. This also indicates that environmental condition has no direct connection with the severity of natural hazards.

3 Exposure Units

Exposure units are the objects affected by various hazards—the congregation of humans, the society where human activities take place, and various resources that are exposed to natural hazards. Exposure units can be divided into population, crops, livestock, buildings, land (e.g., cultivated land, forestland, and grassland), transportation facilities (e.g., railways, highways, bridges, ports, and airports), lifeline systems (e.g., water supply, power supply, gas supply, heat supply, and communication systems), and production systems (e.g., plants, buildings, equipments, and various kinds of instruments). As an important component of the natural disaster system, exposure units are the final source of disaster losses (Shi 1996, 2003; Wang et al. 2006). Therefore, understanding the spatiotemporal characteristics of exposure units of natural disasters should provide important insights on the natural disaster system and change in China.

3.1 Population

Humans are the foremost exposure units of natural disasters. According to the statistics from the Swiss Re-insurance Company, in 2008, deaths and missing people caused by natural disasters reached 234,842 worldwide, 88,928 of which were in China. Reducing personal casualties and population vulnerability has been the primary goal for China in fighting against natural disasters.

Total population: According to the statistics of the *China Statistical Yearbook 2013* (National Bureau of Statistics of China 2013), China is the most populous country in the world with a total of 1.354 billion people by the end of 2012, accounting for 20 % of the world population—an increase of 0.49 % compared to 2011. Huge population base means that there are more people under the risk of hazard impacts, which is also the main reason for huge casualties in catastrophes in China. The enormous population also has imposed great pressure on the environment where they live. Ever-increasing demand on resources and energy will inevitably cause damage to the ecological environment, creating the condition for the occurrence of more human-induced hazards.

Population structure: According to the statistics of the *China Statistical Yearbook 2015* (NBS-China 2015), males account for 51.23 % of the Chinese population, outnumbering females at 33.76 million by the end of 2014. Population aged 65 and older amounts to 137.55 million, accounting for 10.06 % of the total. Figure 7 shows that the proportion of aged population continuously increased from 4.9 % in 1982 to 10.06 % in 2014, indicating a clear aging tendency of the population. The ever-increasing aged population has caused a series of social problems. Meanwhile, increasingly more young people move to cities for employment and are employed at places away from their hometowns, which results in more “empty nest” families in rural and urban areas, increasing the vulnerability of people to natural disasters.

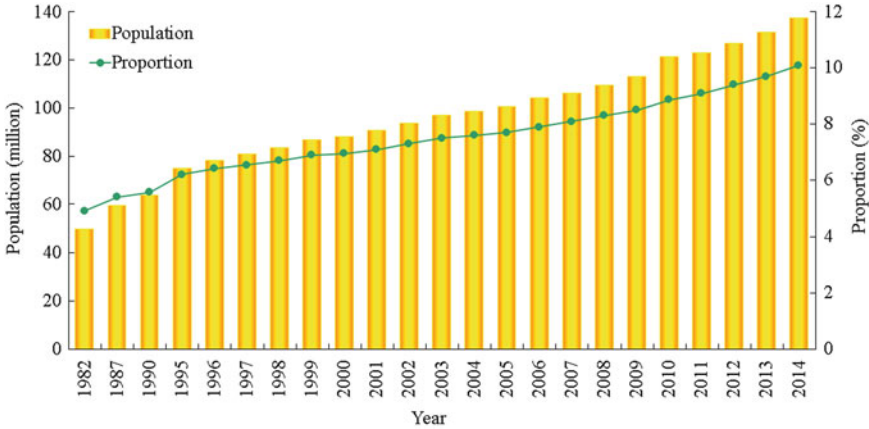


Fig. 7 Population above 65 years in China, 1982–2014 (Data source NBS-China 2015)

Education level of the population: According to the sixth nationwide census of China, people who had received college or above education accounted for 8.93 % of the total population in 2010, and illiteracy rate declined from 6.72 % in 2000 to 4.08 % in 2010, indicating that the overall education level of the population still needs to improve. The low educational level prevents the reduction of vulnerability to disasters.

Population growth: Figure 8 shows that natural growth rate of the population in China steadily declines in recent years, and the growth of the total population is gradually slowing down. The natural population growth rate was 16.61 % in 1987 and dropped to 5.21 % in 2014. It is projected that population growth in China will stabilize toward mid- and late twenty-first century.

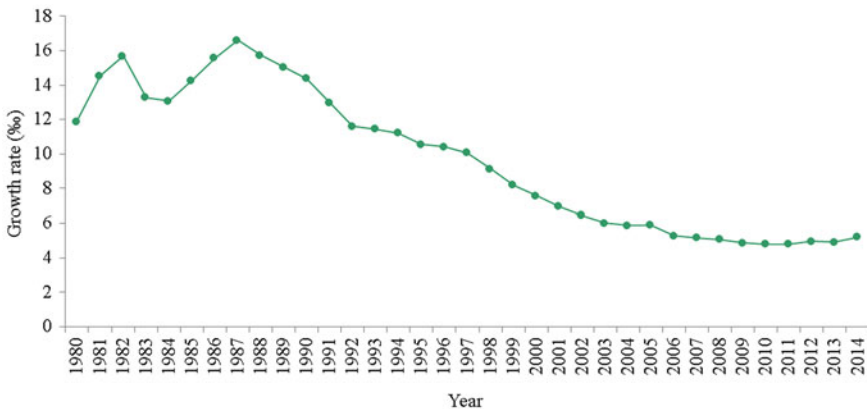


Fig. 8 Natural population growth rate in China, 1980–2014 (Data source NBS-China 2015)

Spatial distribution of population: Affected by the natural environment and socioeconomic development, population in China shows a general pattern of high density in the eastern areas and low density in the western areas.

Population distribution in eastern and western areas varies significantly. Population in the eastern and northeastern areas accounts for 46.34 % of the total population in the country, while population in the vast western areas accounts for only 27.04 % of the total (as shown in Fig. 9). Population density reaches 565 persons per km² in the eastern areas—four times of the national average; and 53 persons per km² in the western areas—37.57 % of the national average level.

Population distribution is greatly restricted by natural conditions. The plain areas are populous while the mountainous areas and plateaus are often sparsely populated. Figure 10 shows that the areas with high population density are mainly

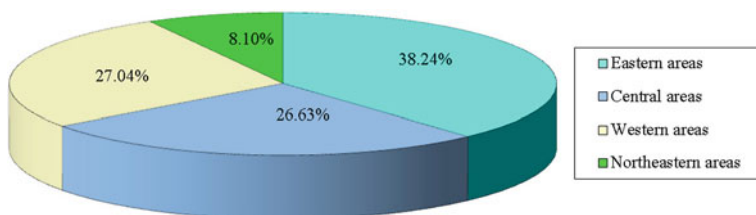


Fig. 9 Regional distribution of population in China, 2013 (Data source NBS-China 2014)

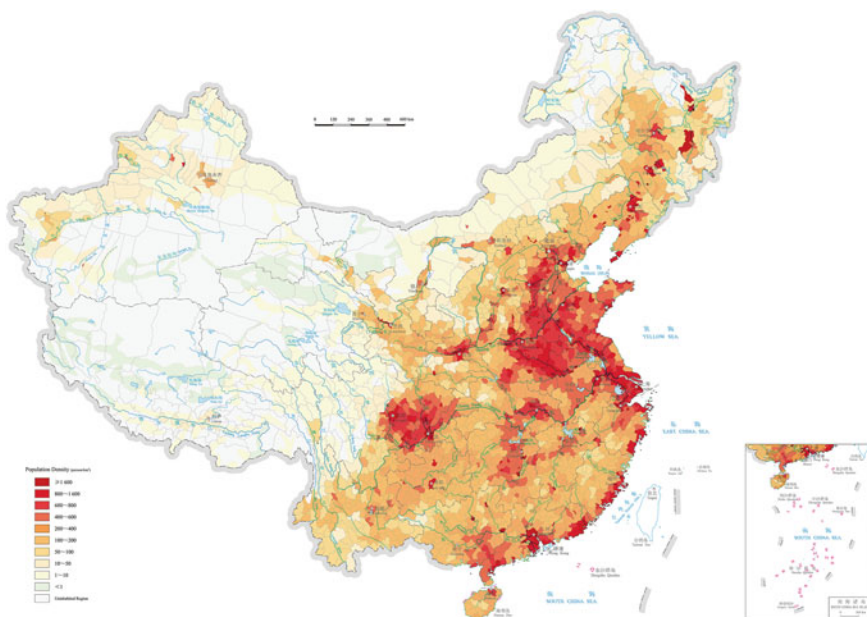


Fig. 10 Population density in China, 2007 (Source Shi 2011, p. 18–19)

distributed in the North China Plain, middle and lower Yangtze River Plain, southeast coastal areas, northeast Songhua River and Nen River Plain, Sichuan Basin, and other areas where the topography is relatively flat, while areas with rugged terrains, such as the southwest Hengduan Mountains, Qinghai–Tibet Plateau, and Inner Mongolian Plateau are sparsely populated. This is closely related to the effect of landform on agriculture, transportation, and urban development. The flat landform in plain areas offers favorable conditions for agricultural development thus these areas became production bases of agricultural products; meanwhile, low cost of transportation and construction facilitates urban development. In mountainous areas, severe natural conditions and topography prevent large-scale development of agricultural production, transportation, and urban systems and thus impose more limits on population growth. In high plateau areas, although transportation development is less restricted, limited water sources and climatic conditions make these places unsuitable for farming and thus limit the size of population. Warm and humid areas have more population than cold and arid areas. Areas with relatively low population density are cold or arid climatic zones, such as the Qinghai–Tibet Plateau, Inner Mongolian Plateau, and northwestern inland arid areas. Densely populated areas are mainly concentrated in warm and moist monsoon region in eastern China. Variation of climatic conditions causes the differentiation of population distribution—warm and moist climatic conditions are more favorable for agriculture and human settlement. The Chinese civilization was originated along the middle and lower reaches of the Yellow River that had favorable climatic conditions, and later expanded to the warmer and more humid Yangtze River valley.

Population in cultivated land areas are more than that in forest and grassland areas. Type and quality of the land greatly affect agricultural production. Areas with cultivated land can produce more cereal crops to supply for urban residents, thus having higher regional population density (for example, the North China Plain, Songhua River and Nen River Plain, and middle and lower Yangtze River Plain are all major grain producing areas in China), while forest and grassland areas (such as southwestern China and Inner Mongolian Plateau) are less populous.

The degree of concentration of cities and towns is in line with population density. Figure 10 shows that population in China is mainly distributed in the Pearl River Delta, Yangtze River Delta, Bohai Rim, urban agglomerations on the Central China Plain, metropolitan areas in the middle and lower Yangtze River Plain, and Chengdu–Chongqing metropolitan areas, which are all concentrated areas of cities and towns, showing a strong correlation between population distribution and the distribution of cities and towns. It is mainly because that cities and towns can provide more employment and education opportunities, which is attractive for surplus-laborers in rural areas. Since the reform and opening-up in China in the late 1970s, especially in southeast coastal areas, rapid population growth is closely related to the rapid economic development of urban areas, among which, Shenzhen is a typical case. Shenzhen has developed into a megacity with more than ten million people from a small fishing village in less than two decades, attracting a great number of people from all over the country.

In conclusion, the pattern of regional distribution of population in China is the result of the joint effect of natural environment and economic and social developments. The difference in population distribution in eastern and western China has close and direct relationship with the differences in the natural environment and socioeconomic conditions in the two regions. Population in China and its distribution directly determine the following characteristics of natural disaster impact: (1) large numbers of people are affected by natural disasters and human casualties are high. Catastrophic disaster risk is high; (2) disaster-affected populations are unevenly distributed. The number of disaster-affected populations in coastal areas and the eastern area are larger than that in the western and northern areas. In areas where both relative intensity of hazards and density of population (as exposure units) are high, such as the North China Plain and the middle and lower Yangtze River Basin, disaster risk is particularly high.

3.2 *Urban Settlements*

As products of regional development, cities and towns are both areas where material wealth is highly concentrated, and the most prominent exposure units affected by natural disasters. Urbanization takes place along with industrialization and modernization and its level is an important indication of the level of development of a country or a region. It is becoming the main driving force of regional economic growth in China (Wang et al. 2006).

Process of urbanization in China: In the past six decades, urbanization in China can be divided into two distinct stages: the first is the period from the founding of the People's Republic of China until the economic reform and opening-up, between 1949 and 1978. The second stage is the period from 1978 onward.

From 1949 to 1978, urbanization rate rose from 10.64 to 17.92 %, with an annual increase of no more than 0.25 %. In the second stage, along with the accelerated socioeconomic development in China, urbanization rate has rapidly increased. It went up from 17.86 % in 1978 to 52.57 % in 2012, with a 1 % average increase each year.

Current situation of urbanization in China: By the end of 2012, there were 18,881 towns, 126 large cities with more than 1 million people, and 108 medium sized cities with 0.5–1 million people. The number of urban residents totaled 71,182 million, and the urbanization rate was 52.57 %.

Urban development in China has concentrated in some regions. In the past decades, city and town concentrated areas, city clusters, and metropolitan areas have gradually formed and developed. City/town clusters or metropolis economic zones have been formed primarily in east coastal areas such as the Yangtze River Delta and the Pearl River Delta, as well as the Beijing–Tianjin–Tangshan area, which have become the main areas leading the economic growth in China and areas that are most likely to achieve modernization. Central and southern

Liaoning Province, Shandong Peninsula, as well as Wuhan, the Central China Plain area, the Central Shanxi Plain, and Chengdu–Chongqing in central and western China are showing a tendency of developing city/town clusters.

In general urban infrastructure in Chinese cities is still underdeveloped and the problem of aging infrastructure is becoming increasingly prominent. These include: the scale, density, and capacity of water distribution networks are unable to meet the ever-increasing urban demand; investment for urban transportation infrastructure development is inadequate and central cities lack high-capacity, rapid, and convenient public transportation system, stationary transportation facilities such as parking lots are in short supply and traffic jams are serious in most cities; drainage and waste water treatment capacities are insufficient, so are solid waste collection and treatment capacities therefore small and medium sized cities and towns have serious problem with garbage dumps; urban energy supply heavily relies on fossil fuels; district heating is not widely adopted, and air pollution from mixed coal burning smoke and vehicle exhaust is aggravating.

Disaster prevention and mitigation capacity in urban areas is generally low. In China, over 70 % cities and towns, more than half of the population and over 75 % of industrial and agricultural production are located in areas with severe natural disasters, including floods, water logging and earthquakes. However, the ability to cope with and fight against natural disasters in cities and towns is weak, resulting in serious losses. Cities and towns focus much of their attention on providing relief to disaster-stricken areas but less emphasis is placed on prevention, therefore, emergency response capacity for large-scale catastrophic disasters and accidents is in urgent need to be improved. The poorly developed disaster insurance cannot meet the actual demand of post-disaster reconstruction.

3.3 Transportation System

Natural disasters may cause a series of damages to transportation networks, including damage to the base and surface of roads, railways, and airports, bridges, culverts, tunnels, stations, and facilities of communication, water supply and power supply; blocking waterways; and causing damage to navigation and port facilities, thus causing direct property losses or threatening transportation safety, even resulting in traffic accidents or interruption of transports, as well as a series of indirect losses or impacts (Wang et al. 2006).

Transportation system consists of railways, highways, inland waterways, maritime transport, and aerial transport: In China, a national transport network taking maritime transport, land transport, and aerial transport as main carriers has been gradually formed. After the Qinghai–Tibet Railway opened to the traffic in 2006, all provinces in China are covered by railways. In 2012, operating railway mileages reached 97.6 thousand km, with passenger capacity amounting to 1.89 billion. Operating mileage of highways reached 4.24 million km, among which expressways was 96.2 thousand km with passenger capacity amounting to 35.57 billion.

Cargo handling capacity at principal seaports reached 6.65 billion tons, and volume of freight amounted to 4.59 billion tons. There were 2457 lines for civil aviation, 180 airports for commercial flights, and the mileage of scheduled flights reached 3.28 million km.

Distribution of transportation networks is in line with the distribution of population and urban areas, denser in the eastern area as compared to western China: This pattern is partly restricted by natural conditions. But it also reflects the demand of economic activities and people. The railway transport network is composed of interconnected trunk lines, branch lines, connection lines, and railroad hubs. It centers at Beijing and the Beijing–Guangzhou Railway and Longhai Railway–Lanzhou–Xinjiang Railway are the trunk lines. Roads in China mainly include the trunk lines of state highways and expressways, and auxiliary lines of provincial highways, interprovincial highways, and county level roads. The national highway network connects major cities, industrial centers, transport hubs, and seaports around the country. Inland navigation is mainly on the Yangtze River, Pearl River, Heilungkiang River, Huaihe River, and the Beijing–Hangzhou Grand Canal. Among them, the Yangtze River is the main waterway for inland navigation in China, accounting for about 70 % of the total volume of traffic for passenger and freight. For maritime transport, the top ten ports with the largest cargo handling capacity in China are Shanghai, Shenzhen, Qingdao, Guangzhou, Ningbo, Tianjin, Xiamen, Dalian, Lianyungang, and Yingkou. The air transport network takes airports in Beijing, Shanghai, and Guangzhou as centers, airports in provincial capitals and tourist cities as hubs, and airports in other cities as branch lines, connecting 127 cities within China and 80 cities in 38 other countries. The main airports include Beijing Capital International Airport, Guangzhou Baiyun International Airport, Shanghai Hongqiao International Airport, Wuhan Tianhe Airport, Guilin Airport, Chengdu Shuangliu Airport, Shaanxi Xianyang Airport, Nanjing Airport, Kunming Wujiaaba Airport, and Hangzhou Airport (Fig. 11).

3.4 *Economy*

The economy as an exposure unit of natural disasters has complex interactions with disaster events: socioeconomic development on the one hand is affected by natural disasters. On the other hand, it imposes increasingly broader and more profound impacts on the natural environment, becoming important conditions for preventing or inducing the occurrence and development of natural disasters. With the increase of population and economic growth, damage range and scale of losses caused by natural disasters continuously expand; meanwhile, overexploitation of resources and damage to the environment by socioeconomic activities continuously aggravate hazards such as droughts, soil erosion, desertification, and red tide. Social progress and economic growth can create important conditions for carrying out disaster-prevention projects, improving emergency response, and facilitating post-disaster recovery and reconstruction, which can significantly reduce the vulnerability and enhance the coping



Fig. 11 Transportation networks in China, 2007 (Source Shi 2011, p. 17)

capacity of affected communities; they can also create better conditions for adaptation through adjustment in production systems and institutions and to certain extent alleviate impacts and losses caused by natural disasters (Wang et al. 2006). Therefore, analyzing the overall characteristics of the Chinese economy and its spatial differentiation is of great importance for understanding the spatial and temporal patterns of natural disasters in China.

Economic aggregate and growth: Since the reform and opening-up in China, especially since the 1990s, the Chinese economy maintained a rapid development with an annual growth rate of about 10 %. GDP of China in 2014 registered RMB 63.64 trillion Yuan, among which, output value of the primary industry, the secondary industry, and the tertiary industry was RMB 5.83, 27.14, and 30.67 trillion Yuan, respectively (National Bureau of Statistics of China 2015). GDP per capita amounted to RMB 46.53 thousand Yuan, 5.92 times of that in 2000. Though impacted by the global financial crises since 2008, the economy still kept a growth rate of over 8 %, and GDP in China has surpassed Germany and Japan in 2010, became the world’s second largest economy.

In terms of industrial growth (Fig. 12), the secondary and tertiary industries maintained a fairly high growth rate, up three times within 14 years from 2000 to 2014, while the primary industry was only 3.90 times higher than that of 14 years ago. Proportion of the primary and secondary industries in the overall economy slightly declined, down from 15.06 to 9.17 % and 45.92 to 42.64 % respectively, while the proportion of the tertiary industry went up from 39.02 to 48.19 %.

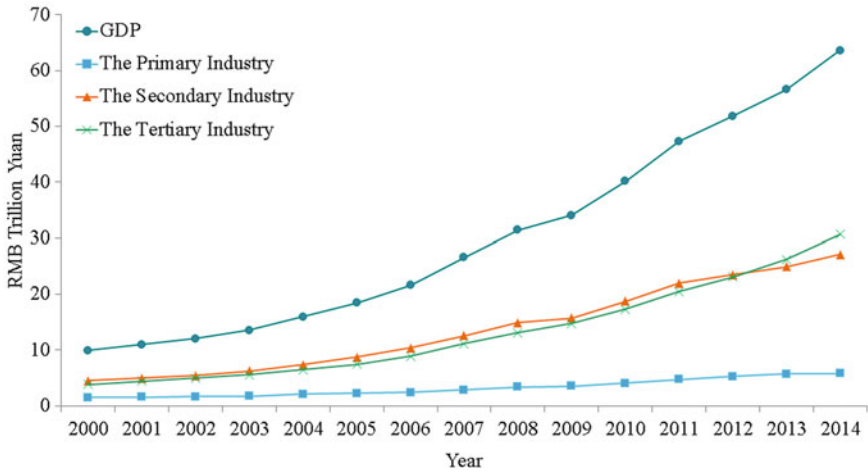


Fig. 12 Economic growth in China, 2000–2014 (Data Source NBS-China 2015)

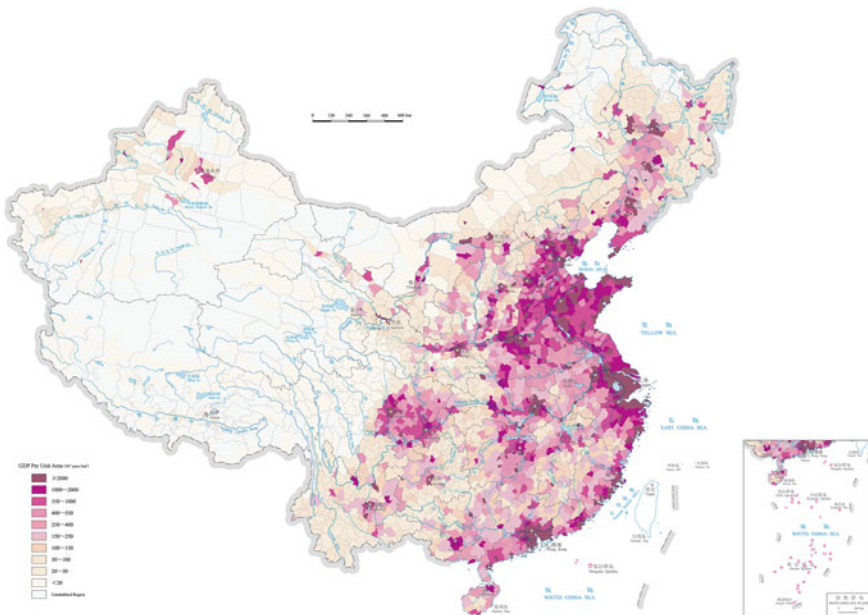


Fig. 13 Distribution of economic output in China, 2007 (Source Shi 2011, p. 20–21)

Regional differentiation of economic growth: Regional differentiation of economic growth in China is quite distinctive. Figure 13 shows the Gross Domestic Production (GDP) per unit area in China. The intensity of economic activities has a similar spatial pattern as population and cities and towns, greatly unbalanced in

geographical distribution. Population and cities and towns are densely concentrated in the eastern area (especially the coastal areas) and the economy there is well developed too, while the western area has low population density and underdeveloped economy. Areas with high GDP are generally located in the east coastal areas and along the main rivers, especially in the metropolitan areas of the Yangtze River Delta, Pearl River Delta, and the Bohai Rim. In the inland areas, major cities and megacities with extremely high economic density are distributed in beaded shape along transportation trunk lines such as along the waterway of the Yangtze River and the Beijing–Kowloon Railway. They have become regional centers of economic activities and have influences through the entire region or nationwide.

It is worth noting that although the Chinese economy has maintained a sustained rapid growth in recent years, the overall level was still low, and GDP per capita is not only much lower than that of developed countries, but also lower than many developing countries. The socioeconomic development in China also face the following challenges: a huge population, relatively low level of education of the population, weak economic foundation, relatively low level of science and technological development and modes of production, and great pressure on resources and environment from economic development. These challenges affect the development of capacity for disaster risk reduction in China.

3.5 Land Use and Land Cover

Land is the most fundamental natural resource and material base on which the survival and development of people depend. On the one hand, natural disasters can cause damage to land resources; on the other hand, land cover change from human activities may lead to natural and environmental disasters.

China is a country with a large proportion of mountainous areas and deeply affected by the monsoon climate. Mountains, hills, plateaus, plains, and basins account for 33.3, 9.90, 26.04, 11.98, and 18.75 % of the total land area, respectively. The area of cultivated land, forestland, and grassland was 13.54, 18.22, and 41.67 % of the total in 2007 (National Bureau of Statistics of China 2008).

The area of cultivated land (including paddy field, irrigated field, and rain-fed agricultural land) in China was 130.04 million hectares in 2007, which were mainly distributed in the humid and subhumid areas to the east of the 400 mm annual precipitation isoline, such as the northeast Songhua and Nen River Plain, North China Plain, middle and lower Yangtze River Plain, Pearl River Delta, the hilly area in southern China, and Sichuan Basin (Fig. 14). Cultivated land in these areas accounts for over 90 % of the total nationwide. The area of forests in China was 174.91 million hectares in 2007, mainly distributed in the northeast Greater Khingan Range and Lesser Khingan Range and Changbai Mountain, west Sichuan, northwest Yunnan, and southeast Tibet in southwestern China, as well as the mountainous areas in southern China such as the Fujian–Zhejiang–Jiangxi Hills, Nanling Hills, and Xuefeng Mountain. Forestlands are also distributed in the Altai

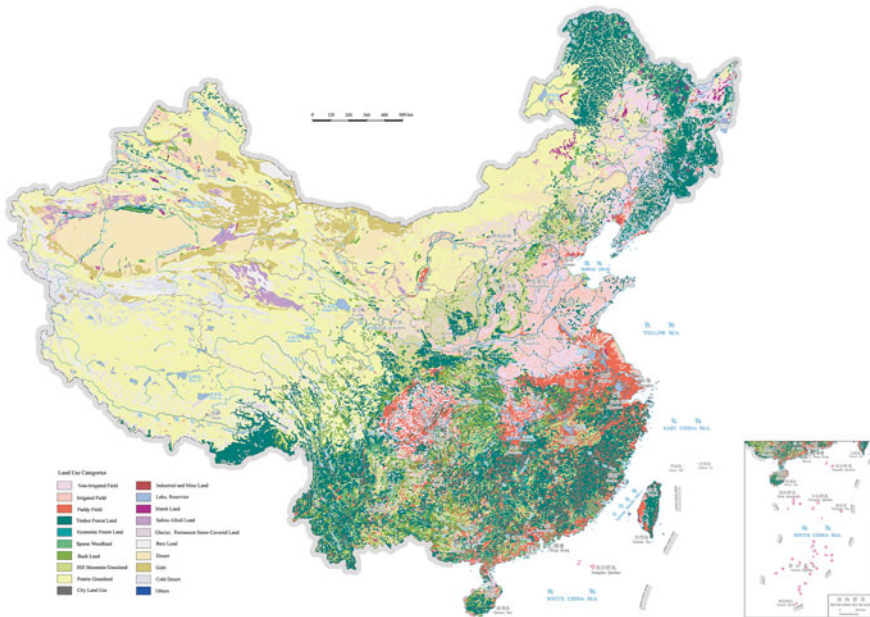


Fig. 14 Land use in China, 2007 (Source Shi 2011, p. 14–15)

and Tianshan Mountains, and Qilian Mountain in northwestern China. The area of the grassland totals 400 million hectares, mainly distributed in the semi-arid and arid areas to the west of the 400 mm annual precipitation isoline, such as the vast plateau, mountains, and basins in the western part of Northeast China, Inner Mongolia, Ningxia, Gansu, Qinghai, Xinjiang, and Tibet. Unused land is mainly located in northwestern China, in the Gobi and desert.

With the rapid development of the Chinese economy and continuous progress of the urbanization process in China, the insatiable demand for land for construction has created great conflicts between different land use and caused remarkable changes in land use and land cover.

Cultivated land: According to the statistics of the Ministry of Land and Resources, the area of cultivated land in China declined from 135.38 million hectares to 135.16 million hectares between 2009 and 2013 (MLR 2015) (Fig. 15). With the strong drive for urban expansion of the local governments, maintaining a stable cultivated land area is still a challenging task.

Forestland: According to the survey data from the State Administration of Forestry, between the mid-1970s and the early twenty-first century, percentage of forest cover in China had experienced the following changes: it was 12.70 % in the mid-1970s, 12.00 % in the later 1970s, 12.36 % in the mid-1980s, 12.98 % in the later 1980s, 13.92 % in the mid-1990s, 16.55 % in the later 1990s, 18.21 % in the early 2000s, 20.36 % in the mid-2000s, and 21.63 % in the later 2000s and early 2010s (Fig. 16) (SAF 2014). The area of forests had experienced a process of

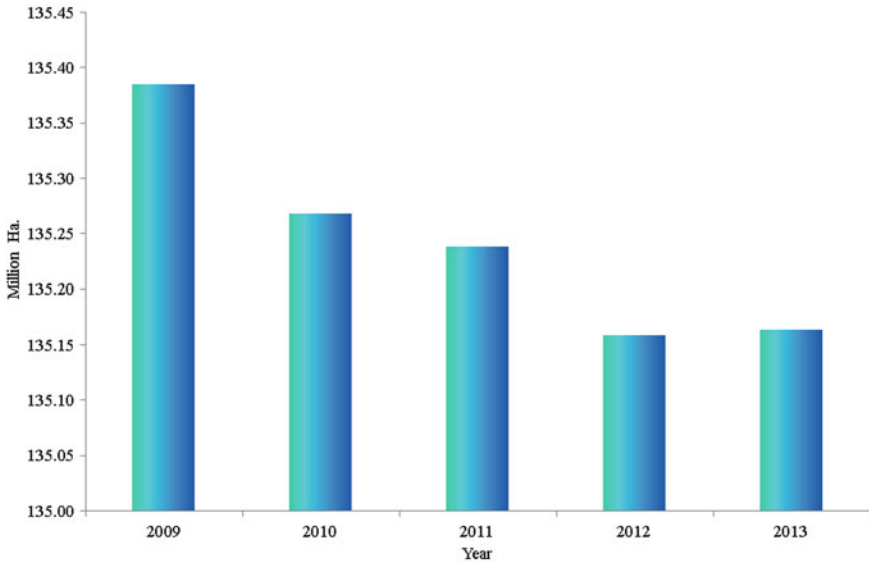


Fig. 15 The area of cultivated land in China, 2009–2013 (Data source MLR 2015)

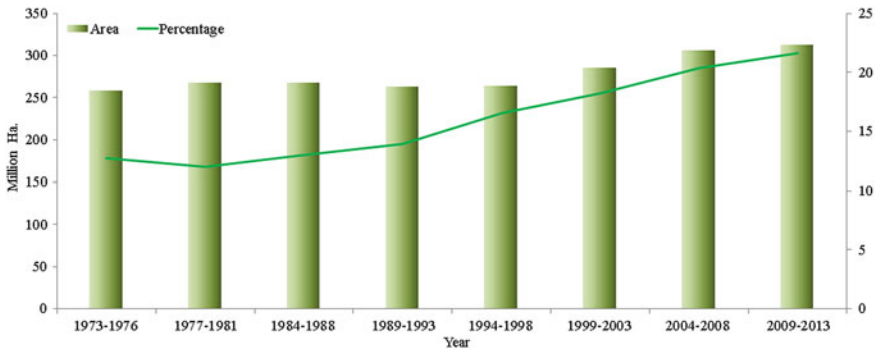


Fig. 16 The area of forest land and percentage of forest coverage in China, 1973–2013 (Data source SAF 2014)

slow decrease to fast growth, which can be mainly attributed to the large-scale reforestation efforts since the 1980s, when the government had recognized the importance of ecological restoration, and carried out a series of ecological construction projects such as the “North China–Northwest China–Northeast China Shelter Forest” project and the “Returning Farmland to Forestry” project, which gradually increased forest cover in the country.

Grassland: According to the statistics of the Ministry of Land and Resources, the area of grassland in the country slightly decreased from 2.638 million hectares to 2.195 million hectares between 2001 and 2013 (MLR 2001, 2015).

Land for construction: Affected by the rapid economic growth and urban and rural development, land for construction increased very fast in recent years. With accelerated urbanization and construction of infrastructure (such as roads, ports, and airports), a large amount of agricultural land was expropriated as construction land. Changes of the built-up areas in the country are as follows: it was 3,873 km² in 1952, 7,438 km² in 1978, 9,522 km² in 1985, 12,856 km² in 1990, 20,214 km² in 1996, 22,439 km² in 2000, 32,521 km² in 2005, and 38,107 km² in 2009 (Wang et al. 2006; NBS-China 2014), with an average annual increase of 5.41 %. According to the statistics of the Ministry of Land and Resources, in 2004 and 2008, the area of residential, industrial, and mining land was 257.2 thousand km² and 269.3 thousand km², with an average annual increase of 1.16 %.

4 Natural Disaster Losses

4.1 Disaster-Affected Population

China is one of the countries in the world that suffered the most from serious natural disasters. Its disaster-affected population and death tolls are among the world's largest. During the period from 1978 to 2014, the total population affected by natural disasters nationwide was on average 350 million a year and the number reached about 500 million in a number of years (Fig. 17). From 1978 to 2014, with a total of 266 thousand people died from natural disasters (average 7,192 a year), the annual number of deaths was in decline, except in the catastrophic disasters of 2008 and 2010 (Fig. 17).

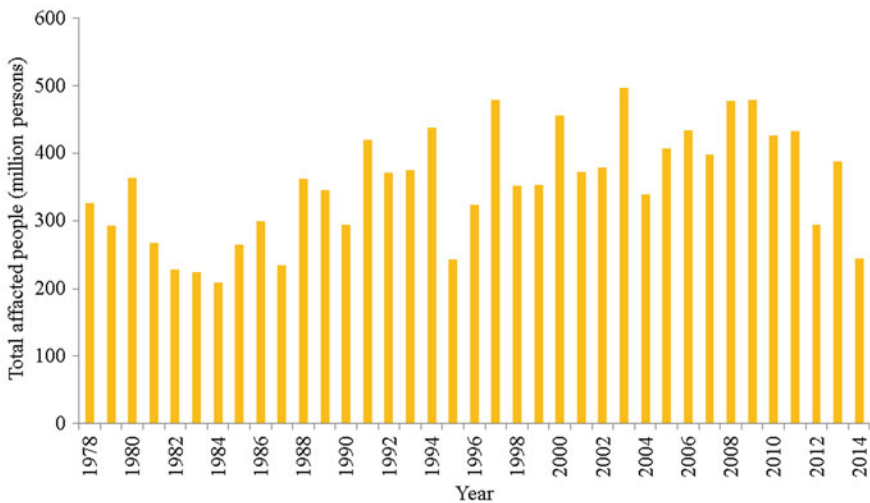


Fig. 17 Population affected by natural disasters in China, 1978–2014 (Data source MCA 2015)

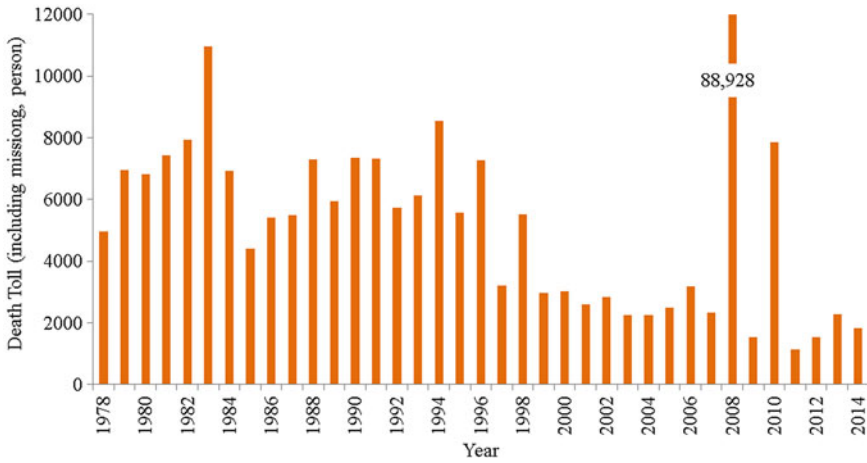


Fig. 18 Death tolls caused by natural disasters, 1978–2014 (Data source MCA 2015)

In 1978–2014, the temporal trend and regional distribution of disaster-affected population was uneven. In the 1980s, total disaster-affected population in the country averaged about 290 million each year. From 1990 to 2000, this number was about 360 million and in 2001–2010, it was about 420 million (Fig. 18). Disaster-affected population in China shows a rising trend since the economic reform and opening-up. Areas with huge disaster-affected population were mainly located in the eastern densely populated areas, especially in the North China Plain, the Fen River–Wei River Valleys, and the middle and lower Yangtze River Plain. The Chengdu–Chongqing area in Sichuan Basin is also an area with high disaster-affected population. In addition, the Pearl River Delta, Northeast Plain, and southeast coastal areas also had high disaster-affected populations.

4.2 Collapsed Buildings

In China, natural disasters that cause building collapses are mainly floods, followed by earthquakes, typhoons, and storm surges, and landslides, debris flows, rockfalls, land subsidence, and wind disasters. From 1978 to 2014, a total of 102 million rooms were collapsed by natural disasters in China, averaged 2.8 million each year. The number of collapsed houses was the largest in the 1990s, with more than 4 million rooms each year on average; and over 10 million rooms were collapsed in 2008 due to the Wenchuan Earthquake (Fig. 19). These numbers were not only affected by the types and strength of the hazards, but also by characteristics of the exposure units such as building density and population density. The regional distribution of collapsed houses in 1978–2014 shows that the most severely stricken areas were Hunan, Sichuan, Anhui, and Henan Provinces, where the population and

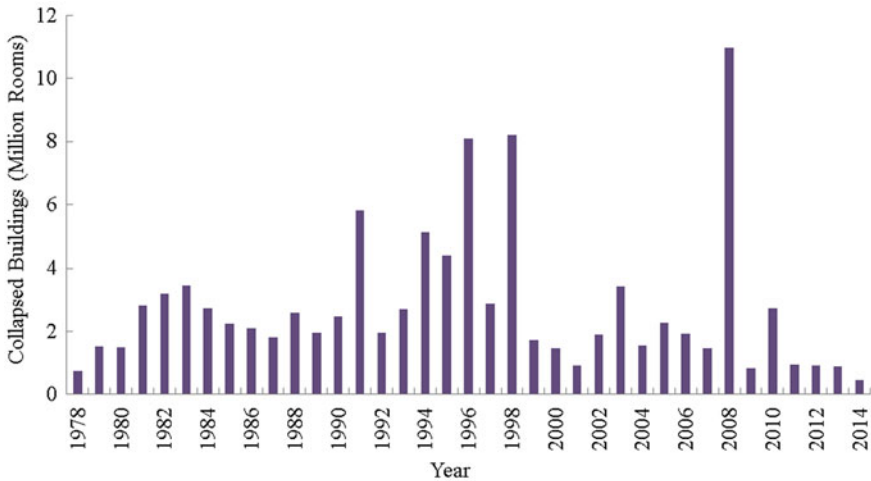


Fig. 19 Collapsed buildings by natural disasters in China, 1978–2014 (Data source MCA 2015)

houses were dense and disasters such as floods and earthquakes were frequent and severe—more than 200 thousand rooms were collapsed each year in each province; these were followed by Jilin, Hebei, Jiangsu, Zhejiang, Fujian, Jiangxi, Shandong, Hubei, Guangdong, Guangxi, Yunnan, and Shaanxi provinces, with 100 thousand–200 thousand rooms collapsed each year. In Shanxi, Inner Mongolia, Liaoning, Heilongjiang, Hainan, Guizhou, Gansu, Qinghai, and Xinjiang, where floods were fewer or less severe, or density of population and houses were relatively low, 10 thousand–100 thousand rooms were collapsed by natural disasters each year during this time period. Beijing, Shanghai, Tianjin, Tibet, and Ningxia had the smallest numbers of damaged houses, with less than 10 thousand rooms collapsed each year.

4.3 Agricultural Losses

Natural disasters are the most important natural factors affecting agricultural production in China. Damage to agriculture caused by natural disasters can be categorized as direct damages and long-term impacts. The former refers to the effect on the volume and value of output of products in agriculture, forestry, animal husbandry, and fishery. The latter refers to the impact on income of farmers, poverty, resources for agricultural production, and capacity of agricultural development. In 1978–1997, the disaster-affected area of crops in China increased. But it has been decreasing since 1997 (Fig. 20).

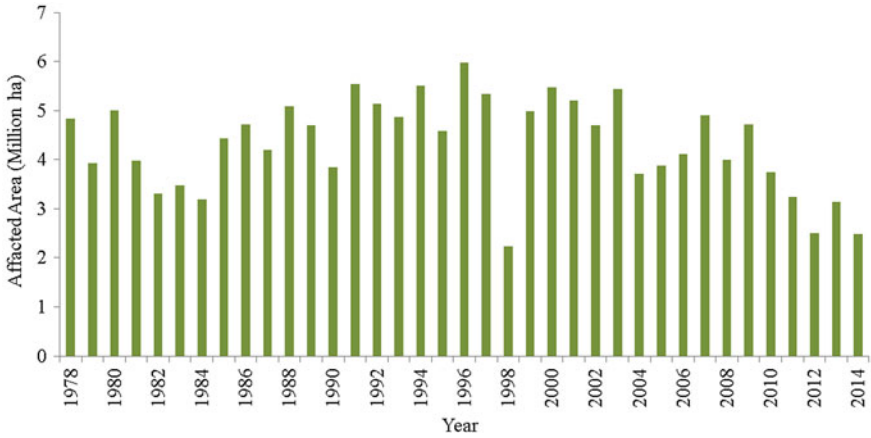


Fig. 20 Area of crops affected by natural disasters in China, 1978–2014 (Data source MCA 2015)

4.4 Direct Economic Losses

Since 1989, direct economic losses caused by natural disasters has seen an overall rising trend (Fig. 21). From 1989 to 1993, the direct economic losses were the lowest, but they accounted for a relatively high proportion of the national GDP in the corresponding years. Between 1994 and 1998, the direct economic losses increased greatly year by year, but the percentage of the losses in national GDP had dropped. During the 10 years from 1999 to 2007, economic losses caused by

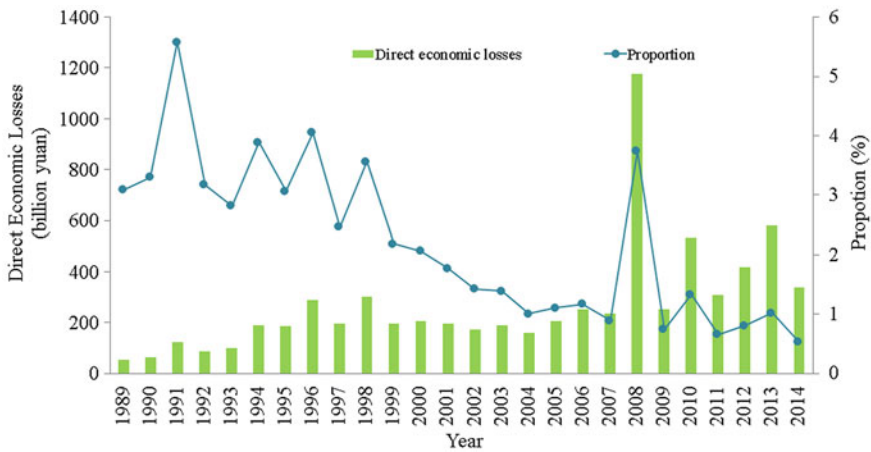


Fig. 21 Direct economic losses caused by natural disasters and proportion in national GDP in China, 1989–2014 (Data source MCA 2015)

natural disasters remained unchanged, and the proportion in national GDP had continuously dropped (Fig. 21).

In the 1990s, direct economic losses caused by natural disasters substantially increased, and the average losses were RMB 172 billion Yuan per year. Annual direct economic losses caused by natural disasters in the 1990s and 2000s amounted to RMB 238 billion Yuan. This situation drastically differs from the previous decades—before the 1980s, economic losses caused by natural disasters on average were very low but the difference between severe disaster years and other years was great—direct economic losses in normal years ranged between RMB 10 billion and 40 billion Yuan, but amounted to more than RMB 100 billion Yuan in severe disaster years. Since the 1990s, losses caused by natural disasters has increased sharply but the interannual differences were relatively small except for 2008 and 2010, due to the 2008 Wenchuan Earthquake and freezing rain and sleet in southern China, and the 2010 Yushu Earthquake and Zhouqu debris flows. This temporal pattern is mainly because comparative economic losses from natural disasters depend on the intensity of the hazards and the level of economic development. In the 1950s and the 1960s, the estimated ratio of direct economic losses from natural disasters to GDP was 15 %, and the ratio of economic losses to fiscal revenue was 50 %, and these ratios exceeded 20 and 100 % respectively in the years of severe disasters. In the 1970s–1990s, these two ratios dropped to 3–7 and 20–30 %, respectively with smaller interannual differences.

5 Natural Disaster Risks

Our assessment of natural disaster risks in China mainly took into consideration the intensity of hazards and vulnerability of exposure units. Due to the limited availability of data for the assessment of some single hazard disaster risks, the assessments can be divided into three types: the first is strict risk evaluation of natural disasters; the second is relative risks of natural disasters since the vulnerability of the exposure units could only be quantified in relative terms despite that the probability of hazard occurrences can be accurately calculated; the third is risk grade of natural disasters, in which case both the probability of hazard occurrences and the vulnerability of exposure units are expressed in relative terms. In Figs. 22, 23, 24, and 25, total risk of natural disasters, risk of human deaths, risk of direct economic losses, and risk of building damages in China are shown, respectively. In the calculation of these risk maps, 12 types of major natural disasters including earthquake, typhoon, flood, drought, landslide and debris flow, dust storm, storm surge, hail storm, snow, frost, forest fire, and grassland fire are selected (Shi 2003). Risk level of each disaster is divided into 10 grades, where Grade 10 is the highest, that is, “Very High Risk” and Grade 1 is the lowest, that is, “Extremely Low Risk.” According to the data in the *Statistics of Major Natural Disasters in China, 1949–2009* (Zheng et al. 2009),



Fig. 22 Total risk level of all major natural disasters in China (Source Shi 2011, p. 142–143)

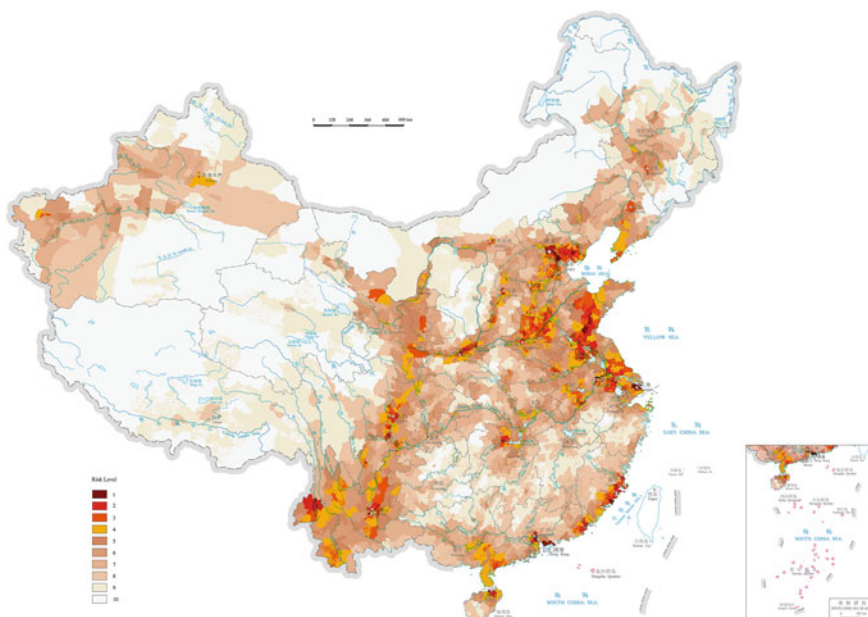


Fig. 23 Risk level of human casualty from natural disasters in China (Source Shi 2011, p. 146–147)

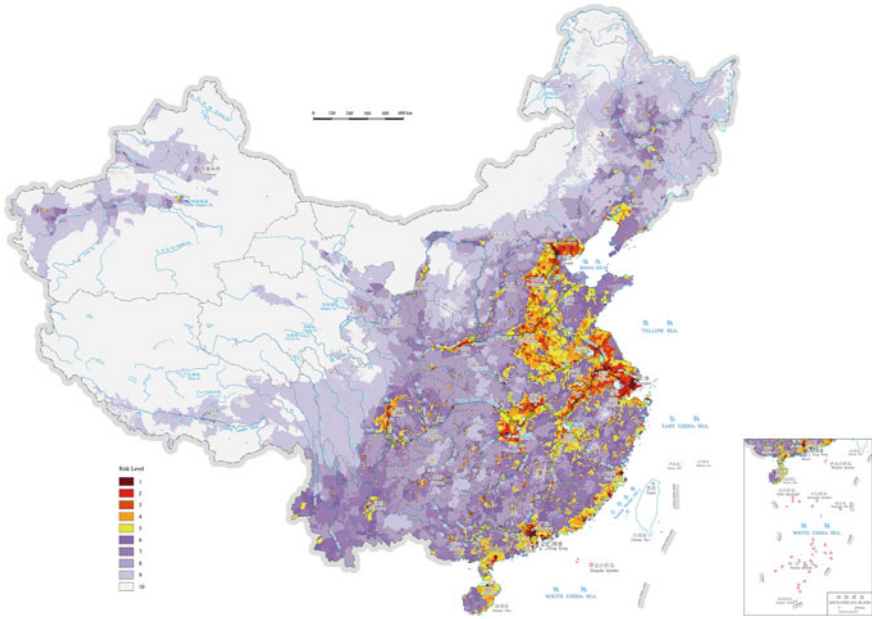


Fig. 24 Risk level of building collapse from natural disasters in China (Source Shi 2011, p. 150–151)

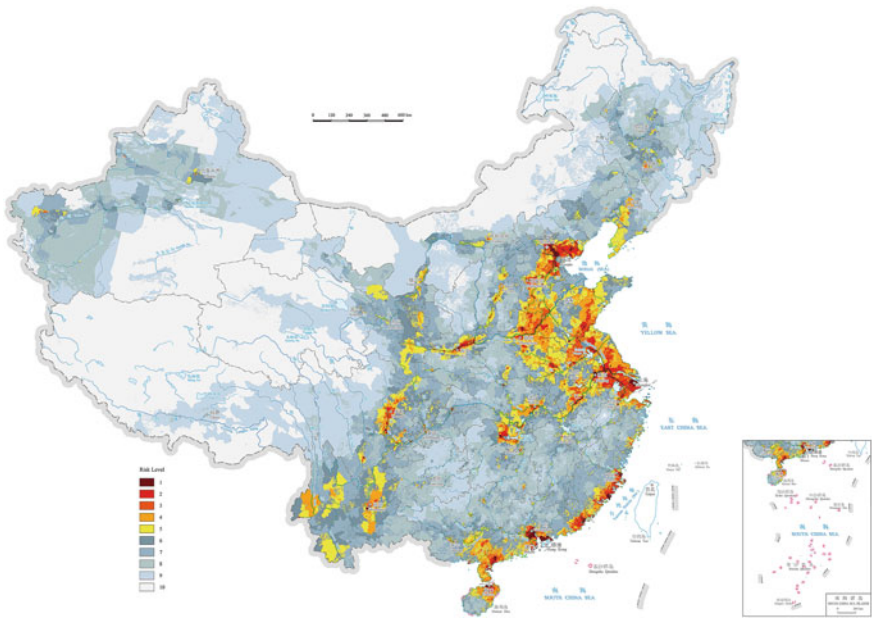


Fig. 25 Risk of economic losses caused by natural disasters in China (Source Shi 2011, p. 152–153)

and based on the number of occurrence of disasters, the number of people affected, the number of collapsed buildings, and direct economic losses, weights of the 12 natural disasters in the calculation of the map of total natural disaster risks in China were calculated respectively (Shi 2011).

5.1 Total Risk of Natural Disasters

The total risk level of all major natural disasters is derived from a comprehensive evaluation based on the result of risk assessment of the 12 single disaster types and the weight (that is, frequency) of each disaster type. The composite risk index is as follows:

$$RI = \sum_{i=1}^n r_i \times w_i \quad (5)$$

where, RI is the total risk of all major natural disasters in an area (which is 1 km grid in this assessment), r_i is the risk level of the i th disaster, w_i is the weight of the i th disaster, n is the 12 natural disasters evaluated in the assessment.

Figure 22 shows that most areas in China have medium and low values of risk of natural disasters. The areas with high risk values are mainly concentrated to the east of the Taihang–Wuling–Dayao Mountains, and the high risk center is located in North China, the middle and lower Yangtze River Basin, and the southeast coastal areas. The areas with medium RI are located to the east of the Greater Khingan–Yin–Hengduan Mountains, where the areas with high RI value are scattered. Northwestern China has low RI values and the lowest risk level is found in northern Tibet, from where risk level gradually rises outward. All three areas with high RI values are densely populated and have highly developed economy. They are mainly in the metropolitan areas in the Yangtze River Delta, the Pearl River Delta, and the Beijing–Tianjin–Tangshan area. This to some extent reflects the spatial distribution of exposure in China. North China is mainly affected by earthquakes, the middle and lower Yangtze River Basin is mainly affected by floods and water logging, and the southeast coastal areas are mainly affected by typhoon. The total risk of all major natural disasters is the result of the combined effect of hazards and exposure.

5.2 Risk of Human Casualty from Natural Disasters

The risk level of casualty caused by all major natural disasters is calculated from a comprehensive evaluation based on the result of risk assessment of the 12 single

disasters and the weight of each disaster (derived from the number of people killed by each type of disaster). The formula is as follows:

$$R_c = \sum_{i=1}^n r_i \times w_i, \quad i = 1, 2, \dots, n \quad (6)$$

where, R_c is the risk of casualty caused by all major natural disasters in an area, r_i is the risk level of the i th disaster, w_i is the weight of the i th disaster, n is the 12 natural disasters evaluated in the assessment.

Figure 23 indicates that casualties of natural disaster in China are clearly clustered spatially—they are mainly distributed in three areas: North China and East China surrounded by the Yanshan–Lvliang–Dabie–Tianmu Mountains; Helan Mountain–Liupan Mountain–southeastern Qinghai–Tibet Plateau–Hengduan Mountains–Wuliang Mountain; and the southeast coastal areas. Central and northern Qinghai–Tibet Plateau, inland areas in northwestern China, as well as the northwest part of northeastern China are areas with relatively low risk. The North China Plain, Yangtze River Delta, southeast coastal areas, and Chengdu–Chongqing areas in Sichuan Basin are densely populated places. Population density does not correlate well with risk level. Except for the southeast coastal areas and a fraction of the basin areas in the middle and lower reaches of the Yangtze River, the high risk areas of human casualty from natural disasters are mainly associated with seismic belts. For example, the North China seismic belt, north–south seismic belt, and Qinghai–Tibet Plateau seismic belt are in line with areas of high casualty. Risk of casualty is mainly controlled by the earthquakes. Although Xinjiang and southern Tibet are also seismotectonic active areas, these areas are sparsely populated, therefore extremely high risk will not occur there. Southeast coastal areas have high risk of typhoon disasters and the basin areas in the middle and lower reaches of the Yangtze River have high risk of flooding and water logging.

5.3 Risk of Building Collapse

The risk level of building collapse caused by all major natural disasters is calculated from a comprehensive evaluation based on the result of risk assessment of the 12 types of single disasters and the weight of each disaster (derived from the numbers of collapsed houses caused by each type of disaster). The formula is as follows:

$$R_h = \sum_{i=1}^n r_i \times w_i \quad (7)$$

where, R_h is the risk level of building collapse caused by all major natural disasters, r_i is the risk level of the i th disaster, w_i is the weight of the i th disaster, n is the 12 natural disasters evaluated in the assessment.

The spatial pattern of risk of building collapse caused by natural disasters in China is shown in Fig. 24. High-value areas with R_h greater than 4 are mainly distributed on the second and third topographical steps to the east of the Qinghai–Tibet Plateau. About 80 % of the high-value areas with R_h greater than 9 coincides with high direct economic losses areas (see the next section), located in the triangular area between Beijing, Changsha, and Shanghai. Other high value areas are scattered. The vast northwestern areas are places with low R_h values. Density of buildings evidently has positive correlation with population density. The area within this triangle has dense population and houses. It is also affected by several major hazards in China.

5.4 Risk of Direct Economic Losses

The risk Level of direct economic losses caused by all major natural disasters is calculated from a comprehensive evaluation based on the result of risk assessment of the 12 types of single disasters and the weight of each disaster (derived from direct economic losses caused by each type of disaster). The formula is as follows:

$$R_e = \sum_{i=1}^n r_i \times w_i, \quad i = 1, 2, \dots, n \tag{8}$$

where, R_e is the risk level of direct economic losses caused by all major natural disasters, r_i is the risk level of the i th disaster, w_i is the weight of the i th disaster, n is the 12 natural disasters evaluated in the assessment.

The spatial distribution of risk of direct economic losses caused by all major natural disasters is shown in Fig. 25. As a whole, the areas with high R_e are mainly distributed in the triangular area between Beijing, Changsha, and Shanghai. Other areas with high R_e are scattered in the southeast coastal areas and eastern Qinghai–Tibet Plateau. Areas with low R_e center at northern Tibet and the risk level increases outward. Between the high and low value areas are areas of medium R_e values. Economic development level has directly positive correlation with the population density. Densely populated areas such as the North China Plain, Yangtze River Delta, southeast coastal areas, and Chengdu–Chongqing areas in Sichuan Basin are also well-developed areas. Comparing Figs. 23 and 25, it is clear that the spatial patterns of R_e and R_c are very consistent, especially in the three areas with high values. Meanwhile, the spatial pattern of R_e is closely related to the distribution of several main hazards, including seismic belts and areas with high frequency of typhoons, floods, landslides, and debris flows.

The all-disaster risk assessment of this section reveals the total risk of all major natural disasters for each 1 km grid in China. Further details on the data, methods, and results are found in Shi (2011).

References

- MCA (Ministry of Civil Affairs). 2015. *China civil affairs' statistical yearbook 2015*. Beijing: China Statistics Press (in Chinese).
- MLR (Ministry of Land and Resources of the Peoples' Republic of China). 2001. 2001 National land and resources bulletin (in Chinese).
- MLR (Ministry of Land and Resources of the Peoples' Republic of China). 2015. 2014 National land and resources bulletin (in Chinese).
- NBS-China (National Bureau of Statistics of China). 2008. *China statistical yearbook 2008*. Beijing: China Statistics Press (in Chinese).
- NBS-China (National Bureau of Statistics of China). 2013. *China statistical yearbook 2013*. Beijing: China Statistics Press (in Chinese).
- NBS-China (National Bureau of Statistics of China). 2014. *China statistical yearbook 2014*. Beijing: China Statistics Press (in Chinese).
- NBS-China (National Bureau of Statistics of China). 2015. *China statistical yearbook 2015*. Beijing: China Statistics Press (in Chinese).
- Research Team for the Major Natural Disaster of National Science and Technology Commission. 1994. *Major natural disasters and disaster mitigation countermeasures in China* (Overview). Beijing: Science Press (in Chinese).
- Shi, P.J. 1991. Study on the theory of disaster research and its practice. *Journal of Nanjing University* (Natural Sciences) 11(supp): 37–42 (in Chinese).
- Shi, P.J. 1996. Theory and practice of disaster study. *Journal of Natural Disasters* 5(4): 6–17 (in Chinese).
- Shi, P.J. 2002. Theory on disaster science and disaster dynamics. *Journal of Natural Disasters* 11 (3): 1–9 (in Chinese).
- Shi, P.J. 2003. *Atlas of natural disaster system of china*. Beijing: Science Press (in Chinese and English).
- Shi, P.J. 2005. Theory and practice on disaster system research—the fourth discussion. *Journal of Natural Disasters* 14(6): 1–7 (in Chinese).
- Shi, P.J. 2009. Theory and practice on disaster system research—the fifth discussion. *Journal of Natural Disasters* 18(5): 1–9 (in Chinese).
- Shi, P.J. 2011. *Atlas of natural disaster risk of China*. Beijing: Science Press (in Chinese and English).
- State Administration of Forestry. 2014. *China forestry database*. <http://cfdb.forestry.gov.cn/lysjk/indexJump.do?url=view/moudle/dataQuery/dataQuery>.
- Wang, J.A., P.J. Shi, and L. Zhu. 1994. A research on regional distribution of major natural hazards in China. *Acta Geographica Sinica* 49(1): 18–26 (in Chinese).
- Wang, J.A., P.J. Shi, P. Wang, et al. 2006. *Spatiotemporal pattern of natural disasters of China*. Beijing: Science Press (in Chinese).
- Zhang, L.S., and E.Z. Liu. 1992. *Atlas of natural disaster of China*. Beijing: Science Press (in Chinese).
- Zheng, G.C. 2009. *Calamities always help to make a nation flourishing—epic of combating natural disasters in sixty years of New China*. Changsha: Hunan People's Press (in Chinese).

Earthquake Disasters in China

Wei Xu, Jifu Liu, Guodong Xu, Ying Wang, Lianyou Liu
and Peijun Shi

Abstract Due to its geological conditions, China is one of the most seismic hazard-prone countries in the world. This chapter first introduces the spatial and temporal patterns of seismic activities and earthquake disasters in China. Seismic risk is then systematically assessed by combing peak ground acceleration (PGA) and building vulnerability curves, and an earthquake disaster risk map with regard to direct economic losses is obtained. Finally, the earthquake emergency response process, disaster response mechanisms, and post-disaster restoration and reconstruction processes are analyzed using the Wenchuan Earthquake case.

Keywords Earthquake disaster · Spatiotemporal pattern · Earthquake risk · Wenchuan Earthquake

Located at the junction of the circum-Pacific seismic belt and the Mediterranean-Himalayan seismic belt, China is one of the countries with most intense continental seismic activity, and earthquake disasters have been one of the most important natural disasters affecting China. According to the statistics, in the Chinese mainland, on average there are 19 earthquakes with magnitude above 5, 4 earthquakes with magnitude above 6, and 0.67 earthquakes with magnitude above 7 every year. Earthquake threats facing the Chinese cities are especially serious. Twenty-two provincial capital cities and 2/3 of the large cities that have more than one million population are located in high seismic hazard regions. Among these, 11 provincial capital cities have the possibility to encounter large earthquakes above magnitude 7 and 17 provincial capital cities have the possibility to encounter large earthquakes

W. Xu · J. Liu · Y. Wang · L. Liu
Key Laboratory of Environmental Change and Natural Disasters of Ministry
of Education, Beijing Normal University, Beijing 100875, China

G. Xu
Institute of Disaster Prevention, Beijing 101601, China

P. Shi (✉)
State Key Laboratory of Earth Surface Processes and Resource Ecology,
Beijing Normal University, Beijing 100875, China
e-mail: spj@bnu.edu.cn

above magnitude 6.5 (Chen et al. 2005). Since the founding of the People Republic of China, the China Seismological Bureau and other related government departments have been established to carry out the development of seismic intensity zoning map and seismic observation network, development of zoning map for ground motion parameters, national earthquake safety plan, and other large projects, laying solid foundation for effectively reducing earthquake risks. The large-scale Observation Network for Crustal Movement in China project has fundamentally improved the backward situation of dynamic monitoring for the Earth's surface crust in China, improved the ability to forecast great earthquakes, and placed China at an advanced level of scientific and technological development internationally for monitoring and studying present-day crustal movement. Seismic disaster risk research has a very positive impact on reducing seismic losses and establishing earthquake-safe communities.

Since 1999, with the support of the Swiss Reinsurance Company, the Ministry of Civil Affairs (MOCA), Ministry of Science and Technology (MOST), and other relevant government departments, the authors have participated in the "Analogy Model for Seism Losses in China" project entrusted by the Swiss Reinsurance Company, the "Research and Demonstration for Key Technologies of Comprehensive Risk Prevention" national science and technology support project (2006BAD20B00), and the rapid assessments for disaster situations of the Wenchuan Earthquake in 2008 and Yushu Earthquake in 2010, as well as the "Technology for Comprehensive Disaster Risk Analysis" sub-project of an national science and technology support project (2008BAK49B04), and the "Technological Research for Risk Evaluation of Natural Disasters in the Yangtze River Delta Area" (2008BAK50B07). We have successively carried out a series of research on spatial and temporal pattern identification, fragility analysis, risk evaluation, and other aspects of seism disasters in China. Contents of this chapter are the integrated summary for the above studies.

1 Spatial and Temporal Patterns of Earthquakes

Situated at the junction of the circum-Pacific seismic belt and the Mediterranean-Himalayan seismic belt, China experiences most intense seismic activities and is one of the most earthquake-prone areas in the world (Wang et al. 2006). Seism in China is characterized by high frequency, wide distribution, great intensity, shallow seismic focus, and clear regional differences.

1.1 *Spatial Distribution of Seismic Activities*

China has rich historical earthquake data. The recorded most ancient earthquake can be traced back to the twenty-third century BC (DEDP 1995). According to the

historical earthquake data, destructive earthquakes have happened in 34 provinces, municipalities, and autonomous regions. Considering that early earthquake records may not have included some strong earthquakes, the earthquake data used in the analysis of this chapter are only from the twentieth century onward.

Most earthquakes in China are shallow focus earthquakes that occurred within the continental crust, with strike-slip type as the principal type; therefore, the horizontal distribution of epicenters can well represent the seismotectonic framework. Figure 1 shows the epicenter distribution of historical earthquakes in China (1900–2014).

From Fig. 1, we can clearly see that seismic activities of inland areas in China is much higher in the west as compared to the east. Seismic activities in western China is characterized by high frequency and great intensity.

According to Lou (1996), the boundary between eastern and western inland China seismic regions is the line connecting Baoji, Hankou, and Guiyang (around 107.5° E). Statistics for seismic activity frequencies in China (1900–2014) based on this division are shown in Table 1.

From the statistics we can see that between 1900 and 2014, the total number of seismic activities ($M_s \geq 6$) in China’s western inland is 8.28 times of that in eastern inland. In the recent over 100 years, there have been no earthquakes above magnitude 8, and only a few earthquakes above magnitude 7 in eastern inland.

To sum up, the spatial pattern of seismic activities in Chinese mainland is featured by strong activities in the west and weak activities in the east. The

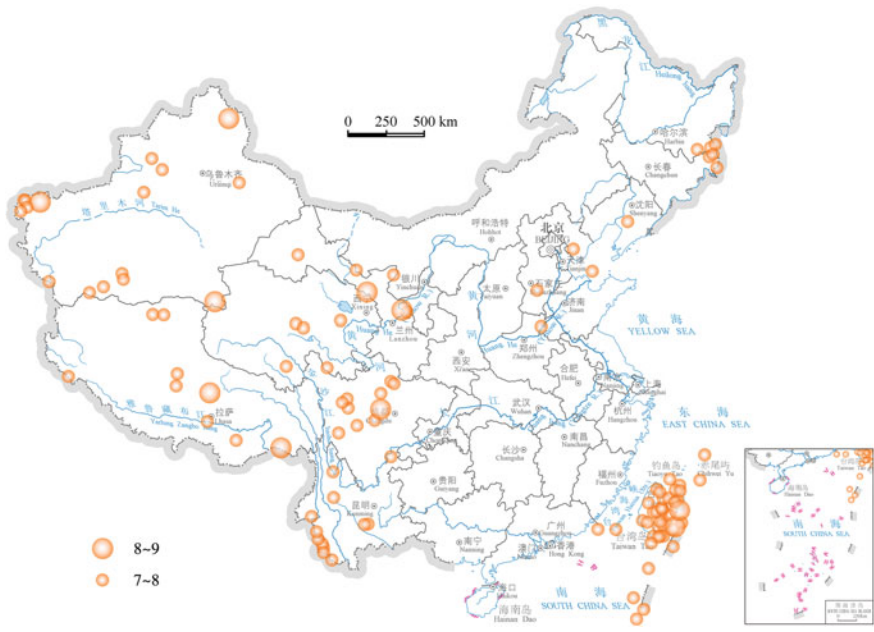


Fig. 1 Epicenters of historical earthquakes in China, 1900–2014

Table 1 Number of earthquakes in China's eastern and western inland, 1900–2014 ($M_s \geq 6$)

Region	$6 \leq M_s < 7$	$7 \leq M_s < 8$	$8 \leq M_s$	Sum
Eastern mainland	35	11	0	46
Western mainland	324	49	8	381
Western: eastern	9.26:1	4.45:1	8:0	8.28:1

Data source CENC (2015), DEDP (1995, 1999)

earthquake-prone areas in China are Xinjiang, Qinghai, Tibet, Sichuan, (west) Yunnan, Hebei, Taiwan, and other eastern provinces.

First, according to the geologic structure, the western inland area can be divided into Xinjiang seismotectonic zone and Qinghai–Tibet seismotectonic zone.

Xinjiang seismotectonic zone: Earthquakes in this area are related to the movements of the huge Cenozoic compressional basins and the orogenic belts in between. There have been very few earthquakes in the Junggar Basin and the Tarim Basin due to their rather stable interiors. The Tianshan Mountains and the Altai Mountains among it upheave intensely, so earthquakes mostly occur at the junction of these mountains and the plains. The earthquake faults are EW strike or NW strike; the faults in NW strike or NNW are mostly the compression and right-slip type.

Qinghai–Tibet seismotectonic zone: This area includes the entire Qinghai–Tibet Plateau and the western part of the Sichuan–Yunnan Plateau. As the region with the most active inland earthquakes in the world, earthquakes above magnitude 7 in the Qinghai–Tibet Plateau account for 43 % of the same magnitude earthquakes in the whole Eurasia, and more than 60 % of the same magnitude earthquakes in Chinese inland. The Qinghai–Tibet plate is located in the north of the subduction zone of the Indian plate and Eurasian plate, with an average elevation of 4,000 m. The Indian plate continuously subducts and compresses northward, which is the major driving force source. This area has the greatest crustal thickness in China, with average thickness of 50 km, and highest of about 73 km. Earthquakes in Qinghai most concentrate in the fracture system spreading in NW–EW–NNW strike and fracture with NE and SN strikes (Ma et al. 1982).

Table 2 shows seismic activities of six provinces (autonomous regions) that experience frequent earthquakes in China's western earthquake zone from 1900 to 2014. From the table, we can see that earthquakes with the highest intensity happened in Xinjiang and Tibet, but the region with the highest earthquake frequency per unit area is in Yunnan and Sichuan.

Second, to the east is the North China seismotectonic zone and the Taiwan seismotectonic zone.

North China seismotectonic zone: Many large earthquakes have occurred in this region since 1949, including the magnitude 6.8 Xingtai Earthquake in 1966 and the magnitude 7.8 Tangshan Earthquake in 1976. Since the Neogene, tectonic movements in this region have been very intense, deep structures manifested as the crust thinning and upper mantle upheaving, some low-velocity layer within local crust are also found; shallow structures manifested as the formation of rift valley and

Table 2 Seismic activities of six provinces (autonomous regions) in China's western earthquake zone, 1900–2014

Province (autonomous region)	Greatest earthquake		Earthquake of $M_s \geq 7.0$			Earthquake of $M_s \geq 5.0$		
	Magnitude	Rank	Frequency		Area frequency Times/ 10^5 km 2	Frequency		Area frequency Times/ 10^5 km 2
			Times	Rank		Times	Rank	
Yunnan	7.8	4	11	2	2.86	303	3	78.80
Xinjiang	8.25	2	17	1	0.98	483	1	29.54
Tibet	8.6	1	9	4	0.75	419	2	34.75
Qinghai	7.7	5	6	5	0.67	176	5	24.54
Gansu	8.0	3	4	6	0.99	59	6	14.50
Sichuan	8.0	3	10	3	2.08	192	4	39.82

Data source CENC (2015), DEDP (1995, 1999)

graben basin as well as fault activities. The strikes of tectonic lines are mainly NNE, followed by NW strike.

Taiwan seismotectonic zone: This zone includes Taiwan Province and its adjacent waters and is the region with the most frequent seismic activities in China. The occurrence of earthquakes related to the Pacific arc tectonic, Taiwan Island, and the surrounding active tectonic movements (including volcanic arc, intermountain depression, depression of the western edge of Cenozoic fold belt). The earthquake faults appear in NNE strike, with reverse-left-lateral strike-slip.

1.2 Temporal Distribution of Seismic Activities

Ma and Jiang studied the records of continental earthquakes in China in the past about 2,000 years and found that the alternation between periods of strong and weak earthquakes, and frequent and less frequent earthquakes is clear, and defined the periods with more frequent and high strength seismic activities as seismic active episodes, and periods with less frequent and low strength seismic activities as seismic inactive episodes (Ma and Jiang 1987). For example, in the twentieth century, $M_s \geq 7$ earthquakes in the Chinese mainland and its adjacent areas showed clear phases, with a duration of active episodes of 13–16 years and duration of largely stable inactive episodes usually of about eight years. The active episodes are: (1) 1897–1912; (2) 1920–1937; (3) 1946–1957; (4) 1966–1976; and (5) 1985 onward (Fig. 2). The time interval between active episodes is the inactive episodes, during which there were relatively fewer strong earthquakes and rarely any $M_s \geq 8$ earthquake.

We analyzed the earthquake data of $M_s \geq 7$ from 1987 to 2009 using the same method (Ma and Jiang 1987) and found that the ending year for the fifth earthquake active period was 2001 and the starting year of the sixth episode was 2008, with the 12 May 2008 Wenchuan Earthquake.

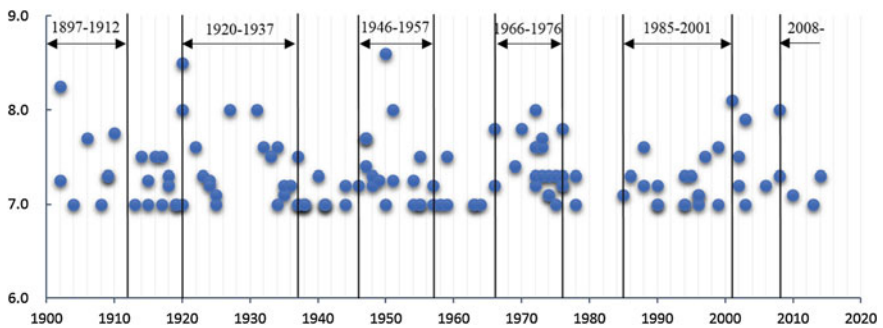


Fig. 2 Six seismically active episodes in Chinese mainland and its adjacent areas (Data source CENC 2015; DEDP 1995, 1999)

The spatial distribution of seismic activities for every earthquake active episode is different. In each episode seismic activities concentrated at one or two seismic belts, and these varied greatly among the episodes.

The main activity area of the first episode was the NE tectonic zone from Pamir to Baikal; the second episode was in the NW tectonic zone along the Hexi Corridor in Gansu; the main activity area of the third episode was the nearly NS seismic belt from eastern Tibet to central Mongolia; the fourth episode included the Sichuan–Yunnan seismic area and the North China seismic area. The main activity area of the fifth episode was the Kunlun Mountains seismic belt. On 14 November 2001, a Ms8.1 violent earthquake occurred in the Kunlun Mountains, which was the second greatest earthquake within Chinese mainland since the founding of the People’s Republic of China in 1949, and ranked only second to the Ms8.5 earthquake in Tibet Medog on 15 August 1950.

According to the records of historical earthquakes and disasters in China (Lou 1996), between the sixteenth and seventeenth century and since the twentieth century, seismic activities were relatively intense while in the fifteenth century and the eighteenth to nineteenth century, seismic activities were relatively weak. As the frequency record of medium and strong earthquakes in the past over 100 years (Fig. 3) indicates, during this time period, earthquake frequency showed an increasing trend. Between 1949 and 2000, at least 50 medium or strong earthquakes struck each year, which is evidently higher than that between 1897 and 1949. Especially since 1999, the frequency of earthquakes clearly has been increasing. If the sixth phase of earthquake active period follows the same pattern as the previous phases, the Chinese mainland area is in the middle of a period of concentrated earthquake occurrences.

Since 1990, the annual fluctuation of death tolls from earthquakes in China has been great and serious disasters and heavy losses occurred frequently. Except 1996, 2003, 2008, 2010, and 2013 during which serious earthquakes happened, annual death tolls from earthquakes were less than one hundred, which indicates that with the socioeconomic development earthquake disaster prevention level has been improving and people’s awareness to earthquake disaster has also increased. As a

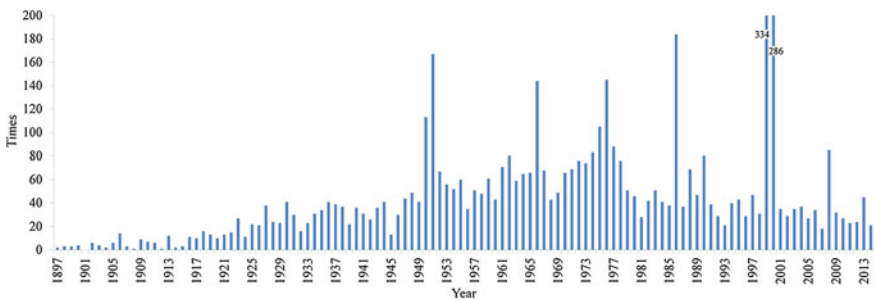


Fig. 3 Annual change of the number of medium and strong earthquakes in China, 1897–2014 (Data source CENC 2015; DEDP 1995, 1999)

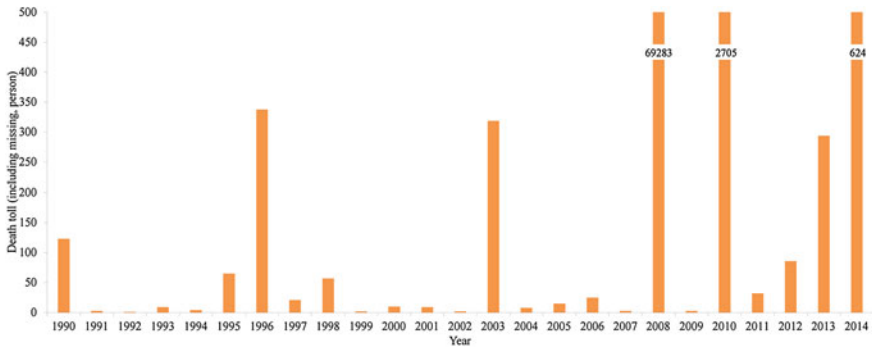


Fig. 4 Deaths and missing people from earthquakes in China, 1990–2013 (Data source Lou 1996; MCA 2015)

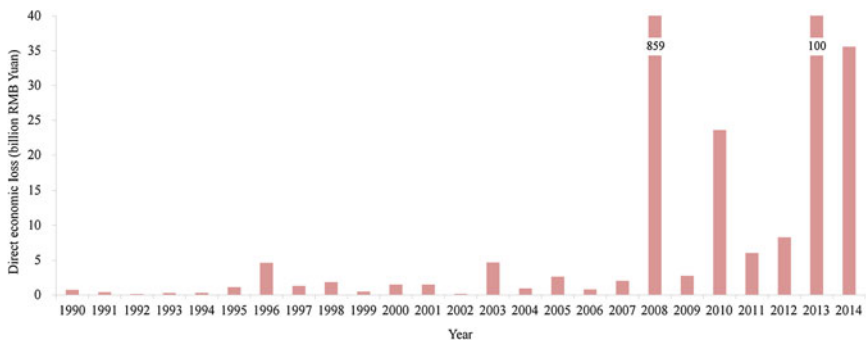


Fig. 5 Direct economic losses caused by earthquakes in China, 1999–2014 (Data source Lou 1996; MCA 2015)

result, the ability to protect life in earthquakes has clearly improved (Fig. 4). However, because of the continuous and rapid growth of the economy, in the recent 20 years, direct economic losses caused by earthquakes has evidently shown an increasing trend (Fig. 5).

2 Formation and Assessment of Earthquake Disasters

Based on existing research and literature, this section presents the fragility curves of different types of buildings in China and the spatial distribution of earthquake risks of provincial- and county-level administrative units based on a comprehensive consideration of earthquake hazard, exposure, as well as fragility, among other factors.

2.1 Earthquake Disasters and Their Assessment

China is one of the countries with the most serious earthquake disasters in the world. The Ms8.0 Wenchuan Earthquake and Ms7.1 Yushu Earthquake have successively occurred in China in recent years, with heavy casualties and huge economic losses.

Earthquake disaster analyses in China have resulted in various zoning maps of earthquake hazard. There are four versions of national earthquake zoning map of China.

In 1957, Lee and colleagues prepared the first generation earthquake zoning map of China, providing the intensity distribution of maximum earthquakes in the country (Lee 1957).

In 1977, the second version of earthquake zoning map of China was published, which was prepared using the medium-term and long-term earthquake forecasting method, providing maximum earthquake intensity that may be encountered within the future 100 years (Deng et al. 1980).

In 1990, the third version of earthquake zoning map of China was published, which was prepared using probability analysis method, providing the intensity value for the exceedance probability of 10 % in 50 years (Compiling Committee of Seismic Zoning Map in China 1992).

All the above three versions of the seismic zoning map adopt earthquake intensities as the mapping parameter.

The Seismic Ground Motion Parameters Zonation Map of China was published in 2001 (GB 18306–2001) (AQSIQ–SAC 2001), with the scale of 1:4,000,000. The single intensity parameter is hard to serve as a design response spectrum when seismic design enters the stage of considering response spectrum; therefore in China earthquake ground motion parameters (including the peak ground acceleration PGA and site characteristic period T_g) are also used in seismic zoning.

In the Seismic Peak Ground Acceleration Zoning Map of China (AQSIQ–SAC 2001), earthquake hazard is represented by the seismic peak ground acceleration value for exceedance probability of 10 % in 50 years, which is divided into seven subregions: region 7 ($PGA \geq 0.40$ g), region 6 ($PGA = 0.30$ g), region 5 ($PGA = 0.20$ g), region 4 ($PGA = 0.15$ g), region 3 ($PGA = 0.10$ g), region 2 ($PGA = 0.05$ g), and region 1 ($PGA < 0.05$ g).

According to the statistical analysis for the occurrence probability of earthquakes in the north, northwest, and southwest areas of China, the seismic intensity for exceedance probability of 63 % in 50 years is the normal intensity—the Code for Seismic Design of Buildings takes this as the first level of intensity; the intensity for exceedance probability of 10 % in 50 years is the basic seismic intensity (also the design basic seismic peak acceleration specified by the Seismic Ground Motion Parameters Zoning Map of China)—the Code takes this as the second level of intensity; the intensity for exceedance probability of 2–3 % in 50 years is the rare intensity—the Code takes this as the third level of intensity. Exceedance probability in 50 years, return period, and peak acceleration of different levels of seismic ground motions are shown in Table 3.

Table 3 Return period (year), peak acceleration (g, acceleration of gravity), and probability of three-level seismic ground motions

Level of seismic ground motion	Exceedance probability in 50 years (%)	Return period (year)	Peak acceleration					
			6°	7°	8°	9°		
Second level of intensity (seismic fortification intensity)	10	475						
First level (frequently occurred seism peak acceleration)	63	51	0.018	0.036	0.054	0.086	0.108	0.144
Second level (design basic peak acceleration)	10	475	0.050	0.100	0.150	0.200	0.300	0.400
Third level (rare seism peak acceleration)	2–3	1,642–2,475	0.120	0.225	0.324	0.405	0.540	0.630

Source Fang et al. (2011, p. 193)

The Seismic Ground Motion Characteristic Period Zoning Map of China (AQSIQ–SAC 2001) shows the three regions of seismic ground motion characteristic period under general site conditions (class II site): region 1 (0.35 s), region 2 (0.40 s), and region 3 (0.45 s).

In generating the Seismic Ground Motion Parameters Zoning Map of China, three assumptions were made: (1) seismic peak ground acceleration is not affected by local site conditions; (2) the influence of site conditions on design ground motion is mainly reflected in the characteristic period; and (3) the zoning of seismic ground motion characteristic period only specifies characteristic periods under general site conditions (class II site). In practice, however, we still need to adjust the characteristic periods according to site classifications based on geological survey data (Table 4).

At present, seismic hazard assessment is mainly based on the levels of historical seismic activity and tectonic conditions of activity, among others. The results of seismic hazard assessment may differ significantly from the actual occurrence of future large earthquakes. The Tangshan Earthquake, Wenchuan Earthquake, and Yushu Earthquake all occurred in areas of low-level seismic activity according to the knowledge prior to the events, and this indicates that the evaluation models, analysis methods, and results of seismic hazard at present are still far from adequate.

Table 4 Values of characteristic period

Subregions of characteristic period	Site classifications				
	I ₀	I ₁	II	III	IV
Region 1 (0.35 s)	0.20	0.25	0.35	0.45	0.65
Region 2 (0.40 s)	0.25	0.30	0.40	0.55	0.75
Region 3 (0.45 s)	0.30	0.35	0.45	0.65	0.90

Source AQSIQ–SAC (2001)

In order to meet the requirements of social and economic development for earthquake prevention and disaster reduction, it is necessary to pay closer attention to research on seismic fragility of potential hazard-affected units and seismic hazard levels, and take reducing seismic disaster risk and developing long-term management approaches of seismic disaster risks as an important part of disaster prevention and mitigation.

2.2 Fragility of Buildings and Assessment

Destruction status and loss ratio of buildings: According to the *Post-Earthquake Field Works—Part 4: Assessment of Direct Loss* (GB/T 18208.4–2005) (AQSIQ–SAC 2005), the extent of damage of buildings can be divided into five types: basically intact, slightly damaged, moderately damaged, severely damaged, and completely destroyed. The loss ratios of buildings of different damage status are shown in Table 5.

Classification and fragility of buildings: Buildings can be classified according to the type of structure, time of construction, number of storeys, height, level of earthquake fortification, geographical location, and so on.

Construction time of buildings in China can be divided into five periods: before 1978, 1978–1989, 1990–2000, 2000–2010, and after 2011.

Geographical location mainly determines the outer wall thickness of masonry buildings under different climatic conditions. In Heilongjiang, Xinjiang, and other northern China provinces, for example, the outer wall thickness of masonry structures is usually 49 cm. In the North China area, this is usually 37 cm; and in southern China provinces, it is usually 24 cm. For brick masonry buildings, the influence of climate on outer wall thickness shall be taken into consideration.

Based on the consideration for seismic performance combined with the classification of buildings in the China Statistical Yearbooks, the type of buildings can be divided into: Type A (mainly reinforced concrete structure); Type B (mainly brick-concrete structure); Type C (mainly brick-timber structure); and Type D (mainly raw-soil structure and dry-laid stone houses). For Type A and Type B buildings, their seismic performance in various seismic fortification subregions

Table 5 Loss ratio of buildings of different damage status

Type of building	Destruction level				
	Basically intact	Slightly damaged	Moderately damaged	Severely damaged	Completely destroyed
Reinforced concrete, masonry buildings	0–5	6–15	16–45	46–80	81–100
Industrial factory buildings	0–4	5–16	17–45	46–80	81–100
One-storey houses in cities and towns, farm buildings	0–5	6–15	16–40	41–70	71–100

Source AQSIQ–SAC (2005)

(seven in total) with different design basic seismic ground motion is different, so Type A and Type B buildings can be classified into seven subclasses, as shown in Table 6. The purpose of this simple classification is to extract statistical data on the spatial distribution of buildings in the China Statistical Yearbooks. More detailed data on the spatial distribution of building types are largely unavailable at the national level.

For different types of buildings, the peak acceleration of seismic ground motion S_a is used as a random variable to describe the fragility characteristics. Assuming that the fragility curve of buildings is the normal distribution function for logarithm ($\ln(S_a)$) of S_a (peak acceleration of seismic ground motion), each destruction status d_s has a corresponding fragility curve.

Assuming that the mean value of S_a under a certain destruction status is $E(S_a)$, the variance is $\text{Var}(S_a)$, then the mean value (μ) and variance (σ^2) for the logarithm of S_a are respectively

$$\mu = \ln(E(S_a)) - \frac{1}{2} \left(1 + \frac{\text{Var}(S_a)}{[E(S_a)]^2} \right). \tag{1}$$

Table 6 Classification of building types

Seismic performance categories of buildings	Main types of building structures	Subregions of design for earthquake	Design basic seismic acceleration	Classification of building types
Type A	Reinforced concrete structure and steel structure	Region 1	None	Region 1 of Type A
		Region 2	0.05 g	Region 2 of Type A
		Region 3	0.10 g	Region 3 of Type A
		Region 4	0.15 g	Region 4 of Type A
		Region 5	0.20 g	Region 5 of Type A
		Region 6	0.30 g	Region 6 of Type A
		Region 7	0.40 g	Region 7 of Type A
Type B	Brick-concrete structure	Region 1	None	Region 1 of Type B
		Region 2	0.05 g	Region 2 of Type B
		Region 3	0.10 g	Region 3 of Type B
		Region 4	0.15 g	Region 4 of Type B
		Region 5	0.20 g	Region 5 of Type B
		Region 6	0.30 g	Region 6 of Type B
		Region 7	0.40 g	Region 7 of Type B
Type C	Brick-timber structure	-	-	Type C
	Masonry structure			
Type D	Raw-soil structure and dry-laid stone houses	-	-	Type D

Source Fang et al. (2011, p. 194)

$$\sigma^2 = \ln \left(1 + \frac{\text{Var}(S_a)}{[E(S_a)]^2} \right) \quad (2)$$

The expression of fragility curve under a certain destruction status d_s is

$$P[d_s|S_a] = \Phi \left[\frac{\ln(S_a) - \mu}{\sigma} \right] \quad (3)$$

where, Φ is the curve for cumulative probability of standard normal distribution.

The points on the fragility curve under a certain destruction status refer to the probability of buildings reaching or exceedance a certain destruction status under the action of a certain S_a . The fragility curve under a certain destruction status is determined by the mean value of spectrum displacement $E(S_a)$ and variance $\text{Var}(S_a)$. The variance of fragility curve shows the variation range—the greater the variance, the gentler the fragility curve; and the smaller the variance, the steeper the fragility curve.

According to the survey for historical earthquakes in china and the results of existing research (Yin et al. 2003; Yin and Yang 2004), this chapter provides the fragility curves for different types of buildings, as shown in Fig. 6.

Unit construction cost for different building types: The unit construction cost of buildings can be determined according to the building types listed in Table 7.

2.3 Earthquake Disaster and Post-disaster Rapid Loss Assessment

Earthquake disaster is the result of seismic hazard, vulnerability of earthquake disaster-affected bodies, and their exposure. Due to the limited availability of data and limitations of modeling, in post-disaster rapid loss assessment we only consider the damage state and number of damaged buildings, direct economic losses from building damages, and the number of affected people. Using the earthquake magnitude and epicenter parameters, the assessment is composed of three steps: (1) determine the spatial distribution of population and buildings by collecting population and socioeconomic data and combining them with land use data; (2) evaluate the degree of exposure of disaster-affected bodies, including population and buildings; (3) determine earthquake-related losses based on the assessment results of the exposure of disaster-affected bodies and building vulnerability.

Based on the experiences in post-earthquake loss assessment of the Wenchuan Earthquake (Xu et al. 2008) and the Yushu Earthquake (Xu et al. 2011), Fig. 7 presents an improved framework of earthquake loss assessment using empirical models:

First, retrieve data for the earthquake parameters (earthquake magnitude and epicenter location) published by the China Earthquake Administration. Select either

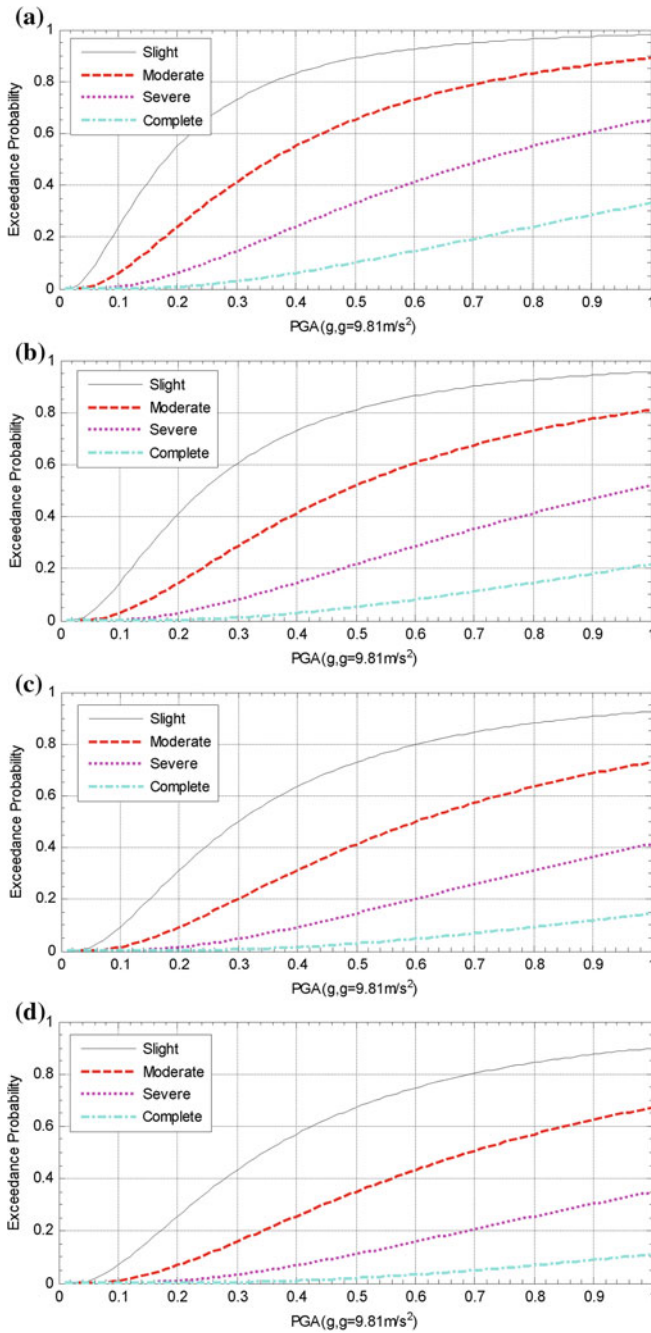


Fig. 6 Fragility curves for buildings by different damage status. **a** Type A in Region 1. **b** Type A in Region 2. **c** Type A in Region 3. **d** Type A in Region 4. **e** Type A in Region 5. **f** Type A in Region 6. **g** Type A in Region 7. **h** Type B in Region 1. **i** Type B in Region 2. **j** Type B in Region 3. **k** Type B in Region 4. **l** Type B in Region 5. **m** Type B in Region 6. **n** Type B in Region 7. **o** Type C. **p** Type D (Source Fang et al. 2011, p. 194–198)

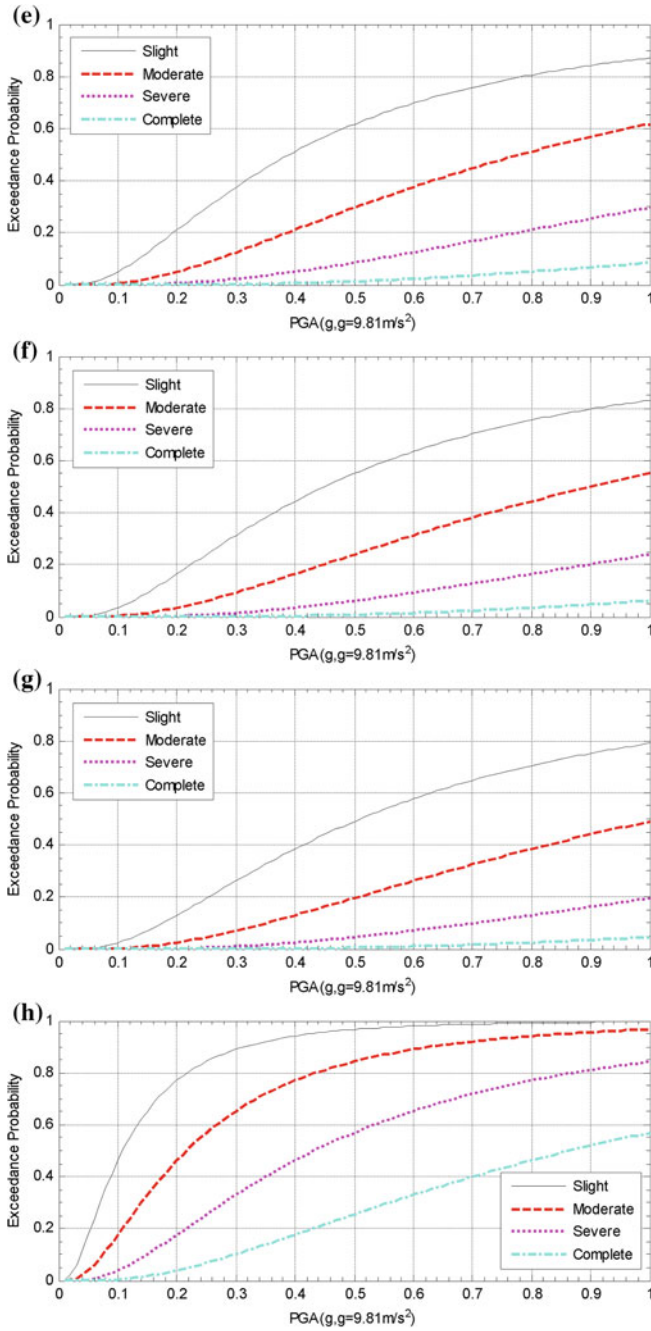


Fig. 6 (continued)

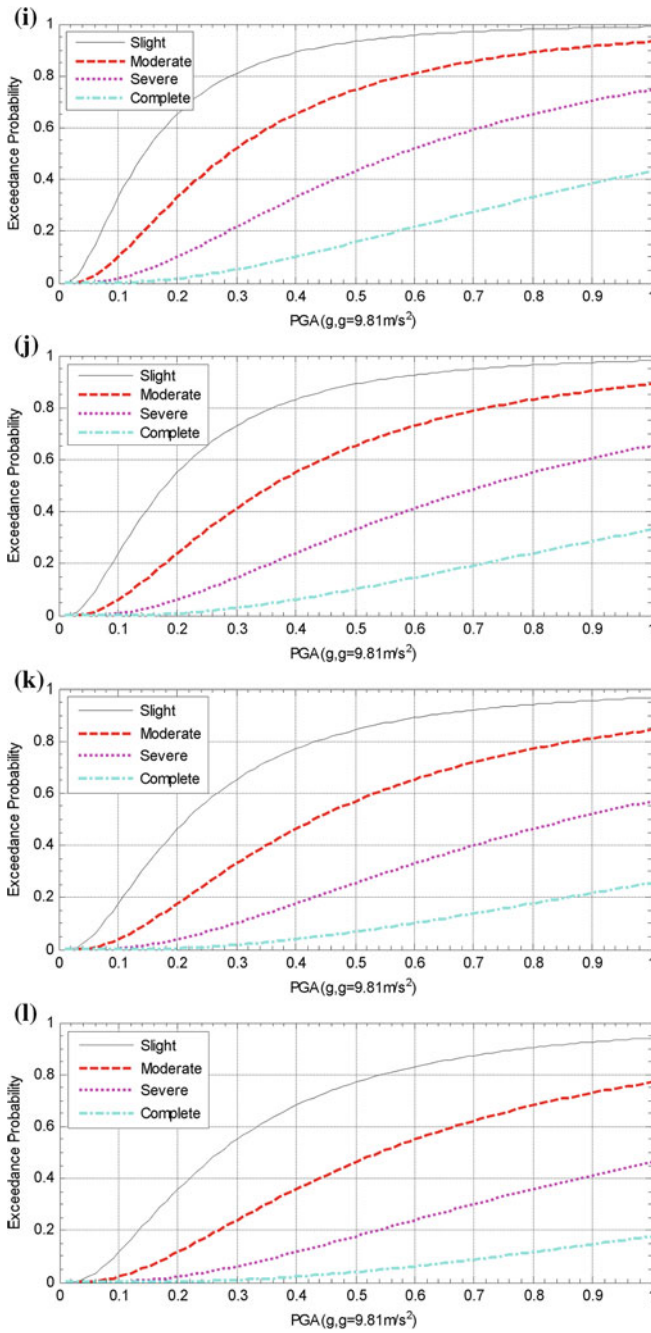


Fig. 6 (continued)

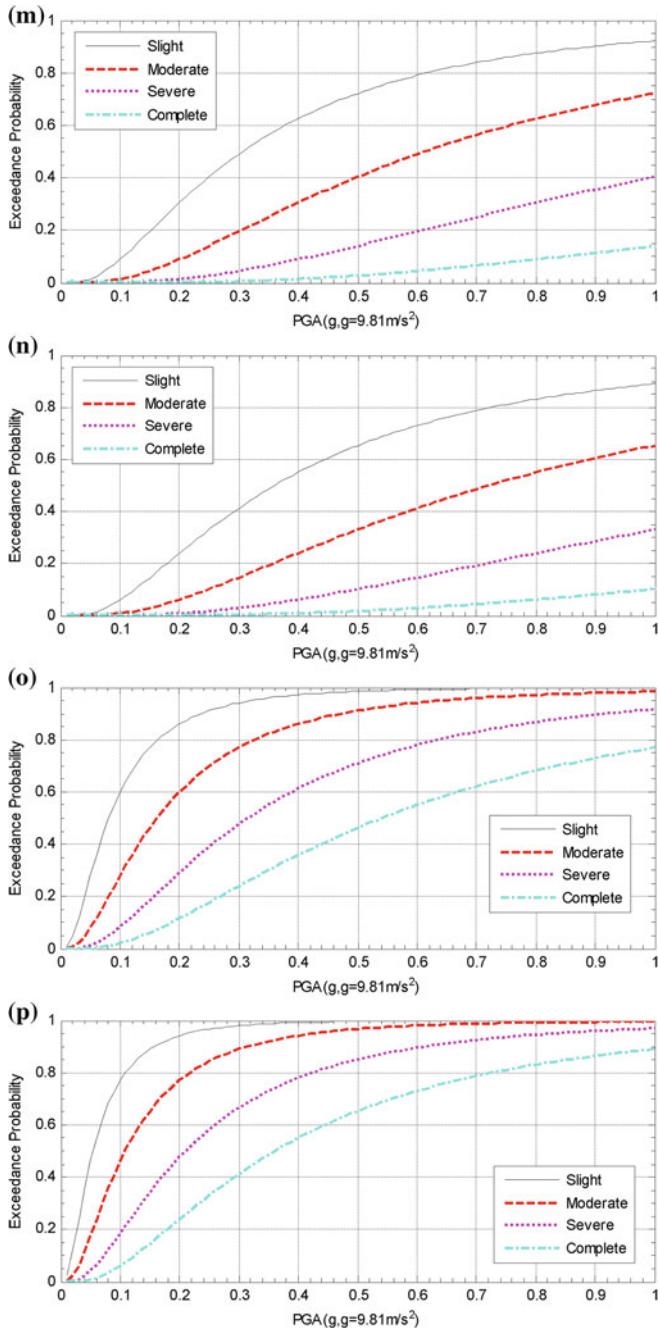


Fig. 6 (continued)

Table 7 Unit construction costs for different building types

Types of houses	Type A	Type B	Type C	Type D
Unit cost (RMB Yuan/m ²)	2,200	1,600	1,000	600

Source Fang et al. (2011)

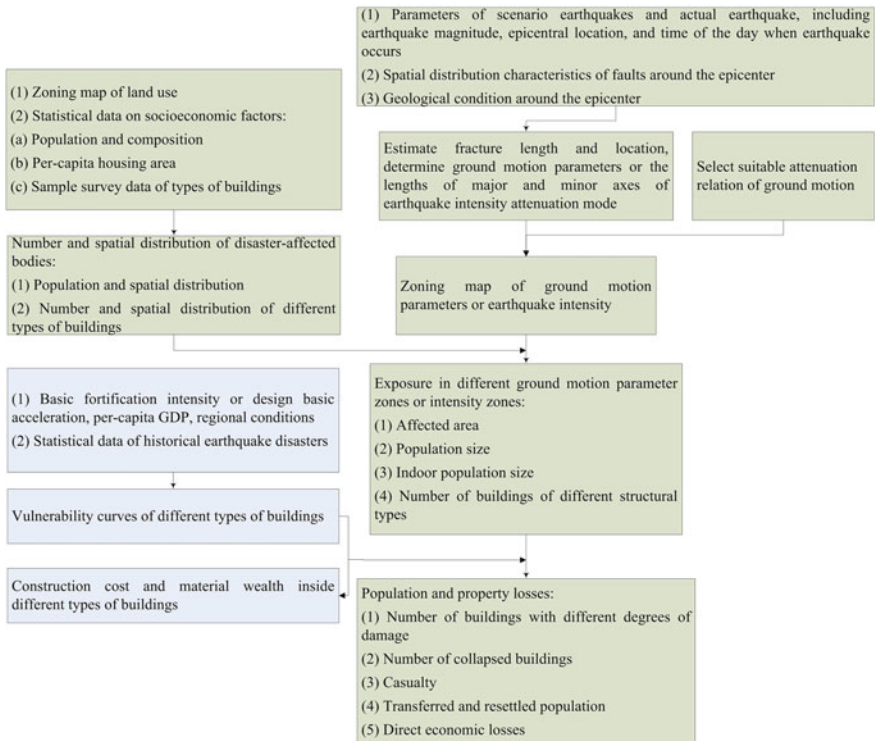


Fig. 7 Earthquake disaster and the framework of post-disaster rapid loss assessment based on empirical models

a point source model or a line source model according to earthquake magnitude, fault spatial distribution characteristics, and seismic geological condition around the epicenter.

In the current practice, spatial distribution models of isoseismic line are the following types: (1) elliptical model based on point source; and (2) equal fault throw model based on fault fracture line. The choice of isoseismic line model shall be made in accordance with the earthquake magnitude, depth of hypocenter, thickness of cover layer in epicentral area, and active structure. In the case of large magnitude earthquake (greater than 6.5), shallow depth of hypocenter, small cover thickness, and obvious active structure in epicentral area, equal fault throw model

based on fault fracture line should be used to compile isoseismic line plan; otherwise elliptical attenuation model based on point source should be adopted.

Second, select suitable attenuation relation model of seismic intensity, compile experiential peak acceleration or intensity isoseismic line chart in accordance with the model of earthquake source.

Third, according to the experiential ground motion parameter or intensity zonation plan and regional land use zonation plan and socioeconomic data (such as population size and composition, per-capita housing area, and sampling statistical data of structure type of buildings), determine the exposure data of different ground motion parameter zones or intensity zones, such as disaster area, population size, indoor population size and percentage, and the number of buildings with different structure types.

Fourth, based on historical seismic damage statistical data of the disaster area or seismic damage statistical data of similar areas and regional socioeconomic development level, earthquake fortification standard of buildings, construction date, and other regional characteristics, vulnerability curves of different types of buildings in the disaster area are calculated.

Fifth, calculate the damage degree of the population and property in different ground motion parameter zones or intensity zones according to the indoor population of different types of housing in the area, unit construction cost of buildings, material wealth inside the buildings, vulnerability of disaster-affected bodies using corresponding damage assessment models. Evaluate earthquake losses (such as the number of buildings with different damage degrees, the number of houses collapsed after the earthquake, the number of initial casualties, transferred and resettled population, and direct economic losses).

This loss assessment framework has been applied post-disaster in the rapid assessment of many earthquake disasters and has been constantly improved.

2.4 Earthquake Disaster Risk Assessment and Mapping

As a product of earthquake hazard, vulnerability of disaster-affected bodies, and their spatial distribution (exposure), earthquake disaster risk is the earthquake damage that an area may be subjected to in a certain period of time in the future. Earthquake disaster risk assessment evaluates the potential earthquake damage of disaster-affected bodies by taking into account potential earthquake hazard, vulnerability of disaster-affected bodies, and the potential degree of exposure of these units in the area.

Earthquake hazard analysis examines the probability of occurrence of earthquakes above a given intensity in a region within a certain period of time in the future. Vulnerability of disaster-affected bodies refers to the probability or possibility of certain degree of damage under the impact of certain earthquake intensity. Degree of exposure refers to the number of disaster-affected bodies or percentage that may be affected by the threat under certain earthquake intensity.

Here, disaster-affected body is a relatively broad concept, including industrial and civil constructions, infrastructure (such as roads and bridges, municipal pipelines, communication networks, embankment dams), population, and so on. Different types of disaster-affected bodies require different methods for vulnerability analysis.

Based on the definition of earthquake disaster risk, its result of analysis is composed of the following types:

Absolute risk: earthquake damage that may be suffered in an area within a certain period of time, including economic losses and casualties. The assessment result shows the total of potential earthquake losses for an area.

Relative risk: earthquake damage that may be suffered per unit area (or per capita or unit of assets) in an area within a certain period of time, including economic losses and casualties. The assessment result shows the relative earthquake risk per unit area of an area.

Single exposure unit risk: earthquake damage that a single disaster-affected body (building or people) may encounter in an area within a certain period of time. The assessment result can provide data support for the determination of premium rate of disaster-affected bodies in an area.

Figure 8 outlines the steps of earthquake disaster risk assessment:

First, determine the number and spatial distribution of each type of disaster-affected bodies. Size of the population and the number of different types of buildings can be determined using county-level administrative divisions, land use divisions, population and composition, proportion of different types of buildings, per-capita housing area, and so on.

Second, determine the ground motion parameter (peak acceleration or seismic intensity) under different return periods. Seismic Peak Ground Acceleration Zoning

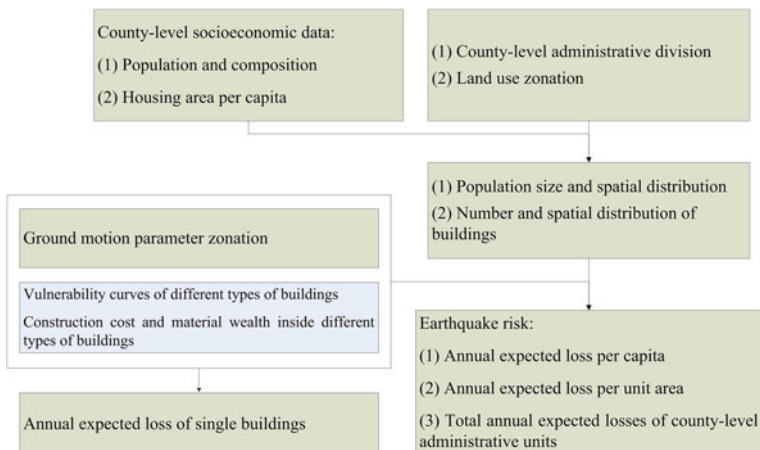


Fig. 8 Framework of earthquake disaster risk assessment (Source Fang et al. 2011, p. 199)

Map of China (AQSIQ–SAC 2001) indicates seismic peak ground acceleration with exceedance probability of 10 % in 50 years (the return period of these medium earthquakes is 475 years); the peak acceleration of strong and rare earthquakes (exceedance probability 2–3 % in 50 years, return period 1,642–2,475 years) and small earthquakes (exceedance probability 63 % in 50 years, return period 51 years) can be determined according to Table 3. Describe earthquake hazard using the three levels seismic peak ground acceleration.

Third, determine the building type and its vulnerability curve (see vulnerability assessment in this section for details).

Fourth, using building vulnerability curves and the three levels of ground motion peak acceleration to determine the annual mean expected earthquake loss rate of certain type of building; then determine the value of the earthquake disaster risk in the area according to the construction cost of different types of buildings and the number and spatial distribution of the disaster-affected bodies.

If annual expected earthquake disaster risk is measured by annual economic losses from building damages caused by earthquakes that may occur within the county administrative units, then the calculation formula is as follows:

$$R = \sum_p \left(C_p \times \sum_{j=I-1}^{I+1} \frac{L_{pj}}{Y_j} \right) \quad (4)$$

where, R is the annual economic losses from building damages that may occur within a county (RMB Yuan/year); p is the type of buildings. Seismic performance of buildings is divided into Type A (mainly of reinforced concrete structures), Type B (mainly brick-concrete structures), Type C (mainly masonry structures), and Type D (mainly raw-soil structures); C_p is the total construction cost of p type building; I is design basic earthquake intensity, $I - 1$, I , $I + 1$ are the corresponding intensity grade of a small earthquake, medium earthquake, and strong earthquake, respectively; Y_j is the return period of intensity grade j , which can be calculated according to the exceedance probability of strong earthquake ($I + 1$), medium earthquake (I), and small earthquake ($I - 1$); L_{pj} refers to the loss rate of p type building under intensity level j , and its calculation formula is:

$$L_{pj} = \sum_{d_s=1}^5 DM_j(d_s) \times LR(d_s) \quad (j = I - 1, I, I + 1) \quad (5)$$

where, d_s is damage state ($d_s = 1, 2, 3, 4, 5$ refer to intact, slightly damaged, moderately damaged, severely damaged, and completely destroyed, respectively); $LR(d_s)$ is loss ratio when the damage state is d_s ; DM is earthquake damage matrix, $DM_j(d_s)$ is the percentage of d_s under j -level intensity.

Table 8 Mean loss ratio of buildings with different degrees of damage

Damage degree of building	Basically intact	Slightly damaged	Moderately damaged	Severely damaged	Completely destroyed
Mean of loss ratio	0.00	0.15	0.40	0.70	1.00

Data source Fang et al. (2011, p. 199)

The unit construction cost of buildings can be decided based on the building types in Table 7. Table 8 shows the mean loss ratio of buildings with different degrees of damage.

2.5 Earthquake Disaster Risk Mapping

Earthquake disaster risk database: risk database for earthquake damage in China is made up of three parts of data: (1) data for earthquake disaster-inducing factor; (2) data for disaster-affected bodies; (3) data for earthquake disaster risk level.

Database for disaster-inducing factor: data for earthquake disaster-inducing factor in China is composed of data for spatial distribution of seismic peak ground acceleration, historical earthquakes, and spatial distribution of active structures. These data are mainly published by the China Earthquake Administration.

Database for disaster-affected bodies in China: this database mainly includes data on land use, population and density, and the number and distribution of different building types. Using the data from the 1 % National Population Sampling Survey of 2005 and considering other local conditions, Type A, B, C, D buildings of each provincial administrative unit are estimated. According to the 2000 National Population Census data, determine the population (including urban population and rural population) and corresponding per-capita construction area of the county units. Based on land use types, assign the population and buildings to the corresponding plots.

Earthquake disaster risk database: this database includes land parcel-level earthquake disaster risk database and county-level earthquake disaster risk database. Where, land parcel-level earthquake disaster risk database is an integrated database including land use, earthquake hazard, and disaster-affected bodies data, loss data of the plot under the impact of design basic earthquake peak acceleration, and earthquake disaster risk data.

Compilation of the county-level administrative unit earthquake disaster risk map of China: Using land use and county-level socioeconomic data, earthquake hazard analysis results, and building vulnerability curves, prepare the land parcel-level earthquake disaster risk map for each province in China (1:10,000). Aggregate the land parcel-level earthquake disaster risk data into county-level data, then compile the county-level administrative unit earthquake disaster risk map of in China (Figs. 9, 10, and 11).

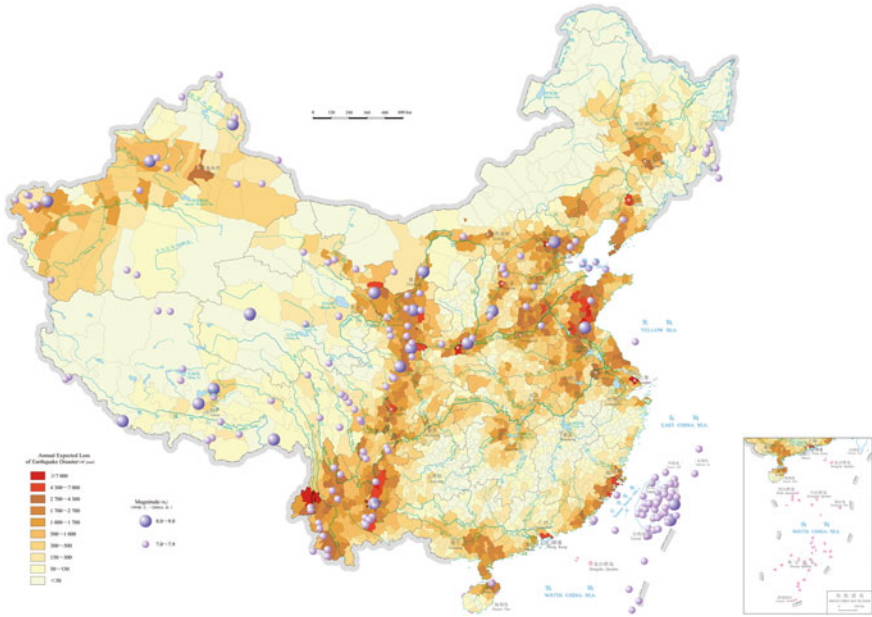


Fig. 9 County-level earthquake disaster risk map of China—Total annual expected losses (Source Shi 2011, p. 28–29)



Fig. 10 County-level earthquake disaster risk map of China—Annual expected losses per unit area (Source Shi 2011, p. 30–31)

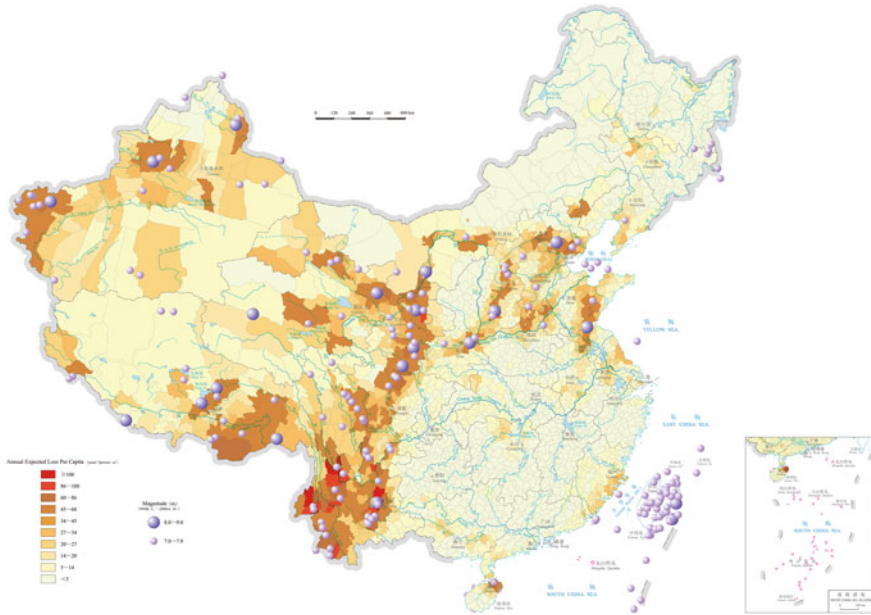


Fig. 11 County-level earthquake disaster risk map of China—annual expected losses per capita (Source Shi 2011, p. 32–33)

3 Assessment Result of Earthquake Disaster Risk of China

Total annual expected economic losses: this is calculated in order to indicate the total annual earthquake disaster risk of an area in the future. In addition to the earthquake hazard level of the area, total annual expected economic losses are also closely related to the size of the population, the total number of buildings, and earthquake resistance capacity of the area. In this chapter, county-level administrative units are taken as the spatial unit of analysis of the total annual expected losses. Figure 9 shows that the counties with higher total annual expected economic losses are mainly distributed on the east coast and in Gansu, Sichuan, and Yunnan Provinces.

Annual expected economic loss per unit area: under the condition that earthquake hazard is at the same level and the total earthquake resistance capacity of buildings is similar for different regions, if the population and the number of buildings in one area is higher, the total earthquake disaster risk of the area will be higher too. In order to better compare the relative degree of earthquake disaster risks in different areas, we normalize the annual expected economic losses into per unit area by administrative district. The annual expected economic loss per unit area

is closely related to the density of disaster-affected bodies in each unit of the land area. Figure 10 shows that the counties with higher annual expected economic loss per unit land area are mainly located on the North China plain, a number of east coastal provinces, and Gansu, Sichuan, and Yunnan Provinces.

Annual expected economic loss per capita: The per-capita annual expected economic loss indicator shows the average annual economic loss per capita caused by earthquakes in an administrative district in the future. This is to facilitate the comparison with the economic losses and disaster risks caused by other disasters. Per-capita annual expected economic loss is closely related to the earthquake hazard level at the place. The county-level administrative units with higher per-capita annual expected economic loss are mainly distributed in Yunnan, Sichuan, Shandong, and Ningxia (Fig. 11). Improving the seismic fortification level is an effective way to reduce the per-capita annual expected economic loss.

4 Responses to the 2008 Wenchuan Earthquake

4.1 Disaster Situation

At 14:28 on 12 May 2008, an Ms8.0 earthquake occurred in Wenchuan County, Sichuan Province. The epicenter was located at Yingxiu Town, Wenchuan County (31.0° N, 103.4° E), with focus depth of 14 km and epicentral intensity of XI degree. The aftershocks occurred more than 30 thousand times, involving 10 provinces and municipality including Sichuan, Gansu, Shaanxi, Chongqing, 417 counties (cities or districts), 4,667 towns, and 48,810 villages. The total disaster area was about 0.5 million square kilometers, wherein severely and very severely hit areas were 0.13 million square kilometers (Table 9), resulting in 69,227 deaths, 17,923 people missing, and 15.1 million people to be urgently transferred and resettled (Earthquake Relief Experts Group of National Committee for Disaster Reduction and Ministry of Science and Technology 2008). A large number of houses collapsed or were damaged, large area of infrastructures was damaged, agriculture and industrial production encountered great losses, ecological environment was severely damaged, and direct economic losses were over RMB 845.1 billion Yuan. Severe secondary disasters such as rock collapse, landslide, mud-rock flow, and formation of barrier lake were also prevalent. The affected area in Sichuan Province alone was 0.27 million km². Disaster areas of Sichuan mainly involved 20 prefectures and cities, including A'ba, Mianyang, Deyang, Chengdu, and Guangyuan, 140 counties (cities or districts), 3,765 villages (towns). The population of the disaster area was 70.6715 million, with 20.4164 million households, and the total affected population was 46.24 million.

Table 9 Areas severely affected by the Wenchuan Earthquake

Impact	Province	County (City or District)
Very severely hit county (city) (10)	Sichuan (10)	Wenchuan County, Beichuan County, Mianzhu City, Shifang City, Qingchuan County, Mao County, An County, Dujiangyan City, Pingwu County, and Pengzhou City
Severely hit county (city or district) (36)	Sichuan (26)	Li County, Jiangyou City, Lizhou District, Chaotian District, Wangcang County, Zitong County, Youxian District, Jingyang District, Xiaojin County, Fucheng District, Luojiang County, Heishui County, Chongzhou City, Jiange County, Santai County, Yanzhong City, Yanting County, Songfan County, Cangxi County, Lushan County, Zhongjiang County, Yuanba District, Dayi County, Baoxing County, Nanjiang County, and Guanghan City
	Gansu (7)	Wen County, Wudu District, Kang County, Cheng County, Hui County, Xihe County, and Liangdang County
	Shaanxi (3)	Ningqiang County, Lueyang County, and Mian County

Data source Earthquake Relief Experts Group of National Committee for Disaster Reduction and Ministry of Science and Technology (2008)

4.2 Emergency Rescue Process

On the day of the Wenchuan Earthquake, the then Premier of the State Council, Wen Jiabao, immediately flew to the disaster area, set up the Earthquake Relief Headquarters and started the national emergency response I. On 17 May 2008, the President and General Secretary of the Central Committee of the Communist Party of China, Hu Jintao, urged at the disaster area that local governments, militaries, and all rescue forces should unify the leadership and command; in particular to strengthen coordination between military and civilian forces and formed a mechanism of vigorous collaboration and close cooperation, to carry out relief work orderly.

On 19 May 2008, with the overall progress of rescue work, the State Council adjusted and improved the composition and structure of the Earthquake Relief Headquarters of the State Council (Table 10). Under the unified command of the Earthquake Relief Headquarters, an earthquake relief campaign with the fastest speed, most broad mobilization, and greatest input in the Chinese history was launched, maximizing life-saving of disaster victims and minimizing disaster losses. A total of 84,017 people were rescued from ruins and 1.49 million people trapped in collapsed buildings were saved. More than 4.3 million sick and injured people received timely treatment and over 10 thousand patients were quickly transferred to 375 hospitals of over 20 provinces and cities. A total of 0.146 million People's Liberation Army soldiers and armed police officers as well as 75 thousand

Table 10 Composition and structure of the Earthquake Relief Headquarters of the State Council

Commander in Chief		Wen Jiabao
Vice Commander in Chief		Li Keqiang and Hui Liangyu
Emergency rescue and disaster relief team	Leading unit	General Staff Headquarters of the People's Liberation Army
	Member unit	Ministry of Public Security, Safety Supervision Bureau, China Earthquake Administration, People's Armed Police Force, and Chengdu Military Region
Public affairs team	Leading unit	Ministry of Civil Affairs
	Member unit	Ministry of Foreign Affairs, National Development and Reform Commission, Ministry of Finance, Ministry of Housing and Urban-Rural Development, Ministry of Commerce, Ministry of Agriculture, and Red Cross
Earthquake monitoring team	Leading unit	China Earthquake Administration
	Member unit	Ministry of Science and Technology, Ministry of Land and Resources, Ministry of Environmental Protection, China Meteorological Administration, and Administration for Science, Technology and Industry for National Defense
Hygiene and disease control team	Leading unit	Ministry of Health
	Member unit	National Development and Reform Commission, Ministry of Agriculture, General Administration of Quality Supervision, Inspection and Quarantine, Food and Drug Administration, General Logistics Department of the People's Liberation Army, and People's Armed Police Force
Communication team	Leading unit	Publicity Department of the Central Committee of the Communist Party of China
	Member unit	Ministry of Foreign Affairs, State Administration of Radio, Film and Television, Office of Taiwan Affairs, News Office of the State Council, Office of Hong Kong and Macao Affairs, and China Meteorological Administration
Production recovery team	Leading unit	Ministry of Industry and Information Technology
	Member unit	National Development and Reform Commission, Ministry of Finance, Ministry of Commerce, Ministry of Human Resources and Social Security, Ministry of Agriculture, State-owned Assets Supervision and Administration Commission, Safety Supervision Bureau, China Insurance Regulatory Commission, and Administration for Science, Technology and Industry for National Defense
Infrastructure recovery and post-disaster reconstruction team	Leading unit	National Development and Reform Commission
	Member unit	Ministry of Industry and Information Technology, Ministry of Civil Affairs, Ministry of Finance, Ministry of Housing and Urban-Rural Development, Ministry of Transport, Ministry of Railways, Ministry of Agriculture, State-owned Assets Supervision and Administration Commission, State

(continued)

Table 10 (continued)

Commander in Chief		Wen Jiabao
Vice Commander in Chief		Li Keqiang and Hui Liangyu
		Administration of Radio, Film and Television, Safety Supervision Bureau, China Banking Regulatory Commission, State Electricity Regulatory Commission, Post Bureau, Civil Aviation Administration, and State Grid Corporation of China
Water conservancy team	Leading unit	Ministry of Water Resources
	Member unit	National Development and Reform Commission, Ministry of Finance, Ministry of Land and Resources, Ministry of Environmental Protection, Ministry of Housing and Urban-Rural Development, Ministry of Health, Ministry of Agriculture, China Earthquake Administration, China Meteorological Administration, State Electricity Regulatory Commission, and Operations Department of the Headquarters of the General Staff of the People's Liberation Army
Social security team	Leading unit	Ministry of Public Security
	Member unit	Ministry of Education, Ministry of Justice, People's Bank of China, China Banking Regulatory Commission, China Securities Regulatory Commission, Tourism Administration, State Bureau for Letters and Calls, and People's Armed Police Force
Experts Committee	Leading unit	Ministry of Science and Technology, Ministry of Education, Ministry of Land and Resources, Ministry of Water Resources, China Earthquake Administration, Chinese Academy of Sciences, Chinese Academy of Engineering, Chinese Academy of Geological Sciences, and China Academy of Building Research

Data source The State Council (2008)

reserve militia-men and women participated in disaster rescue, and the whole nation was mobilized to vigorously support the disaster relief efforts.

As of 25 September 2008, the Ministry of Civil Affairs allocated and transported totally 1.5797 million makeshift tents, 4.8669 million blankets, 14.1013 million clothes, 4.146 million tons of fuel oil, and 8.858 million tons of coal; a total of 677,131 prefabricated houses (movable plank houses) was installed in the earthquake affected areas. Governments at all levels provided totally RMB 80.936 billion Yuan funds for earthquake emergency rescue and disaster relief. Financial input of the central government amounted to RMB 73.457 billion Yuan, wherein RMB 33.132 billion Yuan was used for emergency rescue and relief and RMB 40.325 billion Yuan was used for post-disaster reconstruction. Financial input of local governments was RMB 7.479 billion Yuan.

4.3 *Disaster Response Mechanism*

Information release mechanism: Only 12 min after the Wenchuan Earthquake, the short-message quick report system of the China Earthquake Administration sent out the three earthquake parameters (time, location, and earthquake magnitude) to the relevant staff and members of earthquake rescue teams. At the same time, formal documents about detailed earthquake occurrence information were also reported to the State Council. Upon receiving the Wenchuan Earthquake information, News Media such as the China Central Television (CCTV) rapidly released the news to the nation. Through the development over decades, earthquake information release mechanism of China made great progress and the general public receives earthquake information within a short time after earthquake occurrence. On the second day after the earthquake, the State Council made a decision that all Wenchuan Earthquake-related information should be released by the News Office of the State Council to guarantee consistency and accuracy of the information. Rumors were avoided with open and transparent information release mechanism, and this not only stabilized disaster victims' mood, but also gained support of world opinion, thus speeding up emergency rescue as well as restoration and reconstruction work.

Comprehensive coordination mechanism: In accordance with the deployment of the Central Committee of the Communist Party of China, the State Council and Central Military Commission, under the unified command and coordination of the State Council Earthquake Relief Headquarters, each ministry and commission of the State Council, local governments, military, armed police force, volunteers, and other forces coordinated with each other and carried out emergency rescue and reconstruction efficiently, orderly, and quickly through work division and cooperation. Soon after the earthquake, China mobilized the People's Liberation Army, armed police force, public security police, fire police, and special police (a total of more than 20 professional branches and 150,000 people), as well as 75 thousand reserve militias, and organized 5,257 professional rescue members, and 91.3 thousand medical treatment and public health members. The central financial department arranged relief funds timely, and China Earthquake Administration and other functional departments including civil administration, health, public security, water, education, and transportation launched emergency plans and emergency response actions and developed emergency rescue and other arrangements immediately. Across the country, the public showed great solidarity and made tremendous efforts to support the disaster areas, for example through organizing emergency rescue teams, supplying goods and materials, treating the injured, building temporary and transition shelters, among others. Provinces and cities outside the disaster areas developed counterpart assistance arrangements with the disaster areas; governments of Hong Kong and Macao Special Administrative Regions dispatched helicopters and service teams, rescue teams, infectious disease prevention teams, and medical treatment teams to Sichuan for earthquake relief works; they also raised funds to support the reconstruction of the disaster areas.

Nationwide-mobilization for disaster response mechanism: Through the Wenchuan Earthquake disaster response, China demonstrated its unprecedented national strength, concentrated its military capacity, and achieved great solidarity of the people. Wenchuan Earthquake disaster relief also fully reflected the advantages of the Chinese system in making concerted effort for major undertakings. The Wenchuan Earthquake disaster relief experience shows that the centralized leadership structure of the Chinese system is highly beneficial for reducing decision conflicts in crisis situation and is conducive to forming coordinated actions in national disaster relief; the centralized Chinese administrative system is highly beneficial for ensuring the government to mobilize and integrate various emergency rescue and disaster relief forces, gather resources, and maximally improve the effectiveness of the government's emergency response in crisis situation; the Chinese military system of central command is highly conducive to rapidly mobilize armed forces that act as the main force and the commando in responding to natural catastrophes. Therefore, in future major disaster situations, it is necessary to fully take advantage of the unique Chinese governance system, optimize the leadership system and working mechanism, and further develop the unique Chinese mechanisms for responding to major disasters (Shi and Liu 2009).

4.4 Restoration and Reconstruction

Formulation of restoration and reconstruction policies: Facing the huge losses of collapsed and damaged buildings, damaged infrastructure, and industrial and agricultural production and ecological environment destructions due to the catastrophe, under the leadership of the General Headquarters of Earthquake Rescue and Relief the government made a comprehensive and rapid assessment of the disaster situation, formulated reconstruction plans according to the law, and established a national counterpart assistance mechanism for rapid disaster recovery and reconstruction. On 4 June 2008, the State Council approved the *Regulation on Post-Wenchuan Earthquake Restoration and Reconstruction* (hereinafter referred to as the *Regulation*), which was issued and implemented on 8 June 2008. This is the first law on post-disaster restoration and reconstruction in the history of China in coping with large disasters. The issues of temporary sheltering and resettlement of displaced disaster victims, investigating and assessing disaster losses, developing restoration and reconstruction plans and implementation, fund-raising and policy support for recovery, supervision and management, and legal responsibilities were addressed in the *Regulation*, which laid a solid legal foundation for restoration and reconstruction (Table 11).

According to the *Regulation* and based on the rapid scientific assessment of the Wenchuan Earthquake disaster impact, the central government promulgated a series of plans and policies, including “Directive on Counterpart Assistance for Post-Wenchuan Earthquake Restoration and Reconstruction” on 11 June 2008, “Suggestions on Post-Wenchuan Earthquake Restoration and Reconstruction” on

Table 11 Post-Wenchuan Earthquake restoration and reconstruction policy documents

Time of issuance and implementation	Policy documents
8 June 2008	Regulation on Post-Wenchuan Earthquake Restoration and Reconstruction
11 June 2008	Directive on Counterpart Assistance for Post-Wenchuan Earthquake Restoration and Reconstruction, State Council
29 June 2008	Suggestions on Post-Wenchuan Earthquake Restoration and Reconstruction, State Council
3 July 2008	Guiding Opinions on Post-Wenchuan Earthquake Restoration and Reconstruction
19 September 2008	Overall Plan for Post-Wenchuan Earthquake Restoration and Reconstruction
October–November 2008	Special Plans for Post-Wenchuan Earthquake Restoration and Reconstruction
In and after September 2008–	Plans for Post-Wenchuan Earthquake Restoration and Reconstruction, approved by various regional governments

29 June 2008, “Guiding Opinions on Post Wenchuan Earthquake Restoration and Reconstruction” on 3 July 2008, and the “Overall Plan on Post Wenchuan Earthquake Restoration and Reconstruction” on 19 September 2008 as the policy framework for the catastrophe recovery.

The “Overall Plan on Post Wenchuan Earthquake Restoration and Reconstruction” (Overall Plan) identified the basic principles, objectives, and contents for recovery. It required to invest RMB 1,000 billion Yuan within about 3 years through local government fund allocation, counterpart assistance, public donations, domestic bank loans, capital market financing, foreign emergency loans on favorable terms, urban and rural residents private capital, capital of enterprises, and innovation financing, for earthquake restoration and reconstruction in the 51 significantly affected counties. The objective was to provide housing for all families, ensure employment for households of working population, provide security for each person, improve infrastructure, ensure development in economy, and realize improvement in ecology. The basic living conditions and economic development should reach or surpass the pre-disaster levels. Endeavor to build a new homeland characterized by enjoyable life and work, eco-civilization, security, and harmony, and lay a solid foundation for sustainable socioeconomic development.

In order to achieve the objectives of the Overall Plan and to rationally allocate resources, the central government proposed the “counterpart assistance” mechanism, under which each of 19 individual provinces (municipalities) and Shenzhen Special Economic Zone supported one significantly affected county on a one-on-one basis (Table 12, except that Tianjin Municipality supported two major disaster counties in Shaanxi Province and Shenzhen supported four major disaster counties in Gansu Province) by committing 1 % of the local financial revenue in the preceding year for goods and operation costs every year for three consecutive years. Enterprises, social groups, and individuals in various regions were also encouraged

Table 12 Counterpart assistance arrangement for Post-Wenchuan Earthquake restoration and reconstruction

ID	Supporting area → Supported area	ID	Supporting area → Supported area
1	Shandong Province → Beichuan County, Sichuan Province	11	Shanxi Province → Mao County, Sichuan Province
2	Guangdong Province → Wenchuan County, Sichuan Province	12	Hunan Province → Li County, Sichuan Province
3	Zhejiang Province → Qingchuan County, Sichuan Province	13	Jilin Province → Heishui County, Sichuan Province
4	Jiangsu Province → Mianzhu City, Sichuan Province	14	Anhui Province → Songpan County, Sichuan Province
5	Beijing Municipality → Shifang City, Sichuan Province	15	Jiangxi Province → Xiaojin County, Sichuan Province
6	Shanghai Municipality → Dujiangyan City, Sichuan Province	16	Hubei Province → Hanyuan County, Sichuan Province
7	Hebei Province → Pingwu County, Sichuan Province	17	Chongqing Municipality → Chongzhou City, Sichuan Province
8	Liaoning Province → An County, Sichuan Province	18	Heilongjiang Province → Jiange County, Sichuan Province
9	Henan Province → Jiangyou City, Sichuan Province	19	Shenzhen → Wen County, Kang County, Cheng County, Wudu District of Longnan City, Sichuan Province
10	Fujian Province → Pengzhou City, Sichuan Province	20	Tianjin Municipality → Ningqiang County and Lueyang County in Shaanxi Province

Data source Directive on Counterpart Assistance for Post-Wenchuan Earthquake Restoration and Reconstruction, State Council, 11 June 2008

to invest for starting factories and constructing then operating infrastructures in disaster areas in accordance with the market rules.

In order to further ensure the successful implementation of the Overall Plan and accelerate the restoration and reconstruction process, the National Development and Reform Commission (NDRC) and relevant government departments issued the Special Planning for Urban and Rural Housing Construction in Post-Wenchuan Earthquake Restoration and Reconstruction Project; Special Planning for Cities and Towns System in Post-Wenchuan Earthquake Restoration and Reconstruction Project; Special Planning for Rural Construction in Post-Wenchuan Earthquake Restoration and Reconstruction Project; Special Planning for Public Service Facilities Construction in Post-Wenchuan Earthquake Restoration and Reconstruction Project; Special Planning for Infrastructure Facilities Construction in Post-Wenchuan Earthquake Restoration and Reconstruction Project; Special Planning for Productive Force Distribution and Industrial Adjustment in Post-Wenchuan Earthquake Restoration and Reconstruction Project; Special Planning for Market Service System in Post-Wenchuan Earthquake Restoration and Reconstruction Project; Special Planning for Disaster Prevention and Reduction in Post-Wenchuan Earthquake Restoration and Reconstruction Project;

Special Planning for Ecology Restoration in Post-Wenchuan Earthquake Restoration and Reconstruction Project; and Special Planning for Land Use in Post-Wenchuan Earthquake Restoration and Reconstruction Project successively in October and November 2008, and presented specific objectives and tasks of reconstruction in relevant fields, thus extending and refining the objectives and tasks of the Overall Plan in specific areas (Shi et al. 2012).

Considering the rapid progress of reconstruction in the disaster areas, in March 2009, the Second Session of the Eleventh National People's Congress proposed that the scheduled 3-year reconstruction tasks can be completed in 2 years, that is, complete the tasks specified in the Overall Plan before September 2010.

Implementation of restoration and reconstruction: By May 2011, a total of RMB 1020.5 billion Yuan had been invested in restoration and reconstruction, therein, the central government financial department invested RMB 302.6 billion Yuan. At this point, all national reconstruction projects of disaster areas in Sichuan, Shaanxi, and Gansu had been started; the completed projects accounted for 95 % of all projects; and completed investment took up 95 % of the total investment. The housing conditions of urban and rural residents had been remarkably improved. Within one year after the earthquake, the restoration and reinforcement of damaged houses had been completed; within one and a half years after the earthquake, the reconstruction of rural housing had been totally completed; and within two years after the earthquake, housing reconstruction in cities and towns had been largely completed. In the disaster areas, in the three (Sichuan, Shaanxi, Gansu) provinces 2.92 million rural houses and 1.46 million houses in cities and towns were reinforced and repaired; and 1.91 million rural houses and 290 thousand houses in cities and towns were reconstructed. The public service facilities had been largely improved. Damaged schools and hospitals were fully restored and reconstructed. Furthermore, a large number of social welfare institutions, elderly homes, community service centers, activities center for rural residents, and other public service facilities had also been built. The earthquake fortification standard of schools and hospitals had been increased from 7 to 8. So the buildings became stronger and safer, and the facilities and devices were improved significantly.

On the whole, the focus of the planned projects and investments were mainly on securing the basic safety of disaster victims, infrastructure construction, productive capacity deployment, and industrial readjustment. Investment in disaster prevention and reduction was relatively little.

Summary of the restoration and reconstruction experiences: **Counterpart assistance mechanism** has played an important role in restoration and reconstruction. After the Wenchuan Earthquake, under the unified resource deployment of the Central Committee of the Communist Party of China, the counterpart assistance arrangement organized related provinces and municipalities to provide assistance to the disaster areas in order to speed up post-disaster restoration and reconstruction. The implementation of the “one province assists one hard-hit county” policy demonstrated the strength of the Chinese socialist system and fully mobilized the resource of the whole nation—it became a platform for gathering the forces for restoration and reconstruction, integrating various resources, bridging the

financing gaps in post-disaster reconstruction, providing supports in manpower, materials, and intelligence and helped the disaster areas resolve a large number of urgent problems with regard to people's livelihood, and laid a firm foundation for the long-term development of the disaster areas. In addition, a supervision mechanism for the use of reconstruction funds was created and plans for funds allocation and use were formulated. The funds were well used and the use efficiency was improved, which enabled the implementation of various reconstruction projects. The counterpart assistance arrangement had clearly defined tasks. Through strengthening regional cooperation with provinces (municipalities) that provide counterpart assistance, their resource advantages (location, industry, capital, and others) were fully tapped into. Restoration and reconstruction of residential buildings, agriculture and rural infrastructures, especially in poor areas, were carried out by means of non-disaster areas assisting disaster areas and developed areas assisting undeveloped areas. Through strengthening the regional economic cooperation, the "blood transfusion" function of assistance was transformed into "hematopoiesis" function for local economic development; short-term assistance was changed into long-term economic development measures to promote the adjustment of regional industrial structures, industrial development, and the cooperation and communication among regions, and bring advanced concepts, opening-up channels and communication channels, advanced technology and markets, and so on, thus gradually driving the economic restoration and development of the disaster areas.

In combination with the construction of small towns and poverty alleviation programs, this has laid a solid foundation for the construction of new socialist countryside. The rural restoration and reconstruction after the earthquake disaster are directly related to not only the rural production and living of the rural population, but also the long-term development of the economy and society of the disaster areas and have been integrated with the small town construction and poverty alleviation programs. First, the restoration and reconstruction have paid attention to the coordination of rural living and rural production and properly handled the relationship between living and production development to realize a peaceful life and ensure that all people have houses to live, land to farm, and a secured livelihood in the new villages. Secondly, the restoration and reconstruction have focused on the coordination of reconstruction and region development and appropriately handled the relationship between current and long-term developments, integrated the post-disaster restoration and reconstruction of rural areas with strengthening region development and balancing urban and rural developments, rationally and scientifically determined the direction and objective of development, and focused on the post-disaster restoration and reconstruction and new countryside development pilot projects for demonstration. Thirdly, the restoration and reconstruction have paid attention to the integration of uniformed planning and local characteristics/practices, properly handled the relationship between safe living and economical and practical designs, performed village and farmhouse reconstruction as per the geographical, industrial, and ethnic features of the local areas, realized the integration between seismic resistance and disaster prevention and between uniformed planning and local characteristics and practically, and well managed the relationship between safe

living and development with local characteristics. Fourthly, the restoration and reconstruction have emphasized the integration of reconstruction and ecological restoration, and have paid great attention to the relationship between development and protection and creating a harmonious ecological environment. Lastly, the restoration and reconstruction have emphasized the integration between self-aid of rural residents and government subsidy and social assistance, mobilized all resources, and taken into consideration the interest of all stakeholders to carry out the difficult tasks in post-disaster restoration and reconstruction. According to the surveys, with respect to post-earthquake restoration and reconstruction, especially in rural housing and infrastructure, the new developments in some areas have exceeded the level before the earthquake and reached a higher stage as compared to the plans. This has also laid a foundation for accelerating the new socialist countryside construction locally.

References

- AQSIQ-SAC (General Administration of Quality Supervision, Inspection and Quarantine of the People's Republic of China, Standardization Administration of China). 2001. *Seismic ground motion parameters zoning map of China (GB 18306-2001)*. Beijing: Standards Press of China (in Chinese).
- AQSIQ-SAC (General Administration of Quality Supervision, Inspection and Quarantine of the People's Republic of China, Standardization Administration of China). 2005. *Part 4 of Earthquake site work: Assessment of direct damages caused by disasters (GB/T 18208.4-2005)*. Beijing: Standards Press of China (in Chinese).
- CENC (China Earthquake Network Center). <http://www.ceic.ac.cn/>.
- Chen, Y., Y.T. Chen, G.M. Zhang, et al. 2005. Forecast and early-warning and preparedness measures for great earthquake disasters in China during the period of the 11th five-year plan. *Journal of Catastrophology* 20(1): 1-14 (in Chinese).
- Compiling Committee of Seismic Zoning Map in China. 1992. Seismic intensity zoning map of China (1990) and its explanations. *Earthquake Research in China* 8(4): 1-11.
- DEDP (Department of Earthquake Disaster Prevention), China Earthquake Administration. 1995. *Catalogue of Chinese historical strong earthquakes (B.C. 23-A.D. 1911)*. Beijing: Seismological Press (in Chinese).
- DEDP (Department of Earthquake Disaster Prevention), China Earthquake Administration. 1999. *Catalogue of Chinese modern strong earthquakes (1912-1990)*. Beijing: China Science and Technology Press (in Chinese).
- Deng, Q.D., Y.M. Zhang, W.L. Huan, et al. 1980. Principles and methods of composing the seismic zoning map of China. *Acta Seismologica Sinica* 2(1): 90-110 (in Chinese).
- Earthquake Relief Experts Group of National Committee for Disaster Reduction and Ministry of Science and Technology. 2008. *Comprehensive analysis and assessment of the Wenchuan Earthquake*. Beijing: Science Press (in Chinese).
- Fang, W.H., J.A. Wang, and P.J. Shi. 2011. *Integrated risk governance: Database, risk map and network platform*. Beijing: Science Press (in Chinese).
- Lee, S.P. 1957. The map of seismicity of China. *Acta Geophysica Sinica* 6(2): 127-158 (in Chinese).
- Lou, B.T. 1996. *Summary of Chinese historical earthquake disasters*. Beijing: Seismological Press (in Chinese).

- Ma, Z.J., and M. Jiang. 1987. Strong earthquake period and episodes in China. *Earthquake Research in China* 3(1): 47–50 (in Chinese).
- Ma, Z.J., Z.X. Fu, Y.Z. Zhang, et al. 1982. *Nine major earthquakes in China*. Beijing: Seismological Press (in Chinese).
- MCA (Ministry of Civil Affairs). 2015. *China civil affairs' statistical yearbook 2015*. Beijing: China Statistics Press (in Chinese).
- Shi, P.J. 2011. *Atlas of natural disaster risk of China*. Beijing: Science Press (in Chinese and English).
- Shi, P.J., and Y.H. Liu. 2009. Chinese paradigm for integrated large scale disaster risk governance. *Journal of US-China Public Administration* 6(6): 18–28.
- Shi, P.J., C. Jeager, and Q. Ye. 2012. *Integrated risk governance: Science plan and case studies of large-scale disasters*. Beijing: Beijing Normal University Publishing Group and Berlin Heidelberg: Springer.
- The State Council. 2008. The notice of the composition and structure of the Earthquake Relief Headquarters of the State Council. http://www.gov.cn/zhengce/content/2008-06/02/content_6591.htm.
- Wang, J.A., P.J. Shi, P. Wang, et al. 2006. *Spatiotemporal pattern of natural disasters in China*. Beijing: Science Press (in Chinese).
- Xu, G.D., W.F. Fang, P.J. Shi, et al. 2008. Rapid assessment of the Wenchuan Earthquake. *Journal of Earthquake Engineering and Engineering Vibration* 28(6): 65–74 (in Chinese).
- Xu, G.D., Y. Yuan, W.F. Fang, et al. 2011. Rapid loss assessment of Ms 7.1 Yushu Earthquake. *Journal of Earthquake Engineering and Engineering Vibration* 31(1): 114–123 (in Chinese).
- Yin, Z.Q., and S.W. Yang. 2004. *Seismological damage analysis and fortification standard*. Beijing: Seismological Press (in Chinese).
- Yin, Z.Q., Z. Zhao, and S.W. Yang. 2003. Relationship between vulnerability of buildings and earthquake acceleration spectra (1). *Earthquake Engineering and Engineering Vibration* 23(4): 195–200 (in Chinese).

Landslide and Debris Flow Disasters in China

Yongqiu Wu, Xilin Liu, Jing'ai Wang, Lianyou Liu and Peijun Shi

Abstract China is a nation facing extremely serious landslide and debris flow disaster risks. Considering the current status of research, this chapter starts with examining the hazards of landslides and debris flows in China, then conducts risk classification and zoning, and proposes integrated disaster prevention measures. Finally, the disaster emergency response process, disaster response mechanisms, and post-disaster restoration and reconstruction processes are analyzed using the Zhouqu debris flow case.

Keywords Debris flow · Landslide · Spatiotemporal pattern · Zhouqu debris flow

Although landslides and debris flows are geological disasters that occur under similar conditions, there are significant differences between the two phenomena. Landslide is a phenomenon where bulk rock (or soil) located on a slope slides down as a whole under the effect of groundwater, surface water, and gravity (Yang and Li 2005). Debris flow is a solid–liquid two-phase flow (mixed mud, sand, and stones)—cross between a landslide and water flow. Debris flow is characterized by its sudden onset, fast motion, and a short-lived nature, and may include both laminar and turbulent flow. Both landslides and debris flows are natural phenomena that become disasters when they threaten human habitat, leading to casualties and/or property damage. Under certain circumstances, landslides and debris flows can transform

Y. Wu (✉) · L. Liu

Key Laboratory of Environmental Change and Natural Disasters of Ministry of Education, Beijing Normal University, Beijing 100875, China
e-mail: yqwu@bnu.edu.cn

X. Liu

School of Geography and Planning, Sun Yat-Sen University, Guangzhou 5102754, China

J. Wang

School of Geography, Beijing Normal University, Beijing 100875, China

P. Shi

State Key Laboratory of Earth Surface Processes and Resource Ecology, Beijing Normal University, Beijing 100875, China

from one to the other. One notable example is a large landslide event that blocked a river in Gongte, Tibet, in April 2000: the whole process included collapse→landslide→(debris flow)→river blockage forming barrier lake→lake outburst→flood→valley terrain reconstruction→secondary avalanches and landslides in the valley, therefore forming a complete chain of geological disasters (Huang 2007). Landslide and debris flow risks are defined as the expected losses of lives, properties, and economic activities caused by landslide or debris flow disasters over a given area and time period. Landslide and debris flow risks can be expressed as the product of the risk level of landslide or debris flow and vulnerability.

China is a nation facing extremely serious landslide and debris flow disaster risks. Landslides and debris flows can interrupt traffic, clog rivers, destroy factories and mines, bury villages and towns, and cause casualties and great economic losses, and therefore they are recognized as serious natural disasters. With regard to landslides, large and super-large landslides are predominant in China. In particular, large landslides in the western region of China are well-known for their extensive scale, complex mechanism, and tremendous impacts. The most basic reason for large landslide development in China is its favorable geomorphic conditions. About 80 % large landslides occurred within the first slope-descending zone of continental terrain at the eastern side around the Qinghai–Tibet Plateau (Huang 2007). Debris flows in China are distributed in 31 provinces, municipalities, and autonomous regions and 950 counties, with an active region of 4.3 million km², including 1.3 million km² strong active region. There are a total of more than 80,000 active areas of debris flows, including more than 8,500 very high risk areas. In recent years, debris flows caused economic losses of RMB several billion Yuan and hundreds to thousands of disaster victims every year (Kang et al. 2004; Yu et al. 2010).

This chapter is based on existing research under the support of the National Science and Technology Pillar Program (2006BAD20B00) during the 11th Five-Year Plan in combination with other relevant works carried out by our research group in recent years. Chinese and international landslide and debris flow disaster research mainly focused on the hazards and disaster prevention, and risk assessment is relatively recent. Up until now, there exist no credible landslide and debris flow disaster vulnerability curves; and estimations on exceedance probability of landslide and debris flow disasters are not sufficiently advanced. Risk assessment of landslides and debris flows has been far less prioritized as compared to that of typhoons, floods, and earthquakes.

Considering the current status of research, this chapter starts with examining the hazards of landslides and debris flows in China, then conducts risk classification and zoning, and proposes integrated disaster prevention measures. The main sources of data used in this chapter include: a Chinese newspaper and periodical database of natural disasters (established by Beijing Normal University); a national geological disaster bulletin released by the Ministry of Land and Resources of the People's Republic of China since 2004, statistical data from the National Bureau of Statistics of China, statistical data from the Bureau of Civil Affairs, and the *Chinese Landslide Disaster Distribution Maps* and *Chinese Debris Flow Distribution and*

Hazard Zoning Maps (1:6,000,000) published by the Chengdu Cartographic Press, and published academic papers.

1 Spatial and Temporal Patterns of Landslides and Debris Flows

Landslides and debris flows are geological hazards occurring in mountainous areas. With regard to their spatial distribution, landslides and debris flows mainly occur in the slope-descending zones between the second and the third stage and between the first and the second stage of the topographic divisions in China. Their distribution conforms to the strikes of some major mountain ranges in China. Wherein, the southwestern areas and the upper reach of the Yangtze River witness the most frequent disasters, while the semiarid, dry, and extremely dry areas in northwestern China as well as the northeastern regions have relatively fewer landslide and debris flow disasters. Areas around the Bohai Sea, Huang-Huai-Hai Plain, and Zhejiang-Fujian hilly regions south of the Yangtze River have sparse landslides and debris flows; and other regions are characterized by fewer landslide and debris flow disasters that occur only in areas with hilly terrain (Wang et al. 2006). Landslide and debris flow disasters mainly occur in rainy season of the year, and vary greatly in different years. Their temporal distribution is primarily influenced by climatic conditions. Global warming increases the frequency of extreme climatic events and extreme precipitation is greatly conducive to landslide and debris flow disasters. Generally speaking, landslide and debris flow disasters in China have increased in the recent 30 years.

1.1 Spatial Distribution of Landslide and Debris Flow Disaster

Spatial distribution of landslide disasters: China is one of the countries in the world that suffer from many landslides, and the disaster distribution is spatially uneven. Landslides are mainly distributed in Sichuan, Yunnan, Guizhou, southeastern Tibet and Gansu, the middle and southern part of Shaanxi as well as the south of Ningxia, followed by Shanxi, western Hunan and Hubei, Fujian, and some areas of Guangdong and Guangxi Provinces. Landslides are sparsely distributed in provinces and regions in southern and eastern China (except for the provinces identified above) as well as Qinghai Province. Such disasters seldom occur in the northeast, North china, Inner Mongolian, and Xinjiang (Fig. 1).

Landslide distribution of China is closely related to the topography of the country. The areas facing the most serious landslide disasters are in the middle and lower part of the second stage of the terrain. Taking the Qinling Mountains as a



Fig. 1 Landslide disasters of China (Source Shi 2011, p. 77)

rough boundary, the plateau and mountainous areas in Sichuan and Yunnan are to the south and the loess plateau region is to the north. Common characteristics of this area are large differential neotectonic uplifting and high earthquake magnitude and intensity. Torrential rain and rainy weather prevail in the summer; land use intensity is high; and other human activities are also intense. Landslides in this area are characterized by large scale, dense distribution, fast sliding speed, far sliding distance, high occurrence frequency, and extensive affected scope (Wang et al. 2006).

The areas with serious landslide disasters are mainly distributed in the Bashan Mountain, Wushan Mountain, and Huaying Mountain in eastern Sichuan as well as the plateau and mountainous areas of Sichuan, Hubei, and Guizhou Provinces. Internal and external forces for the formation of landslides in the Three Gorges area of the Yangtze River and the Daba Mountain and Huaying Mountain areas in the north are greater than that of the plateau and mountainous areas of Guizhou and Hubei Provinces. Landslides in this region are known by their medium to large scale, dense distribution, fast sliding speed, and common river clogging phenomenon. Occurrence frequency of landslides is high, with extensive scope. Rainstorm-induced landslides are the major type, followed by engineering-related landslides, and a small part of these is earthquake-induced landslides.

The areas with less serious landslide disasters are mainly distributed at the periphery of the Qinghai–Tibet Plateau, including the Himalayas, Namchabawa Mountain, Shaluli Mountain, Kunlun Mountains, Qinling Range, among others. With regard to the terrain, these areas are located at the highest altitude, and

mountain strikes are controlled by latitudinal structural system. Neotectonic movement in the area is characterized by intense motion, high earthquake magnitude, great earthquake intensity, fast mountain uplift, and deep river valley. Landslides in the area are mainly caused by avalanches and freeze thaw, and show dense distribution, large scale, high occurrence frequency, fast sliding speed, and far sliding distance. Most slide bodies are separated from the slide bed, and river clogging due to landslides is very common.

The areas with moderate landslide disasters are mainly distributed in the extensive hilly and mountainous regions south of the Qinling Mountains and east of the Yunnan–Guizhou Plateau, Sichuan Basin, and mountainous areas of Taiwan. Medium- and small-scale rainstorm-induced landslides prevail in the area, followed by engineering-related landslides. There are also some earthquake-induced landslides in Taiwan. Landslide distribution is relatively sparse, with low occurrence frequency. Most slide bodies are not separated from the slide bed.

The areas with light landslide disasters are located in northwestern China. Latitudinal structure and the Qi-Lv mountain type structural system form the landform framework of the area. Neotectonic movement shows intense uplifting and frequent earthquake activities. The climate is dry with strong weathering. The area is sparsely populated, so influence of human activities on slope instability is little. Landslides in this area are mainly caused by large- and medium-scale undersurface ice melting and sinking. There are also rainstorm-induced and engineering-related landslides in the Taihang–Lvliang mountain areas. The landslides are rather dense, with fast sliding speed and short sliding distance. Most sliding bodies are not separated from the sliding bed and the occurrence frequency is relatively low.

The areas with slight landslide disasters are mainly distributed in the Tongbai–Dabie Mountains in eastern China and northern hilly and mountainous regions. Landform of this area is controlled by the Neocathaysian structure and nearly EW-trending structural systems. Neotectonic movement is slight and the terrain is flat. Freeze thaw-induced landslides prevail in the northern part of the area and rainstorm-induced landslides prevail in the south. The landslides are marked by small scale, sparse distribution, and low occurrence frequency; therefore their impacts on the natural environment and human economic activities are insignificant (Wang et al. 2006).

The areas that almost have no landslide disasters are mainly distributed in the Tarim–Qaidam Basin and Junggar Basin in inland of China and the Songnen Plain, Sanjiang Plain, and middle and lower reaches of the Yangtze River and Yellow River Plains in eastern China. Landslides do not occur in these areas basically because the geomorphic conditions conducive to landslide formation are absent. However, there have been a very small number of landslides due to manual excavation of earth that had very limited impact (Wang et al. 2006).

Spatial distribution of debris flow disasters: Debris flow disasters of China are mainly distributed in the two transitional zones between the three topographic stages of China, that is, the transitional zone between the Qinghai–Tibet Plateau and the lower plateaus and basins (Yunnan–Guizhou Plateau, Loess Plateau, Sichuan



Fig. 2 Debris flow disasters of China (Source Shi 2011, p. 76)

Basin, Tarim Basin, Junggar Basin), including the Kunlun Mountains, Qilian Mountains, Min Mountain, Longmen Mountains, Hengduan Mountains, and Himalayas; and the transitional zone from the lower plateaus and basins to the low mountains and hills in eastern China, including the Daxing'anling and Xiaoxing'anling, Long White Mountain, Yanshan Mountain, Taihang Mountain, Qinling Mountains, Daba Mountain, Wushan Mountain, Yunkai Mountain and so on (Fig. 2). Except for the plateaus and surrounding mountainous areas, debris flows also occur in mountainous areas in North China and northeast China (such as the West Hills of Beijing and Liaoning Province). Debris flows are also distributed in mountainous areas in other regions of China, such as Anxi in Fujian, Nantou and Hualian in Taiwan, and Dayu Mountain and Qingshan Mountain in Hongkong (Kang et al. 2004).

A number of major debris flow areas of China are introduced below.

(1) Debris flow area in the Xiaojiang River Basin of Yunnan Province: The Xiaojiang River originates from the Yuweihoushan Mountain at the northeast plateau of Yunnan. It extends from south to north, passes Xundian County, Dongchuan City, and Huize County and finally flows into the Jinsha River, with a total length of 138 km and a drainage area of 3043 km². The Xiaojiang River valley develops on the famous deep and large Xiaojiang fracture zone, which has complex old structures and is under the influence of very active neotectonic movement. It is also located in a strong earthquake area. With its unique natural conditions and human activities, many favorable factors conducive to forming debris flows interact

here and make the area the most debris flow-prone place in China. Debris flows of this area are mainly induced by rainstorm. At both sides of the Xiaojiang River near Dongchuan City, along about 90 km of the river course, there are 107 V-shaped debris flow sites and countless small-scale slope debris flows densely distribute in groups. In the rainy season, triggered by rainstorms such debris flows originate in mountains and plunge into the Xiaojiang River, which causes serious disasters for cities and towns, mining facilities, roads, farmlands, villages, water resources infrastructure, river regulation engineering works. Debris flow disasters have become a crucial factor impeding the economic development and threatening the safety of people in the Xiaojiang River Basin. In addition, a large amount of silt and stones scoured by the debris flows enters the Jinsha River through the Xiaojiang River, which forms greatly hazardous rapids at the confluence of the two rivers and forces the Jinsha River to extend toward the opposite bank, thus hampering the development and utilization of the Jinsha River channel. With its small river basin and extremely developed debris flows, which occur so frequently and with such intensity that endangers all aspects of the local economy, the Xiaojiang River Basin is a very rare debris flow case in China as well as other mountainous areas of the world (Du et al. 1987).

(2) Debris flow area in the Daying River Basin of Yunnan Province: The Daying River Basin is located near the southwestern border of Yunnan adjacent to Myanmar. It is situated between $91^{\circ} 4' E$ to $98^{\circ} 38' E$ longitude and $24^{\circ} 26' N$ to $25^{\circ} 38' N$ latitude. The Daying River originates from the Jiaoji Mountain in the northeast of Tengchong, passes Tengchong County, Lianghe County, and Yingjiang County and finally flows into the Irrawaddy River in Myanmar. The Daying River is 168 km long in China, with 1,390 m drop height and $5,800 \text{ km}^2$ drainage area. According to the field survey reports and statistics (Zhang and Liu 1989), the river basin has densely distributed debris flows and 116 gullies. The debris flow gullies are the viscous and diluted types. Debris flows in gullies occur frequently and enter the river, making the Daying River a heavily sediment-laden river. Annual sediment discharge at the Xialaxian Hydrological Station reaches 6,470,000 tons. On the other hand, a large amount of sediments also deposit on the river bed, causing the river bed to rise by 5–10 cm every year, which brings great harm to the place (Zhang and Liu 1989).

(3) Debris flow area in the Bailong River Basin of Gansu Province: Spatial density and occurrence frequency of debris flows in the Pai-lung River Basin rank No. 1 in Gansu Province and are nearly the same as in other major debris flow areas of China. These debris flows have generated serious hazard for the basin. According to the preliminary statistics, there are more than 1,000 debris flow sites in the river valley, which are distributed within a $6,400 \text{ km}^2$ area and include 490 large-scale debris flows. Rainfall here is relatively low but the high spatial density of debris flows is caused by widely distributed weak rocks and the active neotectonic movement has played an important role in such occurrences. Solid substances forming the debris flows in this area are mainly supplied by weak rocks from the Silurian period, such as phyllite, slate, shale, and rock bind. They are distributed at the middle and lower parts of slopes and form rockfall and landslide mass easily,

thus becoming major sources for solid substances of debris flows. Neotectonic movement (especially earthquakes) exerts great influence on the formation of debris flows. In Wudu of the Pai-lung River Basin hundreds of earthquakes have been recorded since the start of record, including 15 dangerous earthquakes (Li and Zeng 1982). Zhouqu County, where an extraordinarily serious debris flow occurred in 7–8 August 2010, is located in the Pai-lung River Basin.

(4) Debris flow area in the Anning River Valley of Sichuan Province: The Anning River flows from North to South and enters the Yalong River and then the Jinsha River near Panzhihua, with a total length of 287 km. The three-river basin is located at the eastern edge of the Hengduan Mountain and characterized by rugged terrain as well as rising and falling mountains. The terrain is high in the North and West, and low in the South and east. The altitude of most mountain ridges is about 3,000 m. The highest peak is the main peak of the Maomao Mountain, with a height of 4,621 m and relative height difference of 3,878 m. Mountain ridges in this area are nearly north to south structures. The Anning River develops in a rift valley on a North to South deep and large fracture zone, which is flat and extensive with a width of 5–10 km. The river valley is a vital communication line between the Chengdu Basin and Yunnan Province. Terraces and floodplains are well developed in the valley. Especially at the east bank, in addition to the multilevel terraces, there are also proluvial fans formed by debris flows along the mountain foot. Along the 110 km section from Xide to Dechang, there are dense debris flow sites and 61 debris flow gullies (Kang et al. 2004).

(5) Debris flow area in the Weihe River Valley of Shaanxi and Gansu Provinces: The Weihe River Valley from Baoji (Shaanxi) to Tianshui (Gansu) is about 150 km long and crossed by the Longhai Railway. Mountains at both sides of the Weihe River Valley are high and steep, with relative height difference of 600–1,000 m and gradient of 30°–50°. They are formed by granitic gneiss, dolomite, and metamorphic rocks covered by 20–40 m thick loess. This area mainly suffers from loess earth flow. This section contains 150 debris flow gullies, including 104 gullies along the railway line and 20 gullies severely impairing the safety of the railways (Kang et al. 2004).

(6) Debris flow area along the Sichuan–Tibet Highway: The Sichuan–Tibet Highway starts from Chengdu in the east and ends at Lasa in the west, with a total length of 2,460 km and crosses 14 high mountains with altitude exceeding 3,000 m and more than 10 great rivers. It is an important traffic main road from other inland areas of China to Tibet, and assumes the task of delivering materials and supplies to the Tibetan area. In more than 50 years from December 1954 (when the highway started operating) to date, in rainy seasons the road traffic was interrupted from time to time. The rain often obstructed traffic and the traffic obstruction periods lasted for several days to several months. Although the road was thoroughly maintained and partially upgraded in the mid-1970s, problems are still not solved and serious disasters still occur. Debris flow disasters are one of the important reasons for road traffic interruption and traffic jam. According to an investigation carried out in the 1990s, the Sichuan–Tibet line encounters 1,006 debris flow gullies, including 877 serious and extraordinarily serious gullies (Kang et al. 2004).

1.2 Temporal Distribution of Landslide and Debris Flow Disasters

1.2.1 Hazards

Driving factors of landslides and debris flows are mainly geological and climatic. As far as geological factors are concerned, variation in the occurrence of earthquakes greatly affects the occurrences of landslides and debris flows. If a strong earthquake occurs in a landslide- and debris flow-prone area such as those identified above, the number of landslides and debris flows will significantly increase. For example, the magnitude 8.0 Wenchuan Earthquake in Sichuan in 2008 caused a large number of secondary geological disasters. According to the post-earthquake investigation data from the Ministry of Land and Resources, over 20 thousand geological disasters were induced, including collapses, landslides, debris flows, among others. Most of these disasters were collapse and landslide disasters, covering more than $20 \times 104 \text{ km}^2$ land area (Wang et al. 2010). Under the background of global climate change, activities of summer monsoon in eastern China have increased since the 1980s (Li 1999). Landslide and debris flow occurrences have also taken on an increasing trend.

Systematic recording and statistical data for landslides and debris flows were not available in the Twentieth century. Therefore data for this time period are mainly found in scholarly research. The Ministry of Land and Resources started releasing monthly, quarterly, and yearly “National Geological Disaster Bulletin” from 2004. Thus in this chapter disaster situation data for landslides and debris flows after 2004 are extracted from the bulletins.

Situation of landslide and debris flow hazards in the twenty-first century:

The interannual change of occurrences of landslide and debris flow hazards in China from 2005 to 2014 are shown in Figs. 3 and 4, respectively using the data from the national geological hazard bulletins.

1.2.2 Disasters

Temporal pattern of landslide disaster occurrences in the second half of the

twentieth century: The occurrence frequency of serious landslides in China from the 1950s to the end of the twentieth century is shown in Fig. 5 (Li 1999). From the figure we can see that: (1) landslide occurrences fluctuated but also showed a general rising trend over time; (2) landslide activity seems to have gone through several cycles in 1951–1964, 1964–1977, 1977–1987, and 1987–1996, with the peak years in 1957, 1971, 1981, and 1991; (3) for the five peak years, the first two are low and the numbers of serious landslides in these years were not significantly higher than other years in the same time period. The latter three peaks are much

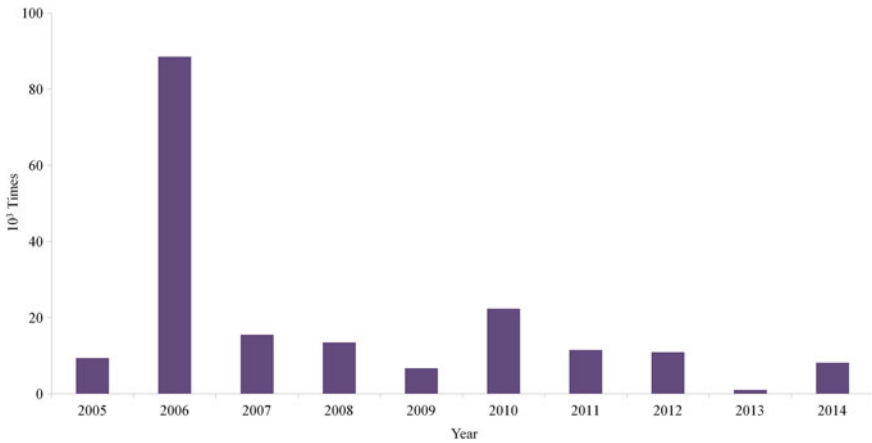


Fig. 3 Number of landslide hazards in China, 2005–2014 (Date source MLR 2005, 2006, 2007, 2008, 2009, 2010, 2011, 2012, 2013, 2014)

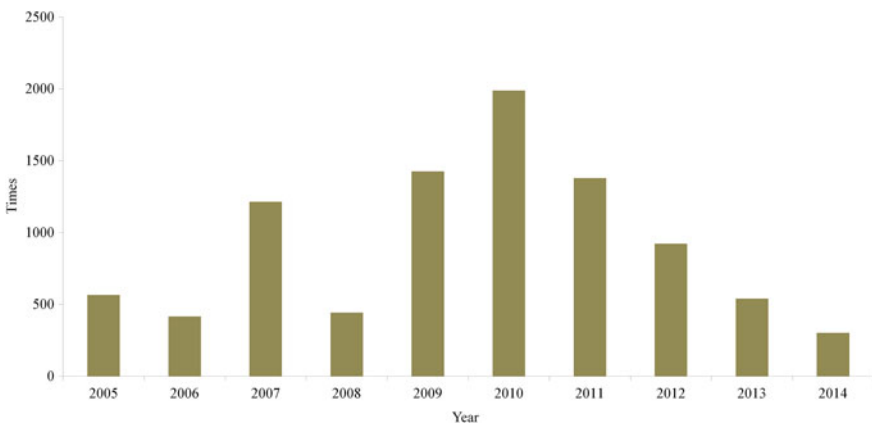


Fig. 4 Number of debris flow hazards in China, 2005–2014 (Date source MLR 2005, 2006, 2007, 2008, 2009, 2010, 2011, 2012, 2013, 2014)

higher, indicating that disaster occurrences have increased dramatically over time; (4) in Fig. 5, time interval between the first and the second peaks is 14 years, but the intervals between other peak years are about 10 years; (5) in 1951–1978, serious landslide frequency was less than 10/year but this became higher than 10 after 1978.

Temporal pattern of debris flow disaster occurrences in the second half of the twentieth century: The temporal pattern of large debris flow occurrences in China (Fig. 6) is very similar to serious landslide disaster occurrences, but the cycle

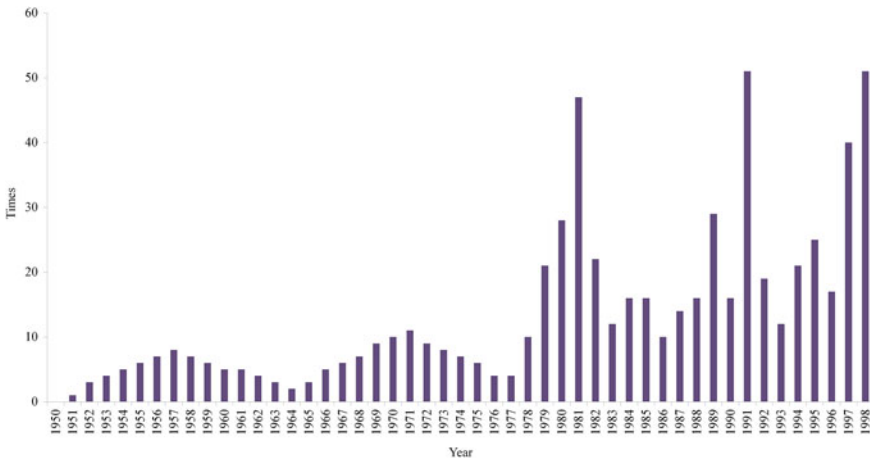


Fig. 5 Number of serious landslide disasters in China, 1950–1998 (Source Li 1999)

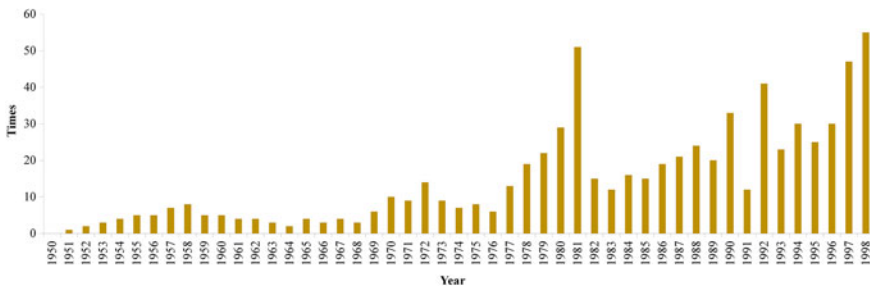


Fig. 6 Number of large debris flow disasters in China, 1950–1998 (Source Li 1999)

of activity seems slightly different. Debris flow occurrences show the following features: (1) the occurrences fluctuated over time but there was a general trend of gradual increase; (2) debris flow activity seems to have gone through several cycles in 1951–1962, 1962–1975, 1975–1986, and 1986–1994, with the peak years in 1958, 1972, 1981, and 1992; (3) for the four peaks, the first two are low and the numbers of large debris flows in these years were not significantly higher than other years in the same time period. Similar to the serious landslides, the latter three peaks are much higher, indicating that disaster occurrences became increasingly frequent over time; (4) in 1949–1968, disaster occurrences were less than 10/year, but the occurrences became higher than 10/year after 1968; (5) comparing the temporal pattern of serious landslide and large debris flow occurrences, we can see that debris flow peaks occurred 1–2 years ahead of landslides (Li 1999).

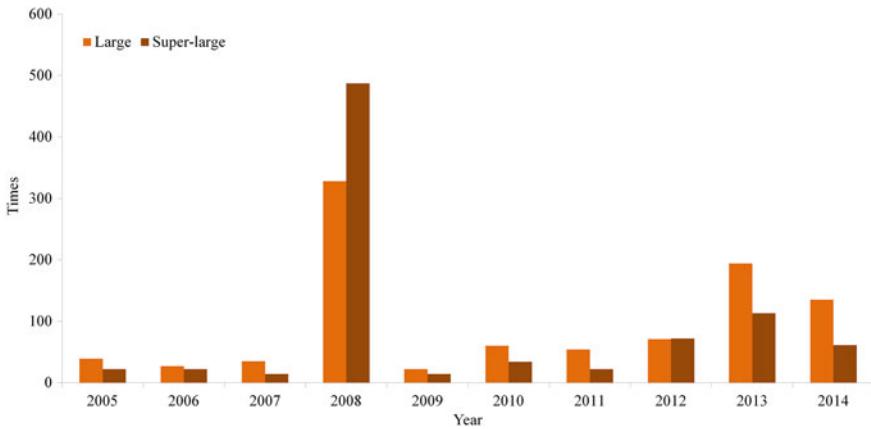


Fig. 7 Number of large and super-large geological hazards in China, 2005–2014 (Date source MLR 2005, 2006, 2007, 2008, 2009, 2010, 2011, 2012, 2013, 2014)

Situation of large and super-large geological disasters in the twenty-first century: On 24 November 2003, Decree No. 394 of the State Council of the People’s Republic of China issued the *Regulation on Geological Hazards Prevention*, which was enforced from 1 March 2004. Accordingly, the Ministry of Land and Resources regularly releases national geological hazard bulletins since 2004. According to the *Regulation on Geological Hazards Prevention*, large geological hazard refers to a hazard causing 10–30 deaths or RMB 5–10 million Yuan direct economic losses; super-large geological hazard refers to a landslide causing more than 30 deaths and above RMB 10 million Yuan direct economic losses. Using the data from the National Geological Disaster Bulletin issued by the Ministry of Land and Resources of the People’s Republic of China, interannual change of occurrences of large and super-large landslide disasters in China from 2005 to 2014 is shown in Fig. 7.

1.2.3 Disaster Losses

Annual economic losses and loss of lives and personal injury caused by geological disasters are related to the frequency of geological disasters. But the secondary debris flow disasters caused by the Wenchuan Earthquake in 2008 and other serious geological disasters such as the debris flow disaster in Zhouqu in 2010 have had extremely significant influences on the loss of lives, personal injury, and economic losses. The losses and impacts of geological disasters are mainly controlled by their spatial scale and intensity (Figs. 8 and 9).

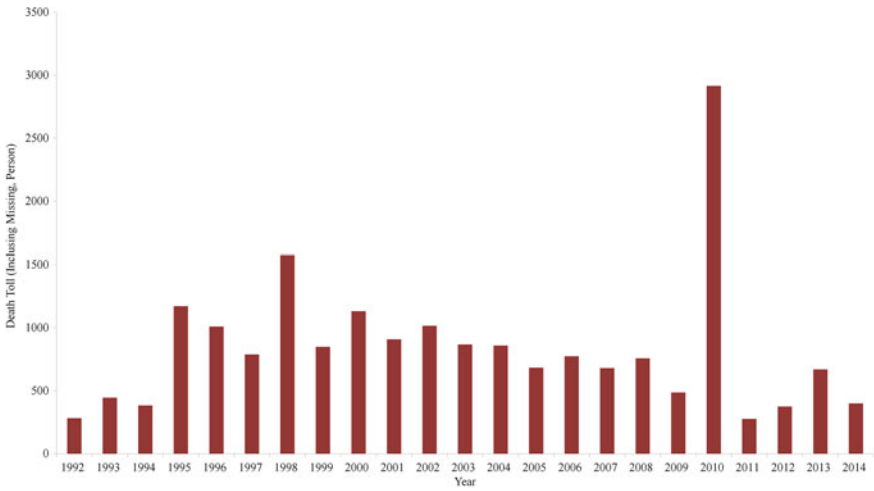


Fig. 8 Death toll (including missing people) in geological disasters in China, 1992–2013 (Date source MLR 2005, 2006, 2007, 2008, 2009, 2010, 2011, 2012, 2013, 2014)

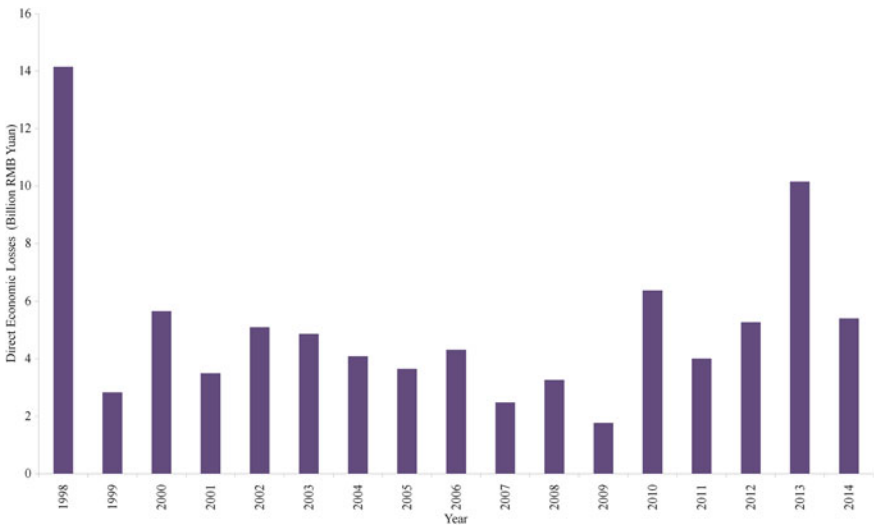


Fig. 9 Direct economic losses caused by geological disasters in China, 1998–2013 (Date source MLR 2005, 2006, 2007, 2008, 2009, 2010, 2011, 2012, 2013, 2014)

2 Formation and Assessment of Landslide and Debris Flow Disasters

Landslides and debris flows are sudden onset geological disasters and widely distributed in high and medium mountains as well as low mountainous and hilly areas. Existing studies often focus on individual debris flows and landslides, and regional study on debris flows and landslides is uncommon. For the prevention and reduction of landslide and debris flow disasters, in addition to continuously working on site-scale engineering measures, non-engineering measures through regional land use planning restrictions and adopting suitable land use are also important means. Landslide and debris flow disaster risk zonation performs classification of the land area into extremely high risk zone, high risk zone, medium risk zone, low risk zone, and extremely low risk zone, thus facilitating the division of corresponding prohibited development zone, limited development zone, and suitable development zone. Land use planning means shall be used to limit unsuitable land development practices to reduce and prevent landslide and debris flow disasters.

The Office for the Coordination of Humanitarian Affairs of the United Nations defined natural disaster risks as expected losses of people's lives, properties, and economic activities caused by specific natural disasters in certain area and given time (United Nations 1992). Quantitative expression of disaster risk is as follows: Risk (R) = Hazard (H) \times Vulnerability (V). This expression takes into account the three factors contributing to the formation of disasters: the disaster-formative environment, hazard, and exposure unit (Shi 2002). Stability of a disaster-formative environment, disaster inducing capability of the hazard, and vulnerability of the exposure units (potential loss and disaster-resistance capability) together determine the occurrence (or not) of disasters. Landslide and debris flow disaster risk assessment of this chapter considers that disaster risk is the product of hazard and vulnerability. Landslide and debris flow disaster risk mainly depends on the geological and geomorphic conditions of an area, potential occurrence frequency and intensity of landslide and debris flow hazards, and vulnerability or socioeconomic conditions and defensive measures of exposure units.

2.1 Landslide and Debris Flow Disaster Risk Assessment and Mapping

Basic hazard data and the landslide and debris flow hazard map: The *Map of Landslide Distribution in China* published by the Chengdu Map Press in 1991 (1:6,000,000) was used for hazard identification. In this map, China is divided into seven landslide hazard zones, including no-hazard, negligible hazard, moderate hazard, slightly serious hazard, moderately serious hazard, serious hazard, and most serious hazard zones. By taking into consideration natural and human factors contributing to the formation of landslide disasters and geomorphological features

of regions, the seven zones are further divided into 28 subzones (Institute of Mountain Hazards and Environment, Chinese Academy of Sciences 1991a). A second map used in the study was the *Distribution and Hazard Zoning Map of Debris Flows in China* also published by the Chengdu Map Press in 1991 (1:6,000,000). In this map, China is divided into four debris flow hazard zones, including negligible or no-hazard, slight hazard, moderate hazard, and serious hazard zones. The first-level division is according to the surface structural stability of different geological and geomorphological units in trunk river drainage areas of great rivers and by taking into consideration the type, frequency, and activity of debris flows affected by the climate within the area that generates outflows to the ocean in the river drainage areas. The second-level division is based on the main tributaries in the drainage areas and by taking into consideration the characteristics of debris flows and the intensity of human activities within the first-level divisions. It results in 15 subzones, wherein two are negligible hazard or no-hazard zones (in Xinjiang, Tibet, and Inner Mongolia and in the Irtysh River Basin) (Institute of Mountain Hazards and Environment, Chinese Academy of Sciences 1991b). The Songhua River and Liaohe River drainage areas (including the Northeast Plain) are classified as a slight hazard zone; the Huanghe, Huaihe, and Haihe drainage areas (including the North China Plain) and the Yangtze River drainage area (including the middle and lower reaches of the Yangtze River and Sichuan Basin) are classified as a moderate hazard zone; and the Pearl River drainage area (including the Pearl River Delta) is classified as a slight hazard zone.

In order to generate a comprehensive hazard map of landslides and debris flows in China, the four hazard levels of debris flows (negligible or no-hazard, slight hazard, moderate hazard, and serious hazard) are assigned values of 0, 2, 4, and 6, respectively and the seven landslide hazard levels (no-hazard, negligible hazard, moderate hazard, slightly serious hazard, moderately serious hazard, serious hazard, and most serious hazard) are assigned values of 0, 1, 2, 3, 4, 5, and 6 respectively. Comprehensive hazard of landslides and debris flows is expressed as the sum of the debris flow hazard and landslide hazard values and ranges between 0 and 12. Dividing the values between 0 and 12 into 5 levels (0–1, 2–4, 5–7, 8–10, and 11–12) and normalizing these values result in five hazard classes: 0–0.084 (extremely low), 0.166–0.334 (low), 0.416–0.584 (moderate), 0.666–0.834 (high), and 0.916–1 (extremely high). Using these criteria and data from the two hazard maps for landslides and debris flows, a comprehensive hazard map of landslides and debris flows of China is generated (Fig. 10).

Vulnerability to landslides and debris flows: Landslides and debris flows are both sudden geological hazards and often triggered by the same events, with similar exposure units, therefore the same evaluation method is used for the evaluation of vulnerability to both hazards. Vulnerability evaluation uses a composite index (Liu and Mo 2002, 2003) composed of four indicators, including gross domestic product (G) per unit area of the disaster year, annual average cumulative investment in fixed asset (P) during the past 10 years, annual average land resource value (L) per unit area, and population density (D) of the year. A number of coefficients can be used to correct the population density data (proportion of those aged 65 and above and

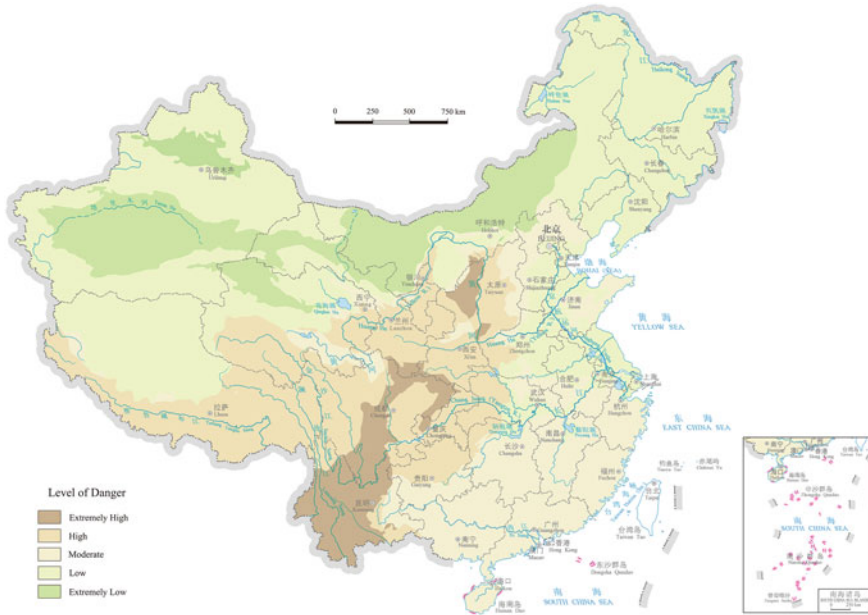


Fig. 10 Comprehensive hazard map of landslides and debris flows in China (Source Shi 2011, p. 76)

children below 15 in total population; proportion of those received only primary or lower education in the total population; and proportion of agricultural population in the total population). This chapter uses a simplified version of the above model with three indicators: gross domestic product, land use type, and population density to evaluate vulnerability to landslides and debris flows:

$$V = \sqrt{\frac{(G + L)/2 + D}{2}} \tag{1}$$

where, V is vulnerability (0–1); G is gross domestic product per unit area; L is the assigned per unit area value for different land use types, and D is population density. G , L , and D are all normalized values (0–1).

This simplified vulnerability model excluded the annual average cumulative investment in fixed asset per unit area indicator, and land resource value is replaced with the assigned per unit area value for different land use types; correction coefficients for population density, are also omitted. The gross domestic product stands for economic vulnerability, land use type for environmental vulnerability, and population density stands for vulnerability of human lives.

Given that the population density data are available from the Fifth Population Census of China in 2000, correspondingly, data from year 2000 are also used for the gross domestic product per unit area and the land use type indicators. The gross domestic product, land use type, and population density spatial data are extracted

from the basic geographic database of China set up by the Institute of Geographic Sciences and Natural Resources Research, Chinese Academy of Sciences, at a resolution of $1 \text{ km} \times 1 \text{ km}$. Gross domestic product is expressed in ten thousand Yuan per km^2 , and population density is expressed in person/ km^2 . Land use type is available as vector data for each province. These are converted into raster images with a spatial resolution of $1 \text{ km} \times 1 \text{ km}$ to facilitate spatial analysis in combination with gross domestic product and population density. Domestic product and population density data are normalized into the range of 0–1, and values in the same range are assigned to different land use types, including unused land (0), water area (0.2), grassland (0.4), forest land (0.6), cultivated land (0.8), and land used for industrial, mining, and residential purposes in urban and rural areas (1).

Using the normalized raster data of gross domestic product (G), land use type (L), and population density (D) and Eq. 1, vulnerability to landslides and debris flows is calculated and the resulting map is shown in Fig. 11. Vulnerability is classified into 5 levels.

Landslide and debris flow disaster risk map: With the natural disaster risk definition from the United Nations (United Nations Office for the Coordination of Humanitarian Affairs 1992; Li et al. 2005), landslide and debris flow disaster risk is calculated as:

$$R = H \times V \tag{2}$$

wherein, R is risk (0–1); H is hazard (0–1); and V is vulnerability (0–1).



Fig. 11 Vulnerability to landslides and debris flows in China (Source Shi 2011, p. 77)

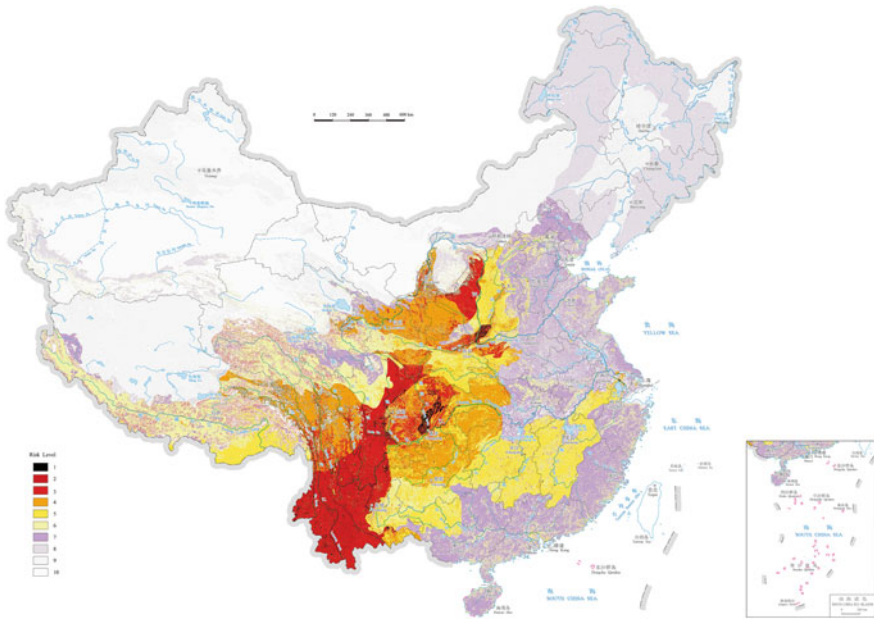


Fig. 12 Landslide and debris flow disaster risks in China (Source Shi 2011, p. 78–79)

The hazard map is rasterized and converted into a 1 km × 1 km resolution raster image. With the spatial analysis function of ArcGIS, the hazard and vulnerability raster data are multiplied to generate the map of landslide and debris flow disaster risks in China. The landslide and debris flow disaster risks are divided into 10 levels (Fig. 12).

2.2 Landslide and Debris Flow Disaster Risk Analysis

The areal percentage of all risk levels is shown in Fig. 13. Regions with extremely high and high risks (levels of 1, 2, and 3) account for 3 % of the total land area, where development should be prohibited and disaster risks should be vigorously reduced and avoided. Regions with moderate risks (levels of 4, 5, 6, and 7) account for 28 % of the total area and are considered as limited development area, where disaster risk prevention should be strengthened and risk should be reduced. Regions with low and extremely low risks account for 68 % of the total area and are considered as suitable development area, where risk can be accepted or neglected. Although landslide and debris flow hazards are very serious in China, on the whole the country does not face extremely high risk of landslide and debris flow disasters, because the western area with serious hazards and the eastern area with high vulnerability do not overlap. However, with further development of the economy

and society and increase of population, economic, environmental, and human vulnerability to landslide and debris flow disasters in China will further increase. In particular, with the gradual development of the western regions and the decrease of economic disparity between the east coastal areas and the west, overlap of areas with high vulnerability and serious hazards will grow. Therefore, before China becomes a moderately developed country and its population starts to decrease, the

Table 1 Risk of landslide and debris flow disasters for some provinces of China

Province	Extremely low risk	Low risk	Moderate risk	High risk	Extremely high risk
Beijing	–	○	○	–	–
Hebei	○	○	○	○	–
Shanxi	○	○	○	○	○
Inner Mongolia	○	○	○	○	–
Liaoning	○	○	○	–	–
Jilin	○	○	○	–	–
Heilongjiang	○	○	○	–	–
Jiangsu	○	○	○	○	–
Zhejiang	○	○	○	○	–
Shandong	○	○	○	–	–
Anhui	○	○	○	○	–
Henan	○	○	○	○	–
Jiangxi	○	○	○	○	–
Hubei	○	○	○	○	–
Hunan	○	○	○	○	–
Fujian	○	○	○	○	–
Guangdong	○	○	○	–	–
Hong Kong	–	○	○	–	–
Hainan	○	○	○	–	–
Sichuan	○	○	○	○	○
Chongqing	–	○	○	○	○
Guangxi	○	○	○	○	–
Guizhou	○	○	○	○	○
Yunnan	○	○	○	○	○
Xizang	○	○	○	○	–
Shaanxi	○	○	○	○	○
Gansu	○	○	○	○	–
Ningxia	○	○	○	○	○
Qinghai	○	○	○	○	–
Xinjiang	○	○	○	–	–

Note ○ indicates “exists”; – indicates “does not exist”

Source Liu et al. (2011)

risk of landslide and debris flow disasters in China will continue to increase and the total area of regions with high risk will also increase.

Risk of landslide and debris flow disasters is a combined result of hazard and vulnerability—risk is not necessarily the highest in areas where the hazard is most serious, nor in areas with the highest vulnerability—risk is extremely high only where the hazard and vulnerability are both at their worst. Therefore, each provincial administrative unit has differentiated risk composition within its area. Extremely low risk areas exist in all provincial-level administrative units except in Beijing, Hong Kong, and Chongqing. The provincial-level administrative units that have high and extremely high risk areas are Sichuan, Chongqing, Guizhou, Yunnan, Shaanxi, Ningxia, and Shanxi (Table 1). In Beijing and Hong Kong, the socioeconomic development level and thus vulnerability is high, and these places do not have any extremely low risk area due to this high vulnerability. On the other hand, Beijing and Hong Kong also do not have high and extremely high risk areas because there is no serious landslide and debris flow hazard areas in these places.

3 Responses to the Flush Flood and Debris Flow Disaster in Zhouqu County, Gansu Province

3.1 Disaster Situation

Flush flood and debris flows in Zhouqu County: Affected by heavy rainstorms, the Sanyanyu and Luojiayu gullies in Zhouqu County of Gansu Province suffered from an ultra-large debris flow disaster from 11 to 12 p.m. on August 7, 2010 (Figs. 13 and 14). After running out of the mountain passes, the debris flows rushed into Yueyuan Village, Beiguan Village, Beijie Village, Dongjie Village, Nanmen Village, Chunchang Village, Luojiayu Village, and Wachang Village along the gully beds, burying farmland and destroying buildings on its way, leveling Sanyanyu to the ground. After running out of the mountain pass, the debris flow from the Sanyanyu gully formed an accumulation area, which is about 2 km in length and 170–270 m (maximum 350, 80 m in the city, average 200 m) in width, with the accumulation thickness of 2–7 m (average about 4 m); after running out of the mountain pass the debris flow from the Luojiayu gully formed an accumulation area with the length of 2.5 km, average width of about 70 m, and average accumulation thickness of 2 m (Hu et al. 2010). The instantaneous maximum speed of flush flood and debris flow front in Sanyanyu at the mountain pass reached 27 m/s, and the debris flow reached the city in 2.1 min after exiting the mountain pass; the instantaneous maximum speed of flush flood and debris flow front in Luojiayu reached 14.76 m/s, and the debris flow reached the city in 4.3 min (Ministry of Land and Resources of the People's Republic of China 2010).

It was estimated that solid deposits carried by the flush flood and debris flows in the Sanyanyu gully and the Luojiayu gully north of the Zhouqu County urban area

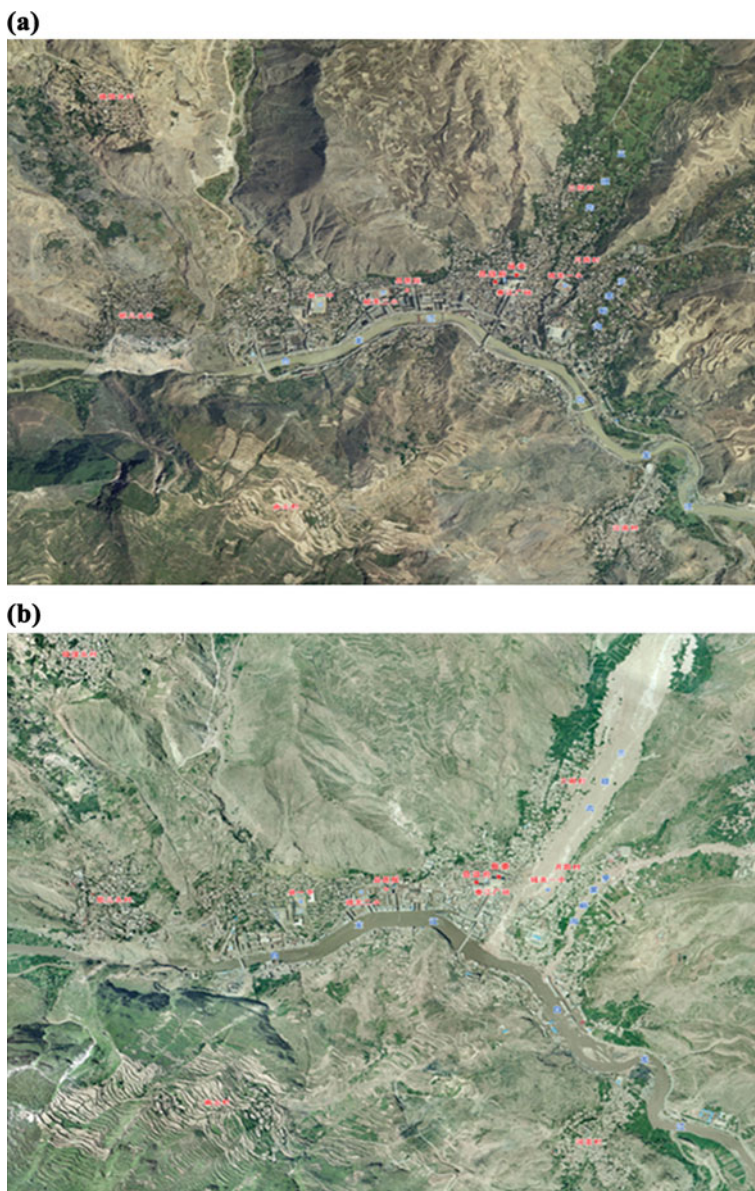


Fig. 13 **a** Aerial photos of the Zhouqu County urban area before (July 2008) and **b** after (August 8 2010) the August 7, 2010 debris flow disaster (scale 1:4,000) (*Source* Ministry of Land and Resources of China and State Bureau of Surveying and Mapping of China 2008, 2010)

amounted to 1.81 million m^3 in total, of which 1.5 million m^3 was deposited by the flush flood and debris flow in the Sanyanyu gully (about 1 million m^3 was deposited on the bank and about 0.5 million m^3 entered the Pai-lung River); solid deposits



Fig. 14 Debris flow site in the Zhouqu County urban area (Source Ministry of Land and Resources of China 2010)

carried by the flush flood and debris flow in the Luojiayu gully reached 0.31 million m^3 (about 0.21 million m^3 was deposited on the bank, and 0.1 million m^3 entered the Pai-lung River) (Ministry of Land and Resources of the People's Republic of China 2010). The length, width, and height of the largest megalith on the debris flow fan in the Sanyanyu gully were 6, 5.8, and 4.9 m, respectively. An additional over 40 other megaliths bigger than 30 tons were left on the debris flow fan; the length, width, and height of the largest megalith on the debris flow fan in the Luojiayu gully were 5.2, 3.5 and 2.4 m respectively. Buildings were mainly destroyed by the megaliths in the debris flows (Yu et al. 2010).

Formation conditions of the flush flood and debris flows in Zhouqu:

(1) Water condition: From 8 a.m. on August 7 to 8 a.m. on August 8, 2010 (Beijing time), southern Gansu experienced a heavy rainstorm. The distribution of the rainstorm belt was in northwest–southeast direction, with the precipitation center located in Dingxi, Minxian, Lintao, and other counties (cities) in Gansu Province. This rainfall process was characterized by short duration, high intensity, strong local concentration, and uneven spatial distribution. According to the observation data from the national basic weather stations, the 24 h accumulated precipitation from 8 a.m. on August 7 to 8 a.m. on August 8 was highest in Dingxi of Gansu (55 mm), followed by Minxian (50.9 mm). Based on the encrypted automatic weather station observation data of Gansu, the 1 h precipitation in the Sanyanyu gully and the Luojiayu gully in Zhouqu County at 11 p.m. on August 7 reached 96.7 mm, while the 0.5 h instantaneous precipitation amounted to 77.3 mm. These 24 h accumulated precipitation and 1 h precipitation intensity

exceeded the extreme value since the local weather records started. It was the sudden heavy rainfall that caused the rare large flush flood and debris flows in this area (Zhao and Cui 2010).

(2) Geological conditions: The exposed lithology in the Zhouqu area is mainly Devonian and Permian gray phyllite, siliceous limestone, carbonaceous shale, and slate, among others. The rocks underwent tectonic movements for many times. The folds, fissures, and joints are well developed and can easily form debris and clay through weathering. Under the influence of tectonic movement and earthquakes, collapse and landslides in Sanyanyu and Luojiayu are relatively developed. The resulting loose materials accumulate in gullies and become the main source of debris flow substances. According to historical data, in 1879, a magnitude 8.0 earthquake occurred in the Wen County and Wudu District area, producing huge amounts of slumped masses that accumulated in gullies, as well as various multi-level fill dams that blocked the gullies (Hu et al. 2010). Wherein, the Dayu and Xiaoyu of Sanyanyu formed four fill dams with heights ranging from 80 to 280 m. The four branch gullies of Sanyanyu underwent eight landslides in total, with a sliding area of 0.88 km^2 , total landslide volume of $1303.9 \times 10^4 \text{ m}^3$, along with 58 collapse bodies that have a volume of about $2830.1 \times 10^4 \text{ m}^3$. In addition, another about $1,029 \times 10^4 \text{ m}^3$ of slump, collapse, and gully deposits accumulated in the Sanyanyu gully. The total of the above reached $5,163 \times 10^4 \text{ m}^3$ in volume, which can provide $2,510 \times 10^4 \text{ m}^3$ loose solid substances for debris flows (Ma and Qi 1997). A field investigation at the Luojiayu gully and the remote sensing images reveal that solid material in the gully was similar to that in Sanyanyu, mainly supplied by deposits from the slopes (Hu et al. 2010).

(3) Topographical condition: The Sanyanyu gully basin is a primary branch of the Pai-lung River at its left bank, with a drainage area of 25.75 km^2 and is scoop shaped. On the whole, the basin spreads along the North–South direction and is higher in the north and lower in the south—a typical mountain and canyons terrain. The elevation of the steep rocky mountain at the peak of the drainage basin is 3,828 m, while the lowest point at the estuary is only 1,340 m in elevation, with relative height difference of 2,488 m. The mountain area is mainly composed of medium/high mountains, with relative height difference of more than 1,000 m and in most cases gradients of more than 50° . There are 59 gullies of different sizes, of which 13 have a length exceeding 1 km. The length of the main gully is 6.8 km, and the average density of gullies is 1.87 km/km^2 . Average gradient of the gullies is 24.1 % (upstream 30 %, midstream 25.5 %, and downstream 9.8 %). Due to the intense erosion of gullies, the cross section shows a “V” shape or a narrow and deep “U” shape. These features of the terrain not only favor flow accumulation, but also provide adequate energy for the formation and movement of debris flows. The area of the debris flow fan in the Sanyanyu gully is 0.87 km^2 and on this the Zhouqu County urban area and 10 natural villages at the suburb are located (Ma and Qi 1997). According to the field survey and interpretation of remote sensing imageries, the terrain and land cover of Luojiayu are similar to that of Sanyanyu, which is conducive to debris flow activity (Hu et al. 2010).

3.1.1 Flush Flood and Debris Flow Disaster

According to the statistics, the debris flow disaster affected 4,496 families and 20,227 people, and buried and destroyed about 93 ha of cultivated land. The flush flood destroyed the houses of 307 households (5,508 rooms), among which 235 were rural houses and 72 were houses of urban residents. An additional 4,189 houses (20,945 rooms) were flooded, among which 1,503 were rural houses and 2,686 were houses for urban residents. Twenty-one government office buildings were destroyed by the flood and 18 vehicles were damaged. The worst-hit Yueyuan Village was nearly buried. The debris flows crossed the urban area of Zhouqu County, destroyed some streets and buildings as well as eight bridges, formed a barrier dam in the Pai-lung River with the length of about 550 m and width of about 70 m. The barrier dam blocked the Pai-lung River and formed a barrier lake with backwater up to 3 km. This caused the submersion of a large highway bridge on the river, and half of the city was flooded. Electricity, communication, and water supplies were interrupted (Yu et al. 2010).

This debris flow disaster is the most severe of its kind in the history of the People's Republic of China. It caused 1,501 deaths and 264 people were missing (MLR 2010).

3.2 *Emergency Rescue and Disaster Response*

After the flush flood and debris flow disaster in Zhouqu County, the Chinese President Hu Jintao and Premier Wen Jiabao made specific requests that the government of Gansu Province and relevant departments should prioritize lifesaving, properly handle the barrier lake problem, and rapidly repair critical infrastructures; the People's Liberation Army and Armed Police Force should fully support the disaster relief work.

In early morning of August 8, Gansu Province promptly established the emergency headquarters for the ultra-large flush flood and debris flow disaster, and simultaneously set up the front headquarter of emergency headquarters and formed eight special working groups led by relevant departments and units to ensure sound disaster relief operations.

Two thousand and eight hundred army officers and soldiers from the Lanzhou Military Region were sent to the disaster area for rescue and relief work in early morning of August 8.

At the noon of August 8, Premier Wen Jiabao, together with leaders of concerned ministries of the State Council, departed for the disaster area. They decided to set up the temporary headquarters of Zhouqu flood rescue and relief work led by the State Council and made specific arrangements on the plane.

On August 9, Premier Wen Jiabao changed the plan of returning to Beijing, and went again to the worse-hit area where secondary disasters may happen, to direct the relief work.

In the morning of August 10, the Standing Committee of the Political Bureau of CCCPC (Central Committee of the Communist Party of China) held a meeting for the comprehensive arrangements of rescue and relief work with regard to the ultra-large flush flood and debris flow disaster in Zhouqu County.

Barriers in the watercourse of the Bai-lung River were removed successfully through the cooperation among the People's Liberation Army, Armed Police Force, and water experts. As a result, the danger of dam break was eliminated at the night of August 12.

National mourning was held on August 15, during which people of all nationalities in China expressed their deep condolences to the victims of the flush flood and debris flow disaster. Meanwhile, leaders of some foreign countries and regional organizations expressed their condolences to the leaders and government of China with regard to the disaster.

By August 15, the Department of Civil Affairs of Gansu Province received donations of RMB 106 million Yuan and goods and materials valued RMB 20.356 million Yuan for Zhouqu disaster relief.

By 6 p.m. on August 16, 66 severely injured people had been hospitalized, among which 58 were transferred to other hospitals for treatment and 5 had recovered. A total of 1,591 people were treated as outpatient, and 1,243 people were successfully rescued.

By August 17, the Red Cross of Gansu Province received disaster relief donation and materials and goods of RMB 47.63 million Yuan, among which donation and goods and materials valued RMB 40.0512 million Yuan and RMB 7.57 million Yuan, respectively.

By August 18, various rescue and dredging work had been performed intensively and orderly in the city. With the dredging being finished on the main North-South street in the city, some shops started to resume business, providing plentiful daily necessities that basically satisfied the needs of the residents in the disaster area. Post-disaster reconstruction had been put on the agenda and it was decided that the reconstruction should be preliminarily on the original sites.

3.3 Restoration and Reconstruction

Debris flow blocking and drainage works located in the Sanyanyu and Luojiayu gullies were almost completely destroyed after the ultra-large debris flow on August 7, resulting in lost disaster prevention and reduction functions. The newly built temporary debris flow drainage gutters in Sanyanyu and Luojiayu have earth embankment and bottom and limited drainage capacity, and can easily be damaged. Protection projects in the Zhaizi gully, Laoya gully, Xiaoshui gully, and Longmiao gully were of low-grade and are dated, some have been partially damaged and out-of-repair for many years, which enormously weakens the disaster prevention capability. On account of the tremendous danger of debris flow around the Zhouqu County urban area and the difficult situation of disaster prevention, it was urgent to

take control measures in the six debris flow gullies including Sanyanyu, Luojiayu, Zhaizi, Laoya, Xiaoshui, and Longmiao gullies near the city. This is critically important for improving the disaster prevention and reduction ability of the city, protecting lives, and properties of this ethnic minority area, improving the regional ecological environment, and ensuring safe floodwater discharge in the lower reach of the river (Ma 2010).

Guiding principles and criteria of disaster prevention and control measures:

Reconstruction work after the disaster must comply with the requirements of a people-orientation approach, taking into adequate consideration of the natural conditions, with scientific planning, sound layout, and strong policy support and joint implementation. Meanwhile, it should be combined with the promotion of harmony and unity for people of different ethnic origins, improvement of people's living standard, enhancement of disaster prevention capacity, and improvement of the ecological environment. In accordance with the characteristics of debris flow formation, flow, and accumulation in the gullies as well as disaster formation mechanism, urban flood control and disaster prevention reality, and layout of the city the following debris flow control principles should be followed: (1) conduct overall planning and comprehensive control; (2) combine engineering control measures and ecological environment protection wherein engineering control should be the main measure; (3) ensure sufficient sediment-retaining capacity of reservoir by combing blocking and drainage works wherein slope stabilization and sediment blocking should be the main measures; (4) combine the control measures on gully and slope wherein those on gully should be the chief measures; (5) make overall plans and take all factors into consideration for the debris flow blocking and drainage works, urban planning and construction, and watercourse maintenance of the Pai-lung River in Zhouqu.

In China, the *Design Code of Debris Flow Prevention and Control Project* (DZ/T0239-2004) issued by the Ministry of Land and Resources of the People's Republic of China is often used as a reference for the debris flow prevention and control works, and the design of debris flow prevention and control projects in urban areas applies the *Flood Prevention Standard* (GB50201-94) and the *Urban Flood Prevention Project Design Code* (GBJ79-2002). For the Zhouqu County urban area, a small city with a population less than 200,000, the debris flow defense standard should be 50-year return period, and the debris flow defense project in Sanyanyu designed in 1997 had met this standard. However, the debris flow defense works were totally damaged during the ultra-large debris flow disaster on August 7, indicating that the previous defense level is clearly too low.

The occurrence frequency of the ultra-large debris flow disaster on August 7, 2010 is extremely low—with a 200-year return period, but it can cause great damage. Therefore, the defense level by rainfall frequency and flood prevention standard is much lower than what is necessary for protection against the debris flow of this scale and frequency. According to the experiences of Chinese and international flush flood and debris flow disaster prevention and control, experts propose to take the largest disaster in history (that is, the ultra-large debris flow on August 7—as a common practice) rather than rainfall frequency or flood frequency as the

defense standard for debris flow in Sanyanyu and Luojiayu, and adopt 100-year return period defense standard for Zhaizi gully, Laoya gully, Xiaoshui gully, and Longmiao gully (Ma 2010).

Control measures: According to the formation, flow, accumulation characteristics and disaster formation mechanism of debris flows in the six gullies including Sanyanyu, Luojiayu, the existing layout of the Zhouqu urban area, as well as the watercourse conditions and hydrological characteristics of the Pai-lung River section near the city, and by taking into consideration the guiding principles identified above, experts put forward a comprehensive treatment scheme combining blocking and draining measures and biological control measures and integrating draining engineering, urban planning, and dredging of the Pai-lung River channel (Ma 2010), as the implementation program for debris flow disaster prevention and control in Zhouqu County. Starting from the debris flow source area, this program aims to eliminate the possibility of hazard formation and forms a complete and systematic debris flow prevention system together with a series of measures adopted in the flow course area, accumulation area, and before entering the river. It will reduce the amount of solid substances supply, retain the solid substances in debris flows, stabilize the gully beds and slopes, reduce the peak flow of debris flows, and the amount of sediments they carry, and relieve the pressure of sediments on the floodwater drainage network of the city and the Pai-lung River. Specifically, this is done mainly through building slope stabilizing dams, anti-slide piles, slope protection retaining walls, bank protection dams, sediment storage dams, anti-scour lips, and planting trees and grass. Meanwhile, build new debris flow drainage works and upgrade some debris flow drainage works to new design standards, improve urban planning for the debris flow-prone area in the city, dredge the blocked channel in the Pai-lung River section near the city, and smoothly drain the controlled debris flow into the Pai-lung River, to protect lives and properties in the city.

References

- Du, R.H., Z.C. Kang, X.Q. Chen, et al. 1987. *Comprehensive investigation and control planning for debris flows in the Xiaojiang River Basin of Yunnan Province*. Chongqing: Chongqing Branch of Science and Technology Academic Press (in Chinese).
- Hu, K.H., Y.G. Ge, P. Cui, et al. 2010. Preliminary analysis of extra-large-scale debris flow disaster in Zhouqu County of Gansu Province. *Journal of Mountain Science* 28(5): 628–634.
- Huang, R.Q. 2007. Large-scale landslides and their sliding mechanism in China since the 20th century. *Chinese Journal of Rock Mechanics and Engineering* 26(3): 433–454 (in Chinese).
- Institute of Mountain Hazards and Environment, Chinese Academy of Sciences. 1991a. *Map of landslide Distribution in China* (1: 6,000,000). Chengdu: Chengdu Maps Press (in Chinese).
- Institute of Mountain Hazards and Environment, Chinese Academy of Sciences, 1991b. *Distribution and hazard zoning map of debris flows in China* (1:6,000,000). Chengdu: Chengdu Maps Press (in Chinese).
- Kang, Z.C., C.F. Li, A.N. Ma, et al. 2004. *Research on debris flow in China*. Beijing: Science Press (in Chinese).
- Li, S.D. 1999. The temporal and spatial distribution of landslide and debris flow disasters in China. *Research of Soil and Water Conservation* 6(4): 33–37 (in Chinese).

- Li, H.L., and S.W. Zeng. 1982. *Debris flow in Gansu*. Beijing: China Communications Press (in Chinese).
- Li, Y.S., J.H. Gu, L.Y. Zou, et al. 2005. *Collections of basic terms relevant to disaster management in English and Chinese*. Beijing: Standard Press of China (in Chinese).
- Liu, X.L., and D.W. Mo. 2002. Site-specific debris flow vulnerability assessment. *Geographical Research* 21(5): 569–577 (in Chinese).
- Liu, X.L., and D.W. Mo. 2003. *Evaluation of debris flow risk*. Chengdu: Sichuan Science and Technology Press (in Chinese).
- Liu, X.L., C.J. Yu, and Z.H. Shang. 2011. Risk mapping and spatial pattern of debris flow and landslide hazards in China. *Journal of Basic Science and Engineering*. 19(5): 721–731 (in Chinese).
- Ma, D.T. 2010. Some suggestions on controlling catastrophic debris flows on Aug. 8th, 2010 in Zhouqu, Gansu. *Journal of Mountain Science* 28(5): 635–640 (in Chinese).
- Ma, D.T., and L. Qi. 1997. Study on comprehensive controlling of debris flow hazard in Sanyanyu gully. *Bulletin of Soil and Water Conservation* 17(4): 26–31 (in Chinese).
- MLR (Ministry of Land and Resources of the Peoples' Republic of China). 2005. *National geological disaster bulletin, August* (in Chinese).
- MLR (Ministry of Land and Resources of the Peoples' Republic of China). 2006. *National geological disaster bulletin, August* (in Chinese).
- MLR (Ministry of Land and Resources of the Peoples' Republic of China). 2007. *National geological disaster bulletin, August* (in Chinese).
- MLR (Ministry of Land and Resources of the Peoples' Republic of China). 2008. *National geological disaster bulletin, August* (in Chinese).
- MLR (Ministry of Land and Resources of the Peoples' Republic of China). 2009. *National geological disaster bulletin, August* (in Chinese).
- MLR (Ministry of Land and Resources of the Peoples' Republic of China). 2010. *National geological disaster bulletin, August* (in Chinese).
- MLR (Ministry of Land and Resources of the Peoples' Republic of China). 2011. *National geological disaster bulletin, August* (in Chinese).
- MLR (Ministry of Land and Resources of the Peoples' Republic of China). 2012. *National geological disaster bulletin, August* (in Chinese).
- MLR (Ministry of Land and Resources of the Peoples' Republic of China). 2013. *National geological disaster bulletin, August* (in Chinese).
- MLR (Ministry of Land and Resources of the Peoples' Republic of China). 2014. *National geological disaster bulletin, August* (in Chinese).
- Shi, P.J. 2002. Theory on disaster science and disaster dynamics. *Journal of Natural Disasters* 11 (3): 1–9 (in Chinese).
- Shi, P. 2011. *Atlas of natural disaster risk of China*. Beijing: Science Press (in Chinese and English).
- United Nations Office for the Coordination of Humanitarian Affairs. 1992. *Internationally agreed glossary of basic terms related to disaster management, DNA/93/36*. Geneva: United Nations.
- Wang, X.Y., G.Z. Nie, and D.W. Wang. 2010. Research on the relationship between landslides and peak ground accelerations induced by Wenchuan Earthquake. *Chinese Journal of Rock Mechanics and Engineering* 29(1): 82–89 (in Chinese).
- Wang, J.A., P.J. Shi, P. Wang, et al. 2006. *Spatiotemporal patterns of natural disasters in China*. Beijing: Science Press (in Chinese).
- Yang, J.C., and Y.L. Li. 2005. *Geomorphology theory*. Beijing: Peking University Press (in Chinese).
- Yu, B., Y.H. Yang, Y.C. Su, et al. 2010. Research on the giant debris flow hazards in Zhouqu County, Gansu Province on August 7, 2010. *Journal of Engineering Geology* 18(4): 437–444 (in Chinese).

- Zhao, Y.C., and C.G. Cui. 2010. A study of rainstorm process triggering Zhouqu extreme mudslide on 8 August 2010. *Torrential Rain and Disasters* 29(3): 289–295 (in Chinese).
- Zhang, X.B., and J. Liu. 1989. *Debris flow area in the Daying River Basin of Yunnan Province*. Chendu: Chendu Cartographic Publishing House (in Chinese).

Typhoon Disasters in China

Weihua Fang, Xingchun Zhong and Xianwu Shi

Abstract This chapter first introduces the spatial and temporal patterns of typhoon activities and its induced disaster losses in China from 1949 to 2010. Typhoon risk is then systematically assessed by taking into account the hazard, vulnerability, and exposure. Typhoon disaster risk in terms of direct economic losses is mapped. Finally, disaster response and coping mechanisms are analyzed through the cases of Typhoon Wanda and Typhoon Saomai.

Keywords Typhoon · Spatiotemporal pattern · Risk assessment

According to the statistics of typhoon best track data issued by the China Meteorological Administration from 1949 to 2009, the Northwest Pacific regions had generated a total of 2,035 tropical cyclones, 33.4 per year on average; 1,646 cyclones were above tropical storm level, at 27.0 per year. Frequent typhoons have posed a serious threat to people's lives and property in the southeastern coastal areas of China. According to the typhoon disaster loss data of China during 1985–2002, deaths caused by typhoon each year is, on an average, 483 people, while 490,000 houses collapsed, and the direct economic losses were RMB 34.7 billion Yuan (price in 2000). In recent years, with rapid socioeconomic development in the southeast coastal areas, various damages caused by typhoon assume an clear upward trend.

With the support of the Ministry of Science and Technology, we have participated in the research of typhoon disaster and risk in the third topic Comprehensive Risk Prevention Technology Integration Platform Research (2006BAD20B03) of the National Eleventh Five-Year Science and Technology Support Project—Comprehensive Risk Management Key Technology Research and Demonstration,

W. Fang (✉) · X. Zhong
Key Laboratory of Environmental Change and Natural Disasters
of Ministry of Education, Beijing Normal University, Beijing 100875, China
e-mail: weihua.fang@bnu.edu.cn

X. Shi
National Marine Hazard Mitigation Service, Beijing 100194, China

using 1×1 km grid as the unit to assess the expected exceeding probability of GDP loss rate, rural housing collapse rate, and agricultural disaster rate. Moreover, we were involved in the fourth topic Comprehensive Study of Disasters and Risk Analysis Technology (2008BAK49B04) of the National Eleventh Five-Year Science and Technology Support Project—Catastrophe Emergent Relief Information Integration System and Demonstration in China, and carried out research and system development of China's typhoon disaster rapid loss assessment index model; meanwhile, we have participated in the typhoon and storm surge correlational research in the seventh topic “Research on Yangtze River Delta Region Natural Disaster Risk Assessment Technology” (2008BAK50B07) of the National Eleventh Five-Year Science and Technology Support Project—Research on Comprehensive Evaluation Technology of China's Major Natural Disaster Risk. This chapter is a summary of the above research.

Partial results of this chapter were achieved on the basis of the *Integrated Risk Governance: Database, Risk Mapping and Network Platform* (Fang et al. 2011) and *Atlas of Natural Disaster Risk of China* (Shi 2011).

1 Spatial and Temporal Patterns of Typhoon Disasters

1.1 Frequency of Historical Typhoon Events

Typhoons happened in China are mainly concentrated in 18° – 26° N, which covers various southern provinces from Hainan to Fujian (Chen et al. 1999). In light of the influence range of typhoons, the vast coastal areas, north from Liaoning Province and south to Hainan Province, are subject to typhoon attacks. Nearly 20 provinces and direct controlled municipalities in eastern China are directly affected by tropical cyclones.

According to recent statistics, the area southeast of the Hainan Island is most frequently experiencing tropical cyclones on annual basis; among all the coastal provinces, direct controlled municipalities and autonomous regions of China, Guangdong, and Guangxi Provinces are most frequently stricken by tropical cyclones, followed by Hainan Province. Along the east coast from south to north, from Fujian, Zhejiang, Jiangsu, Shandong, to Liaoning Provinces, tropical cyclone occurrences decrease. Meanwhile, from the coastal region to inland, the frequency of tropical cyclones also decreases. To the west, Qinghai, Gansu, Tibet, and Xinjiang Provinces/Autonomous Regions have never been hit by tropical cyclones.

Since 1949, the overall frequency of both the tropical cyclones or typhoons (that is, tropical storm and strong tropical storm, typhoon, strong typhoon, super typhoon with equivalent strength or above) originated in Northwest Pacific and tropical cyclones or typhoons landing China (Fig. 1) has decreased; however, the proportion of typhoons in total tropical cyclones is increasing gradually.

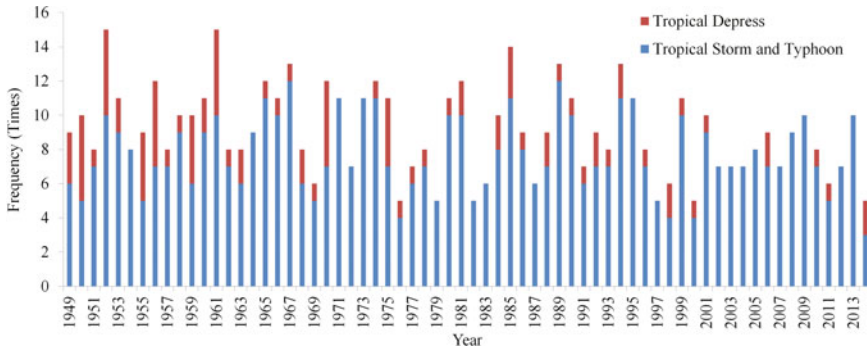


Fig. 1 Frequency of Northwest Pacific tropical cyclone and typhoon landfalls in China, 1949–2014 (Data Source CMA 2015)

1.2 Spatial and Temporal Patterns of Historical Typhoon Tracks

Decadal variation of tracks: The number of tropical cyclone tracks for each 1×1 km grid in every decade between 1949 and 2009 is shown in Fig. 2. The general spatial patterns of tracks in the six decades are very similar, with frequent tracks in South China Sea and east of the Philippines. The frequency of tropical cyclone reveals two distinct dividing track areas, one is along Japan, Ryukyu Island, the Island of Taiwan of China, and the Philippines, and another is China’s mainland coastline. Decadal differences, although not significant, do exist. For example, in the 1950s, the tracks moved eastward, almost all high value areas appeared to the east of the Philippines. In the 1980s, no clear high frequency area existed. It should be noted that in all six time periods tropical cyclones spread to the middle Yangtze River basin, indicating that tropical cyclones advance along the Yangtze River to inland.

Seasonal variation of tracks: The total tropical cyclone tracks by grid in each season over the Northwest Pacific basin is displayed in Fig. 3. It is clear that there are great seasonal variations. The summer (June, July, and August) and the autumn (September, October, and November) are the two seasons with highest (up to 50 in total) tropical cyclone occurrences. In the winter (December, January, and February) the frequency is low, which is only about one fourth of the annual average. The Taiwan Island becomes an obstacle when tropical cyclone moves to mainland China. In the spring (March, April, and May) the high value area moves slightly northward.

On the other hand, existing research on the latitude of typhoon landing points (Chen et al. 1999) indicates that typhoon moves gradually northward from the spring to the summer and up to the northernmost point in the summer. Then it gradually returns in the autumn. This is consistent with the seasonal variation of tropical cyclone track frequency. The seasonal variation of tropical cyclone origins also shows the same spatial pattern (Chen 1990). Tropical cyclone track frequency varies seasonally.

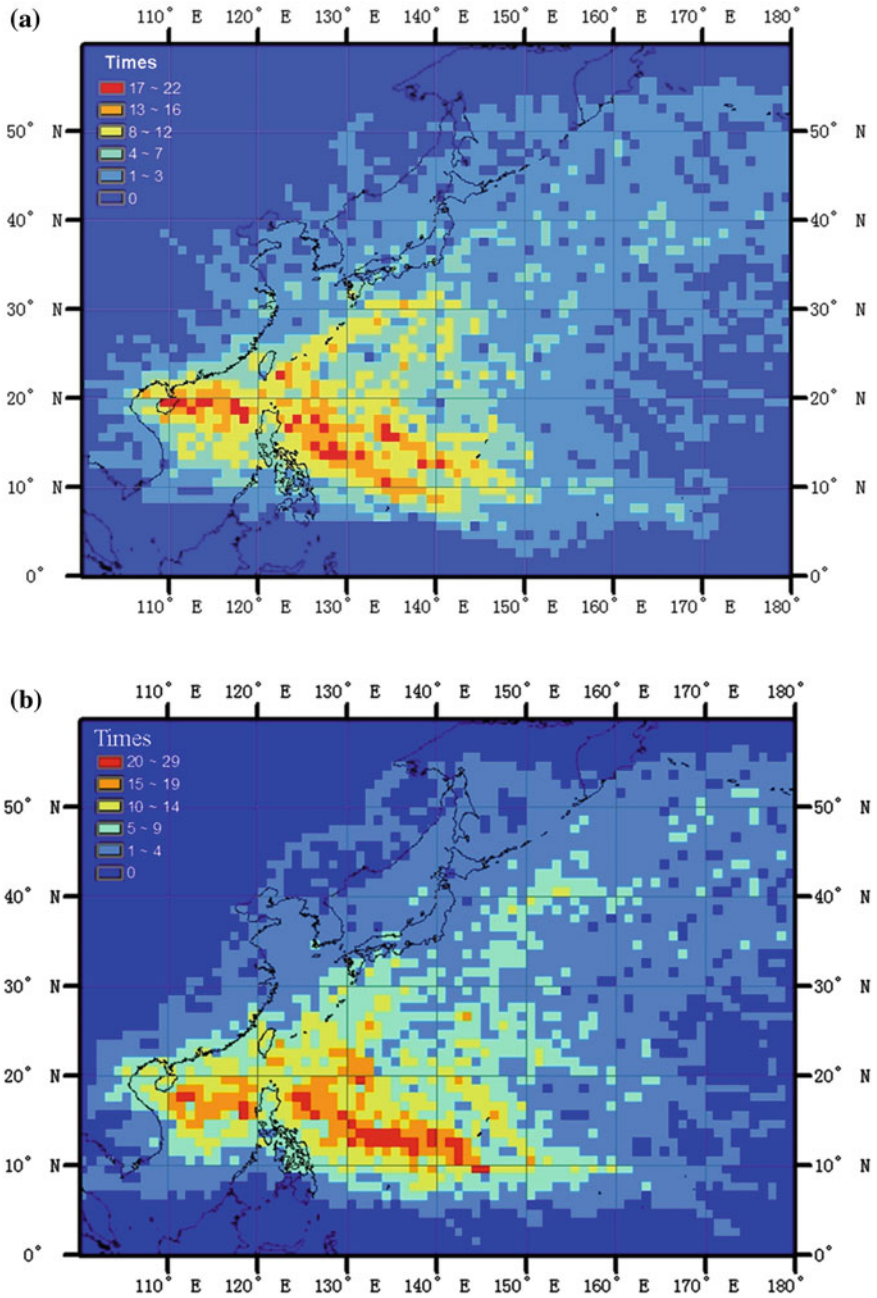


Fig. 2 Decadal variations of tropical cyclone tracks in Northwest Pacific, 1949–2009: Number of tropical cyclone tracks **a** from 1949 to 1960; **b** from 1961 to 1970; **c** from 1971 to 1980; **d** from 1981 to 1990; **e** from 1991 to 2000; and **f** from 2001 to 2009

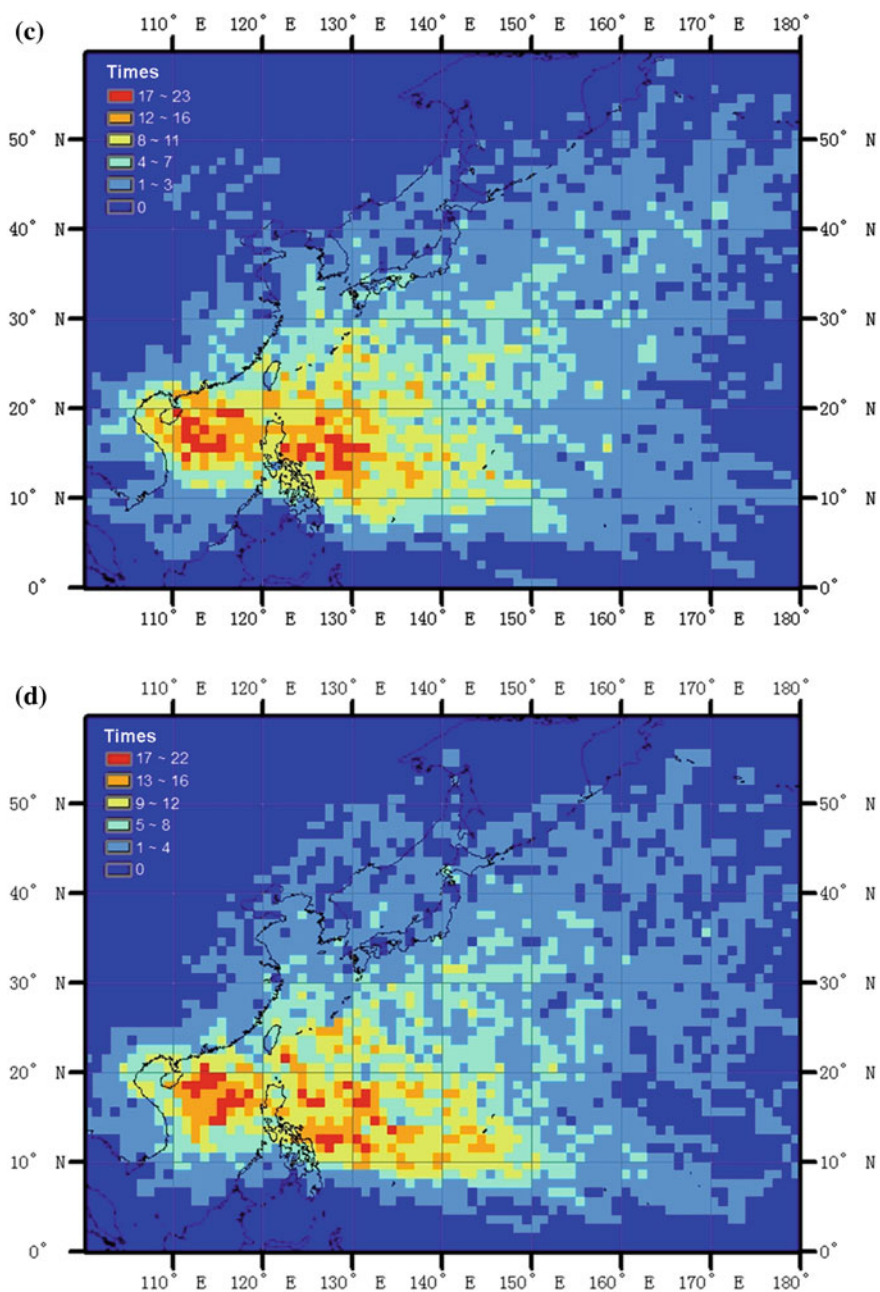


Fig. 2 (continued)

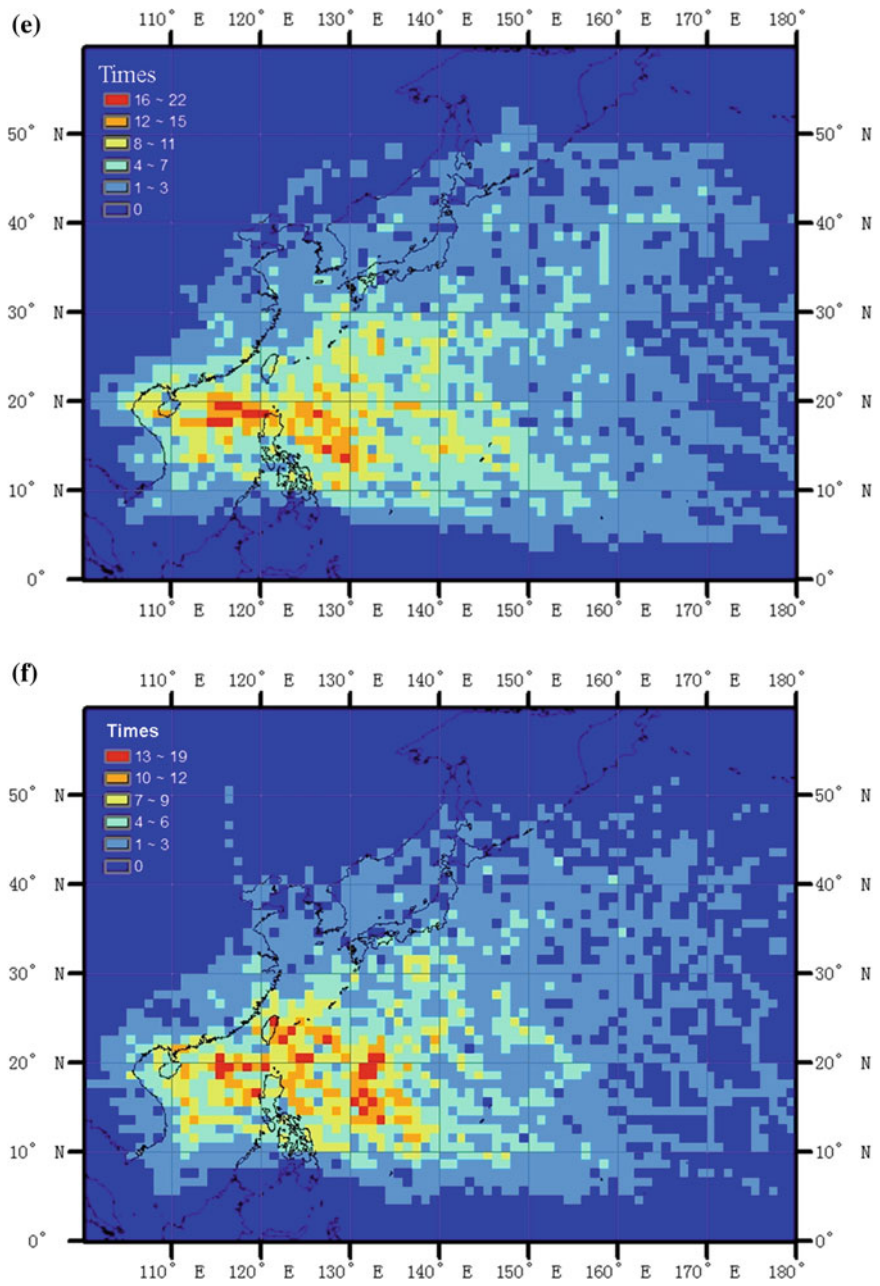


Fig. 2 (continued)

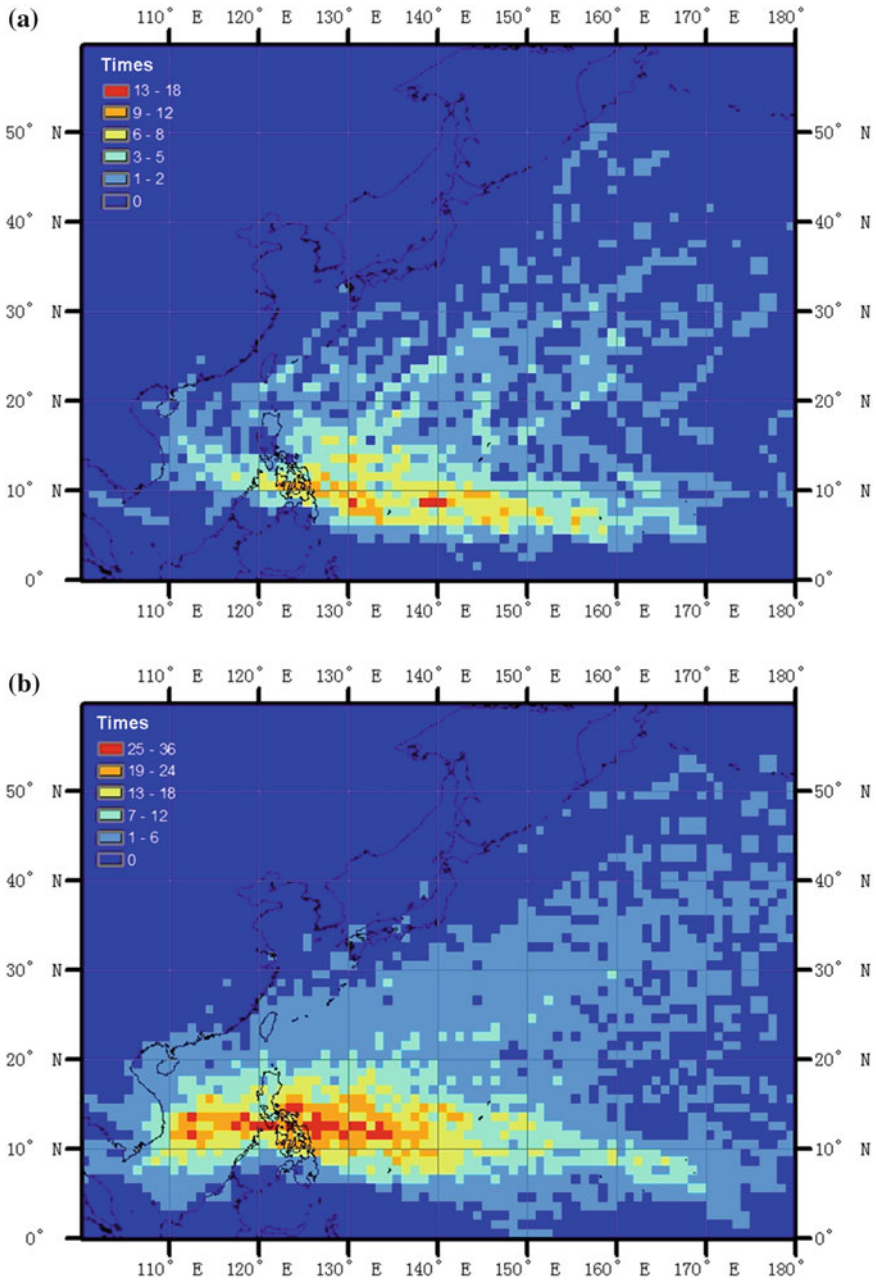


Fig. 3 Seasonal variations of tropical cyclones in Northwestern Pacific, 1949–2009: Number of tropical cyclone tracks **a** in the spring (March, April, and May); **b** in the summer (June, July, and August); **c** in the autumn (September, October, and November); and **d** in the winter (December, January, and February)

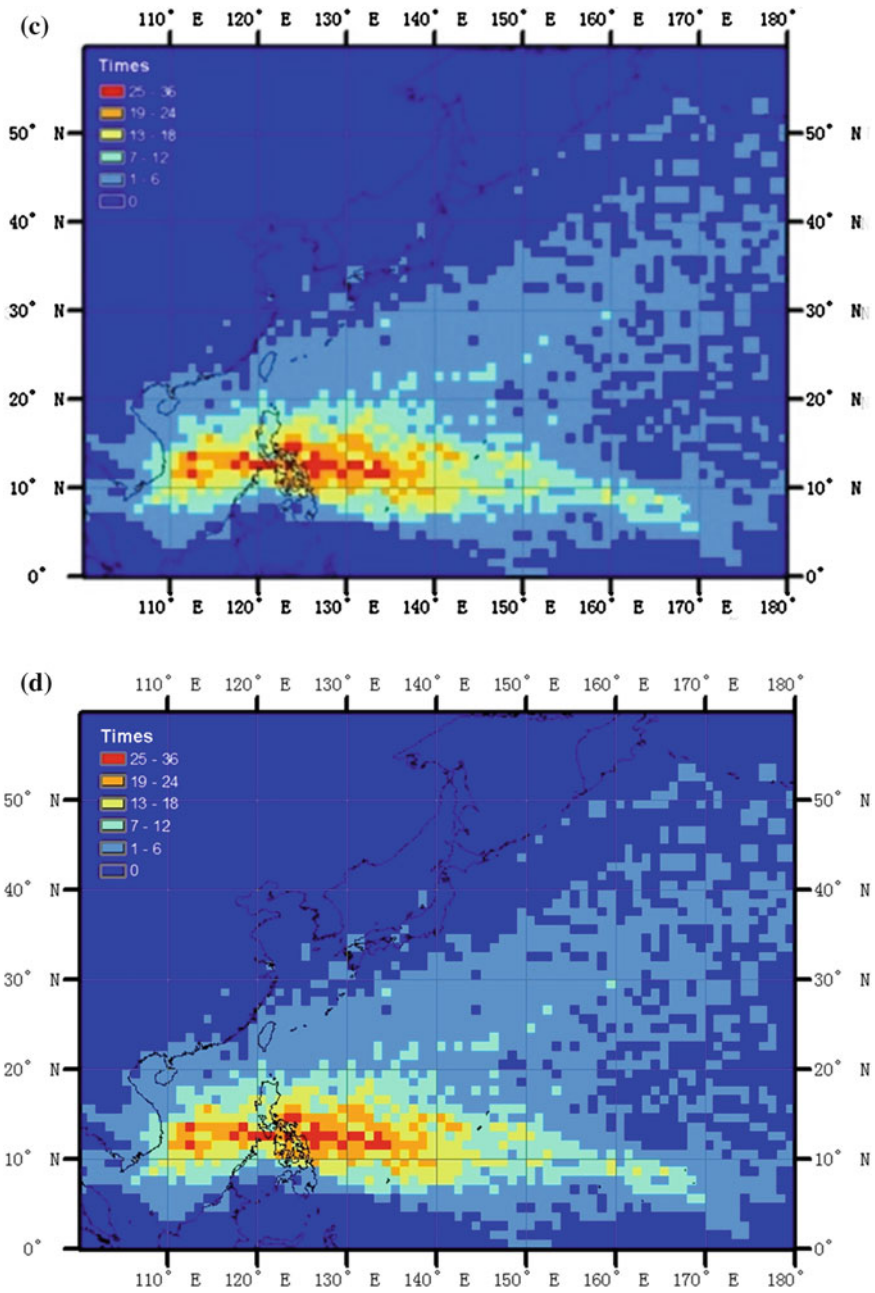


Fig. 3 (continued)

1.3 Spatial and Temporal Patterns of Typhoon Hazard

According to the best track data set issued by the Shanghai Typhoon Institute of China Meteorological Administration, we analyzed the distribution of various degrees of tropical cyclones on Northwest Pacific within 6 h. The results show that typhoon and tropical cyclones with the same strength or above are mainly concentrated in the ocean of 15°–25° N and 120°–140° E. Further to the north and with the landing of tropical cyclones, the cyclone strength becomes significantly weaker. What influence China inland are mostly strong tropical storms and tropical cyclones with lower strength; however, tropical cyclones that directly impact the Taiwan and Hainan Islands have a relatively higher strength.

According to data recorded during the recent 60 years on tropical cyclones, we depicted the spatial distribution of meteorological factors such as daily maximum precipitation and maximum wind speed, respectively for different return periods through modeling. Maximum precipitation and wind speed of tropical cyclones with 20 years return period are taken as an example and shown in Figs. 4 and 5. Typhoon precipitation in China decreases gradually from southeast to northwest and so does the distribution of maximum wind speed. Areas with the strongest typhoon hazard are the Hainan Island and the coastal area of Guangdong Province, followed by the coastal areas of Fujian and Zhejiang Provinces. The smaller the

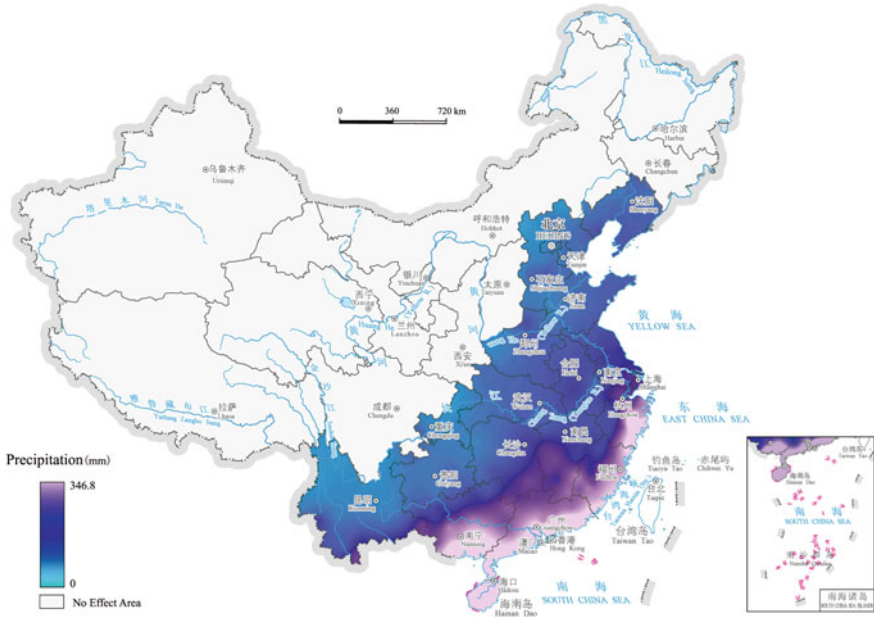


Fig. 4 Daily maximum precipitation of tropical cyclone with return period of 20 years (Source Shi 2011, p. 34)

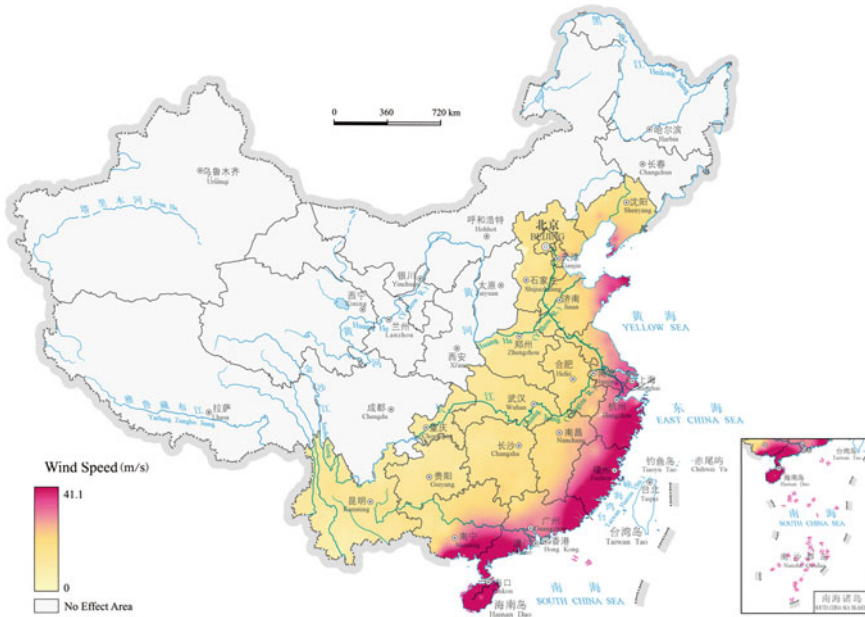


Fig. 5 Daily maximum wind speed of tropical cyclone with return period of 20 years (Source Shi 2011, p. 38)

exceeding probability, the longer the return period is and the larger the typhoon the maximum precipitation and wind speed are. The influenced areas extend westward and northward into provinces inland, such as Yunnan, Guizhou, Chongqing, Henan, and Liaoning Provinces, where the typhoon prevention level is relatively low. Stricken by strong typhoon with low exceeding probability, catastrophe losses may be caused in these areas. Northeast China is also affected by typhoons. The maximum precipitation and wind speed distribution of typhoon is directly connected with its landing point, track, and strength, among other factors.

1.4 Spatial and Temporal Patterns of Typhoon Disaster Losses

Strong wind and storm brought by typhoons are the main causes of disaster losses. The southeast coastal areas of China are highly developed with large population and high density of houses. In case of a devastating typhoon, people living in large areas is hit, houses are collapsed, and farmlands are flooded, which incur huge economic losses. Number of human casualties, damaged areas, collapsed houses, and direct economic losses are the main indicators of disaster losses and important basis for measuring disaster prevention and mitigation effect. Therefore, we conducted a

statistical analysis of typhoon disasters from 1985 mainly based on these four indicators. The typhoon disaster data for 1985–2002 used in this chapter are from the loss database of 124 typical typhoon disasters compiled by Zhou (2005); due to the unavailability of data, disasters in 2003 are not included. Typhoon disaster data for 2004–2008 are from the China meteorological disaster yearbooks (China Meteorological Administration 2006, 2007a, 2007b, 2008, 2009), and the main indicators include damaged area, the number of deaths, the number of injured, houses collapsed and damaged, and economic losses.

Figure 6 shows the number of human deaths, flooded farmlands, collapsed houses, and direct economic losses during 1985–2008 in China caused by typhoon disasters. The number of annual total deaths nationwide exceeded 500 in 1985, 1989, 1990, 1994, 1996, and 2006. Total direct economic losses caused by typhoons exceeded RMB 50 billion Yuan (price in 2000) in 1994, 1996, 1997, 2002, and 2006. More than 500 thousand houses collapsed in 1986, 1994, 1996, 1997, and 2006, especially in 1986 when the number was about 3 million. In 1985, 1990, 1992, 1994, 1996, and 1997, close to or over 5 million hectares of farmlands were damaged by typhoons. On the whole, 1990, 1994, 1996, 1997, and 2006 were major typhoon disaster years because the number of deaths, damaged farmlands, collapsed houses, and direct economic losses in these years all exceeded that of normal years to a large degree.

Because typhoons have distinctive regional distribution, the losses are mainly concentrated in coastal areas, while typhoons in inland areas are relatively few. Nevertheless, some typhoons still have great impact on inland areas. *Report on Significant Disaster Reasons of Property Insurance in China* (Wang 2006)

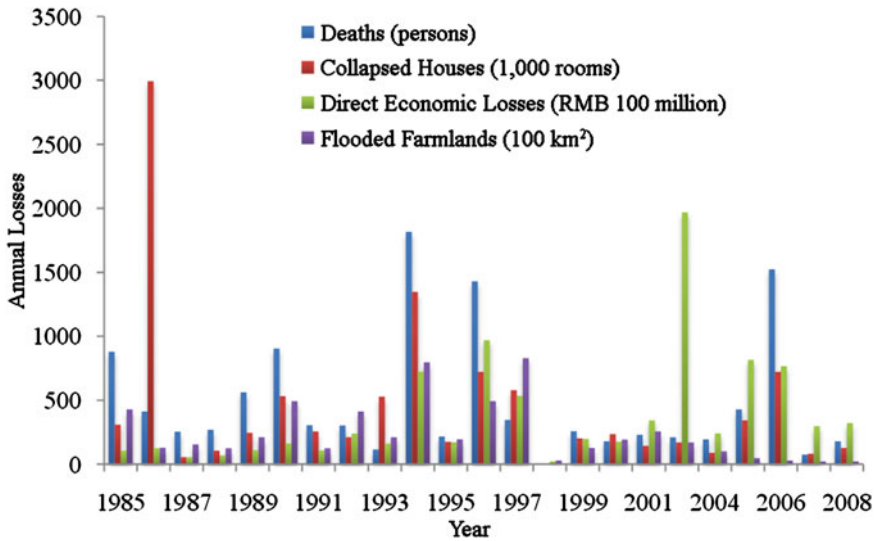


Fig. 6 Losses caused by typhoon disasters in China, 1985–2008

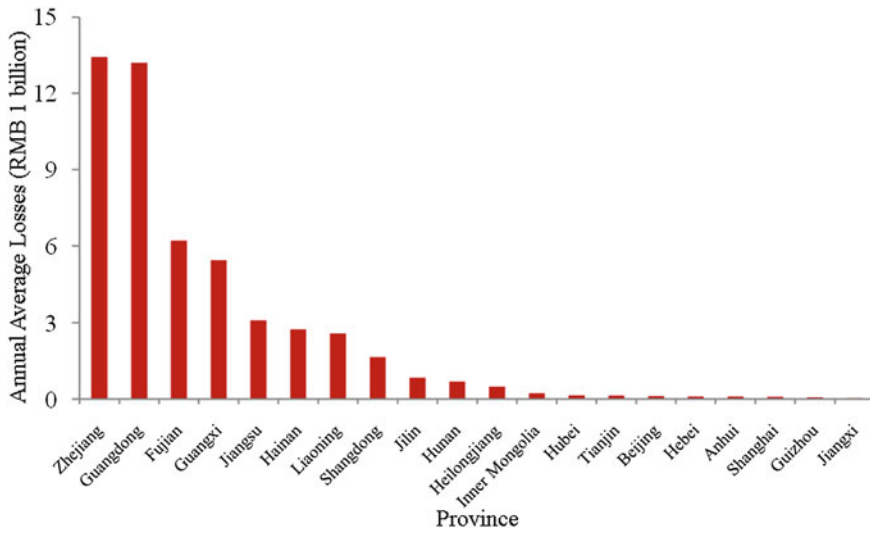


Fig. 7 Annual provincial average economic losses caused by typhoon disasters, 1988–2004

provided statistics on the total economic losses and average annual losses caused by typhoons in each Chinese province from 1988 to 2004 (the loss data were adjusted based on the price level in 2004). The result is shown in Fig. 7.

According to the ranking of losses in each province, Zhejiang, Guangdong, Fujian, Guangxi, Jiangsu, Hainan, and other southeast coastal provinces are most severely affected. Typhoons are relatively active in these provinces. However, the losses in Liaoning, Shandong, and Jilin Provinces are relatively high with respect to the lower frequency of typhoons. By analyzing the data, we found that two major typhoons (No. 9406 and 9415) hit Liaoning Province in 1994 and caused a loss of RMB 13.05 billion Yuan (at the price level in 2004), thus leading to a relatively high average annual loss in the province. Similarly, the relatively high average annual losses in Shandong Province and Jilin Province are also caused by rare high damage events. The regional distribution of economic losses caused by typhoons shows a clear declining trend from southeastern to northwestern China.

2 Formation and Assessment of Typhoon Disaster Risks

2.1 Typhoon Disaster Situation and Disaster Risk

Typhoon hazards are characterized by high frequency, wide influence, abruptness, clustered outbreak, and high hazard intensity (Liang et al. 1995). Typhoon hazard and other meteorological and hydrological factors form a complex hazard chain. The majority of serious typhoon disasters is caused by the joint impact of strong

winds, rainstorms, and storm surges accompanying the landfall of typhoons. The strong wind and rainstorm associated with typhoon can give rise to secondary hazards such as flooding and storm surges, which can further cause rock falls, landslides, debris flows, surges, floods, and other hazards, leading to more serious threats to the society.

The formation process of typhoon disaster involves the hazard and the disaster-formative environment. Generally, it is believed that essential conditions for the formation of the typhoon hazard are as follows: vast and warm (above 26–27 °C) sea surface, initial disturbance, certain Coriolis force, and small vertical wind shear. China is in the west bank of the North Pacific, where the low pressure disturbance generated on low-latitude surface of the Pacific Ocean moves westwards under the guidance of east wind airflow in trade wind zone. Some tropical disturbances on warm and humid ocean surface may form typhoon between May and November under the action of CISK (Conditional Instability of Second Kind) mechanism. When the intense cyclonic vortex with huge energy lands in China at high speed, it will lead to sudden drop in pressure and sharp increase in wind speed in areas it passes. Intense ground friction and other actions will result in strong latent heat release of cyclone, cloud and rain, even rainstorm, and may further lead to water logging, flush floods as well as secondary disasters such as landslides and debris flows. According to the statistics, almost all tropical storms and typhoons landing in China generate rainstorms, 95 % of which is heavy rainstorms (daily precipitation ≥ 100 mm) and 60 % is super-large rainstorms (daily precipitation ≥ 250 mm). The combination of typhoon disaster-formative environments and typhoon hazard can strengthen or weaken the impact of the hazard and secondary hazards to some extent, and directly affect the disaster situation.

The formation process of typhoon disaster also involves exposure units that experience damages from a typhoon of certain intensity, which leads to the loss of these exposure units. Exposure units of typhoon disaster refer to various subjects suffering from a typhoon disaster, including people, crop, water conservancy facilities, communication and transportation facilities as well as buildings. The disaster-bearing capability (vulnerability) of exposure units is an important determinant of disaster formation. When encountering typhoons of equivalent intensity, the loss resulted is lower if the disaster-bearing capability of the exposure units is higher. Therefore, vulnerability assessment of exposure units of typhoons is an important part of typhoon disaster risk assessment.

Typhoon disaster risk is the probability distribution of losses caused by typhoons of different intensities that will occur in the future. The formation of typhoon disaster risk is the result of interactions between exposure units, hazards, and disaster-formative environment. Because the frequency and intensity of typhoon hazards are uncertain, the resulted losses of typhoon disasters also have great uncertainties.

In conclusion, the forming of typhoon disaster risk is due to a comprehensive effect of the instability of disaster-formative environments, severity of hazards, and vulnerability of exposure units. Understanding the formation mechanism of typhoon disaster risk is significant for national and regional disaster prevention and reduction planning, rapid loss assessment, risk zoning, and risk transfer.

2.2 Physical Vulnerability

Based on the available historical loss data and information of exposure units, the vulnerability curves of GDP, rural residential buildings, and farmlands are fitted. First, a dataset of typhoon exposure was developed. The gross domestic product (GDP) and rural residential building survey data of certain level of administrative units (in this case county) were disaggregated into 1 km grids using a well validated algorithm. Farmland distribution was obtained with supervised classification of 30 m resolution remote sensing images and aggregated to 1 km grids. These data as raster layers in GIS formats were utilized as exposure to typhoon hazards. Second, historical loss data were carefully checked and categorized into three types, that is, loss of GDP, loss of rural residential buildings, and farmland damage ratio. Third, an exponential function was selected to fit loss ratio (LR) with hazard intensity indicators (I), such as wind speed and amount of rainfall after exploring various types of empirical functions, as shown in Eq. 1. In this equation, a and b are coefficients.

$$LR = ae^{bI} \tag{1}$$

Figures 8, 9, and 10 are scatter plots of sample historical disaster losses and hazard intensity, and their fitted vulnerability curves, using the data of Zhejiang Province, which is one of the most severely affected provinces by typhoon in China. The GDP and farmland loss data were obtained from the Ministry of Civil Affairs of China, and rural residential building loss data were from the People’s Insurance Company of China (PICC).

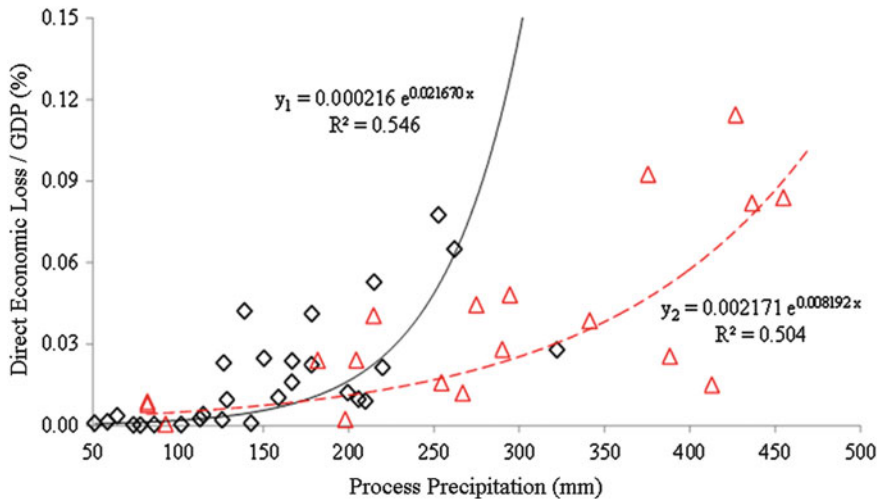


Fig. 8 Process precipitation versus direct economic loss ratio (Red line coastal area; Black line inland area) (Source Fang et al. 2011)

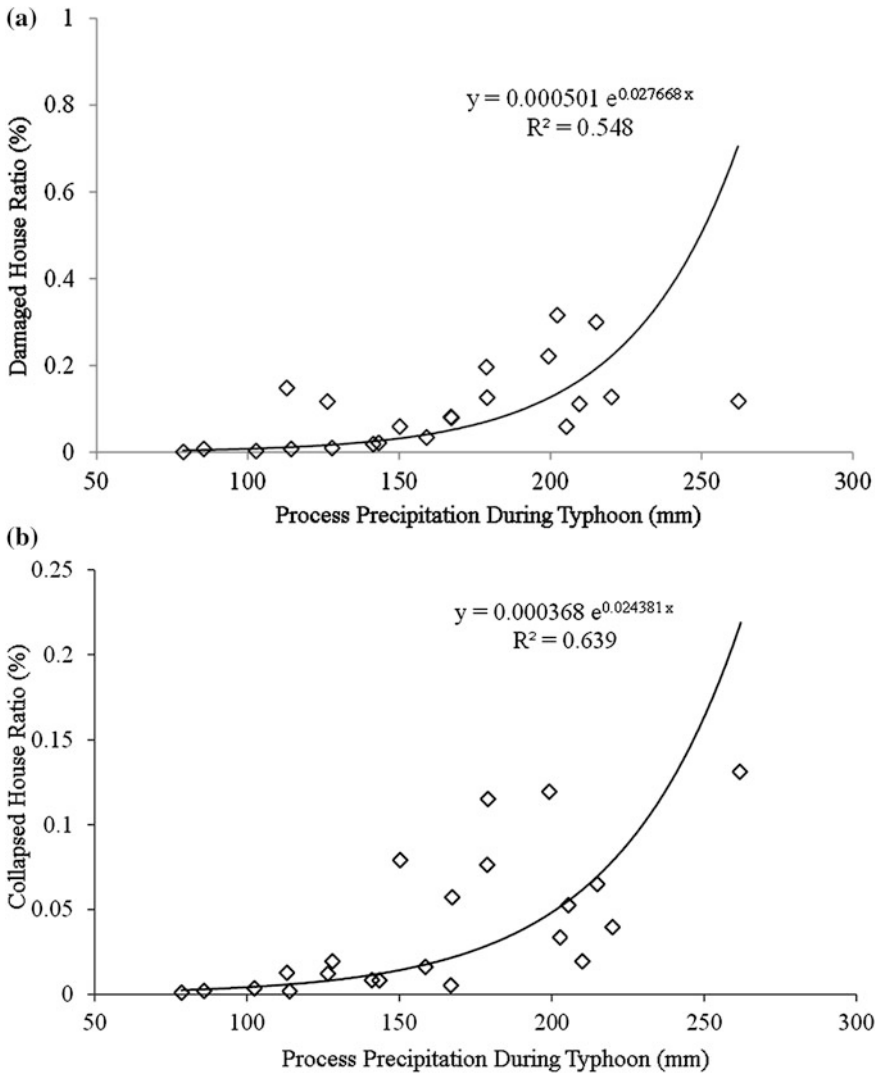


Fig. 9 Relations between process precipitation with **a** rural damaged house ration and **b** rural collapsed house ratio (Source Fang et al. 2011)

It can be seen in Fig. 8 that, when process precipitation exceeds 100 mm, direct economic losses begin to rise significantly. When hazard intensity exceeds a certain threshold value, for example process precipitation is greater than 250 mm, GDP loss ratio in inland areas increases rapidly. According to Fig. 9a, b, when process precipitation is lower than 150 mm, the loss of rural house is not heavy. With the increase of process precipitation, the ratios of damaged and collapsed rural houses rise gradually. When process precipitation exceeds 150 mm, such ratios rise rapidly. These ratios rise dramatically when process precipitation exceeds 200 mm.

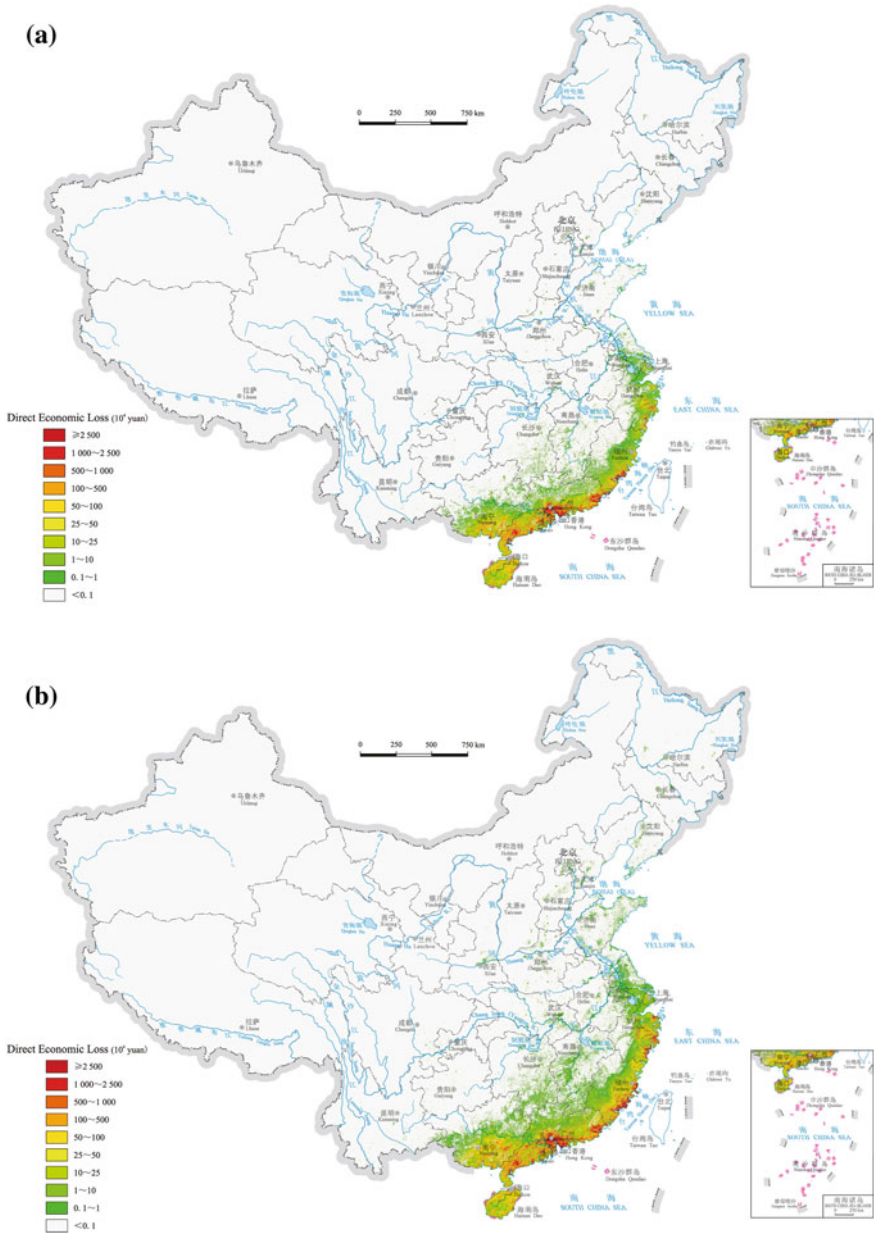


Fig. 10 Direct economic losses with different return period years: **a** 5 years; **b** 10 years; **c** 20 years; **d** 50 years (Source Shi 2011, p. 40–41)

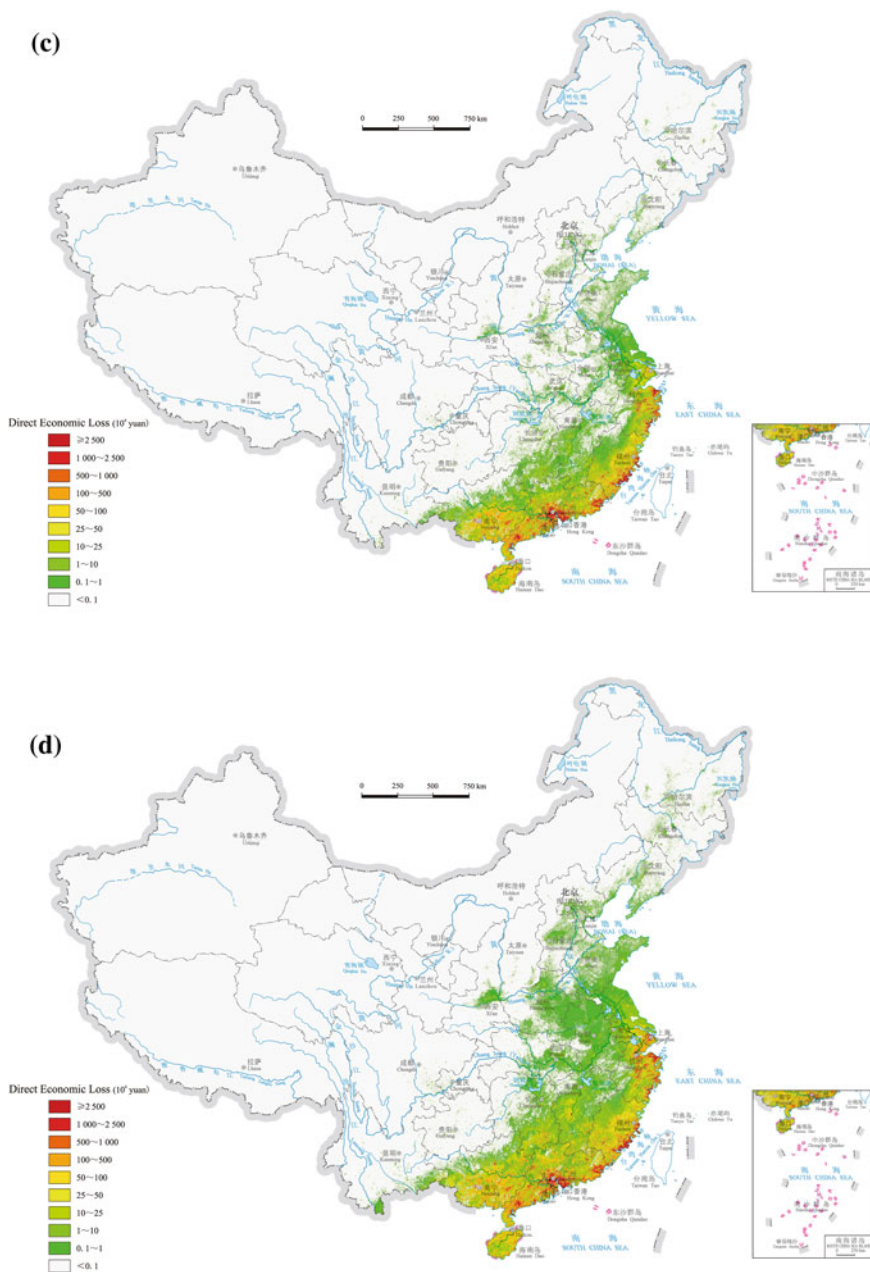


Fig. 10 (continued)

2.3 Risk Assessment

Typhoon disaster risk is defined as the expected annual loss of human lives or property caused by typhoon hazard and secondary disasters. Risk is the function of hazard intensity and its probability distribution, vulnerability curves, and exposure:

$$R = H \times V \times E \quad (2)$$

where, R refers to typhoon disaster risk, H refers to hazard; V refers to vulnerability, and E refers to exposure. The assessment is based on 1 km grid.

The probability that a loss is to be exceeded is referred to as the probability of exceedance. Based on probability distribution, if X is assumed to be continuous random variable, the cumulative probability less than x is presented as $F(X)$ for any real number x . EP refers to probability of exceedance, thus

$$EP = 1 - F(X) = 1 - P(X < x) = 1 - \int_{-\infty}^x f(x) dx \quad (3)$$

where, $f(x)$ refers to probability density function of continuous random variable X . The relation between exceedance probability (EP) of loss and reoccurrence period of cumulative probability (N) is as follows:

$$EP = 1 - F(X) = \frac{1}{N} \quad (4)$$

Taking the calculation of loss with 100-year return period as an example, we first estimate the hazard intensity with 100-year return period as developed by Generalized Extreme Value fitting, and define it as $H_k(100)$. For grid k and exposure value E_k , with corresponding vulnerability $V_k(x)$, the estimated loss with return period 100 years, or $R_k(100)$ is defined as follows:

$$R_k(100) = V_k[H_k(100)] \times E_k \quad (5)$$

The expected annual loss in a certain studied long-time period is expressed as follows:

$$R_k = \sum_{i=1}^N P_k(i) \times V_k[H_k(i)] \times E_k \quad (6)$$

where P_i is the probability of a hazard intensity with return period i .

For direct economic (GDP) losses as shown in Figs. 10 and 11, the impact of typhoon is likely to continuously expand toward the west and the north, and the most inland provinces that the impact can reach are Yunnan, Sichuan, Chongqing, Shaanxi, Hebei, Liaoning, Jilin, and Heilongjiang Provinces. However, these inland provinces are less prepared and therefore more vulnerable than the coastal areas. If a

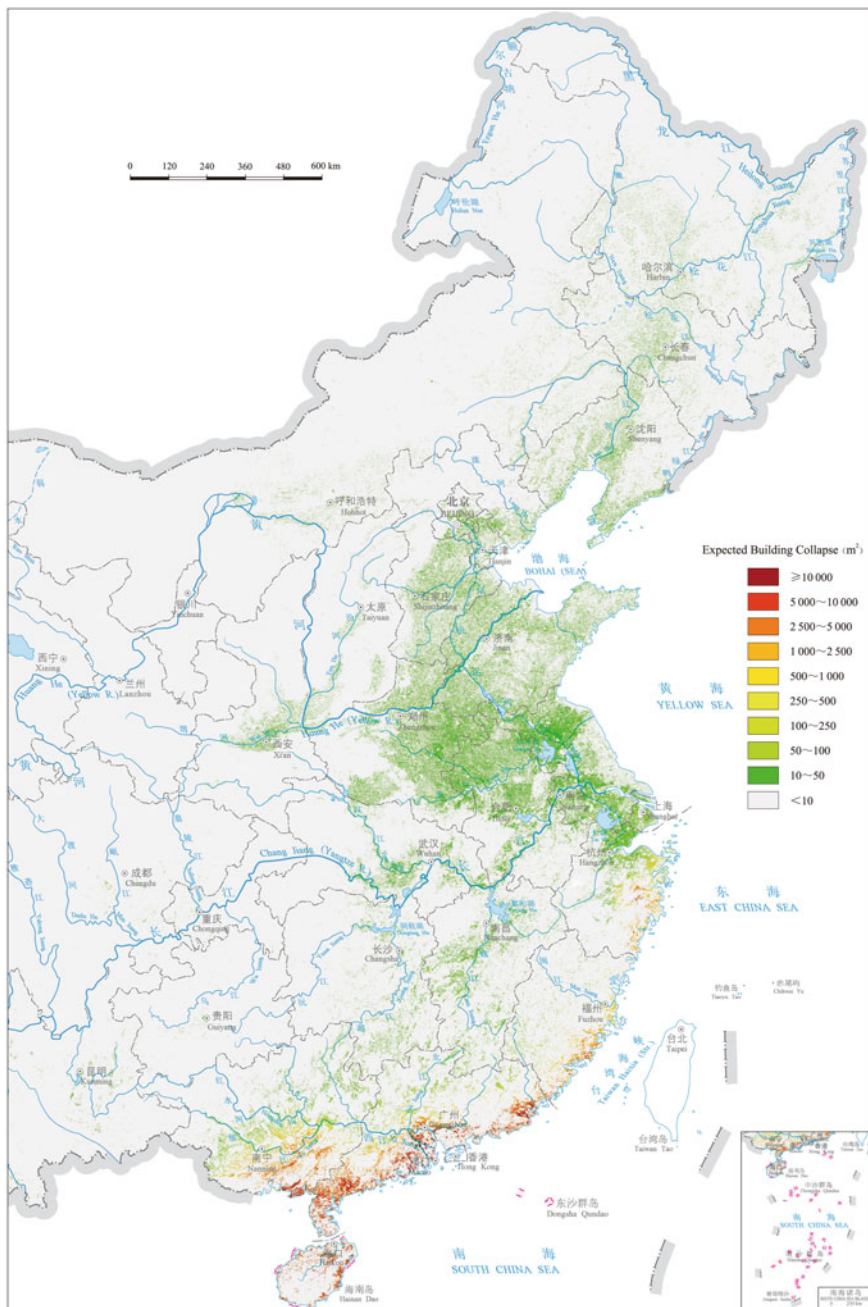


Fig. 11 Expected direct economic losses (Source Shi 2011, p. 45)

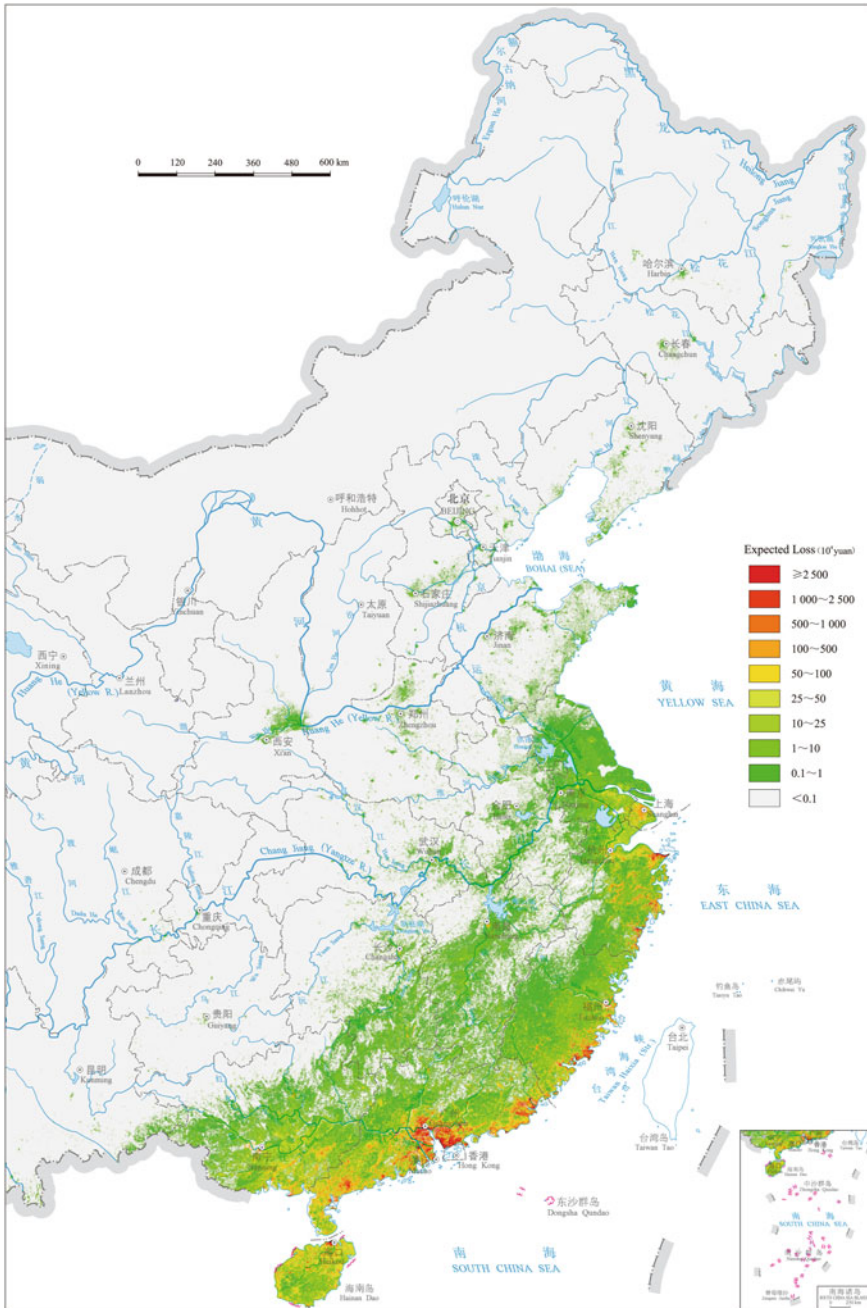


Fig. 12 Expected losses of rural buildings (Source Shi 2011, p. 44)

typhoon with long return period hit these areas, their risks or expected losses of property are higher than the coastal provinces.

The risk of rural buildings being damaged by strong wind and rainfall of typhoons is high in the coastal areas of Guangdong Province, the Leizhou Peninsula, the coastal areas of Guangxi Province and the Hainan Island, followed by the coastal areas of Fujian and Zhejiang Provinces (Fig. 12). Southern Guangxi Province is also a high-risk area due to high vulnerability caused by low income and poorly designed residential buildings.

3 Response to Catastrophic Typhoons

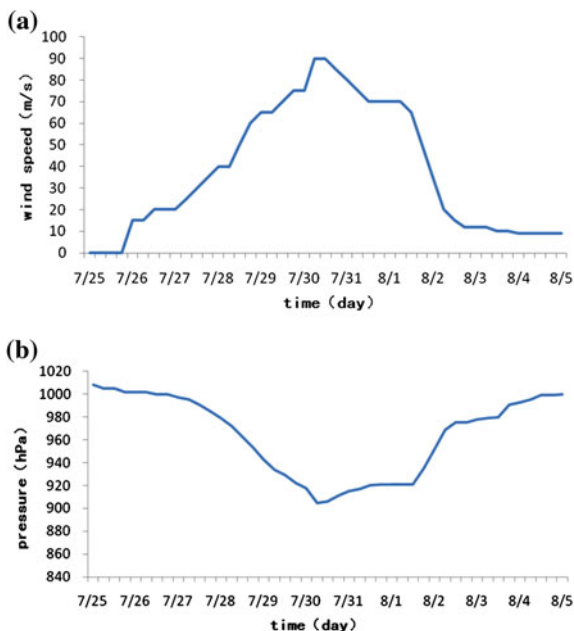
3.1 Typhoon Wanda (No. 5612)

On July 26, 1956 Typhoon Wanda (No. 5612) was generated at the latitude of 13.2° N and longitude of 144.8° E near the Mariana Islands of the Northwest Pacific (Fig. 13), and its central pressure and maximum wind speed are shown in Fig. 14. At the beginning of its generation, the typhoon center moved toward north, and then it moved toward west by 27 July under the influence of subtropical high. On 28 July, the maximum wind speed was up to 100 kt (knots, nautical mile/hour) as measured by the observation airplane of the United States, and the typhoon was given a number. During its movement, the environmental conditions were conducive to its further development: good divergence, weak wind shear, and



Fig. 13 Center and tracks of Typhoon Wanda (No. 5612)

Fig. 14 a Maximum wind speed and **b** atmospheric pressure of Typhoon Wanda (No. 5612)



appropriate water temperature; thus, its intensity started to continuously increase and the wind speed was up to 120 kt. On July 29, the intensity was further increased, and wind speed reached 145 kt. On July 30 at 6 a.m. UTC, Wanda's intensity reached the peak; observation data of the United States showed that atmospheric pressure in the middle of the typhoon fell to 902 hPa, wind speed reached 160 kt (82 m/s, 18-scale wind), and the wind speed at the Central Meteorological Station of China (NMC) was 90 m/s.

Affected by the huge solar halo, the whole Island of Taiwan experienced rainstorm before Wanda landed in mainland China. From July 31 to August 2, process rainfall in Taipei City reached 297.3 mm, where it was 190 mm on July 31 alone. At the time, Taipei was 500 km away from Wanda center.

On August 1, Wanda entered into the NMC 24-h warning line of the East China Sea with intensity of about 140 kt and had the lowest weakening speed on record before landing. At 16:00 p.m., Wanda solar halo began to influence the Zhejiang coast, rainstorm occurred everywhere and tide surged. At 24:00 on August 1, typhoon landed in Xiangshan County, Zhoushan, Zhejiang Province. Its central pressure was 923 hPa and wind speed was 65 m/s when landed. When wind eye passed Shipu Town, Zhejiang Province, observation data showed that the local atmospheric pressure was 914.5 hPa, which was 923 hPa when converted into sea level pressure, and this was the lowest measured atmospheric pressure since the founding of the People's Republic of China. After landing, Wanda's intensity decreased gradually due to the influence of the landform and receded into a tropical

storm in the north of Anhui. Due to the impelling action of the subtropical high, Wanda continuously went deep into China's inland, and the general circulation affected up to 10 provinces. Even regions such as Tianjin, Xiamen, and Qinling were covered by 8-scale wind of Wanda, and wind speed reached 12-scale in parts of Anhui. Wanda became the first tropical cyclone affecting Beijing since 1949. Later its intensity further decreased and it died out on the border of Shaanxi and Inner Mongolia on 5 August.

Disaster situation of the typhoon: Known as the "8·1 Storm," severe Typhoon Wanda brought an unprecedented havoc to many provinces and cities all over China, causing 4,935 human deaths and 16,617 injuries; the area affected was up to 1.562 million ha, and the direct economic losses reached RMB 80 million Yuan (Wen 2006).

Zhejiang Province was one of the worst-hit provinces, with 75 cities and counties badly affected, 2.2 million houses damaged, over 0.4 million ha farmland flooded, 87 medium and small reservoirs destroyed, 902 fishing boats sunk and 2,233 damaged, and 10 sections of the Zhejiang–Jiangxi railway line washed away. In addition, 38.5 % of the primary roads within the province were damaged to a different extent, and direct economic losses were about RMB 0.362 billion Yuan. On the day Wanda landed, 5.02 m storm water was generated in Ganpu, Zhejiang Province, and this record was retained for 24 years thereafter. The highest tide in history, 4.7 m, appeared in the typhoon landing site of Xiangshan County. Over 400 seawalls were destroyed across Zhejiang coastal areas, and Nanzhuang Plain became a world of water. Across the county, a total of 3,402 people died, 5,614 were injured, 77,395 houses and 465 seawalls and gates were destroyed, 7,774 ha of farmland were flooded with grain losses of 20,380 tons, 102 boats were washed away, and materials valued over RMB 615,000 Yuan were lost.

Disaster relief: From August 1 to 5, the Zhejiang Provincial Committee of the Communist Party of China, Standing Committee of the Zhejiang Provincial People's Congress, Zhejiang Provincial Headquarters for Flood Control, and Provincial Military District launched emergency rescue work. Camping at Zhejiang Province, the land army, sea navy, and air forces based in Zhejiang Province immediately dispatched 63,000 officers and soldiers, 16 airplanes, over 40 automobiles, and several rescue boats to save people's lives and properties. 20 thousand JinTen tons of foods were air dropped at the badly hit counties such as Xiangshan, and Yuhang, etc., and 11,500 people were rescued from the flood. On August 4, the State Council allocated RMB 10 million Yuan of emergency fund, 21 million Yuan of agricultural loans, and 3.2 million Yuan of restoration expenditure fund for damaged engineering work, and assigned special people delegates to express convey sympathy and solicitude for disaster victims and cadres, the public, and officers and soldiers fighting the disaster in devastated areas. At the same time, relevant departments of Zhejiang Province allocated 27,900 tons of relief fertilizer, 1.16 million pieces of moso bamboos, 0.35 million pieces of cotton cloth, 637.5 tons of grain seeds, 104.9 tons of vegetable seeds, 3,345 tons of pesticides, and 4,000 tons of cement for disaster relief and recovery.

Experiences and lessons learned: On July 30 when Wanda entered into the 48-h warning line, NMC released a severe-typhoon alarm and delivered it to primary level meteorological departments. Weather experts soon realized that a powerful typhoon was coming. Despite the excellent forecasting system and timely warning at the central level, however, Wanda still caused a large number of casualties, primarily because of following reasons:

- (1) Standards for disaster prevention construction were low. Wanda came at the beginning of the People's Republic of China, at a time when productivity level was low and materials were in great shortage nationwide; funding and technology were both insufficient. Therefore, high-standard typhoon prevention constructions were completely unavailable. Consequently, dams were washed away, a large number of houses collapsed, and all public facilities could not withstand a single blow of Wanda.
- (2) The emergency early warning mechanism was imperfect, and the government did not provide timely emergency disposal. On the one hand, the Wenzhou local meteorological department did not have an efficient information transmission method to disseminate the typhoon warning to tens of thousands of households, and failed to alarm the people at risk to evacuate. On the other hand, after the main typhoon alarm was released, some people who had received the warning did not understand its meaning and took Wanda as a common 12-scale typhoon. The government also did not provide timely disaster response in terms of protecting properties and organizing large-scale evacuation of the local residents.
- (3) The government made improper decisions for fighting the typhoon impact. After the typhoon's arrival, the government held that "human can conquer nature" and organized many cadres and the general public to defend seawalls amidst the 17-scale fierce wind, which caused a large number of casualties.

3.2 *Typhoon Saomai (No. 0608)*

At 20:00 on August 5 2006, the No. 0608 Saomai typhoon was formed over the sea near Guam. It intensified into a severe tropical storm at 8 a.m. on August 7, reinforced to become a typhoon at 2 p.m. on August 7 and a violent typhoon at 11 a.m. on August 9, which further developed into a super typhoon at 6 p.m. on August 9 and then landed in Mazhan Town, Cangnan County, Wenzhou City at 17:25 on August 10. It continued to move west-northwesterly, and arrived in Jiangxi Province at 6 a.m. on August 11. As Saomai was a small circulation, it was weakened significantly on land and reduced to a violent typhoon within 2 h after debarkation and a tropical depression in the morning of August 11, and died out at 6 p.m. on August 11 in Hubei Province. The route of Saomai is shown in Fig. 15, and its central pressure and maximum wind speed are shown in Fig. 16.

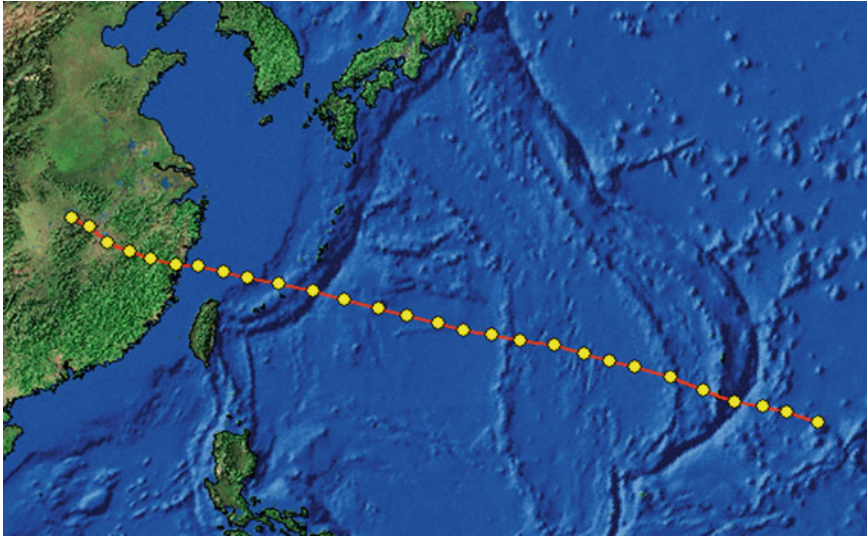
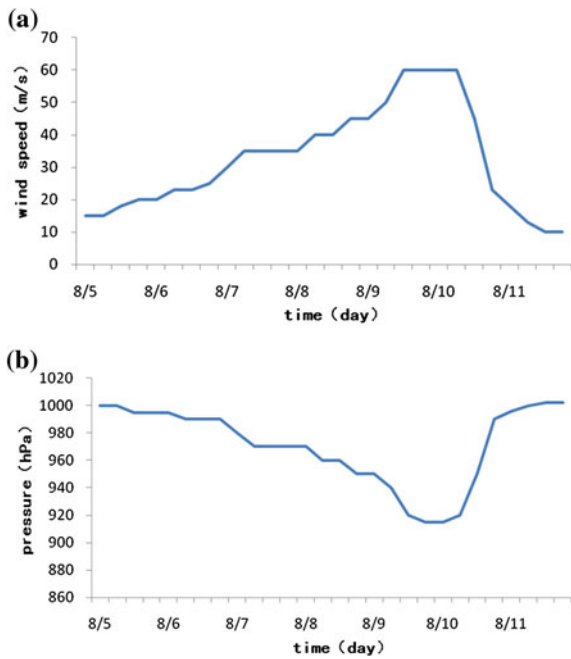


Fig. 15 Center and track of Typhoon Saomai (No. 0608)

Fig. 16 a Maximum wind speed and b atmospheric pressure of Typhoon Saomai (No. 0608)



Saomai was characterized by low central pressure, great wind speed, and heavy rainfall. The central pressure reached 920 hPa when it landed, which was lower than the pressure of the No. 5612 typhoon Wanda (923 hPa) in 1956. The low pressure level of Saomai is rare in the past 50 years and it is the strongest typhoon in China since the founding of the People's Republic of China. Although the typhoon range was relatively limited, the wind speed was high. The maximum wind speed measured in Xiaguan Town, Cangnan County was 68 m/s, which was stronger than the maximum wind speed (62 m/s) of Wanda. Due to the influence of Saomai, Zhejiang Province experienced a large-scale precipitation from 5 a.m. on August 10. Rainfall areas were mainly concentrated in Wenzhou and Taizhou, and there were 33 sites with accumulated rainfall above 100 mm, 13 sites above 200 mm, and 9 sites above 300 mm. The accumulated rainfall at 4 sites was above 350 mm: Changchan Town, Cangnan County (466 mm), Jinxiang County (379 mm), Yucangshan (377 mm), and Fanshan Town (369 mm). Rainfall of above 100, 200, and 300 mm covered 3,512, 509, and 113 km² respectively.

Disaster situation of the typhoon: As the landing time of Typhoon Saomai coincided with the astronomy high tide of the lunar month of July and due to the influence of small circulation, Saomai had caused a catastrophic disaster to many northern areas of Zhejiang and Fujian Provinces.

In Zhejiang Province, due to the influence of Typhoon Saomai, 3.455 million people in 377 towns of 23 counties (cities, districts) were hit by flood, strong wind, and various other impacts and a total of 39 thousand houses toppled; the affected area, disaster area, and area with total loss of harvest of the farmland were 103,500, 51,100, and 16,600 ha, respectively. Grain production was reduced by 140,000 tons; 10,600 ha of aquaculture area were affected and loss of aquatic products amounted to 20,000 tons; production at 13,710 industrial and mining enterprises halted; at 828 places roads were destroyed; 552.6 km of road subgrade and road surface, 864.7 km of electricity transmission lines, 499.1 km of communication lines, and 5,180 dikes with a total length of 396.4 km were damaged; 674 dikes breached at a total length of 81.1 km; 1,833 revetments, 70 sluices, 678 dams, 9,122 irrigation facilities, 55 boreholes, 36 hydrometric stations, 346 electrical pumping stations, and 94 hydropower stations were destroyed. The disaster caused direct economic losses of RMB 12.73 billion Yuan, and 193 people were killed and 11 were missing.

In Fujian Province, 14 cities and counties, 164 towns were affected by Typhoon Saomai, 1,455,200 people were hit, 45,700 houses collapsed, 215 people died, and 157 people were missing in the disaster. A larger number of vessels were damaged and sunk. Among these, the sunken vessels in Shacheng Port of Fuding City alone reached 952, and 1,139 vessels were damaged. The affected area and disaster area of crops were 68,800 and 44,230 ha, respectively. Moreover, 234 industrial and mining enterprises stopped production, and the direct economic losses reached RMB 6.357 billion Yuan.

Disaster relief: All quarters of the society provided help to the people in the disaster areas following Typhoon Saomai. Overseas Chinese associations of various countries contributed RMB 1.269 million Yuan for disaster relief, the Fujian

Branch of Industry and Commerce Bank of China donated RMB 3 million Yuan, and relief funds from all reached RMB 16.435 million Yuan.

On the day of impact, Fujian Province allocated emergency relief funds of RMB 2 million Yuan, subsequently distributed aid of RMB 35 million Yuan, and sent emergency relief goods to disaster areas that include 5,900 tents, 5,000 quilts, 18,000 cases of instant noodles, 13,000 cases of mineral water, 6,000 cases of biscuits, 60 tons of rice, 50,000 pieces of clothing, among others. Local communist party committees and governments of Shacheng, Longan, and other places dispatched ships for search and rescue immediately after the typhoon in the night of August 10. Meanwhile, Flood Prevention Office of Fujian Province also coordinated with the armed police force at all levels, the army, border troops, and militias to carry out maritime search and rescue operations. Many lives were saved through these efforts due to the adequate preparation and rapid actions. After the reach and rescue, a large-scale salvage work at sea was carried out. On August 17, a Deputy Director of the Ministry of Transport led a team from the Maritime Search and Rescue Center of the Ministry of Transport, Rescue and Salvage Bureau of the Ministry of Transport, Shanghai Rescue and Salvage Bureau, and Fujian Maritime Administration to Fuding City to guide the work of shipwrecks salvage. As of October 7, a total of 73 shipwrecks were salvaged and 18 bodies were found.

Zhejiang Province also made preparations before Saomai's arrival, started the disaster prevention plan, and disseminated the plan through the Wenzhou Agriculture Information Network. Various levels of governments of Zhejiang Province allocated relief funds of RMB 62.8 million Yuan following the disaster. All quarters of society also supported the affected population with money and goods for reconstruction. The then provincial Communist Party Leader Xi Jinping and Leaders of the provincial government and army went to the worst-hit areas for condoling with cadres and the general public as well as inspecting and directing the relief efforts. The 1,935 injured disaster victims were treated in the health centers and great effort was made to control infectious diseases. Water and power supply, transportation, communication, and water conservancy departments also actively engaged in repairing damaged facilities to ensure the basic living condition of the public. Meanwhile, experts and technicians were dispatched by various regions to the affected communities and guided farmer to perform self-help in production in the field.

Experiences and lessons learned: (1) Pre-disaster preparedness is an important mechanism for reducing disaster losses. Fujian Province made a very detailed disaster response plan before Saomai's coming. The provincial Communist Party Secretary Lu Zhongong made three visits to the Provincial Flood Control and Drought Relief Headquarters and inspected the anti-typhoon work of Shacheng four times. An Executive Vice Governor took command at the Provincial Flood Control and Drought Relief Headquarters. The army and people in the province started the emergency response plan and dedicated to fighting against Typhoon Saomai before its arrival.

Evacuation before disaster is an essential part of emergency plans. Zhejiang Province evacuated 989,937 people successfully before the arrival of Saomai,

among which 509,708 were from Wenzhou, 89,480 from Ningbo, 25,002 from Jinhua, 17,216 from Lishui, 29,409 from Shaoxing, 25,820 from Zhoushan, 1,744 from Jiaying, 285,606 from Taizhou, and 5,952 from Huzhou. Fujian Province also evacuated a larger number of people. Six evacuation plans were formulated by Fuding City, which include evacuating marine fishing platoon personnel, people living in geological disaster spots, in low-lying and reclamation areas, in dangerous houses, near the sea, and ship crews. The whole city evacuated 15 thousand people who lived in dangerous areas and only 28 people were killed in the disaster. Timely evacuation minimized the losses caused by Typhoon Saomai.

(2) Information release plays an important role in improving disaster awareness. Relevant departments at all levels of the government released typhoon forecasts and warning information via multiple platforms of the modern communication system during the whole process of the typhoon. All cable television channels and big-screen TVs in commercial districts kept broadcasting programs on typhoon disaster prevention; meanwhile, related news was broadcast on radios. Government and meteorological department websites also updated latest information on the typhoon tendency, and reminded as many people as possible of preparation for flood control and anti-typhoon through mobile telephone short message services, speech on propaganda car and loudspeakers, among other ways. The extensive and in-depth publicity penetrated into thousands of households and enhanced the awareness of the public.

(3) Coordination enhances the effectiveness of disaster prevention. With the overall coordination of the State Flood Control and Drought Relief Headquarters, the meteorological, flood prevention, water conservancy, marine and marine affairs, land and resources, education, tourism, civil affairs, health, and press and publicity departments of the government closely collaborated and fulfilled their duties, worked together to control the disaster and improved the effectiveness of reducing the impact of the super typhoon.

References

- Chen, S.R. 1990. Source regions of tropical storms over northwest Pacific Ocean. *Meteorological Monthly* 16(1): 23–26. (in Chinese).
- Chen, M., Y.G. Zheng, and Z.Y. Tao. 1999. An analysis on tropical cyclones' climatic feature in the western north pacific for 1949–1996. *Journal of Tropical Meteorology* 15(1): 10–16. (in Chinese).
- China Meteorological Administration. 2006. *Meteorological disaster yearbook 2005 of China*. Beijing: Meteorological Press. (in Chinese).
- China Meteorological Administration. 2007a. *Meteorological disaster yearbook 2006 of China*. Beijing: Meteorological Press. (in Chinese).
- China Meteorological Administration. 2007b. *Meteorological disaster yearbook 2007 of China*. Beijing: Meteorological Press. (in Chinese).
- China Meteorological Administration. 2008. *Meteorological disaster yearbook 2008 of China*. Beijing: Meteorological Press. (in Chinese).

- China Meteorological Administration. 2009. *Meteorological disaster yearbook 2009 of China*. Beijing: Meteorological Press. (in Chinese).
- China Meteorological Administration. 2015. <http://data.cma.gov.cn/>.
- Fang, W.F., J.A. Wang, and P.J. Shi. 2011. *Integrated risk governance: Database, risk mapping and internet platform*. Beijing: Science Press. (in Chinese).
- Liang, B.Q., J.P. Liang, and Z.P. Wen. 1995. Study of typhoon disaster and its affects in China. *Journal of Natural Disasters* 14(1): 86–91. (in Chinese).
- Shi, P.J. 2011. *Atlas of natural disaster risk of china*. Beijing: Science Press. (in Chinese and English).
- Wang, Y. 2006. *Report on significant disaster reasons of property insurance in china*. Beijing: China Financial and Economic Publishing House. (in Chinese).
- Wen, K.G. 2006. *Meteorological disasters dictionary of China: Zhejiang Section*. Beijing: China Meteorological Press.
- Zhou, J.H. 2005. *Research on the integrated risk assessment of typhoon disaster in China*. Ph.D. dissertation. Beijing, China: Beijing Normal University (in Chinese).

Floods in China

Juan Du, Feng Kong, Shiqiang Du, Ning Li, Ying Li and Peijun Shi

Abstract As one of the high exposure areas to natural disasters in the world, China has been afflicted by frequent and severe floods throughout history. This chapter analyzes flood hazard and flood losses in China, and reveals their spatial patterns and temporal changes in the past 60 years, from the beginning of the People's Republic of China. The analyses cover several spatial scales—the national, typical flooding area, and county levels. The chapter outlines the flood disaster formation processes by examining flood hazards, human-environmental conditions under which the disasters occur, and exposure units to establish the basis for flood risk assessment. An integrated indicator method based on recurrence intervals and climatic and geomorphological factors, as well as the occurrences of historical floods is used for flood risk zoning. Finally, this chapter takes the great floods in 1998 as an example to introduce China's experience and lessons learned in coping with flood disasters.

Keywords Flood · Spatiotemporal pattern · Flood disaster formation process · 1998 great floods

Flood (including waterlogging) is a serious natural disaster. China is one of the few countries in the world that are most severely afflicted by floods. Flood in China is frequent and spatially extensive. According to the statistics by civil affairs departments, flooding and waterlogging caused an annual average grain production loss of 20 million tons in the past 10 years in mainland China, and the annual

J. Du · F. Kong · N. Li · Y. Li
Key Laboratory of Environmental Change and Natural Disasters
of Ministry of Education, Beijing Normal University, Beijing 100875, China

S. Du
School of Tourism, Shanghai Normal University, Shanghai 200234, China

P. Shi (✉)
State Key Laboratory of Earth Surface Processes and Resource Ecology,
Beijing Normal University, Beijing 100875, China
e-mail: spj@bnu.edu.cn

economic losses were nearly RMB 200 billion Yuan. The continuous flooding and waterlogging in the Yangtze River and Huai River basins in summer 1991 and the severe floods in the South China area in 1994, for example, each resulted in an economic loss of over one hundred billion Yuan. The great floods in the Yangtze River, Songhua River, and Nen River areas in 1998 caused over 260 billion Yuan economic losses and more than 3,000 casualties. In the broad context of deteriorating global environmental conditions, a warming climate, and escalating flood risks, an in-depth exploration of the spatial and temporal aspects of floods in China and the formation process of flood disasters, assessment of regional flood risks, comprehensive analysis of flood impacts, and discussion on integrated flood risk management paradigms are of great significance for national and regional flood risk governance, mitigation, and transfer in China.

Since 1998, with the support of the Chinese National Natural Science Foundation, Ministry of Science and Technology, and the Swiss Reinsurance Company (SwissRe) and other organizations, we carried out a series of research including the Hunan Dongting Lake Area Flood Risk Assessment under the International Cooperation Program of the National Natural Science Foundation (40521140276) (2004–2007) led by Chinese and Austrian scientists; the Integrated Natural Disaster Risk Assessment and Disaster Reduction Paradigms in Rapidly Urbanized Areas of the National Natural Science Foundation Key Program (40535024) (2006–2009); Theme 3: Research on Developing a Comprehensive Technological Platform for Integrated Risk Governance of the National 11th Five-Year Plan Science and Technology Supporting Program on Key Technology Research and Demonstration for Integrated Disaster Risk Governance (2006BAD20B03); the SwissRe project, Study of Flood in China (1998–2001); and Theme 7: Technology Research for the Assessment of Natural Disaster Risk Grade in the Yangtze River Delta Area, under the Technology Research for the Comprehensive Assessment of Severe Natural Disaster Risk Grade in China project, supported by the National 11th Five-Year Plan Science and Technology Supporting Program (2008BAK50B07) (2008–2011). These studies addressed the spatial and temporal patterns of natural disasters in China, flood risks, vulnerability to floods, disaster resilience, flood risk formation mechanism in China, and the spatial and temporal patterns of flood risks, and obtained some important research results (Shi 2003; Wang et al. 2006; Shi 2010; Fang et al. 2011). This chapter is a comprehensive summary of these studies.

1 Spatial and Temporal Patterns of Floods

1.1 Spatial Distribution of Floods

According to the flood frequency map of 1949–1989, major floods occurred in the middle- and lower-reaches of the seven large rivers in China (Yangtze River, Yellow River, Huai River, Hai River, Pearl River, Liao River, and Songhua River)

and their tributaries and exhibited contiguous distribution in the area to the east of the second topographic ladder¹ (Ma 1994). Based on the statistics of the total number of floods resulting from heavy rains in 1951–1990, China Meteorological Administration found that two- to three-year return period flooding and waterlogging were concentrated in the Huai River Plain, Dongting Lake Plain, Poyang Lake Plain, and the area between the Hangzhou Bay and the Leizhou Peninsula (CMA 1995). Fan (1998) established a comprehensive risk index based on loss data (disaster area, collapsed houses, casualties, and economic losses) from heavy rains and floods in 26 provinces and autonomous regions of China in 1989–1993. The result shows that risk was greater in eastern and southern China than the west and north, with the high-risk areas located in the Yangtze River, Huai River, Nen River, and Songhua River basins. Wang et al. (1997) compiled a county-level map of flood occurrences based on the 1990–1994 flood statistics, which shows that floods mainly occurred to the east of the Hu Huanyong Line,² and the highest occurrences were found in the Yangtze and Huai River basins and the coastal areas of southern China. Xu et al. (2000) examined reports in provincial-level newspapers on floods in China in 1998 and summarized their spatial distribution in this year of great floods. They concluded that flood areas were in the Songhua and Nen River basins of Northeast China, the middle- and lower-reaches of the Yangtze River, and the Dongting Lake and Poyang Lake Plains, with contiguous distribution but also a number of local high value centers.

Spatial pattern of extreme precipitation in China: Fig. 1 shows the spatial patterns of decadal storm rainfall in China from 1951 to 2010. The threshold of storm is set at 50 mm/24 h based on the precipitation intensity grading standards promulgated by China Meteorological Administration. Since 1951, the storm rainfall keeps increasing and its spatial coverage also expands from the coastal areas in the southeast to the inland areas in the northwest. In 1951–1960, most of China’s meteorological stations reported a total storm rainfall below 5,000 mm, few reported 5,000–8,000 mm, and a tiny number of meteorological stations in the coastal areas reported over 8,000 mm (Fig. 1a). In 1961–1970, more and more meteorological stations, mainly in the coastal areas including Guangdong, Guangxi, and Hainan as well as the highly urbanized middle and lower reaches of the Yangtze River, registered total storm rainfall above 8,000 mm (Fig. 1b). In 1971–1980, the majority of meteorological stations located east of Shandong Peninsula-southwest Guangxi, especially those in Guangdong, Guangxi and Hainan recorded decadal storm rainfall over 5,000 mm (Fig. 1c). In 1981–1990, all the

¹The second topographic ladder refers to the area east of the Kunlun, Qilian, and Hengduan mountains and west of the Daxing’anling, Taihang, Wu, and Xuefeng mountains.

²The Hu Huanyong Line is also called the Heihe–Tengchong Line, which is known internationally as the “Hu Line.” It stretches from the city of Heihe in the north to Tengchong County in the south diagonally across China. The line marks a striking contrast in the distribution of China’s population: the area west of this line accounts for 57 % of the total land area but has only 6 % of the population of China; the area east of this line accounts for 43 % of the total land area but has 94 % of the population.

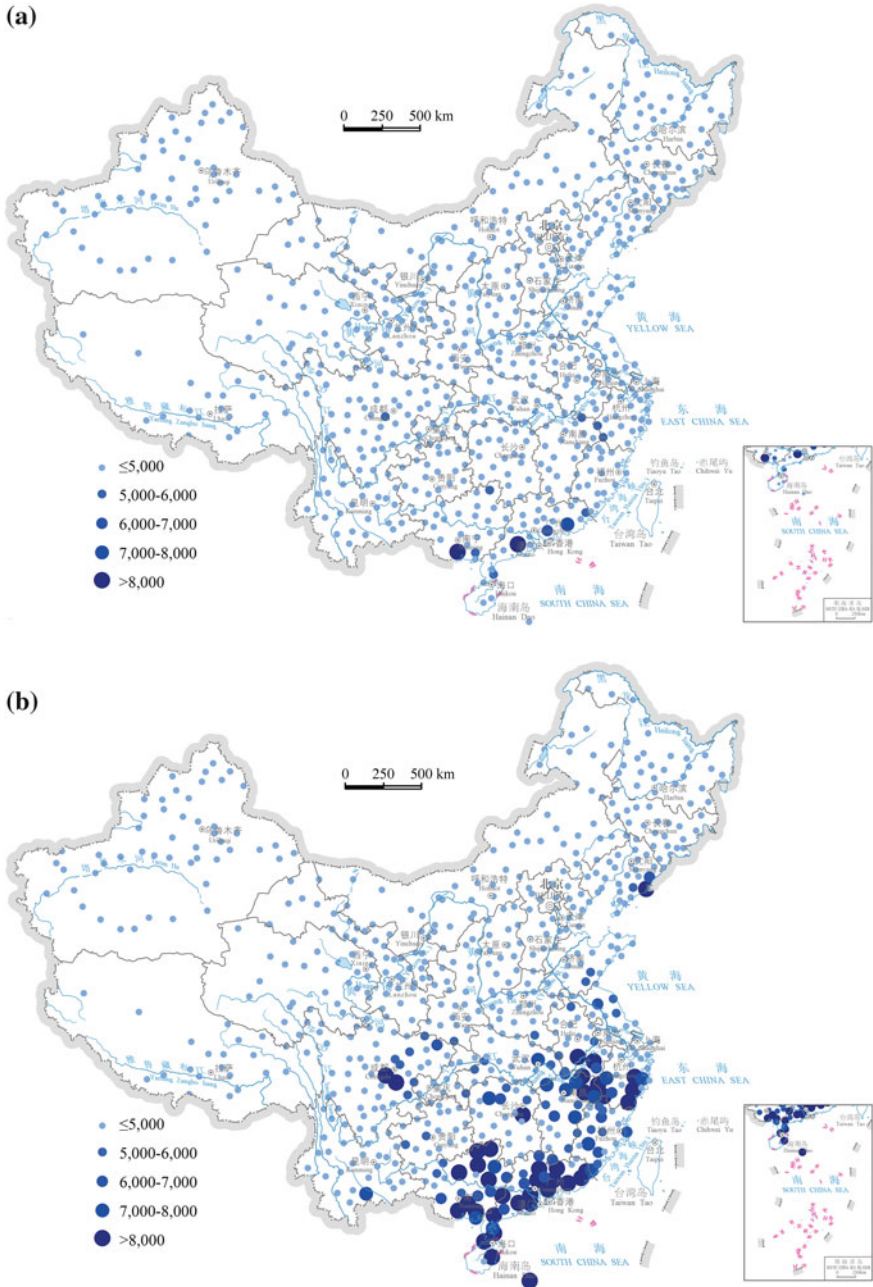
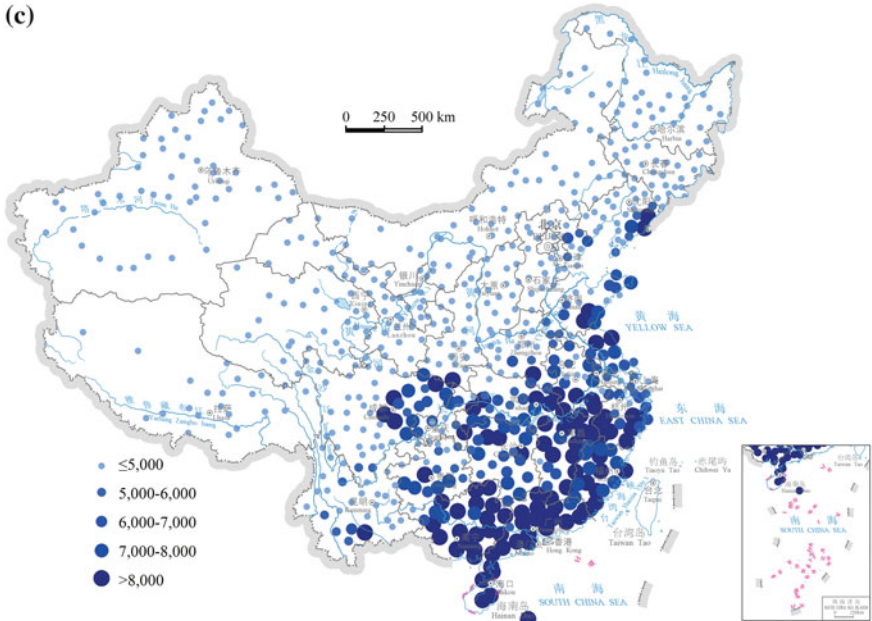


Fig. 1 Spatial distribution of Decadal Storm Rainfall in China, 1951–2010: **a** 1951–1960; **b** 1961–1970; **c** 1971–1980; **d** 1981–1990; **e** 1991–2000; **f** 2001–2010 (Source Shi et al. 2014)

(c)



(d)

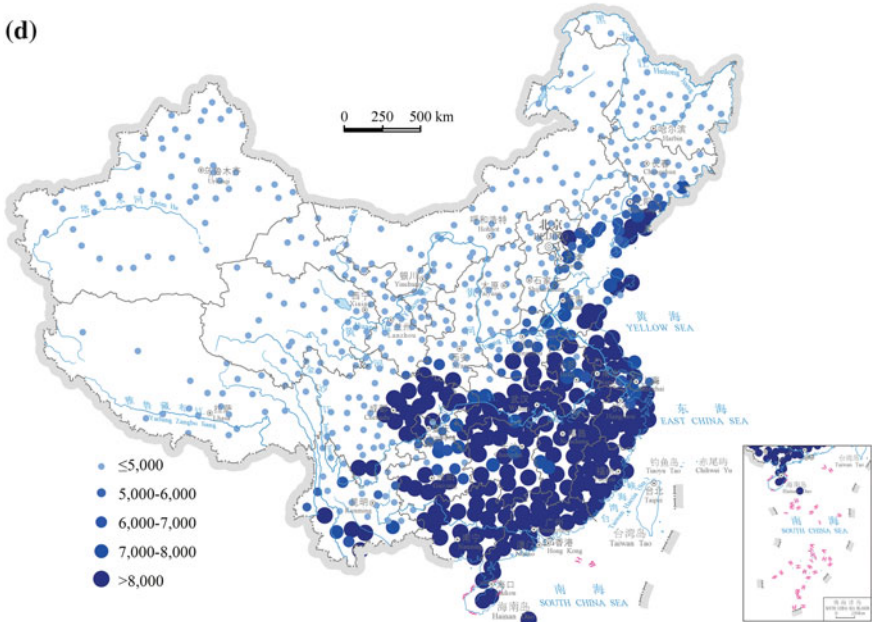
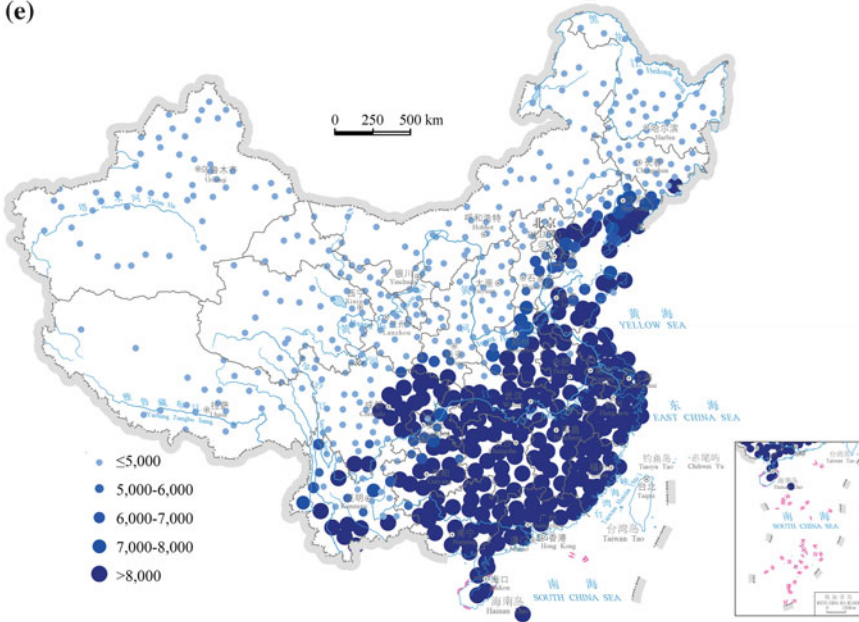


Fig. 1 (continued)

(e)



(f)

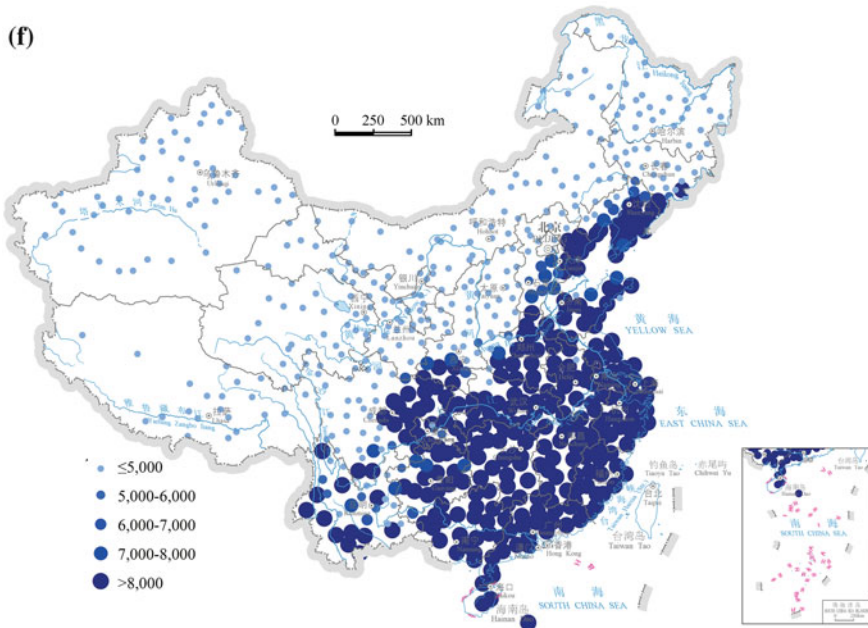


Fig. 1 (continued)

stations east of Shandong Peninsula-southwest Guangxi reported decadal storm rainfall of over 5,000 mm, and most of them reported over 8,000 mm (Fig. 1d). In 1991–2000, nearly all the stations east of Shandong Peninsula-southwest Guangxi reported decadal storm rainfall of over 6,000 mm and the spatial distribution of those reported over 8,000 mm expanded to the inland areas in northwest China (Fig. 1e). In 2001–2010, the situation worsened, when nearly all the stations east of Shandong Peninsula-southwest Guangxi reported decadal storm rainfall over 7,000 mm and the spatial distribution of those reported over 8,000 mm further expanded to the northwest (Fig. 1f). From 1951 to 2010, the decadal storm rainfall reported by meteorological stations in the northwest region generally stayed below 5,000 mm.

Spatial pattern of floods in China: Based on information from provincial-level newspaper archives and databases, we estimated the spatial distribution of floods in China in 1949–2000. There was a clear spatial differentiation in flood occurrences between eastern China and western China from 1949 to 1965. Counties suffered from floods were mainly located east of the Hu Huanyong Line, especially east of the second topographic ladder. Between 1978 and 2000, flood distribution showed a southeast to northwest trend in four zones, with the most severe flood stricken area located east of the Hu Huanyong Line, followed by the semiarid areas. Flood was also serious in northern Xinjiang but least serious in the cold and arid areas.

A comparison of the 1949–1965 and 1978–2000 average annual flood occurrence maps (Figs. 2 and 3) shows that floods were more severe in the latter period,

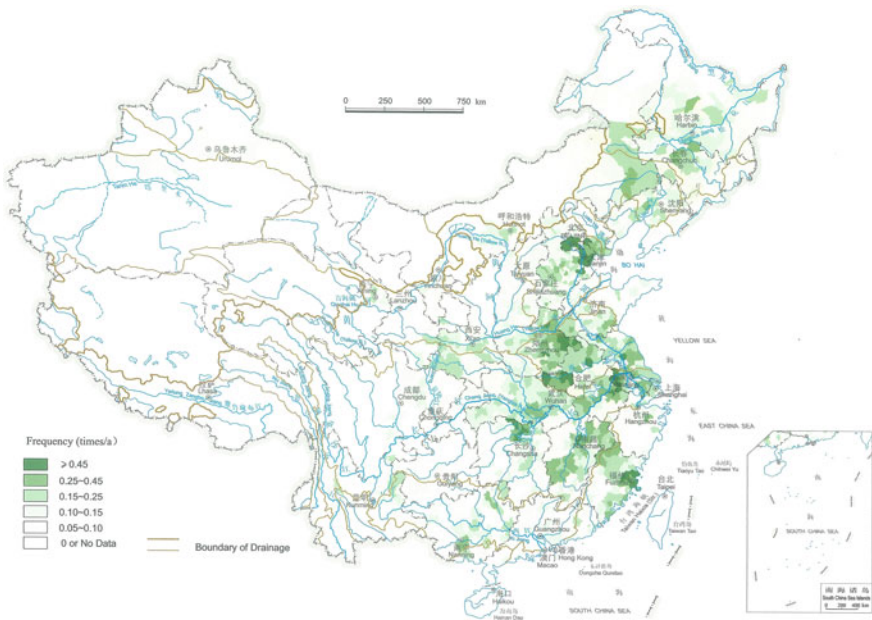


Fig. 2 Average annual floods in China at the county level, 1949–1965 (Source Shi 2003, p. 99)

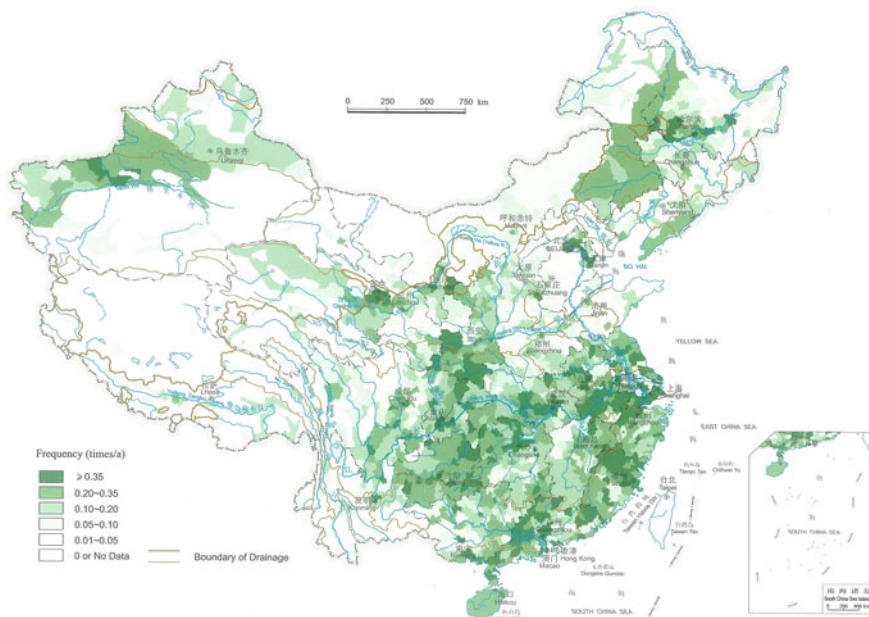


Fig. 3 Average annual floods in China at the county level, 1978–2000 (Source Shi 2003, p. 99)

in terms of both the spatial extensiveness and the overall frequency. The high occurrence center spread from the North China Plain centered around Henan Province to the south, north, and southwest. We believe that the reduced relative frequency in the previously worst-hit area of the North China Plain was a result of the construction of flood control embankments along the Yellow River and the Huai River, which greatly reduced flooding. Change in the spatial pattern of floods in China was mainly determined by land-use changes. On the one hand, human activities in the plain areas encroached into the low-lying wetlands—the reclamation of the wetland areas of Northeast China and the construction of polders and reclamation of lake areas in the middle- and lower-reaches of the Yangtze River are examples. On the other hand, vigorously cultivated hills and forest land resulted in environmental degradation and soil erosion. The destruction of vegetation cover along the Daxing’anling Mountains and the eastern edge of the Qinghai–Tibet Plateau where the source areas of major rivers in China are located directly contributed to the heightened intensity of flash floods and impacts.

By examining the spatial distribution pattern of floods for each year in the 1949–1965 and 1978–1998 periods at the county level, six distribution types can be identified—nationwide distribution, and scattered, northern, eastern, southeastern, and northwestern–southeastern types (Table 1). Floods in China are mainly distributed in the eastern part of the country where the population density is high. The eastern and southeastern types were most common, occurred in 21.6 and 18.9 % of the 37 years, respectively, and the northern type was 13.5 % of the total. Eastern

Table 1 Statistics of China’s flood distribution types based on county level data for 1949–1965 and 1978–1998

Distribution type	Nationwide	Scattered	Northern	Eastern	South-eastern	Northwestern–Southeastern	Total
No. of years	6	7	5	8	7	4	37
Percentage of the total	16.2 %	18.9 %	13.5 %	21.6 %	18.9 %	10.8 %	100 %
Typical flood year	1991	1987	1962	1980	1963	1992	

China has the highest incidences of floods—all together floods occurred in the east in 53 % of the years. Regional distribution of frequent floods overlaps with the densely populated area on the low-lying eastern China plains. This is determined by the natural conditions of this area where monsoon influence is stronger, but it also reflects the socioeconomic characteristics of the exposure units, that is, highly developed economy and densely settled human population. Thus, the densely populated eastern plains are the key areas of flood prevention and control.

1.2 Temporal Distribution of Floods

Interannual variability of extreme precipitation in China: From the time dimension, the yearly total rainfall amounts display distinct trends before and after 1980. Despite the ups and downs, it showed an ascending trend in 1951–1980 while a descending tendency in 1980–2010 (Fig. 4). The yearly total storm rainfall undulates but generally ascends, which was slower in 1970–1990 while faster in 1950–1970 and 2000–2010 (Fig. 5). Figures 4 and 5 show that, after 1980, the total rainfall goes down but the storm rainfall goes up, meaning the total rainfall of

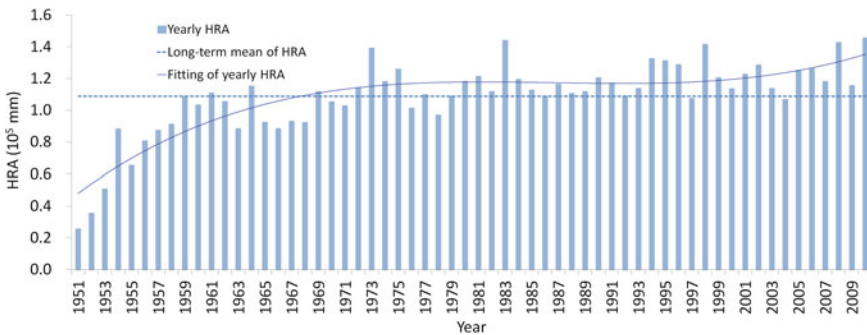


Fig. 4 Yearly total rainfall amounts (TRA) in China, 1951–2010 (Source Shi et al. 2014)

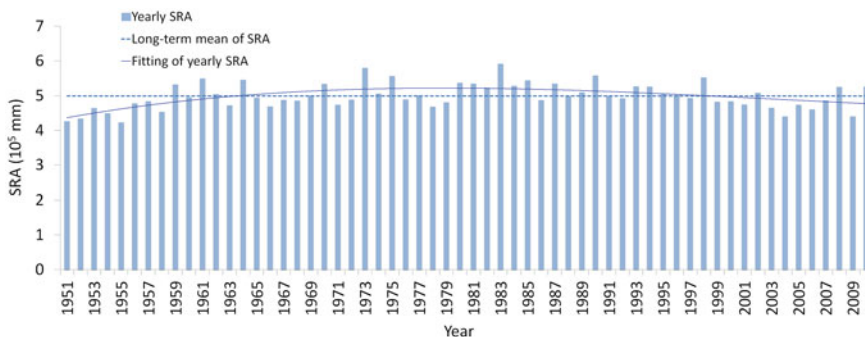


Fig. 5 Yearly storm rainfall amounts (SRA) in China, 1951–2010 (Source Shi et al. 2014)

drizzles, light, moderate and heavy rains are decreasing and storms are increasingly contributing to China’s precipitation. This is possibly an important cause to the aggravating flooding and waterlogging in cities.

Interannual variability of flood disasters in China: Statistical analysis of China’s annual total flood affected area and disaster area of agriculture in 1978–2012 (Fig. 6) found that flooding in China peaked in 1991, 1998, and 2003, with greater total flood affected area and disaster area in these years. Records indicate that these were also typical flood years in China. In the recent three and half decades, the average annual flood affected area in China amounted to 11.48 million ha, and the average annual disaster area reached 6.42 million ha.

Based on the characteristics of floods in various time periods over the past 35 years, interannual variability of flood can be divided into three distinctive stages.

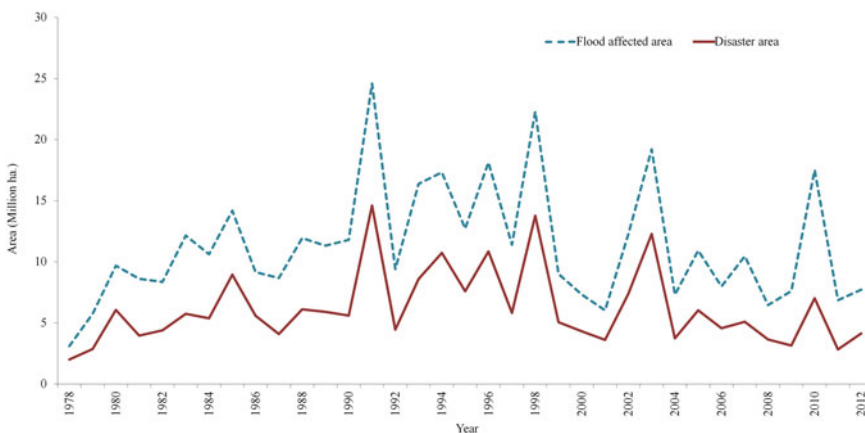


Fig. 6 Interannual variability of total flood affected area and total disaster area of Chinese agriculture, 1978–2012 (Data source China Rural Statistical Yearbook 2013)

Between 1987 and 1990, annual total flood affected area and disaster area in China were relatively small and stable. From 1990 to 1999 during the peak flooding period, flood affected area and disaster area were generally at a high level and fluctuated greatly. Into the twenty-first century, floods returned to a relatively low level and remained stable. But overall, extreme flood events were frequent in the past 35 years.

Direct economic losses caused by floods since 1990 (Fig. 7) indicate that 1990–1993 was the period of low flood damage. In 1994–1999 the flood damage was high. In the first 10 years of the twenty-first century, flood damage appears to be at a stable low level. Affected by the continuous rains in 2010, floods occurred in the seven main river basins including the Yangtze River, the Huai River, the Yellow River, the Liao River, the Songhua River, and the Hai River. Although the flooding situation was less severe than in the great floods of 1998, debris flows and flash floods occurred widely and the damages to agricultural production and livelihood were very high, especially from the most serious debris flow disasters occurred in areas such as Zhouqu of Gansu Province.

Global climate change and El Nino and La Nina under this background are creating increasingly more serious flooding situation in China (Chen et al. 2013). At the same time, population growth and the expansion of economic activities along with environmental degradation make the control of floods increasingly more difficult. Currently, flood defense capacity is high along the main river channels of the seven large rivers and the Min River and Qiantang River. But in mountain areas and along medium and small rivers including tributaries of some of the large rivers flood defense standard is low and the weak flood control capacity is difficult to improve. Flood disasters will continue to occur in these areas.

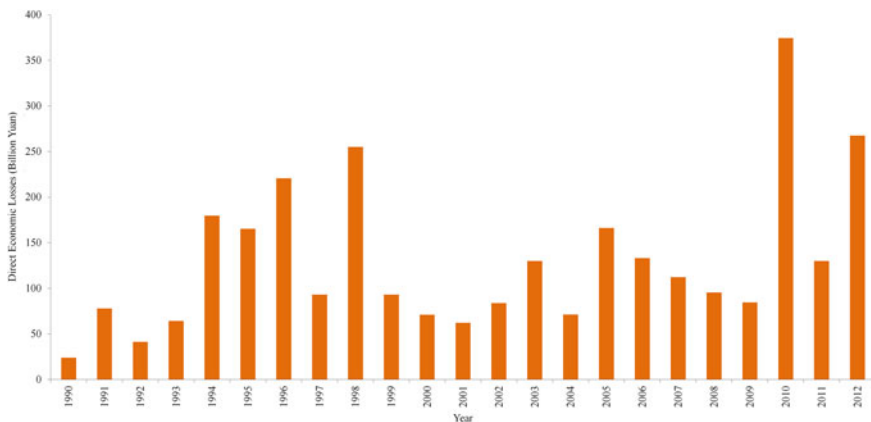


Fig. 7 Direct economic losses caused by floods, 1990–2012 (Data source Bulletin of flood and drought disasters in China 2012)

2 Formation and Risk Assessment of Flood Disasters

2.1 Flood Disaster Formation

Flood risk is a product of interactions between flood hazard, exposure units, and the contextual environment (or human-environmental conditions) of a flood-prone area.

Flood hazard refers to the physical factor that causes a flood disaster event. This hazard is released by a potential source—rivers and reservoirs are typical sources—and forms certain spatial and temporal distribution patterns through hydrological processes. Within a disaster-formative environment the hazard causes harm to the exposure units. For example, surface runoff or flood resulting from heavy rains is the fundamental cause of inundation of and damage to houses and crops. Flood is generally measured by depth and duration.

With flood hazard or a direct disaster-formative force but without an exposure unit there will be no disaster. Exposure units are objects and systems such as people, valuable items, and lifeline systems in the affected area that can potentially be harmed by flood hazard. In general, exposure units can be divided into humans, human settlements, industrial and mining facilities, agriculture, forestry, animal husbandry, fishery, transportation infrastructures, and the environment. Exposure units have certain ability to withstand a disaster. Certain socioeconomic characteristics of the exposure units can make them more vulnerable to disasters. The percentage loss of economic values of the exposure units after experiencing floods of various severities is an indication of vulnerability of the exposure units.

Disaster losses are the ultimate manifestation of disasters. Losses can be divided into direct losses, indirect losses, and secondary derivative losses according to their characteristics. Losses from natural disasters are often measured by the number of people affected and the amount of lost economic values. The number of people affected further includes the number of deaths, people injured, missing, and people who are only affected in other ways. The amount of economic losses includes those from direct losses and indirect losses.

In summary, the formation of flood disaster is a sequential process through closely linked hazard, contextual environment, exposure units, and disaster losses, as shown in Fig. 8. A clear explanation of the flood disaster formation process bears significant importance for guiding flood risk assessment.

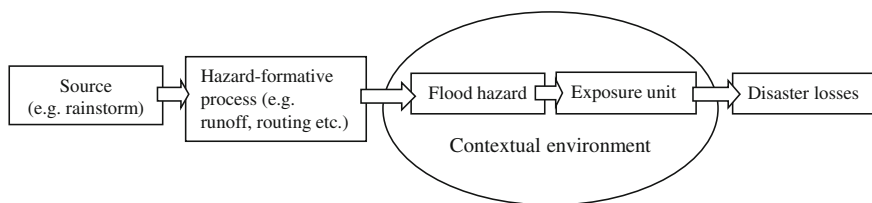


Fig. 8 Flood disaster formation process

2.2 Flood Risk Assessment

2.2.1 China’s Flood Risk by Recurrence Interval

Indicator analysis is one of the methods used for flood risk zoning. By focusing on flood formation mechanism and through the analysis of various factors (indicators) that have affected the formation of a flood, this method assigns weight to every indicator and later integrates the indicators into a single index through a model to assess the overall risk of flood in a study area (Fang et al. 2011). This section analyzes China’s flood risk by recurrence interval, taking into account climatic and geomorphological factors as well as the occurrences of historical floods (Fig. 9).

Among the climatic factors, heavy rain is the most direct factor that causes flooding, and regional climatic differences determine the distribution of floods (Li 1999). We selected heavy rain and regional climate as two indicators for the impact of climate on flood risk. We used the highest three-day precipitation at certain recurrence intervals to evaluate the impact of heavy rains. The data used are rainfall at the 756 national-level meteorological stations provided by the China Meteorological Administration (n.d.). Maximum three-day precipitation with different probabilities at 1 km grid cells was obtained through fitting and interpolation based on the Pearson III distribution. Division of climatic zones followed the definition in *China Physical Geography: Overview* (ECCPGCAS 1985). Among the geomorphological factors, elevation and slope of terrain have the greatest impact on flood formation. Areas with lower elevation and smaller variation in

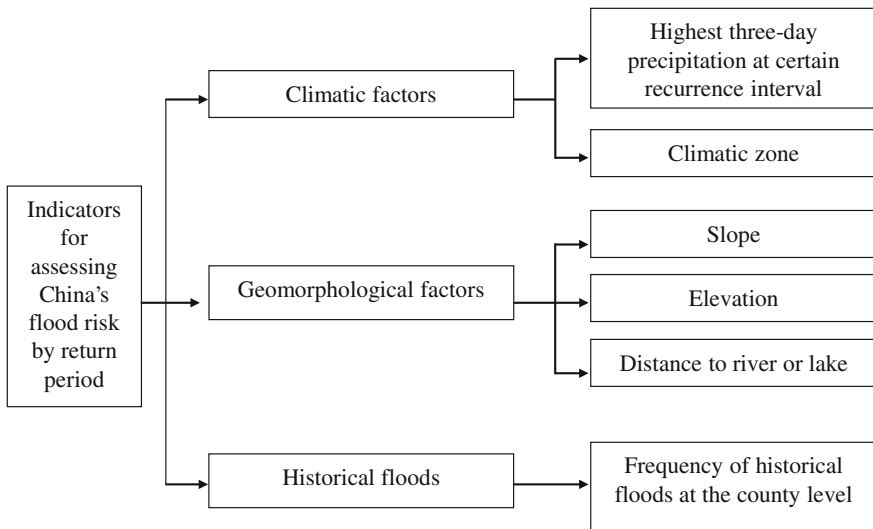


Fig. 9 Indicators for assessing China’s flood risk by return period

topography are more prone to flooding (Tian et al. 2006). We selected elevation, slope, and distance to rivers and lakes as indicators for the impact of geomorphology on flood risk at various recurrence intervals. Elevation data was derived from SRTM DEM, slope data was calculated by ArcGIS spatial analysis based on the elevation data, and the distance to rivers and lakes was calculated in ArcGIS.

Frequency of historical floods across the country indicates the spatial distribution of past flood events in China and is an important indicator for evaluating future flood risks. The data were obtained from the Newspaper-Based China Natural Disaster Database created by the Key Laboratory of Environmental Change and Natural Disasters of the Ministry of Education of China at Beijing Normal University. The data include frequency of floods at the county level for 57 years between 1949 and 2005.

Flood risk by recurrence interval is an integrated assessment on the basis of the six selected indicators. The formula used for creating the composite index is as follows:

$$R_{fI} = a_1 \times x_1 + a_2 \times x_2 + a_3 \times x_3 + a_4 \times x_4 + a_5 \times x_5 + a_6 \times x_6 \quad (1)$$

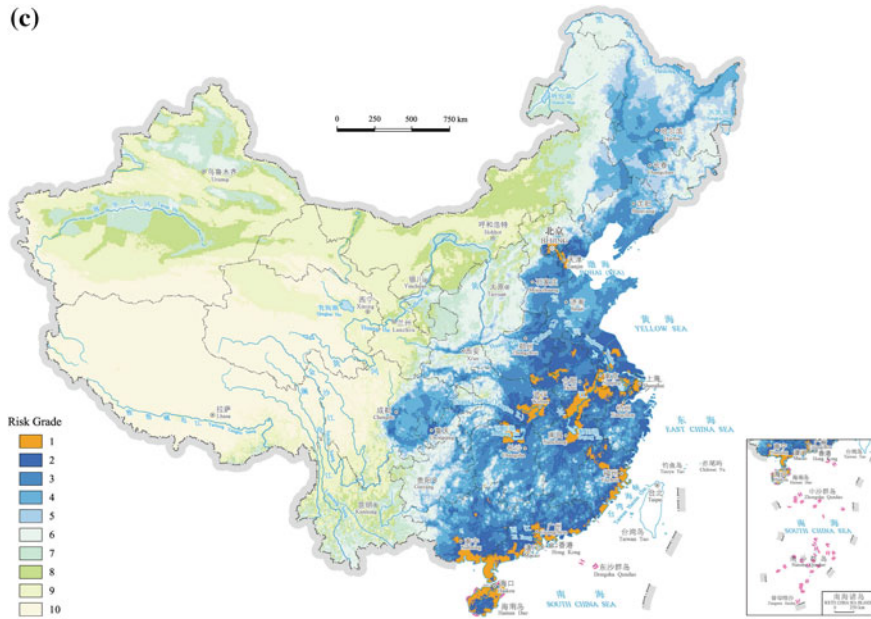
where R_{fI} is flood risk by recurrence interval; x_1 is the highest three-day precipitation at certain recurrence intervals (once in 5 years, once in 20 years, once in 50 years, and once in 100 years); x_2 represents the score of the specific climatic zone based on its impact on flood risk (Shi 2011); x_3 is the score of a given slope of the terrain, x_4 is the score of the specific elevation, and x_5 is the score of a given proximity to a river or lake, all based on their impacts on flood risk (Shi 2011); and x_6 is the frequency of historical floods (1049–2005) at the county level. a_1, a_2, \dots, a_6 are weights of the six indicators, calculated using the Analytic Hierarchy Process (AHP). In this research, these weights are 0.1442, 0.1109, 0.1966, 0.1884, 0.1562, and 0.2036 respectively. Figure 10 shows flood risk grade at 5, 20, 50, and 100 year recurrence intervals.

2.2.2 A Comprehensive Assessment of China's Flood Risk

Frequency of historical floods reflects the consequences of both the natural and human processes. The newspaper-based historical flood database as presented above can provide critical information for flood risk assessment. However, historical floods were recorded at the county level. It cannot represent the heterogeneity of flood risk within a specific county. In this section, we calculated the fine-scale flood risk by downscaling flood frequency in a county to the 1 km grid level.

Within each county for each grid cell, historical flood frequency was recalculated according to both the county-level flood frequency and main contributing factors to the spatial differentiation of flooding frequencies within a county, namely the cell's elevation and distance to rivers/lakes. Elevation and distance to rivers/lakes are the main factors that determine the spatial distribution of exposure, and thus are the main contributing factors to the spatial differentiation of flooding

(c)



(d)

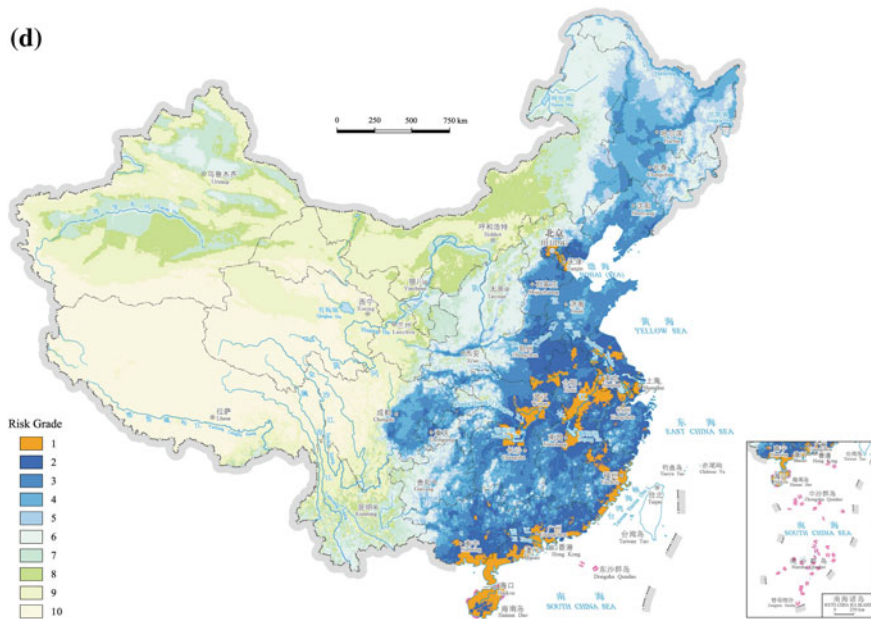


Fig. 10 (continued)

frequencies within a county (Shi et al. 1999). Frequency of historical floods at each grid cell was calculated as follows:

$$d_f = d \times h \times f_c \tag{2}$$

where d_f is the frequency of historical floods at the grid cell level; f_c is flood frequency for the county-level administrative unit; d and h are distribution factors for distance to rivers/lakes and elevation. We used expert scores to derive the relative contribution of various distances (d) and elevation (h) values to flood risk and the result is presented in Table 2.

Considering the possibility that statistical data may be incomplete especially for small floods, we calibrated the results with frequency of heavy rains. Calibration of the result with frequency of heavy rains to compensate for the effect of incomplete statistical data is done as follows:

$$R_f = a \times d_f + b \times s \tag{3}$$

where R_f is comprehensive flood risk index; d_f is normalized historical flood frequency at the grid cell level; S is normalized frequency of heavy rainfall; a and b are weights of d_f and S derived using AHP. In this research, a and b are 0.85 and 0.15.

The result of the above analysis is continuous values for the flood risk of the grid cells. Therefore we divide these results into 10 grades, with a gradually increasing risk level from 1 to 10. Figure 11 indicates the overall level of flood risk in China.

Figure 11 shows that the 10 largest flood-prone areas in China are the Yangtze River Delta region, the area between Nanchang and Nanjing along the Yangtze River, the middle and lower parts of the Gan River region, the Dongting and Poyang Lake areas in the middle- and lower-Yangtze River basin, the Huai River basin, the piedmont region of the Taihang Mountains, the lower parts of the Hai River and Luan River, the Pearl River Delta, the lower part of the Liao River region, the Sanjiang Plain in Northeast China, the Wei River Plain, and the Sichuan Basin.

Table 2 Contribution of various d and h values to flood risk at the grid cell level

Distance to rivers/lakes (km)	Difference in elevation between river channel and a grid cell (m)					
	0–10	10–20	20–30	30–50	50–100	>200
0–5	1.0	0.8	0.6	0.4	0.2	0.1
5–20	0.8	0.6	0.4	0.2	0.1	0.0
20–50	0.6	0.4	0.2	0.1	0.0	0.0
50–100	0.4	0.2	0.1	0.0	0.0	0.0
100–200	0.2	0.1	0.0	0.0	0.0	0.0
>200	0.0	0.0	0.0	0.0	0.0	0.0

Note Values in the table are proportions of grid cell level flood frequency in county level flood frequency

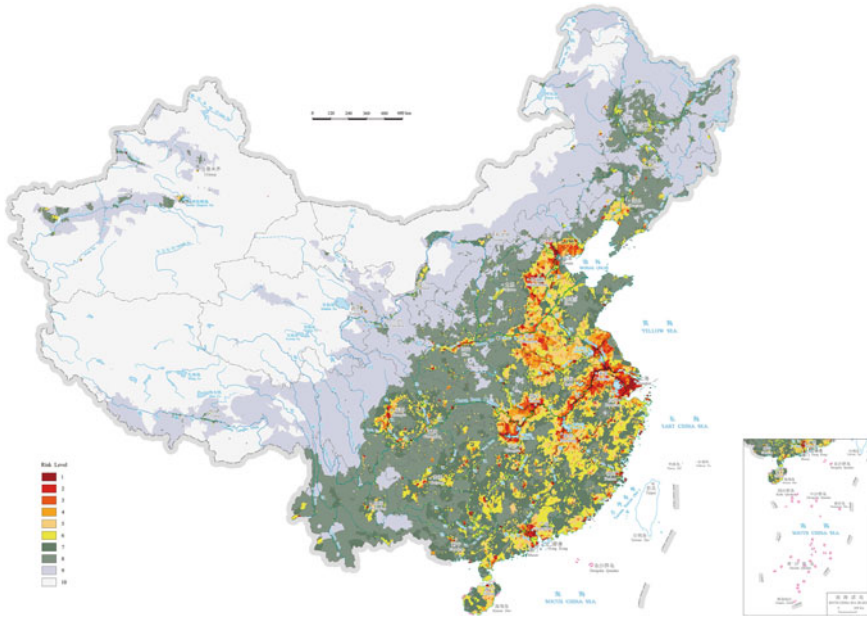


Fig. 11 Comprehensive assessment of China's flood risk (Source Shi 2011, p. 48–49)

3 Responses to the Great Floods in 1998

In 1998, great floods occurred in a number of major rivers in China, including the Yangtze River, Songhua River, Pearl River, and Min River. The 1998 Yangtze River flood was the second largest basin-wide flood in the twentieth century, only next to the 1954 flood. The Songhua River flood ranked the greatest for the river in this time period. In Xijiang River of the Pearl River basin, the 1998 flood was the second largest of the twentieth century, and the Min River flood was the largest. Under the strong leadership of the Communist Party of China (CPC) Central Committee and with an extraordinary flood-fighting spirit, and by relying on the flood control systems created over a 50-year period since the founding of the People's Republic of China (PRC), as well as the material basis built since the economic reform from the early 1980s, local residents and the army launched a battle against the floods. As a result, major damage to the Yangtze and Songhua River dikes and those along other major rivers was avoided; safety of key cities and major transportation routes as well as lives and properties was protected; flood losses were reduced to the largest extent possible; and a victory of flood rescue and relief was achieved. The State Council immediately started on a series of deployments for post-disaster reconstruction, rehabilitation of rivers and lakes, and water conservancy after the disasters.

3.1 Affected Area and Duration of the Floods

The 1998 floods in China occurred mainly in the middle- and lower-reaches of the Yangtze River region (Fig. 12) and the Pearl River, Min River, and Songhua River basins.

The total number of counties that were affected by the floods in the Yangtze River basin amounted to 162, accounting for 22 % of all counties in the basin. Among those, severely affected counties were 46, accounting for 6 % of the total. The affected region was mainly located in the plain areas in the middle- and lower-reaches of the Yangtze River basin. Hunan, Hubei, and Jiangxi Provinces experienced the most severe losses and had the largest affected areas (Table 3).

During the 1998 great floods, floods in the Yangtze River basin occurred between June and August. Due to the concentration of heavy rainfall from mid- and late June to July and early August, frequent rainfall events occurred, and the total precipitation greatly exceeded the historical high in this region. Coupled with changes in land cover, surface runoff increased and quickly discharged into river channels, resulting in rising water levels in river channels and the formation of multiple flood peaks.

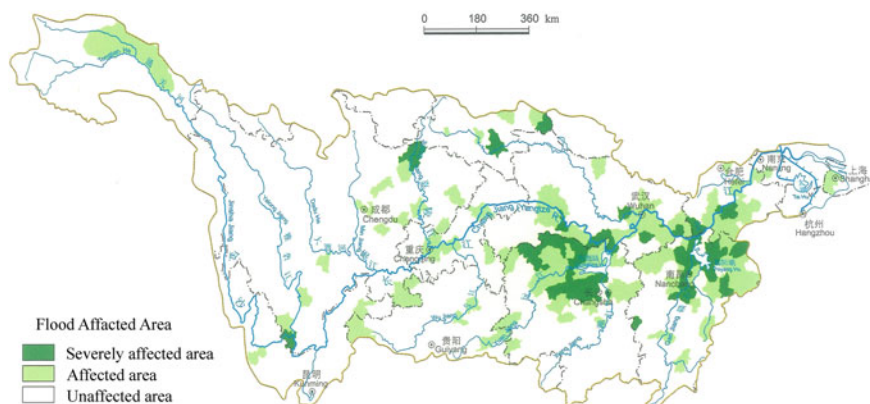


Fig. 12 Severity of the 1998 floods in the Yangtze River basin (Data source Shi 2003, p. 111)

Table 3 The number of affected counties in the Yangtze River basin by the 1998 flood

	Number of counties affected	Percentage of the total	Number of severely affected counties	Percentage of the total
Yangtze River Basin	162	22	46	6
Hunan	39	20	31	16
Hubei	22	27	10	12
Jiangxi	24	27	15	17

3.2 Factors Affected the Formation of the Floods

Factors leading to the occurrence of this basin-wide great flood in the Yangtze River are multiple, originated from both natural and human causes.

Abnormal climatic conditions: Climate anomalies including the 1998 El Nino, above-normal snow accumulation in Eurasia and the Tibet Plateau in the winter and spring, exceptionally strong subtropical high in western Pacific, mid-latitude circulation anomalies in Asia, and frequent activities of the blocking high resulted in the clearly above-normal precipitation during the flooding season in 1998 (Fig. 13). In the mid- to late June, heavy rainfall occurred in the northern part of the region south of the Yangtze River and the western part of South China and the first flood peak in the Yangtze River had already appeared. In late July, sustained heavy rains fell again in the middle- and lower-Yangtze region. In August, the upper-Yangtze region experienced frequent rainfall, floods from this region converged with that from the middle-Yangtze region and thus resulted in the basin-wide great flood. Because the total amount of precipitation was high and concentrated, it led to high floodwater levels and multiple peaks as well as long flood duration. Therefore severe flood disasters broke out in the Yangtze River region.

Topographic factors: The Yangtze River flows through the three topographic ladders of China and can be divided into three reaches accordingly. The upper-reach runs between the source and Yichang in Hubei Province; the middle-reach extends from Yichang to Hukou in Jiangxi Province; and the lower-reach is from Hukou downwards. The upper-reach is located in mountainous areas. Once a heavy rainfall event occur, the convergence time for flood water is very short and the time left for the middle- and lower-reach areas to prepare for

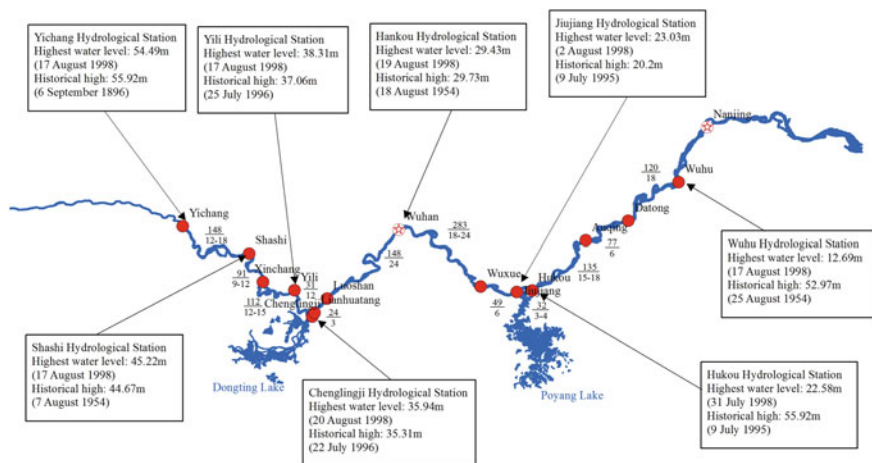


Fig. 13 Water level at the main hydrological stations on the Yangtze River in 1998 (Data source Provincial level newspapers in June–August 1998)

flood control is short. The middle- and lower-reaches of the river are located on alluvial plains. River course gradient is relatively low, especially in the middle-reach area. Slow discharge extends the period of high floodwater level. In 1998, water levels measured at hydrological stations along the river exceeded the historical highs in more than 30 days, and in about 60 days it was above the warning level.

Impacts of human activities: Human activities first involved the large-scale reclamation of the lakes and the reduction of water storage capacity. In 1998 the first four maximum flows of the Yangtze River did not exceed 60,000 m³/s at Yichang, but the fifth, also the largest in history, reached 61,000 m³/s and the water level was above the historical high. It indicates that the floodwater discharge and storage functions of the middle- and lower-reaches of the river and lakes had significantly declined. Between 1949 and 1998, the eight major lakes that take in and store the Yangtze River floodwater experienced a total areal reduction of 5,500 km², accounting for 1/3 of the previous lake areas. Among these, the area of the Dongting Lake was reduced from 4,200 km² to less than 3,000 km² in 1998; the Poyang Lake area changed from 5,000 km² to less than 4,000 km²; and the Tai Lake area declined from 3,200–2,900 km². The reduction rates ranged from 5 to 90 % (Table 4). Two main reasons contributed to the reduction of water area of the lakes—destruction of vegetation cover upstreams and the subsequent soil erosion and siltation of rivers and lakes, and reclamation in the middle- and lower-reaches of the Yangtze River region that directly altered the area of rivers and lakes.

Second, the impacts of human activities were manifested in changing land cover within the basin that reduced the capacity of the land surface to infiltrate rainwater. Upon reaching the ground, rainwater quickly converged and emptied into main river channels. This not only reduced the convergence time, but also increased the total amount of runoff and thus resulted in the historical high of floodwater levels.

Socioeconomic factors: In addition to natural factors, socioeconomic factors also contributed greatly to the flooding problem. With economic development, social progress, and rapid population growth, per unit land area population and property values increased dramatically, which led to the corresponding increase in absolute losses. In 1998 the total population of the Yangtze River region was 400 million. In Sichuan, Chongqing, Hubei, Hunan, Jiangxi, and Anhui alone it was 340.9 million, which more than doubled since 1953 (170.4 million). Annual population growth rate was 1.7–2.1 % from 1949–1998 for the region as a whole. Increased investment in fixed assets was also a problem. With rapid population growth, migration to high-risk flood zones increased, so was the investment. In

Table 4 Reduction rate of lake area in the Yangtze River basin

Lake	Poyang Lake	Dongting Lake	Tai Lake	Liangzi Lake	Xiliang Lake	Hong Lake	Diaocha Lake	Chao Lake
Reduction rate	20	29	9.3	50	80	50	90	5

1952 when the Jing River flood diversion area was first established, only 170 thousand people lived in the area and the number of people displaced during a flood diversion event was only 60 thousand. In 1998, more than 500 thousand people live in the area and the value of fixed assets had reached 2 billion Yuan. Heightened value in fixed assets made flood diversion increasingly impossible and floodwater was retained in the main river channel, and thus resulted in the high water level, long duration, and severe losses of the 1998 flood.

Many factors contributed to the basin-wide flood of the Yangtze River in 1998, including natural factors and human activities, but also socioeconomic factors. Among these, abnormal climatic conditions and human modification of the land are the primary factors. A greater concentration of population and economy also reduced the disaster resistance capacities of the human society and contributed to the very serious disaster losses. Therefore, flood risk reduction should take into account disaster-formative conditions and focuses on not only controlling natural variability, but also improving the resilience of the exposure units in order to adapt to the changing environment.

3.3 *Flood Disasters*

Disaster losses nationwide: As confirmed by the Ministry of Civil Affairs, Ministry of Water Resources, Ministry of Agriculture, State Statistics Bureau, and China Meteorological Administration at the end of the year, flood was the most severe of all disasters in China in 1998. A total of 29 provinces (autonomous regions, municipalities) suffered various degrees of flooding, 180 million people (times) were affected by the floods, 4,150 people died, and 18.4 million people were evacuated. The collapsed houses amounted to 6.85 million, while 13.3 million houses were damaged. A total of 22.3 million ha of croplands was affected, the disaster area for agriculture was 13.8 million ha, and harvest was completely lost on 5.3 million ha of croplands. The floods caused direct economic losses of 255.1 billion Yuan (Table 5). Jiangxi, Hunan, Hubei, Anhui, Heilongjiang, Jilin, Inner Mongolia, Fujian, Guangxi, Sichuan, and Chongqing were the most affected provinces (autonomous regions, municipality) (Fig. 12).

Yangtze River floods: During the flooding season in 1998, eight peak flows occurred in the upper-Yangtze River and the floodwater encountered floods from the middle- and lower-reaches of the river thus formed basin-wide floods. The total volume of floodwater from the upper-Yangtze River was high in 1998, but the peak flow was lower than in 1954. Peak flow at Yichang was equivalent to a flood of 6- to 8-year return period. At the Yichang Station, the maximum 30-day flood volume in 1998 was similar to that in 1954, and was 31.4 billion m³ higher than that in 1931 (Table 6); the maximum 60-day flood volume was 9.7 billion m³ higher than in

Table 5 Disaster losses during the 1998 floods

		Nen River and Songhua River	Five Provinces in the Yangtze River Basin (Hunan, Hubei, Jiangxi, Anhui, Jiangsu)	Nationwide
Affected Population (thousand)		1,335	8,411	18,600
Affected Cropland (thousand ha)		4,830		22,000
Disaster area of agriculture (thousand ha)			6,525	13,800
Collapsed Houses (thousand)		1,750	3,290	6,850
Death Toll (persons)		156	1,562	4,150
Direct Economic losses (billion Yuan)		51.7	134.5	255.1
Breached structures	Affected Population (thousand)	534	406	
	Collapsed Houses (thousand)	770	1,290	
	Death Toll (persons)	94	241	
	Direct Economic losses (billion Yuan)	27.2	19.4	

Table 6 Floodwater volume (*unit* billion m³)

Station		1998		1954		1931	
		30 days	60 days	30 days	60 days	30 days	60 days
Yichang	Observed	137.9	254.5	138.6	244.8	106.5	189.3
Hankou	Observed	175.4	336.5	173.0	322		
	Calculated	188.5	353.6	218.2	383	192.2	330.2
Datong	Observed	202.7	395.1	219.4	421		
	Calculated	219.3	417.4	257.6	490		

Note The “calculated” numbers in the table are the sums of water volumes passed through breached dykes and diverted to floodwater diversion areas

1954, and 62.5 billion m³ higher than in 1931. Seen from the total floodwater volume, the 1998 flood was an event of 100-year recurrence interval and was the second largest basin-wide flood in the twentieth century, only smaller than the 1954 flood (Fig. 13).

Songhua River floods: Since the start of the 1998 flooding season, precipitation in the Nen River basin at the upper-reach of the Songhua River was clearly above normal, and three major floods eventually formed. The first flood occurred in late June to early July. Floodwater mainly originated from the upper-Nen River and its

tributaries. The second flood occurred in late July to early August and the flood-water was primarily from the middle- and lower-Nen River. The third flood occurred in early and mid-August and was a basin-wide flood in the Nen River basin, with a return period of 100–1000 years. Affected by the runoff from the tributaries, the Nen River water level rose rapidly. At the Qiqihar Hydrological Stations, the highest water level was 149.30 m, 0.69 m higher than the observed highest historical water level. The highest water level of 120.89 m occurred in Harbin on the Songhua River on August 22, 0.84 m higher than the observed historical high, with a flow of 16,600 m³/s. The flood was of about 150-year return period and the greatest of the century (Fig. 14).

Xijiang River and Min River floods: In June 1998, a 100-year return period flood occurred in the Xijiang River of the Pearl River basin. On Xijiang River's tributary Gui River, the Guilin Hydrological Station experienced four consecutive peak flows in June, with the highest water level of 147.70 m, the highest ever observed. Affected by the runoff from the upstream and the tributaries in combination with runoff from localized rainfall, Wuzhou Station on the Xijiang River observed a maximum flow of 52,900 m³/s and a water level of 26.51 m. The flood was the second greatest in the Xijiang River basin in the twentieth century.

Also in this flooding season, heavy rains fell in basins of the tributaries of the Min River in Fujian Province, resulting in major floods in the Min River and its tributaries. At Shuikou Power Station on the Min River, the largest inflow reached

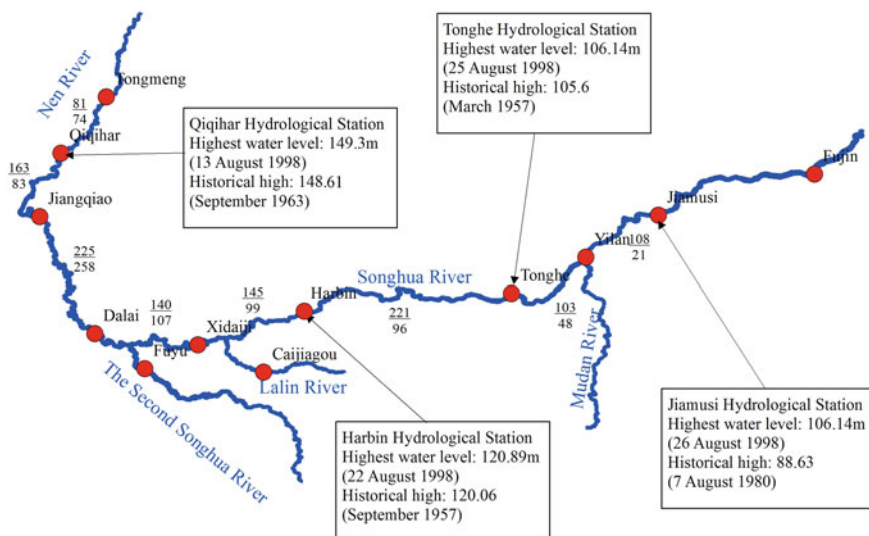


Fig. 14 Water level at the main hydrological stations on the Songhua River in 1998 (*Data source* Provincial level newspapers in June–August 1998)

37,000 m³/s. At the Zhuqi Station on the Min River below the reservoir, the highest water level was 16.95 m and the maximum flow was still as high as 33,800 m³/s—the largest flood of the century.

3.4 *Flood Disaster Responses*

Upon the occurrence of the flood disasters, the CPC Central Committee and State Council attached great importance to fighting the floods. Through the State Flood Control and Drought Relief Headquarters (SFCDRH), the State Council mobilized the River Basin Commissions (RBCs) to fully engage in the flood relief work. The then Party General Secretary Jiang Zemin and Premier Li Peng commanded at the frontline on flood relief.

Mobilization of rescue and relief forces nationwide: A total of 180 thousand members of the People's Liberation Army and more than five million armed police, militia, and reservists were mobilized for emergency rescue and disaster relief. A total of 4.3 million persons (trips) were involved, and more than 110 generals took command at the frontlines. A total of 1,289 flights and 236.8 thousand vehicle and 37.5 thousand boat trips were ordered. The largest number of troops from the Army for combating a natural disaster since the founding of the PRC was sent to the disaster area. A total of 22,728 medical teams and 125 thousand volunteers—the largest numbers in history—participated in disaster relief and assistance. Facing the catastrophic floods that had rarely been seen in history, the nation set off on rescue and relief according to the unified arrangements of the CPC Central Committee and the State Council.

Mobilization of resources: China Meteorological Administration and Ministry of Water Resources closely monitored the flooding situation and hydrological conditions and issued early warning and optimized coordination. Ministry of Civil Affairs (MCA) closely followed the disaster and disaster relief processes in various regions, accurately grasped disaster related information and assessed losses, and reported in a timely fashion to the State Council and communicated to the international community about the disasters and relief work. MCA also actively coordinated the support to the disaster area from relevant government departments, and swiftly allocated relief funds and materials. Under the CPC Central Committee and the State Council's unified plan, the largest disaster relief donation since the founding of the PRC was organized. According to the statistics, 11.37 billion Yuan of funds and relief materials in 1998 alone were acquired from the central government and disaster relief donations for helping with the living of the disaster affected people, together with an emergency allocation of 130 thousand special disaster relief tents. In addition, MCA also organized in 13 provinces (autonomous regions and municipalities) to collect 56.98 million pieces unlined clothes, 35.75 million pieces winter clothes, and 6.08 million quilts to help those in severely affected provinces (autonomous regions and municipalities) in a counterpart assistance effort. As of August 19, SFCDRH allocated a total of 73.73 million

textile bags, 5.7 million sacks, 550 assault boats, 2,345 rubber boats, 298 thousand life jackets, 69 thousand life buoys, 1.61 million m² nonwoven cloth, 8.57 million m² weaving cloth, 260 tons plastic film, 455 tons steel wire, and 27 thousand m³ sand and gravel for construction, at a total value of 200 million Yuan, which was the highest compared with in all previous disasters.

In 1998 the central government allocated 8.33 billion Yuan disaster relief funds and a large number of disaster relief supplies. Among these, catastrophic natural disaster relief subsidies amounted to 2.89 billion Yuan, post-disaster reconstruction funds 1.22 billion Yuan, flood control funds 2.89 billion Yuan, restoration funds for damaged structures 50 million Yuan, disaster epidemic prevention funds 283.5 million Yuan, relief funding for cultural and educational institutions 749.8 million Yuan, fertilizer 200 thousand tons, and diesels 500 thousand tons.

Mobilization of social forces for disaster relief: According to the Department of Disaster Relief of the Ministry of Civil Affairs, MCA, China Charity Federation, Red Cross Society of China, and local civil affairs departments together received contributions of 3.52 billion Yuan and 3.74 billion Yuan worth of materials, at a total of 7.26 billion Yuan. MCA directly received donations of 1.05 billion Yuan and 834 million Yuan worth of materials, at a total of 1.88 billion Yuan; China Charity Federation received donations of 328 million Yuan and 235 million Yuan worth of materials, at a total of 563 million Yuan; Red Cross Society of China received 130 million Yuan donations and 140 million Yuan worth of materials, at a total of 270 million Yuan; and local civil affairs departments received donations of 2.01 billion Yuan and 2.54 billion Yuan worth of materials, at a total of 4.54 billion Yuan.

Among these contributions, donations received in mainland China amounted to 2.91 billion Yuan and 3.50 billion Yuan worth of materials, at a total of 6.41 billion Yuan, accounting for 88.35 % of the total donations for disaster relief; donations from Hong Kong, Macao, and Taiwan totaled 352 million Yuan, and the donated materials were at a net worth of 22 million Yuan, which together become 374 million Yuan, accounting for 5.14 % of total disaster relief donations; foreign governments, international organizations, and others from overseas donated 253 million Yuan and 219 million Yuan worth of materials, at a total of 472 million Yuan, accounting for 6.51 % of the total disaster relief donations.

References

- China Meteorological Administration. n.d. China meteorological data sharing service system. <http://cdc.cma.gov.cn/home.do>. Accessed May 2014 (in Chinese).
- Chen, H.P., J.Q. Sun, and X.L. Chen. 2013. Future changes of drought and flood events in China under a global warming scenario. *Atmospheric and Oceanic Science Letters* 6(1): 8–13.
- China Meteorological Administration (CMA). 1995. Maps of rainstorm flood disaster distribution in China from 1951–1990 (in Chinese).
- ECCPGCAS (Editorial Board of China Physical Geography, Chinese Academy of Sciences). 1985. *China Physical geography: Overview*. Beijing: Science Press (in Chinese).

- Fan, B.J. 1998. *Natural disaster and disaster management in China*. Harbin: Heilongjiang Education Press. (in Chinese).
- Fang, W.H., J.A. Wang, and P.J. Shi. 2011. *Integrated risk governance: Database, risk mapping and network platform*. Beijing: Science Press. (in Chinese).
- Li, J.S. 1999. *Series books of river flood control in China: Overview*. Beijing: China Water Power Press. (in Chinese).
- Ma, Z.J. 1994. *China's major natural disasters and disaster mitigation measures*. Beijing: Science Press. (in Chinese).
- Shi, P.J. 2003. *Atlas of natural disaster system of China*. Beijing: Science Press. (in Chinese and English).
- Shi, P.J. 2011. *Atlas of natural disaster risk of China*. Beijing: Science Press. (in Chinese and English).
- Shi, P.J., F. Kong, and J.Y. Fang. 2014. Spatio-temporal patterns of China decadal storm rainfall. *Scientia Geographica Sinica* 34(11): 1281–1290.
- Shi, P.J., W.G. Zhou, W.H. Fang, et al. 1999. Mechanism of influence of landuse change on agriculture natural disaster (II)-Based on the home inquiry, field investigation and GPS analysis. *Journal of Natural Disasters* 8(3): 22–29.
- Tian, G.Z., X.L. Liu, P. Wang, et al. 2006. Flood risk zoning and causal analysis in China. *Journal of Catastrophology* 21(2): 1–6. (in Chinese).
- Wang, J.A., P.J. Shi, and X.L. Zhao. 1997. Regional patterns and monthly changes of natural disasters in China during last five years. *Journal of Natural Disasters* 6(3): 10–15. (in Chinese).
- Wang, J.A., P.J. Shi, P. Wang, et al. 2006. *Spatiotemporal pattern of natural disasters in China*. Beijing: Science Press. (in Chinese).
- Xu, X., J.A. Wang, and W.Y. Wang. 2000. The construction and application of the natural disaster case database in china. *Journal of Beijing Normal University (Natural Science)* 36(2): 274–280. (in Chinese).

Droughts in China

Tao Ye, Huicong Jia, Yongdeng Lei, Peijun Shi and Jing'ai Wang

Abstract China is a country frequently hit by droughts and enormous losses, particularly in agriculture, were claimed in the past years. This chapter discusses drought in China. It first explores the spatial and temporal patterns and dynamic change of historical droughts based on statistical data. Causal factors and mechanisms of agricultural drought, which substantially differ from region to region, are carefully examined through regional cases studies. Agricultural drought risks of China, including those for paddy rice, maize, and wheat, are mapped based on a quantitative assessment of physical vulnerability function of crops to drought stresses. Last but not the least, the Chinese strategies for drought disaster response is discussed via three major drought disaster cases.

Keywords Drought · Spatiotemporal pattern · Physical vulnerability · Risk assessment · Response strategy

Drought is a phenomenon that occurs when precipitation is significantly below normal recorded levels, causing serious hydrological imbalance and resulting in a series of negative impacts on land resources and production systems (IPCC 2001a, b). Drought is regarded as a disaster if losses are incurred in the exposed socioeconomic and ecological systems. The impact of drought could reach nearly every area of

T. Ye · P. Shi

State Key Laboratory of Earth Surface Processes and Resource Ecology,
Beijing Normal University, Beijing 100875, China

H. Jia

Institute of Remote Sensing and Digital Earth, Chinese Academy of Sciences,
Beijing 100094, China

Y. Lei

Key Laboratory of Region Geography, Beijing Normal University,
Beijing 100875, China

J. Wang (✉)

School of Geography, Beijing Normal University, Beijing 100875, China
e-mail: jwang@bnu.edu.cn

socioeconomic life and the natural system due to the fundamental importance of water.

As the world's most populous agricultural country, China is frequently hit by drought disasters and enormous losses were claimed in the past years (Gao 2005). China's food security is not only the nation's own problem, but also may influence the world's political and economic situations. During the past 50 years, in the context of global warming and the drying trend in the northern part of the country, the impact of drought in China has increased (Wang et al. 2002). Therefore it is of great importance to analyze the spatial and temporal patterns and process of drought risks and summarize the Chinese society's drought risk management paradigm in the context of climate change.

Since the 1990s, in response to the International Decade for Natural Disaster Reduction, the departments of meteorology, water conservancy, and agriculture of the Chinese Government funded various research projects on drought and its management. The disaster risk research group at Beijing Normal University also launched its drought studies correspondingly. The group has completed several research projects on droughts of China. Two of these projects, funded by the National Natural Science Foundation of China (NSFC), focused on agricultural drought: "*Diagnosis and Evaluation of Agricultural Vulnerability during the Formation Process of Regional Agricultural Drought Disasters*" (NSFC No. 40271005) (2003–2005) and "*Regional Assessment Methods of Agricultural Drought Disaster Recovery and Mechanism of Comprehensive Disaster Reduction*" (NSFC No. 40271003) (2007–2009). Meanwhile, the group also participated in a National Science and Technology Support Program "*Key Technologies in Integrated Disaster Risk Management and Demonstrations*" of the Ministry of Science and Technology (MOST). The group mainly worked in the third subproject "*Platform of Integrated Risk Management*" (2006BAD20B03) under the theme of "*Drought Disaster Database and Drought Risk Mapping (1:1 million)*," which was finalized in August 2010. The group is presently participating in a China Meteorological Administration (CMA) funded project, "*Regionalization of China Meteorological Disaster Risk under Global Change*" (GYHY200906019). Through these projects, the group has examined the spatial and temporal patterns of agricultural droughts, agricultural drought vulnerability, and the formation of agricultural droughts, and conducted quantitative evaluations of post-drought recovery. This chapter is an integrated summary of the results of these projects and studies (Wang et al. 2006; Shi 2003, 2011).

1 Spatial and Temporal Patterns of Droughts

This section introduces the spatial and temporal patterns of droughts in China. The major sources of information for research on drought patterns are data from weather stations, record of severe historical drought events, provincial-level disaster statistical data, among others (Table 1; Wang et al. 2002).

Table 1 Data sources supporting pattern analysis

Data	Content	Period (year)	Source
Statistical data of drought disasters	Drought-affected areas and disaster areas of each province	1978–2009	China statistical yearbooks; China agricultural statistical database
Statistical data and reports of drought events from newspapers and other media	Start and end of droughts and drought intensity at the county level	1949–2010	Provincial newspapers and other major mass media

1.1 Spatial Distribution of Droughts

In order to reveal the spatial distribution of droughts, annual frequency of occurrence of droughts is extracted from the database of newspaper and other media reported droughts at the county level. The annual frequency of occurrence is used as the variable for depicting the spatial pattern (Fig. 1).

Figure 1 shows a primarily East–West disparity of droughts and some difference between the North and South. There are 169 counties in the country whose drought frequency is over 0.15 and these counties account for 7.2 % of the total number of counties in China; for another 513 counties drought frequency is above 0.10. These counties account for 22 % of the total nationwide.

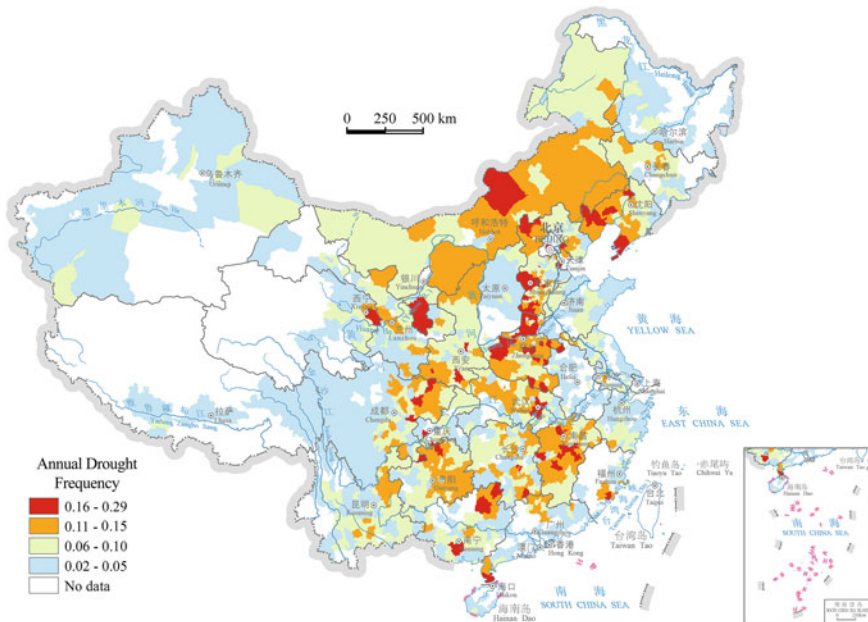


Fig. 1 Drought frequency of counties in China, 1949–2010

High frequency centers of droughts in China are located in the central and western regions of Inner Mongolia, Ningxia, Hebei, Henan, Anhui, East Sichuan, and Chongqing. The regions with the second highest level of frequency (0.10–0.15) are mostly connected to the high frequency centers, covering near half of the areas in eastern and central China.

The spatial distribution of the drought centers and affected areas are surprisingly similar to the agricultural zones in China. Regions with high drought frequency overlap with the rain-fed agricultural area producing cereals in the transitional zone between the agricultural and pastoral areas in northern China, irrigated agricultural area producing winter wheat and summer corn in the Huang-Huai-Hai Rivers Plain, and the paddy agricultural area producing rice in Hunan Province.

Comparing the spatial patterns of drought frequency and China's population density and GDP of recent years, it shows that the vast majority of counties with lower per capita GDP suffered relatively high-frequency droughts, indicating that the occurrence of droughts and their severity are closely related to regional economic development and vulnerability. Heavy reliance on agriculture of the less developed regions entails higher vulnerability to droughts. Exceptions to this pattern are that some regions with relatively high per capita GDP in the past decade were also affected by severe droughts, such as Ordos in Inner Mongolia and northern Shaanxi. This situation may be attributed to the area's extremely rapid economic development in the past decade due to its rich energy resources and low investments to drought-relief facilities.

1.2 Temporal Distribution of Droughts

The temporal distribution of droughts in China is represented by the time series of agricultural losses claimed by droughts in the past 30 years (Fig. 2).

The annual average affected area and disaster area are 25 million and 14 million hectares in the past 30 years, respectively. There is no apparent trend detected with this time series. There are five peaks of droughts in China: 1978, 1992, 1997, 1999–2001, and 2007 (three more major drought events occurred in 2009 and 2010, but the statistical data were not available at the time of this research). In the years of severe droughts, China experienced serious drought-related disaster losses. For instance, during 1999–2001, China went through a multi-year continuous drought. In 1999, 30 provinces, autonomous regions, and direct-controlled municipalities experienced droughts and more than 30 million hectares of crops are affected. In 2000, over 20 provinces and equivalent administrative units experienced droughts and more than 40 million hectares of crops were affected. The drought in this year updated the records of yield and direct economic losses claimed by droughts since 1949. Particularly, this drought lasted into 2001, when 30 provinces, autonomous regions, and municipalities again experienced droughts with over 38 million hectares of crops affected.

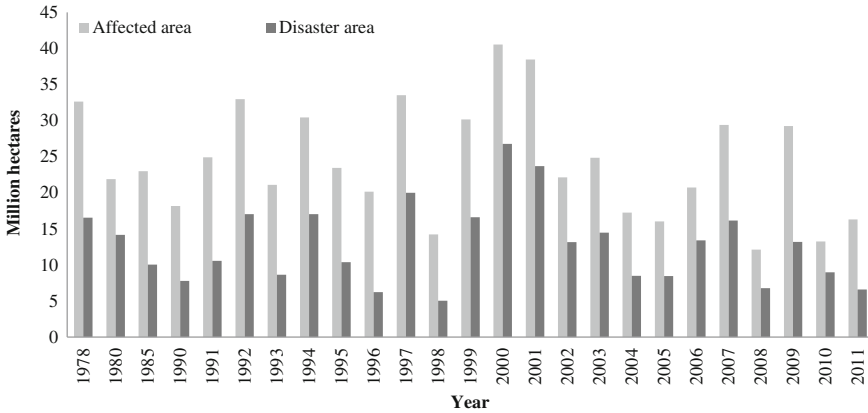


Fig. 2 Temporal pattern of agricultural droughts in China, 1978–2011 (“Affected area” and “disaster area” are the measurements of drought severity commonly used in China. The former refers to the area of crops that experienced a loss of over 10 % of normal yield for the place while the latter refers to the area of crops that experienced a loss of over 30 % normal yield.) [Data source China Statistical Yearbook 2009 (National Bureau of Statistics of China 2012)]

1.3 The Dynamic Spatial and Temporal Patterns of Droughts

In order to show the dynamic changes of drought to annual drought frequency index is calculated (Fig. 3). The index measures the average occurrence of drought per county per year in each province.

It is the total occurrence of drought measured by the total number of counties affected by drought in a year¹ divided by the total number of counties in the province. As droughts normally affect tens of counties, so the provincial total occurrence measured at the county scale is much larger than the one measured at the provincial scale.

In this figure, both the spatial distribution of droughts and the trend of each province are presented. The dynamic change shows a North–South disparity rather than the east–west difference as observed in Fig. 1. In the northern part of China, most of the provinces experienced an increasing drought occurrence over the six decades. This phenomenon can be mainly attributed to the rapid expansion of rain-fed agriculture and the increasing aridity in northern China (Shi and Zhang 1995; Li 2001). With the expansion of agriculture exposure and global warming, these regions are increasingly affected by summer and autumn droughts. In some places rapid urbanization and industrialization also contributed to this change—one such example is the drastic increase in water demand from non-agricultural sectors in Shandong Province. On the other hand, in the southern part of China (south of the

¹It is very common that multiple counties are affected simultaneously by the same drought.

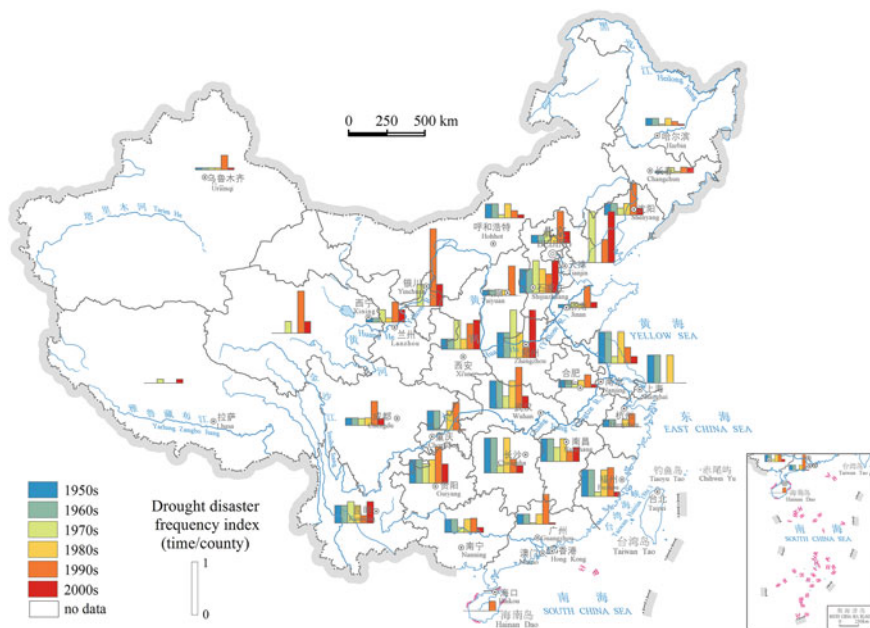


Fig. 3 Regional discrepancy of drought disaster dynamics in China, 1951–2010

Yangtze River), the increase is much slower, except for Yunnan, Guangxi, Hunan, and Jiangxi Provinces.

China’s drought dynamics has three main characteristics. First, the frequency of droughts in the East is higher than the West (with the East-to-West boundary at the Hu Huan-yong population density line), also higher in the North than the South. Second, the proportion of drought-affected counties had risen from 83 % (the average level during 1949–1965) to about 94 % (the average level during 1978–2000). Therefore in the later period, on average almost every county was hit by drought once a year. Drought-prone areas extended to the northeast and southwest, especially to the areas where dry land farming had expanded. Third, high drought severity places in the pastoral area in central and eastern Inner Mongolia remained relatively unchanged in the past decades. Drought centers in rural areas changed greatly, in general shifted from the South to the North.

The pattern of drought dynamics has a number of important implications. For the natural environmental system, in the past 30 years, there was a regional warming and drying trend in northern China (Fu and Ma 2008). Especially in the northeast, North China, and the eastern part of the northwest, continuous droughts have been a serious threat to the living environment of people, leading to a severe shortage of local water resources, environmental degradation, and desertification. In eastern Inner Mongolia, sandy desertification expanded at a rate of 2.4 % annually in the past 10 years. Stream flow in the Yellow River has been decreasing. Meanwhile, the main agricultural areas in the northern arid areas have expanded. The decreased

precipitation and increased temperature in northern China is the main cause of the recent droughts in most regions.

Socioeconomic activities have also played a significant role in this transition. Studies (Liu et al. 2007; Lu and Mei 2007) show that from the 1970s to the 2000s, the proportion of grain produced in the northern part of China increased from 52.5 to 58.9 %. Contribution to the growth of harvest from northern China increased from 53.9 % in the 1970s to 85.1 % in the 2000s. Taking the national average per capita grain consumption as the criterion, regions with surplus of grain changed from Northeast China, the Yangtze River Basin, and South China in the 1970s to Northeast China and North China in the 2000s. From the 1970s to the mid-1990s, food grain was transported from the South to the North (Nan Liang Bei Yun in Chinese) and now the flow is in the opposite direction (Bei Liang Nan Yun in Chinese). The reasons for this change are complex, which include regional climate change, change in input of agricultural factors (cultivated land, labor, and irrigation facilities) and macroeconomic conditions (food structure), technological advances, and so on (Lu and Mei 2007). Consequently, China has increased agricultural exposure to droughts because agricultural production relies more on regions with poor water resources and drought prone. The increased overall vulnerability substantially increases the chance of occurrence of drought conditions.

The Chinese government is implementing the “National plan of increasing grain production capacity of 50 million tons (2009–2020),” which could further increase the grain production requirement for the northern part of the country. Associated with the regional warming and drying trend in northern China, the probability of spatial coupling of drought hazards and food production will increase significantly, which could heighten drought risks in China, especially in the north.

2 Formation and Assessment of Agriculture Drought Disasters

2.1 The Development of Agricultural Drought Disasters

The triggering and development of an agricultural drought disaster can be categorized into several types, according to the theoretical framework of regional disaster system (Fig. 4). It involves two processes: the formation of drought hazards and the formation of losses. The climate and weather system determines precipitation and the local environment determines the redistribution of water resources. If precipitation and water resources in a local area drop below some threshold and last long enough, a drought hazard may occur. The exposure unit—agricultural system will then be affected. The severity of the impact and the size of losses depend not only on the inherent drought-resistant ability of the crops (genetic fragility), but also on the input of drought relief (social vulnerability).

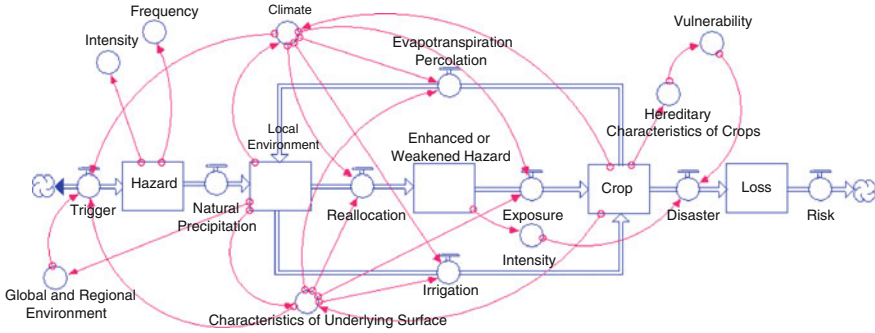


Fig. 4 Conceptual model of regional agricultural drought disaster processes (Source He 2010)

Two important features of the process of drought disaster formation differentiate it from some other natural disasters. On the one hand, the term “local” must be emphasized because local environment such as landform, soil type, and wind speed, may cause redistribution of moisture, temperature, and water. Empirical relationship between drought intensity at the macro scale (for example, regional precipitation) and losses in most cases do not apply to specific local areas. This is similar to flood disasters, in which rain water is redistributed according to the landform and in river streams. On the other hand, drought is a very typical slow onset disaster—a single drought event can last for days or even months. During the process interventions can be carried out to reduce the impact and potential losses. In this sense, societal response to drought is critical, in addition to the genetic fragility of crops (tolerance to water shortage). This is particularly meaningful for drought management.

2.2 Crop Drought Vulnerability

Types of agricultural drought disasters: With regard to water resource utilization, there are three main types of cropping systems—rain-fed agriculture, paddy agriculture, and irrigated agriculture. The spatial distribution of these systems creates significant regional differences in the formation of agricultural drought disasters. Typical areas of these systems correspond precisely to the high frequency centers of drought in Fig. 2. For instance, the region of rain-fed agriculture in the transitional zone between the agricultural and pastoral areas near Inner Mongolia is a high frequency center of drought. The Huang-Huai-Hai River Plain is the region with well-developed irrigation systems, producing mainly winter wheat and maize. Hunan Province is a typical area of paddy cropping, which is also a center of drought in southern China. Although these three regions all have high drought frequency, the driving factors are very different. They are examined below.

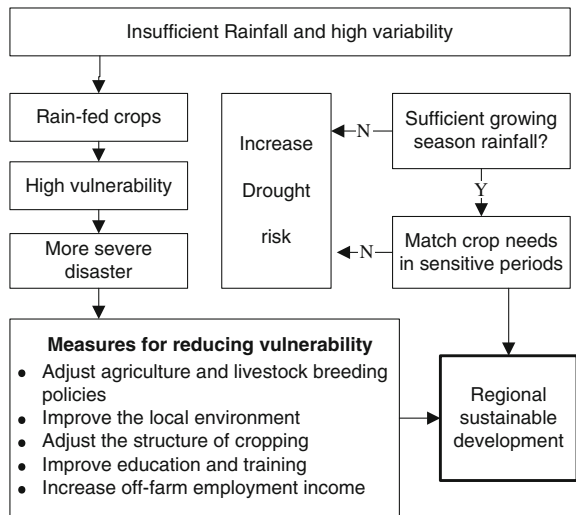
Droughts in rain-fed agriculture regions of China: Rain-fed agriculture refers to agricultural production that solely relies on natural precipitation. It is mainly

practiced in northern China’s arid and semi-arid areas. These regions have low precipitation but the seasonal and interannual variability of precipitation is high. The root cause of drought in these areas is the mismatch between water supply from precipitation and water demand by crops in the growing season (Fig. 5). Rainfall deficiency and interannual variations create great problems for farmers since the amount of precipitation is the key factor that determines the size of production outputs. Extremely low precipitation over large cultivated areas in a year could cause huge losses.

Drought in irrigated agriculture regions of China: Irrigated agriculture is a type of agricultural production for which irrigation facilities is provided and water supply is guaranteed to some degree. Irrigated agriculture allows more stable and higher outputs. In addition to the general cause of extremely low precipitation, drought in irrigated agricultural regions can also be triggered by the imbalance between regional water resource availability and the demand from agricultural production (Fig. 6). For instance, in urbanized and industrialized areas, the demand of water from non-agricultural sectors is getting increasingly high. The quotas of water allocated to the agriculture sector often decreased. In some parts of China, for example the North China Plain, agricultural production is seriously challenging the regional water supply limits.

Drought in the paddy agriculture regions of China: Paddy agriculture is a type of agricultural production that grows water-based crops in the cropland with ridges (that provide water storage) in areas with plenty of water. China’s paddy fields are generally located in the monsoon region in the South. In these areas, water resources are abundant, but annual and seasonal variations can be drastic. For instance, in the Dingcheng District of Changde, Hunan Province, 68–79 % of the annual precipitation occurs in the summer, while only 16–24 % falls in the autumn. In the seasons with plenty of water, drought is not likely to occur but the risk of

Fig. 5 Drought processes in rain-fed agriculture areas in China



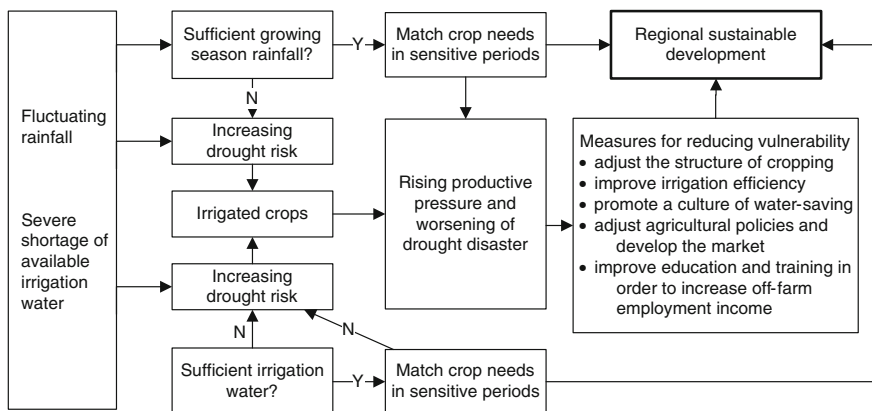


Fig. 6 Drought processes in irrigated agriculture areas in China

water logging is high. In the season with little precipitation, drought could be triggered because of the mismatch between demand and supply (Fig. 7).

In summary, water supply for crops comes from precipitation and irrigation, which is ultimately restricted by precipitation of an area. When the rain falls onto the ground, water either becomes directly available to crops, or is reallocated through runoff and stream flows and later made available to crops through irrigation systems. In this process, if the amount of precipitation is low in rain-fed agricultural

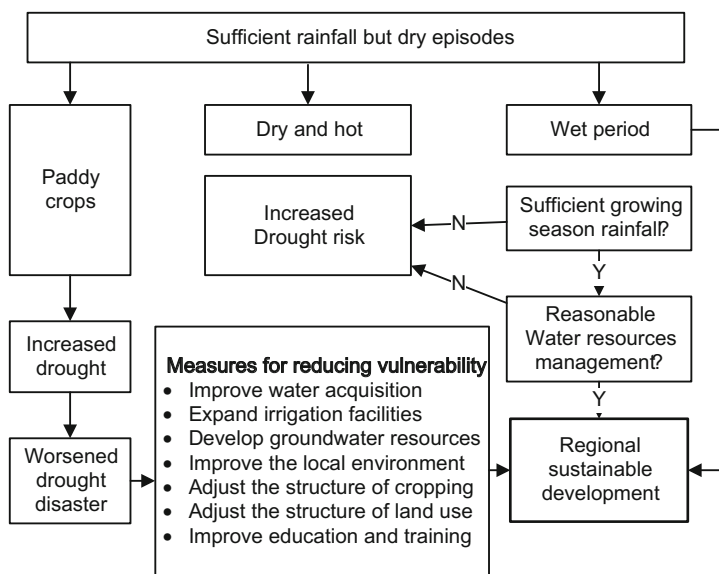


Fig. 7 Drought processes in paddy agriculture areas in China

regions or sufficiently low to be compensated by regional water conservancy and irrigation systems, crops will not receive sufficient amount of water for growth. In such case, agricultural drought is triggered.

2.3 Drought Vulnerability of Three Main Crops

The key factor determining agricultural drought is surface soil moisture. During the growth period of crops, water is supplied from surface soil and its moisture content directly affects crop growth and development. In this sense, quantifying vulnerability of crops to agricultural drought is to establish the quantitative relationship between the degree of water shortage and loss ratio of crops. Such relationship differs by the type of crops and local conditions, including soil conditions, temperature, field management, etc.

There are several approaches to derive such relationships. Examining historical disaster records is a good way to extract the empirical relationship between drought intensity and loss ratio of crops. When historical loss records are limited and feasibility of conducting field experiments are low, some substitutions can fill the gap. Lab experiment is a useful traditional approach, in which crops are planted in a laboratory with controlled environment. Loss in productivity is measured when controlled degree of water deficiency is introduced. The approach is, however, time consuming and costly. An alternative to the experiment method is to simulate with crop growth models. These models, based on principles of systems analysis and computer simulation techniques, quantify the process of crop growth, development, and yield and its response to environmental conditions (Whisler et al. 1986). A large number of growth simulation models have been developed by researchers (Williams et al. 1989).

In our study, we calculated the vulnerability curves of winter wheat, corn, and paddy rice for different regions of China (Wang 2009; Wang et al. 2013; Jia 2010; Lei et al. 2011). Ideally, crops' response to drought hazard is determined by inherent biophysical characteristics (genetic issue), local environment (soil type, temperature, wind speed, land form etc.), and field management practice (crop calendar, fertilizer and other inputs). Therefore, the term "vulnerability curve" is used here instead of "fragility curve". Vulnerability curves of wheat and corn are derived using the Environmental Policy Integrated Climate (EPIC) model (Gassman 2005). The EPIC model is a field scale crop model capable of simulating daily crop growth and yield under various climate and environment conditions, as well as complex management schemes, and operates on a continuous basin using a daily time step and can perform long-term simulations for hundreds of years (Wang et al. 2013). Vulnerability curves of paddy rice are determined by using historical disaster records.

Intensity of drought hazard is represented by different variables in different approaches. In the EPIC model, water stress is used, which is a variable based on the relationship between water supply and demand. Due to the long-lasting feature

of drought, both the degree and duration of water stress affect drought intensity. Crop drought hazard intensity is formulated as follows:

$$H_{yj} = \frac{\sum_{i=1}^n (1 - WS_i) - \min \mathbf{H}}{\max \mathbf{H} - \min \mathbf{H}}, \quad (1)$$

where H_{yj} is drought hazard intensity for year y and station j ; $(1 - WS_i)$ is water stress of day i for the current year and site; n denotes the number of days that the crop has experienced water stress; \mathbf{H} is the vector of water stress for all years and all sites, and its minimum and maximum values are used to normalize the index to the range $[0, 1]$.

In order to derive the loss ratio, two scenarios were set in the EPIC model: (1) perfect fertile and water supply (S1, the control); (2) perfect fertile but rain-fed (S2). Crop yields were simulated in each scenario. Since S1 is regarded as the ideal crop productivity, the difference between the simulated yields of S2 and S1 was then treated as the yield loss induced by water stress and drought. In order to allow cross region and crop comparison, absolute yield loss was converted to a relative value, loss ratio. Then we regress the loss ratio with drought intensity and the statistical relationship between the two variables is derived.

Historical disaster records used for deriving the vulnerability curves of paddy rice come from China Meteorological Disasters Collection (Ding 2008) and China Agricultural Statistical Data (Chen 2009), containing information about drought-affected and severely impacted areas and no harvest areas, production loss, etc.

Vulnerability curves of different regions and crops are not identical. The vulnerability curves are very different for different types of crops (for example, Yongning spring wheat vs. Wenmai spring wheat, Fig. 9) and by region (for example, maize and paddy rice in different regions of China, Figs. 8 and 10). Several factors contribute to this situation. When deriving the vulnerability curves, both type of crop and regional natural environmental conditions are used as inputs, including temperature, soil type, landform, fertilizer, as well as field management. The difference among the curves reflects not only the genetic drought-resistance of crops, but also the natural environment conditions of the concerned areas. Also, local farming and field management practices are different.

2.4 Agricultural Drought Disaster Risk

Drought risk assessment results were derived by integrating return-period drought intensities and regional drought vulnerability curves for each crop. Crop drought hazard intensity indexes are calculated according to Eq. 1 for each 1-km grid. Based on historical data, return-period drought intensity measured as intensity index for each grid are derived. Taking regional vulnerability curves into account,

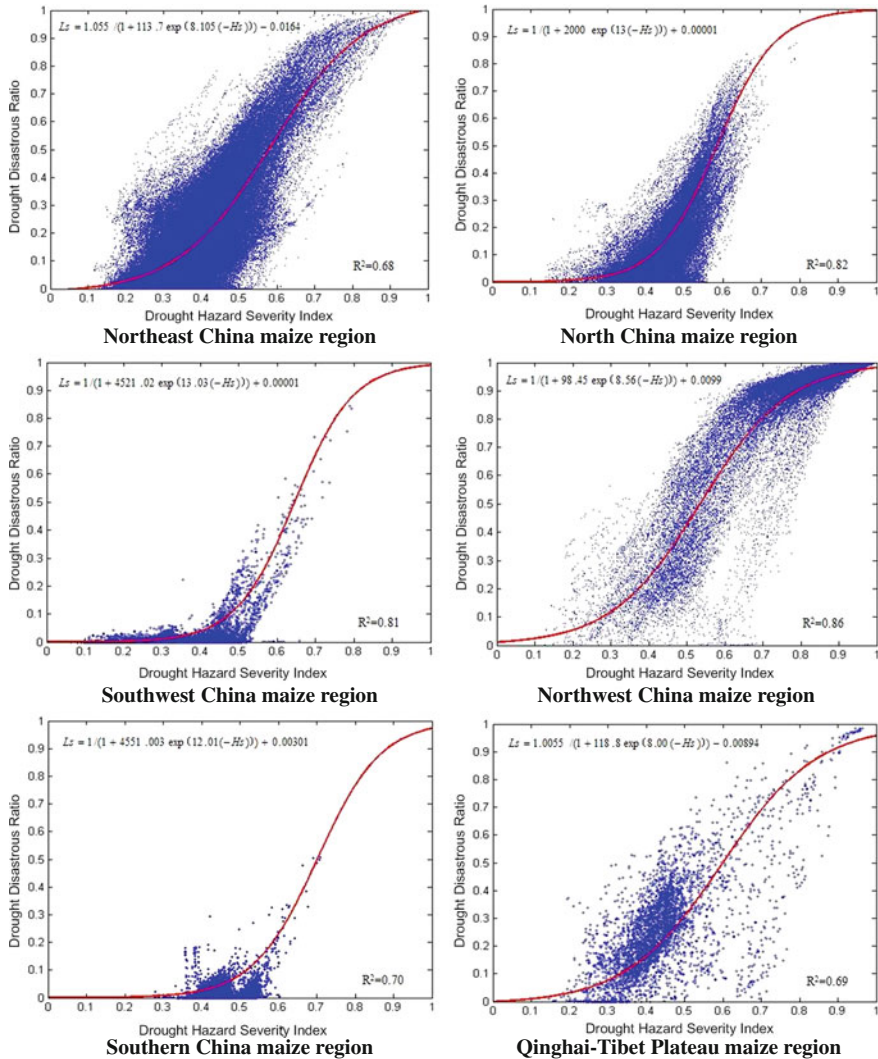


Fig. 8 Vulnerability curves of maize in different parts of China (Source Jia 2010)

crop drought loss measured as yield loss ratio (%) at the four return periods level are then calculated and mapped.

Drought risk of wheat in China: The result of risk assessment of drought for winter wheat is shown in Fig. 11 (Shi 2011). Yield loss decreases from the north (the semi-humid region) to the South. Risk of yield loss for spring wheat is higher than winter wheat. For spring wheat, yield loss level of the North China and northern Xinjiang regions are the highest. For winter wheat, yield loss risk of

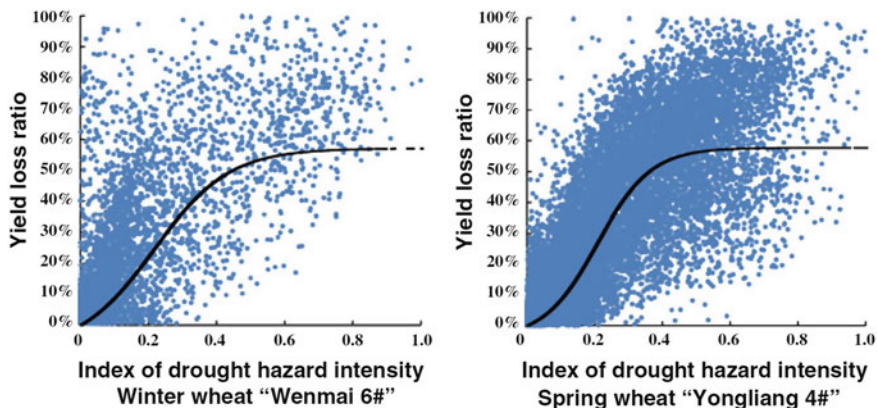


Fig. 9 Vulnerability curves of two types of wheat in China (Source Wang et al. 2013)

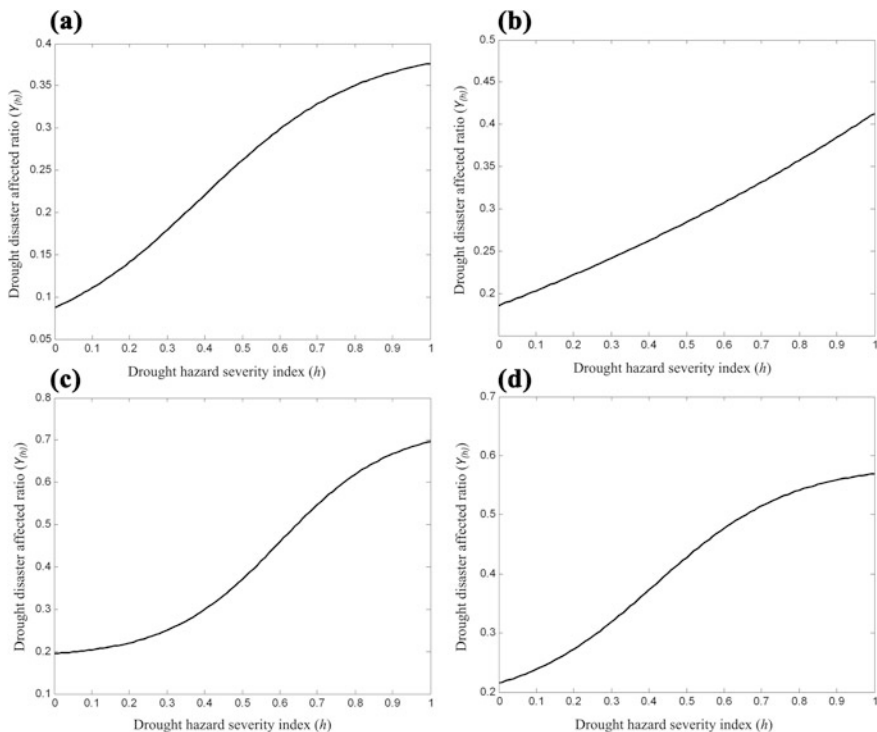


Fig. 10 Vulnerability curves of paddy rice in different regions of China: **a** mid-season paddy in South China; **b** mid-season paddy in North China; **c** mid-season paddy in Northeast China; **d** mid-season paddy in Northwest China (Source Lei et al. 2011)

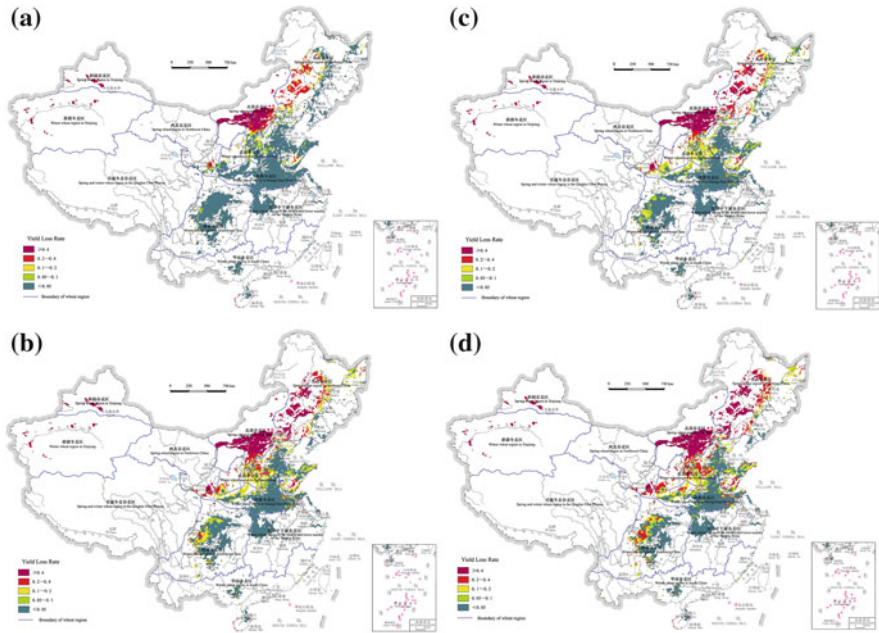


Fig. 11 Risk maps of drought for wheat in China: **a** once every 2 years; **b** once every 5 years; **c** once every 10 years; **d** once every 20 years (Source Shi 2011, p. 62–63)

Xinjiang is the highest, followed by the Huang-Huai-Hai River Plain, the south-western part of China, the Yangtze River region, and South China winter wheat areas. The central part of Inner Mongolia and the wheat producing area in Xinjiang is worth noting, because the yield loss ratio in these areas is particularly high (>0.4) even with the lowest drought intensity (once in every 2 years drought). According to this result, these areas should consider planting alternative local crops instead of wheat.

Drought risk of corn in China: Drought risk of corn decreases from the northwest to the southeast part of China (Fig. 12). With the hazard intensity of once in every 2 years drought, 5 years, 10 years, and 20 years, the total area of the regions with the lowest yield loss ratio (0–0.1) accounts for 54.53, 28.10, 19.80, and 16.93 % of the corn producing area of the country, respectively. The areas with a loss ratio of 0.1–0.2 account for 28.73, 35.95, 32.29, and 24.54 % of the total, respectively. Northwest irrigated corn area and the northwest Hetao Irrigation District is likely to encounter high yield loss even with the lowest drought intensity (once in every 2 years drought). It means that corn production in these regions is extremely vulnerable and a change in production practice is necessary. In addition to these two regions, corn production in the Huan-Huai-Hai River Plain is also of high risk, particularly in Hebei Province. Water resource in this region is not able

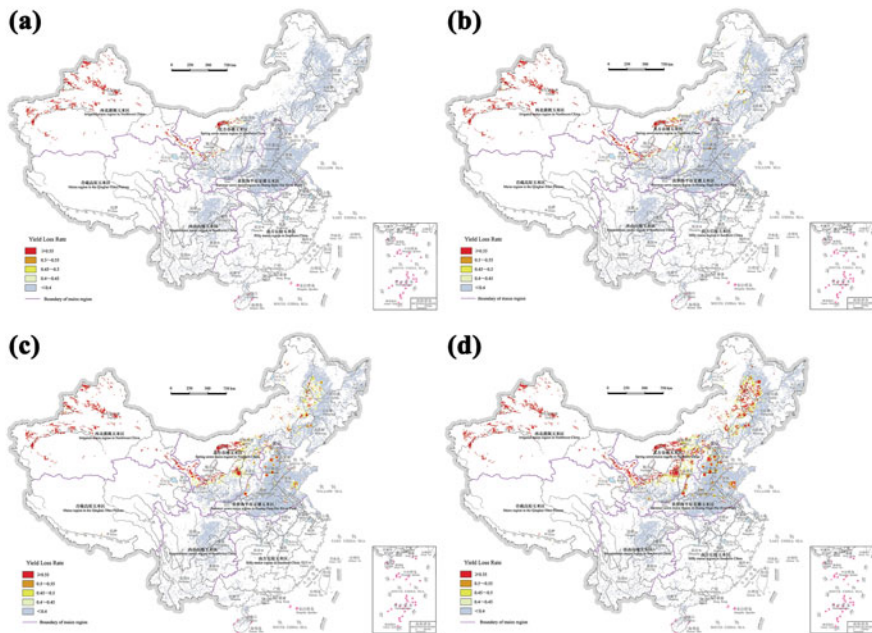


Fig. 12 Risk maps of drought for maize in China: **a** once every 2 years; **b** once every 5 years; **c** once every 10 years; **d** once every 20 years (Source Shi 2011, p. 68–69)

to meet the increasing demand because of the rapid socioeconomic development and increase of cropping. In order to reduce drought risk, water-efficient technologies for agriculture and a water-saving culture in the urban areas in this region are urgently needed.

Drought risk of paddy rice in China: Fig. 13 shows that the regional drought risk of paddy rice shows a clear differentiation between North and South, mainly determined by the difference of precipitation and temperature. The drought risk of the three northeastern provinces is the highest, with high loss rate even under the low intensity scenario (once in every 5 years drought). This region is, however, an important base of paddy rice production in China, which is also famous for its high quality of rice. The next high risk area is the rice producing region along the Yangtze River. Paddy rice in this region may experience medium loss rate when the intensity of drought reaches that of the once in every 20 years drought. For such regions, risk transfer arrangements, such as agricultural insurance, could be helpful for the local producers to manage risks. Further towards the southern part of China, drought risk of paddy rice is much lower than the other parts of the country. Even with severe droughts (for example, once in every 40 years), loss rate is still below 0.4.

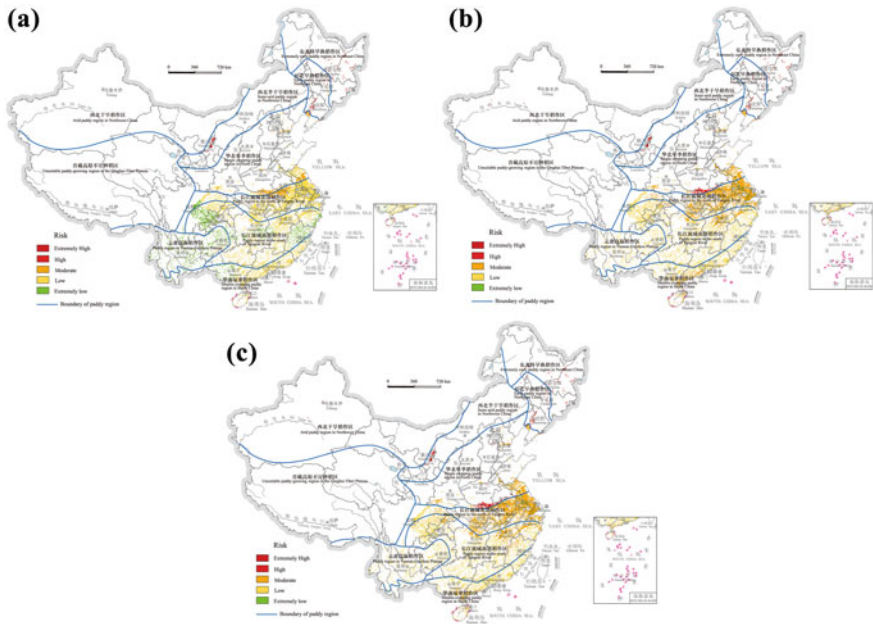


Fig. 13 Risk maps of drought for paddy rice in China: under **a** once every 5 years drought; **b** once every 10 years drought; **c** once every 20 years drought (Source Shi 2011, p. 71)

3 Response to Great Drought Disasters in 2009 and 2010

In this section, three major drought disasters that occurred in China in 2009 and 2010 are presented as the representative case of droughts in China. They are the droughts which affected (1) the major winter wheat production area in North China in spring 2009 (the “2009 Spring Drought”), (2) six provinces in northern China in summer 2009 (the “2009 Summer Drought”), and (3) five provinces in the south-western part of China in spring 2010 (the “2010 Spring Drought”), respectively. The three droughts are representative in terms of their intensity (once in every 50 years event), affected region (in the three drought centers of China), affected crops (major grain crops), and the timing (almost covered the four seasons) (Table 2).

3.1 The 2009 Spring Drought in North China

Metrological drought process: The 2009 Spring Drought started in the early winter of 2008. In the process of its development, the rainfall in the affected areas was generally lower than normal by 50–80 %. Hebei Province observed the lowest

Table 2 Basic features of the 2009–2010 severe droughts in China

Features	2009 Spring Drought	2009 Summer Drought	2010 Spring Drought
Began around	Mid-November 2008	End of June 2009	Early September 2009
Ended around	End of February 2009	Early November 2009	Early May 2010
Duration	3 months	5 months	6 months
Peak time of the drought	7 February 2009	16 August 2009	–
Major affected area	Henan, Anhui, Shandong, Jiangsu, Shanxi, Shaanxi, Hebei, and Gansu	Southeastern Inner Mongolia; northern Shanxi, Hebei, Liaoning, southwestern Jilin, and Heilongjiang	Guangxi, Yunnan, Guizhou, Sichuan, and Chongqing
Major types of crops affected	Winter wheat	Maize, soy bean, sorghum, grains	Spring grain crops and cash crops
Meteorological trigger	Relatively high temperature and low precipitation	High temperature and low precipitation	High temperature and low precipitation
Severity	1/30a–1/50a	1/50a–1/100a	1/50a–1/100a

rainfall for the corresponding period since 1951 and Henan Province observed the third lowest rainfall for the same time period (NCC-CMA 2009a). In early February 2009, the drought reached its peak, affecting the major winter-wheat production areas of the Yellow River, Huai River, and Hai River plains (the Huang-Huai-Hai River Plains) (NCC-CMA 2009b). From 3 February 2009, several precipitation processes occurred in the affected area and the meteorological drought was gradually relieved (NCC-CMA 2009c).

Drought impact and disaster losses: The impact of the drought was spatially extensive, intensive, and destructive, with an estimated intensity of 1/30a–50a drought. The impact changed with precipitation and drought-relief inputs (Fig. 14).

According to the data from National Disaster Reduction Center of China, Ministry of Civil Affairs (NDRCC-MCA 2009a, by 9 February 2009, in total 87.31 million people in the eight North China provinces were affected. By the end of February, 2.21 million hectares of crops were affected, with 2.41 million people and 0.99 million livestock short of drinking water supply.

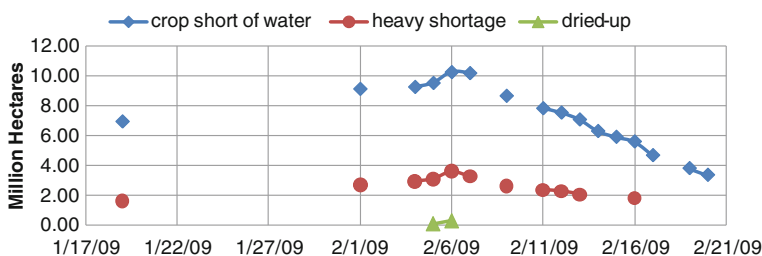


Fig. 14 Dynamics of the impact of the 2009 Spring Drought (Source State Flood Control and Drought Relief Headquarters 2009)

Disaster relief: The Central Committee of the Communist Party of China (CPC), the State Council, and the top leaders of the country were very concerned about the relief of this drought.

The State Flood Control and Drought Relief Headquarter (SFDH) announced the state of emergency of level III, II, and I on 20 January, 4 February, and 5 February, respectively. A number of central government meetings were held to coordinate related government agencies and to issue specific instructions on drought relief.

According to the State Flood Control and Drought Relief Headquarters (2009), by 15 February, the Chinese government organized 12.75 million people, 1.3 million boreholes, 19 thousand pumping stations, 2.32 million drought-relief equipments, 170 thousand water transportation vehicles as daily drought relief-input. RMB 3.9 billion Yuan was spent on drought relief since late December 2008. In total 1.74 billion cubic meters of water was pumped from the Yellow River by Henan and Shandong Provinces, irrigating 1.45 million hectares of crops. Great input resulted in significant reduction of the disaster impact (Fig. 15).

Crop insurance also served well in the recovery process. In Anhui Province, Guoyuan Insurance Company paid RMB 120 million Yuan (Tong 2009) that indemnified half a million winter-wheat producers. The PICC Property and Casualty Company, Ltd. (PICC) offered relevant insurance policies in all the eight provinces except Gansu, with a final payment of RMB 140 million Yuan.

Lack of coping capacities exacerbating drought impact: In the North China region, rural laborers are generally migrated to nearly mid- and large cities for off-farm employment. The largest proportion of household income is not from wheat production but salary of temporary or seasonal employment in urban areas. In this sense, the opportunity cost of wheat production is low and consequently it is often not taken great care of by the rural households. A very typical case was found in a field survey to a local village in Xingtai County in Hebei Province during this drought (Jia et al. 2009). Outside the village, three adjacent plots of wheat field show significantly different degrees of drought impact (Fig. 16). As the size of these plots is small and they are next to each other, the natural conditions including soil type and water condition (drought intensity) could be regarded as the same. The

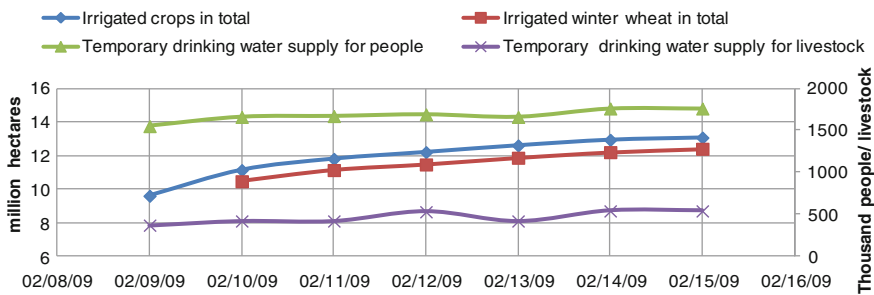


Fig. 15 Drought-relief achievements against the 2009 Spring Drought (Source State Flood Control and Drought Relief Headquarters 2009)

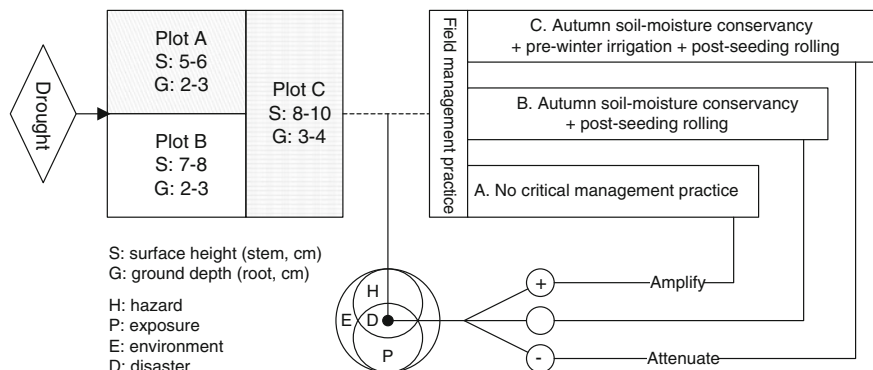


Fig. 16 Amplification and attenuation of drought impact due to field management practice (Source Jia et al. 2009)

difference is clearly induced by farming practice. Wheat growth was the best in plot C, which was carefully managed with autumn soil-moisture conservancy techniques, pre-winter irrigation, and post-seeding soil rolling to reduce evaporation. Those three practices are critically important for winter wheat production in this region—they allow the surface soil to maintain moisture and temperature, preparing for the demand in early spring from wheat plants. In contrast, plot A was the worst, without any field management. This case demonstrates that wheat producers' farming practice significantly changes the vulnerability to drought at the local level and may amplify the impact of drought.

In the same case, after the 2009 spring drought occurred, producers in some villages refused to irrigate their wheat fields simply because the cost of irrigation could be higher than the slim profit margin of wheat harvest (according to a summary survey report from the National Disaster Reduction Commission Expert Panel (NDRCEP 2009a; Reuters 2009)). Such response worsened the impact of drought and aggravated the final losses of wheat production. The impact on the livelihoods of the producers, however, was not as serious as for the wheat production because for the majority of the rural households, agricultural income constituted only a small portion of household income.

3.2 The 2009 Summer Drought in Northern China

Metrological drought process: From June to 15 August 2009, in the affected areas the rainfall was 30–80 % lower than normal. The average rainfall for the five provinces (Liaoning, Jilin, Inner Mongolia, Hebei, and Shanxi) was only 127.6 mm, which was the lowest for the corresponding period since 1951 (NCC-CMA 2009d). The drought lasted until the cropping time of the autumn crops (NCC-CMA 2009e).

Drought impact and disaster losses: The impact of the drought was equivalent to a 50a event, with the following characteristics: (1) in the severely hit areas it was extremely difficult to provide drinking water for the rural population and livestock, (2) huge areas of grain crops were affected, (3) animal husbandry was seriously hit because of the shortage of drinking water and forage grass, and (4) forestry and fruit production suffered from huge losses. Some statistics are provided by NDRCC-MCA to show the immediate impact and final losses claimed by the disaster (Table 3).

This drought caused a reduction of 0.6 % of autumn crop harvests nationwide (2.30 million tons). The direct economic losses were RMB 22.87 billion Yuan.

Disaster relief: Relief of this disaster also attracted great attention of the top leadership of the country. SFDH announced the state of emergency of level IV on 14 August and upgraded it to Level III on 16 August. It also launched a series of relief activities.

By 16 August 2009, Shanxi, Inner Mongolia, Liaoning, and Jilin Provinces organized 5.74 million people, 670 thousand boreholes, 3.46 thousand pumping stations, 386 thousand drought-relief equipments, and 33.6 thousand water transportation vehicles for drought relief in a single day. With these inputs, temporary drinking water supply was provided to 1.5 million people and 890 thousand livestock. 3.13 million hectares of crops were irrigated. In total RMB 490, 179, and 227 million Yuan were spent in drought relief by Inner Mongolia, Liaoning, and Heilongjiang Provinces, respectively (NDRCEP 2009b).

The MCA announced the state of emergency of disaster relief level IV and level II on 10 and 16 August. Drought relief funds and goods were sent to affected areas.

In addition, crop insurance played a significant role in the recovery process. Insurance companies paid RMB 1.95 billion Yuan in Inner Mongolia, Liaoning, and Jilin, covering 3.47 million hectares of crops—almost half of the affected cropland in the three provinces.

Drought and poverty: The impact of drought has cascading effects, with a number of primary impacts followed by multiple secondary or lower level impacts. One of the significant long-term socioeconomic impacts of the 2009 summer drought is the pauperization of the rural residents. The affected region of this

Table 3 Impact and disaster losses of the 2009 Summer Drought

Province	Drinking water shortage		Affected population (1,000 people)	Crop with yield loss (1,000 ha)		Direct economic losses (billion Yuan)
	(1,000 people)	(1,000 livestock)		>10 %	100 %	
Heilongjiang	–	–	1,659	1346.3	50.9	0.76
Inner Mongolia	1,342	4,694	7,945	3531.9	992.1	4.66
Hebei	812	251	4,237	635.0	339.3	2.41
Jilin	151	63	8,175	3056.5	599.0	10.83
Liaoning	705	163	3,018	754.3	260.3	2.71

Source NDRCC-MCA (2009b)

drought was mainly in the transitional zone between the agricultural and pastoral areas in China. In this region, income of local households mainly comes from grazing or farming, or a mixture of these. A small portion of income may come from off-farm employment in large cities outside of the region. In 2009, the impact of the global financial crisis was still ongoing and consequently many seasonal migrant workers who worked in urban areas before failed to find jobs. In the spring of the year, rain water was abundant and the farmers expected a good harvest. Therefore investment in farming (seeds and fertilizer) and grazing was significantly higher than other years. When the severe drought occurred unexpectedly and claimed huge losses, many local households got no return from the investment. According to a government survey, the population lived below the poverty line in Chaoyang City of Liaoning Province increased from 0.65 to 1.54 million. The drought made nearly 0.9 million people poverty-stricken. Once a household falls in poverty, it will be very difficult recover and get out of it, which is generally referred to as the “poverty trap.” The main reason is that the household has lost the critical fund for investment in farming or grazing. The burden on the local governments also increased significantly because they had to provide the budget for subsistence expenditures for the poor.

3.3 The 2010 Spring Drought in Southwest China

Metrological drought process: From early September 2009, the rainfall in southwestern China was lower than normal. In the months followed, Guangxi, Yunnan, Guizhou, Sichuan, Chongqing, and the eastern part of Tibet observed lasting high temperature and scanty rainfall. From 1 September 2009 to 23 February 2010, the average rainfall in Yunnan Province was 163.3 mm, the lowest since 1952. Meanwhile, the average temperature of the province was 15.1 °C, the highest for the same time period (NCC-CMA 2010a). Severe meteorological droughts lasted until late April when precipitation arrived. The drought was completely relieved in early May after massive rainfall occurred in the affected regions (NCC-CMA 2010b).

Drought impact and disaster losses: The drought was extremely severe with intensities of 1/50a and 1/100a in Yunnan Province. Millions hectares of cultivated land and crops were affected and millions hectares of cultivated land were prevented from planting because of the lack of water, and the local population and livestock were in severe shortage of drinking water. According to the MCA, by March 31 2010, there were 69.106 million people in 58 cities and 443 counties in the five provinces (Guangxi, Chongqing, Sichuan, Guizhou, and Yunnan) affected. A total of 5.77 million hectares of crops experienced yield loss, of which 1.18 million experienced full damage. 19.76 million people and 13.37 million livestock suffered from drinking water shortage. The direct economic losses claimed by this drought was RMB 26.62 billion Yuan (NDRCC 2009a, b).

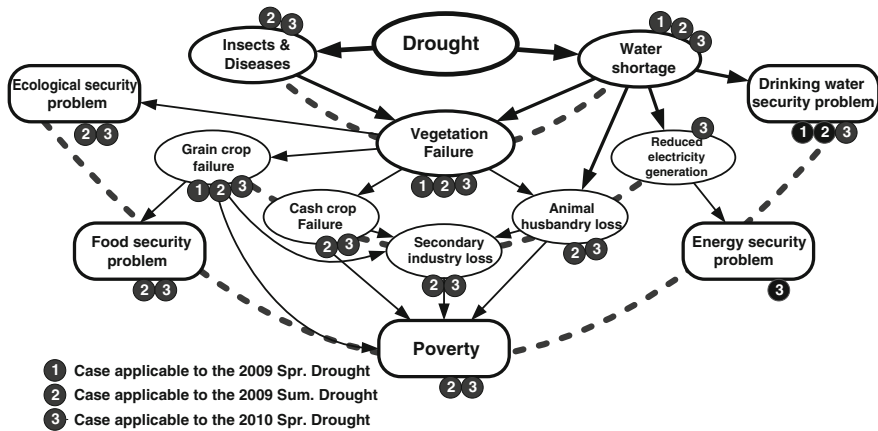


Fig. 17 Drought disaster chain of the 2010 Spring Drought in Southwestern China (Source Ye et al. 2012)

In addition to the direct impacts on people, livestock, and agricultural production, the drought caused a series of further impacts through a series of cascading effects or “disaster chain” (Fig. 17). Water shortage caused operation failure of some local power stations and created pressure on the regional power grid. The loss in agricultural production and animal husbandry largely reduced the raw material supply for secondary industries. In Yunnan Province, sugar production suffered from lack of raw material and consequently a loss of RMB 2 billion Yuan was incurred. Investment return of local households significantly declined and poverty problem emerged, as was the case in the 2009 Summer Drought. Moreover, insects and disease for crops, shrubs, and forests occurred simultaneously, further aggravating the damage to vegetation and the local ecosystem and environment.

Disaster relief: During this major disaster event, the Central Committee of CPC and the State Council again showed great concern over its relief. The main principle for the relief activities was “prioritizing life saving and placing production recovery at a secondary place.” Local governments at all levels were requested to guarantee drinking water supply in local areas with top priority. Relief of agricultural drought came the second. Local governments were also instructed to organize local people to recover their livelihoods by replanting or engaging in off-farm employments. They were also responsible for regulating local markets of foodstuff and preventing secondary disasters and protecting the regional ecosystems.

SFDH announced the state of emergency for drought relief of level III and level II on 5 and 24 February, respectively. By 29 March 2010, the five provinces in total had organized 25.26 million people, 1.14 million drought-relief equipments, 380 thousand water transportation vehicles for drought relief, and irrigated 1.72 million hectares of crops. A total of 257 thousand persons of military forces and paramilitary troops joined in the relief. The Chinese central government allocated a special budget of RMB 155 million Yuan in addition to the regular funding of RMB 800

million Yuan for drought relief. Meanwhile, the 6.3 billion Yuan that had already been allocated for rural drinking water supply projects and irrigation facilities was distributed in advance. With this fund, 18 thousand emergency wells were set up, 7,615 water transportation vehicles were bought, 4,307 small water diversion projects were implemented, and more than 70 thousand small irrigation projects and 20 thousand kilometers of pipelines were constructed (NDRCEP 2010).

NDRC and MCA were very active in providing aid to local victims. The level IV state of emergency of disaster relief was announced for Yunnan and Guangxi on 2 Feb 2010, and upgraded to level III and level II on 5 and 25 Feb, respectively. Ministry of Finance (MOF) and MCA raised a fund of RMB 160 million Yuan for disaster relief to help the local people to cope with food and water shortages. Besides, MCA enhanced regular aids² to local poor people. An extra fund of RMB 200 million Yuan was appropriated in addition to the regular funding of RMB 792 million Yuan (MCA website).

Local capacity building for drought mitigation: In southwest China water resources are plentiful. The five provinces affected in the 2010 Spring Drought are among those with rich water resource endowments. Water resource availability in these provinces is also better than average. Yunnan Province has the richest water resources among the five provinces—it comes the third in per capita water resources in the country, following Qinghai and Tibet. There are, however, very few water conservancy projects covering this Region. Therefore, water supply, regulation, and storage capacity in these areas lag far behind other provinces in China, such as those affected in the 2009 Spring Drought (Figs. 15 and 17). The capacity of water conservancy in this region is very limited.

Two important reasons have contributed to this situation. On the one hand, the affected regions are mainly mountainous or hilly areas. Residents live in small settlements so developing pipeline networks for water supply is much more expensive than other regions. Yunnan and Guizhou Provinces are both to the southwest of the Sichuan Basin, in the central Yunnan alpine region and basin, southwest Yunnan alpine region, and Yunnan–Guizhou Plateau with typical karst landform. In this region, water resources exploitation and utilization is extremely difficult either because of the mountainous terrain or the karst landform. Water is available in surface streams and underground rivers or karst caves. On the other hand, sufficient water supply in normal years weakened people's awareness of drought disaster risks and construction of water conservancy facilities and adoption of water-efficient techniques are not taken seriously by the local population. People living in villages believe that small ponds and cisterns are adequate for providing for their daily needs and agricultural production. Only when severe drought strikes people started to pay attention to the problems with water supply, such as the case

²There are basically two types of aids provided by MCA to rural residents. Regular aid is provided in a specific time of a year to help some rural households to overcome temporary food shortages in between harvest seasons. Aid for contingency is provided when a disaster reaches certain intensity. In the case of the 2009 Spring Drought, the disaster broke out at a time when regular aids were scheduled.

in the 2010 Spring Drought. The statistical data in Figs. 15 and 17 show that the proportions of cropland with water-saving irrigation techniques in Chongqing, Yunnan, and Guizhou Provinces were below 10 %, and those in Guangxi and Sichuan Provinces were below 20 %. Besides, the five provinces had less than half of the cropland equipped with irrigation facility, among which Guizhou Province had less than 20 %, which was the worst in all of China.

References

- Chen, X.H. 2009. *China agricultural statistical data*. Beijing: China Agriculture Press (in Chinese).
- Ding, Y.H. 2008. *China meteorological disasters collection*. Beijing: China Meteorological Press (in Chinese).
- Fu, C.B., and Z.G. Ma. 2008. Global change and regional aridification. *Chinese Journal of Atmospheric Sciences* 32(4): 752–760 (in Chinese).
- Gao, Q.H. 2005. *Analysis of China's natural disaster risk and regional safety*. Beijing: China Meteorological Press (in Chinese).
- Gassman, P.W., J.R. Williams, V.R. Benson, R.C. Izaurralde, L.M. Hauck, C.A. Jones, J.D. Atwood, J.R. Kiniry, and J.D. Flowers. 2005. *Historical development and applications of the EPIC and APEX models*. http://apex.tamu.edu/media/16371/epic_a.pdf.
- He, F. 2010. *Study on regional agricultural drought disaster system—a case study in Zhengshui Basin of Hunan Province*. Doctoral thesis, Beijing Normal University, Beijing, China (in Chinese).
- Intergovernmental Panel on Climate Change (IPCC). 2001a. *Climate change 2001: Impacts, adaptation and vulnerability, summary for policymakers. A report of Working Group II of the Intergovernmental Panel on Climate Change*. Geneva: World Meteorological Organization.
- Intergovernmental Panel on Climate Change (IPCC). 2001b. *Technical summary: Climate change 2001: Impacts, adaptation, and vulnerability. A report of Working Group II of the Intergovernmental Panel on Climate Change*. Cambridge: Cambridge University Press.
- Jia, H.C. 2010. *Corn drought disaster risk assessment of China*. Doctoral thesis, Beijing Normal University, Beijing, China (in Chinese).
- Jia, H.C., J.A. Wang, Y.J. Yue, H.J. Zhou, R. Li, T. Gao, and Y. Bai. 2009. Construction and application of index system of winter wheat drought risk assessment—a preliminary reflection based on fieldwork of Spring Drought in North China in 2009. *Journal of Catastrophology* 4: 20–25 (in Chinese).
- Lei, Y.D., J.A. Wang, and L.L. Luo. 2011. Drought risk assessment of China's mid-season paddy. *International Journal of Disaster Risk Science* 2(2): 32–40.
- Li, J.S. 2001. Temporal variation of droughts in northern parts of China. *Agricultural Research in the Arid Areas* 19(3): 42–51 (in Chinese).
- Liu, Y.J., Y.Z. Yang, and Z.M. Feng. 2007. The change of the main regions for China's food grain production and its implications. *Resources Science* 29(2): 8–14 (in Chinese).
- Lu, W.C., and Y. Mei. 2007. Empirical studies on the variation and contributing factors of regional grain production structure in China—based on spatial econometrics models. *China Agricultural University Journal, Social Sciences Edition* 24(3): 140–152 (in Chinese).
- National Climate Center of China Meteorological Administration (NCC-CMA). 2009a. *China drought & flood climate bulletin*. 227. Beijing: NCC-CMA (in Chinese).
- National Climate Center of China Meteorological Administration (NCC-CMA). 2009b. *China drought & flood climate bulletin*. 289. Beijing: NCC-CMA (in Chinese).
- National Climate Center of China Meteorological Administration (NCC-CMA). 2009c. *China drought & flood climate bulletin*. 242. Beijing: NCC-CMA (in Chinese).

- National Climate Center of China Meteorological Administration (NCC-CMA). 2009d. *China drought & flood climate bulletin*. 251. Beijing: NCC-CMA (in Chinese).
- National Climate Center of China Meteorological Administration (NCC-CMA). 2009e. *China drought & flood climate bulletin*. 253. Beijing: NCC-CMA (in Chinese).
- National Climate Center of China Meteorological Administration (NCC-CMA). 2010a. *China drought & flood climate bulletin*. 250. Beijing: NCC-CMA (in Chinese).
- National Climate Center of China Meteorological Administration (NCC-CMA). 2010b. *China drought & flood climate bulletin*. 252. Beijing: NCC-CMA (in Chinese).
- National Disaster Reduction Commission Expert Panel (NDRCEP). 2009a. Northern China drought disaster survey report. September 2009 (Internal Report, in Chinese).
- NDRCEP. 2009b. Northern China drought disaster survey report. September 2009b. Internal Report (in Chinese).
- NDRCEP. 2010. Yunnan drought disaster survey report. March 2010. Internal report (in Chinese).
- National Disaster Reduction Center of China, Ministry of Civil Affairs (NDRCC-MCA). 2009a. *Monthly Report of Disasters Nationwide* 4: 61–63 (in Chinese).
- NDRCC-MCA. 2009b. Nationwide disaster monthly. *China Disaster Reduction* 11: 58–62 (in Chinese).
- Reuters. 2009. *Despite drought “emergency”, China Wheat Crop OK*. <http://www.reuters.com/article/idUSSP427363>.
- Shi, P.J. 2003. *Atlas of natural disaster system of China*. Beijing: Science Press (in Chinese and English).
- Shi, P.J. 2011. *Atlas of natural disaster risk of China*. Beijing: Science Press (in Chinese and English).
- Shi, Y.F., and S.X. Zhang. 1995. The impact of climate change on the surface water resources in Northwest China arid regions and its future trend. *Science in China: Series B* 25(9): 968–977.
- Tong, J.S. 2009. Guoyuan agricultural insurance company pays drought indemnity, benefiting 500 thousand farmers. *China Insurance News*, 2009/8/6-001 (in Chinese).
- Wang, J.A., H. Sun, W. Xu, and J. Zhou. 2002. Spatio-temporal change of drought disaster in China in recent fifty year. *Journal of Natural Disasters* 11(2): 1–6 (in Chinese).
- Wang, J.A., P.J. Shi, P. Wang, et al. 2006. *Spatial-temporal pattern of natural disasters in China*. Beijing: Science Press (in Chinese).
- Wang, Z.Q. 2009. *On the drought risk of wheat in China based on physical vulnerability assessment*. Doctoral thesis, Beijing Normal University, Beijing, China (in Chinese).
- Wang, Z.Q., F. He, W.H. Fang, et al. 2013. Assessment of physical vulnerability to agricultural drought in China. *Natural Hazards* 67(2): 645–657.
- Whisler, F.D., B. Acock, D.N. Baker, et al. 1986. Crop simulation models in agronomic systems. *Advances in Agronomy* 40: 141–208.
- Williams, J., C. Jones, and J. Kiniry et al. 1989. The EPIC crop growth model. *Transactions of the American Society of Agricultural Engineers* (2): 489–511.
- Ye, T., P.J. Shi, J.A. Wang, et al. 2012. China’s drought disaster risk management: Perspective of severe droughts in 2009–2010. *International Journal of Disaster Risk Science* 3(2): 84–97.

Snow, Frost, and Hail Disasters in China

Jing'ai Wang, Yaojie Yue, Jingtao Zhao, Yuan Bai, Lili Lv, Peijun Shi
and Wenjie Dong

Abstract Snow, frost, and hail are the main agro-meteorological hazards in China. Currently, research on snow, frost, and hail hazards mainly focuses on the formation, spatial and temporal distribution, and disaster-loss evaluation of various exposure units, but little has involved disaster risk assessment and governance. Supported by the “Research and Demonstration of Key Technologies for Integrated Risk Governance” project of the National 11th Five-Year Science and Technology Pillar Program and the Public Welfare Project “Risk Regionalization Research of Meteorological Disasters in China under the Background of Global Change” of the China Meteorological Administration, the natural disaster research team of Beijing Normal University, respectively, studied theory and methods for assessing and mapping snow, frost, and hail disaster risks, and set up a database of snow. This chapter is based on the outcomes of these works.

Keywords Heavy snow frequency · Frost days · Hail frequency · Risk · Spatiotemporal pattern, China

Snow, frost, and hail are the main meteorological hazards in China. Snow hazard is due to heavy snowfalls that cause harm to people’s daily life and damage to production and other economic activities. Frost hazard is related to low temperature

J. Wang (✉) · Y. Yue
School of Geography, Beijing Normal University,
Beijing 100875, China
e-mail: jwang@bnu.edu.cn

J. Zhao · Y. Bai
Key Laboratory of Regional Geography, Beijing Normal University,
Beijing 100875, China

L. Lv · P. Shi · W. Dong
Stake Key Laboratory of Earth Surface Processes and Resource Ecology,
Beijing Normal University, Beijing 100875, China

(Zhang et al. 1991; Li et al. 2005). It often occurs in the transitional periods between the autumn and the winter and between the winter and the spring. With sudden temperature change at night and the ground or plant surface temperature dropping below 0 °C, water in the plants gets frozen so metabolism is damaged and as the result, plants will suffer or die (Feng et al. 1999, 2000; Feng and He 2000). Hail hazard often has short duration and limited spatial scope (Zhang et al. 1991) but is sudden onset and intense (Zhou et al. 2014; Hu et al. 2015; Yue et al. 2015; Zhao et al. 2015; Wang et al. 2016).

Snow disasters of various severities almost occur every year in the pastoral areas of China, especially in Inner Mongolia, Xinjiang, Qinghai and Tibet—the four major pastoral areas. Severe snowstorms occurred periodically and affected large areas, especially with regard to pastoral production.

Frost disasters also occur within a broad spatial scope, involving a number of grain crops and cash crops, and often resulting in significant economic losses to agriculture. The damage of agriculture caused by frost disasters depend on the intensity and duration of the low temperature, the occurrence of the season, and crop types. The reactions of crops to low temperature also vary in different growth periods. As an important agro-meteorological hazard in China, frost mainly occurs in the northwest, northeast, east, and south of China and the North China Plain. The main exposures include winter wheat, cotton, maize, rice, sweet potatoes, sorghum, vegetables, and fruits. Frost disasters often results in significant economic losses to agriculture.

According to the statistics of the World Meteorological Organization (WMO), globally economic losses each year caused by hails are about two billion U.S. dollars (Dong and Zhang 2004). China is one of the countries in the world that suffer the most severe hail disasters. About 2×10^6 ha area is affected by hail every year (CMA 2008). Crops can be damaged greatly by hails—leaves, stems, and growing points of plants are often damaged or completely destroyed (An et al. 2004).

This chapter first introduces the spatial and temporal patterns of snow, frost, and hail hazards in China. Snow, frost, and hail disaster impacts in agriculture are then assessed separately, and their corresponding disaster risk maps are presented. Finally, emergency responses to the low-temperature freezing rain and snow disaster in southern China in 2008 are analyzed. The main sources of data used in this chapter include: a Chinese newspaper and periodical database of natural disasters by Beijing Normal University; meteorological disaster library and yearbooks by the China Meteorological Administration; meteorological data, land use maps, agricultural production statistical data from various sources, among others. Table 1 lists the important data used in this study.

Table 1 Data used in the study

	Database	Key information	Source
Case data	Disaster cases of China from Newspapers and Periodicals	Historical disasters in Chinese counties (1949–2013)	Key Laboratory of Regional Geography, Beijing Normal University
	Meteorological Disasters Library of China	Historical disasters in Chinese counties (1949–2000)	China Meteorological Administration (2001)
	Meteorological Disasters Yearbooks of China	Disasters in Chinese counties (2005–2007)	China Meteorological Administration, China Meteorological Publishing House (2006, 2007, 2008)
	Disaster Reduction of China	Disasters in Chinese counties (2001–2004)	National Disaster Reduction Center of China (2005)
	Online sources	Disasters in Chinese counties (2008)	The Internet
Hazard data	Meteorological data	Temperature data (1955–2005), from 744 meteorological observation stations in China	China Meteorological Administration
	Chinese snow depth time series dataset 1978–2005	Derived from passive microwave remote sensing MMR1 (1978–1987) and SSM/I2 (1987–2005) brightness temperature data	Cold and Arid Regions Environmental and Engineering Research Institute
Exposure data	National Agricultural Atlas of China	Cropland distribution in China	China Cartographic Publishing House (1989)
	1:250,000 Land-use Maps of China	Growing regions of crops and acreage in counties of China	Institute of geographic sciences and natural resources Research, Chinese Academy of Sciences (2001)
	Statistical Yearbook of the Economy of Chinese Counties (Cities) in 2008	Crop yield data in counties of China	China Statistics Publishing House (2008)
	Frost and Frozen Disaster Level of Crops (QX/T 88-2008)	Frost disaster meteorology standard	China Meteorological Administration (2009)

(continued)

Table 1 (continued)

	Database	Key information	Source
	1:250,000 Topographic Map	Elevation, slope	National Administration of Surveying, Mapping and Geoinformation of China (2005)
	Atlas of Road Transport in China 2008	Transportation network data including state trunk highways, provincial trunk highways, county and township roads, other smaller roads and paths, and other elements of the transportation network	China Cartographic Publishing House (2009)

1 Spatial and Temporal Patterns of Heavy Snow, Frost, and Hails

1.1 Spatial and Temporal Distribution of Heavy Snow

Heavy snow and snowstorms are an important hazard restricting the development of animal husbandry in the northern and western pastoral areas of China as well as affecting road transport and other economic activities in this area and elsewhere. Therefore, research on heavy snow and the disaster risk is of great significance for animal husbandry, urban development, and transportation in China.

Grasslands in China account for about 13 % of the world's grassland area and 40 % of the land area of the country, with a total area of 0.313 billion ha and mainly distributed in Inner Mongolia, Xinjiang, and Tibet Autonomous Regions and Qinghai and Gansu Provinces. These autonomous regions and provinces produce annually about 1/5 of the animal products nationwide. Therefore, snow disasters have serious impacts on the economy and livelihood of people in the area.

According to the frequency distribution of heavy snow in China (Fig. 1) extracted from the "Disaster Cases of China from Newspapers and Periodicals" database (1949–2013), basic features of the spatial distribution of heavy snow in China are as follows: (1) The distribution of heavy snow is relatively centralized. There are 399 snow stricken counties, concentrated in four provinces and autonomous regions, including Inner Mongolia, Xinjiang, Qinghai, and Tibet. Three regions are frequently stricken by heavy snow—the vast areas west of the Greater Khingan Mountains and north of the Yinshan Mountains of Inner Mongolia; the areas north of the Tianshan Mountain of Xinjiang; and the Qinghai–Tibet Plateau. (2) There are three regional centers where heavy snow frequently occur—East Ujimqin Banner, West Ujimqin Banner, Sonid Right Banner, and Abag Banner in the Xilingol League of Inner Mongolia; Tacheng, Fuyun, Altay, Hoboksar, and Yining north of the Tianshan Mountain in Xinjiang; and Yushu, Chengduo,

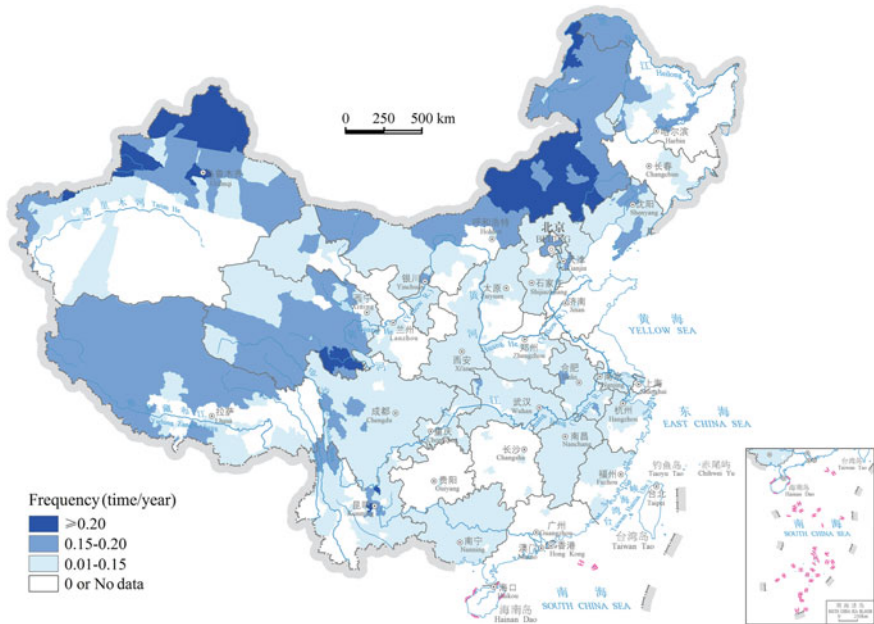


Fig. 1 Frequency of heavy snow in China, 1949–2013

Nangqian, Dari, Gande, and Maqin near the Bayan Har Mountains in northwestern Qinghai–Tibet Plateau.

In order to show the change in the spatial distribution of heavy snow over the past decades, we divided the data into three periods: 1949–1965 (Fig. 2a), 1978–1990 (Fig. 2b), and 1991–2013 (Fig. 2c). Average heavy snow frequency of various counties is used to map the spatial distribution of heavy snow. Figure 2 shows that from 1949 to 1965 (Fig. 2a), the regions with high heavy snow frequency were mainly distributed in areas north of Tianshan in Xinjiang and the central areas of Inner Mongolia. From 1978 to 1990, the regions with high snow frequency mainly distributed in areas northwest of Tianshan in Xinjiang and in the central eastern areas of Inner Mongolia, as well as the northeastern areas of the Qinghai–Tibet Plateau. In the second period (Fig. 2b), the high frequency center of Xinjiang moved towards the west, and that of Inner Mongolia expanded to the transitional zone between agriculture and animal husbandry in southeast. Both sides of the Bayan Har Mountains in northeastern Qinghai–Tibet Plateau also had high heavy snow frequencies. In 1991–2013 (Fig. 2c), the high-frequency areas were similar to that of the previous period, but the total area expanded. The transitional zone between agriculture and animal husbandry in Inner Mongolia, which was a high frequency area in the previous period, had lower heavy snow frequency in this period. This is likely connected to the improvements in the ecological environment of the area and recent developments in animal husbandry, especially the reduced dependence on grazing on open pastures. From 1949 to 2013, the number of

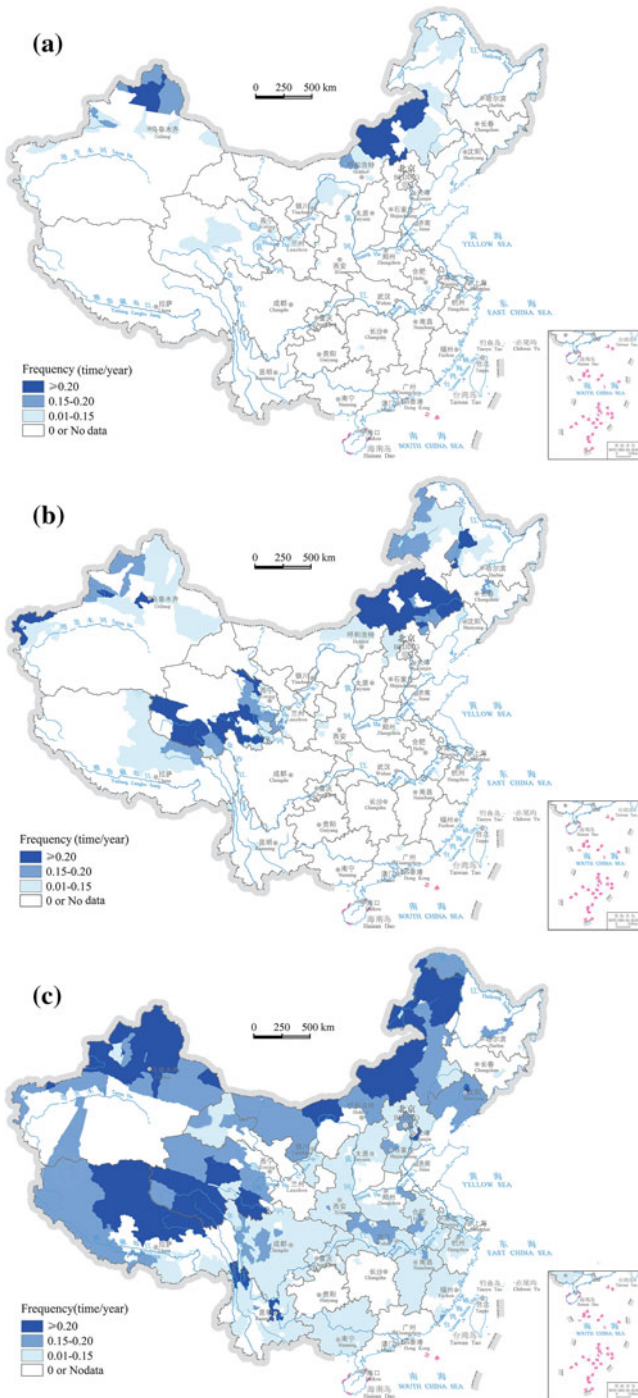


Fig. 2 Frequency of heavy snow in China: a 1949–1965, b 1978–1990, and c 1991–2013

counties with high and relatively high heavy snow frequencies clearly increased, and the expansion of high and relatively high frequency areas accelerated, which is the result of increased hazard severity and greater vulnerability, including aggravated grassland degradation.

1.2 Spatial Distribution of Frost

In China, south and east of the Huaihe–Qinling–Hengduan Mountains, the frost days are below 50 over the year, and frost days are generally above 50 in the rest of the country. Areas with frost days above 200 are mainly distributed in northeastern Inner Mongolia and northern Heilongjiang in the Northeast as well as most parts of the Qinghai–Tibet Plateau, and the highest frost days are 327, which are found in the central part of the Qinghai–Tibet Plateau. Areas with frost days between 100–200 are widely distributed in the Northeast Plain and North China Plain in the northern part of China as well as in Shaanxi, Ningxia, Gansu, and Xinjiang in the northwest. Since agricultural disasters caused by frost mainly occur in the Northwest, North China, the Northeast, East China, the central part of southern China, and the South China areas, crops stricken are mainly winter wheat, cotton, maize, rice, sweet potato, broomcorn, and vegetables and fruits.

Wheat cropping areas in China are broadly subject to the impact of frost, which occurs in wheat-cropping areas ranging from the subtropical and warm temperate zones to the temperate climate region. Generally, frost is frequent and severe in plain areas but less frequent and milder in oceanic climate zones and piedmont plain areas, and frost occurrence in high and cold mountain areas is relatively complicated. Frost-affected wheat production areas are mainly in the region between 105°–120° E and 33°–38° N, and the severely affected areas are located between 110°–118° E and 34°–36° N, that is, in the Huanghe–Huaihe Plain wheat production region (Fig. 3).

Maize is planted in almost every area of the country, from Taiwan in the east to Xinjiang in the west, and from the Hainan Island in the south to the Songnen Plain in the north (Fig. 4). According to the natural conditions, maize production areas in China are divided into six regions. The areas that experience the most severe frost hazard are the northern spring maize production region and the northwest irrigated maize production region, including three northeast provinces, Inner Mongolia Autonomous Region, Ningxia Autonomous Region, the northern part of Hebei and Shaanxi Provinces, most areas of Shanxi and Gansu Provinces, as well as the northern part of Xinjiang Autonomous Region. On the whole, frost hazard in maize production areas in China mainly occurs in areas north of the line connecting Zhuanghe, Jinzhou, Xinglong, Wei County, Qin County, Pucheng, Tianshui, Danqu, and Songfan as well as the areas in the Hexi Corridor and the northern part of Xinjiang.

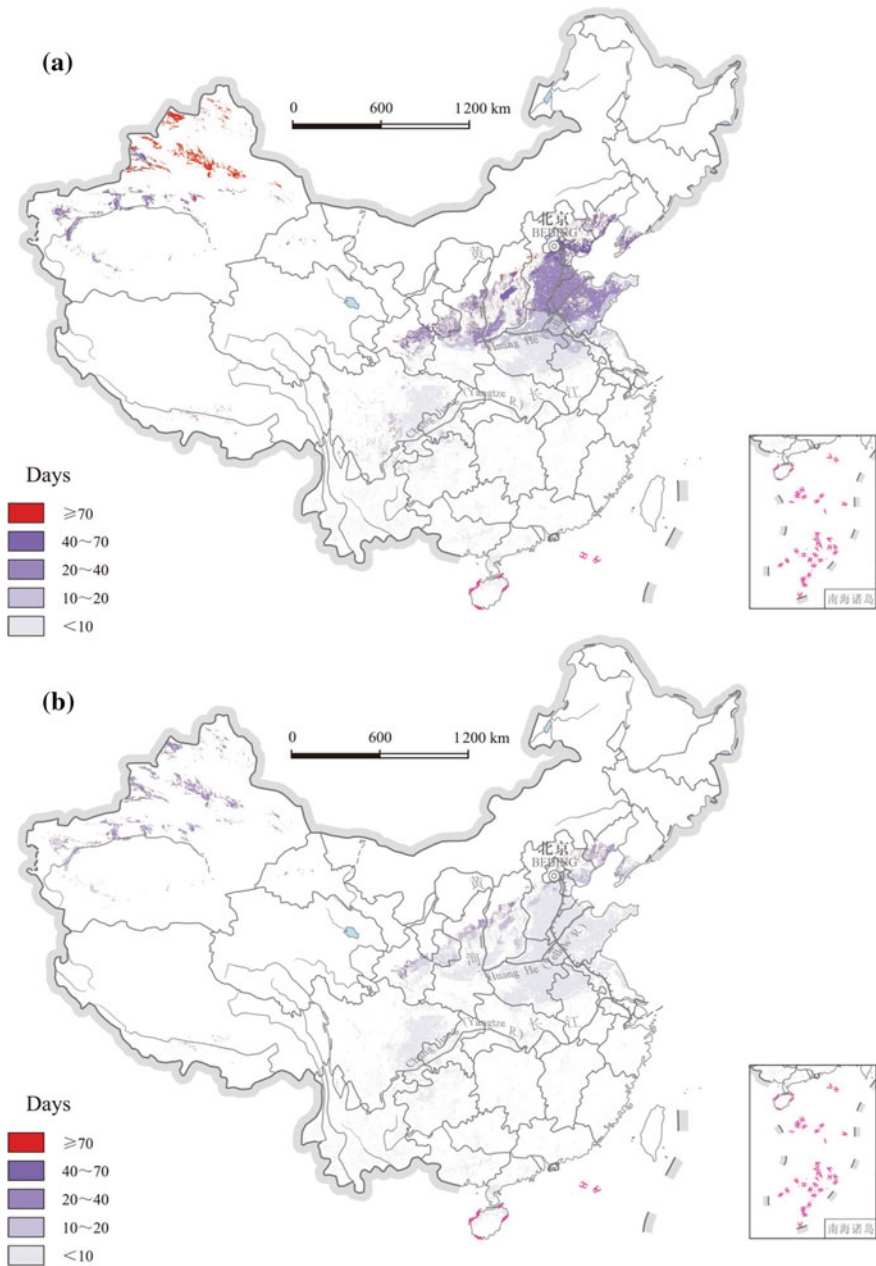


Fig. 3 Distribution of frost days in wheat production areas: **a** Spring frost days in winter wheat production areas; **b** Autumn frost days in winter wheat production areas; **c** Spring frost days in spring wheat production areas; **d** Autumn frost days in spring wheat production areas (Source Shi 2011, p112)

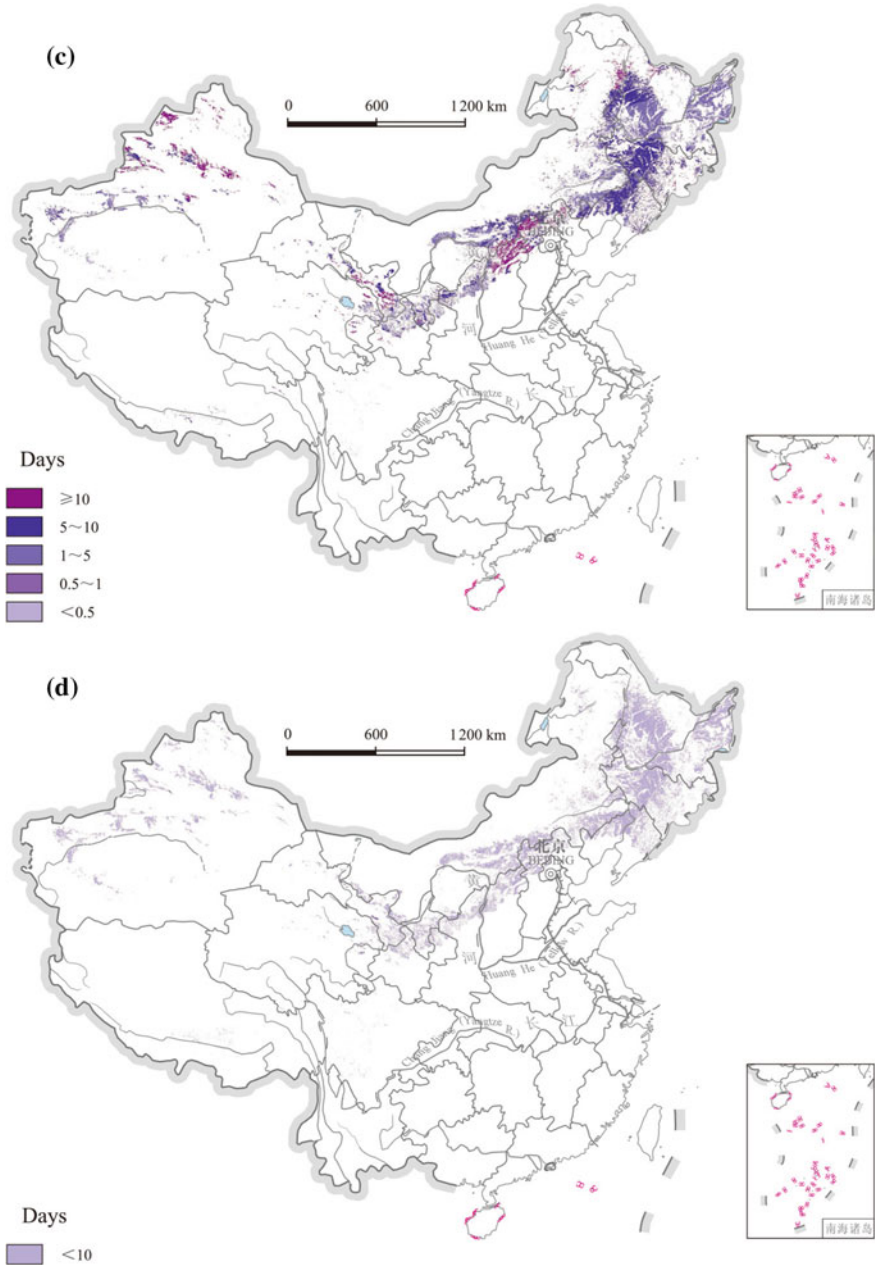


Fig. 3 (continued)

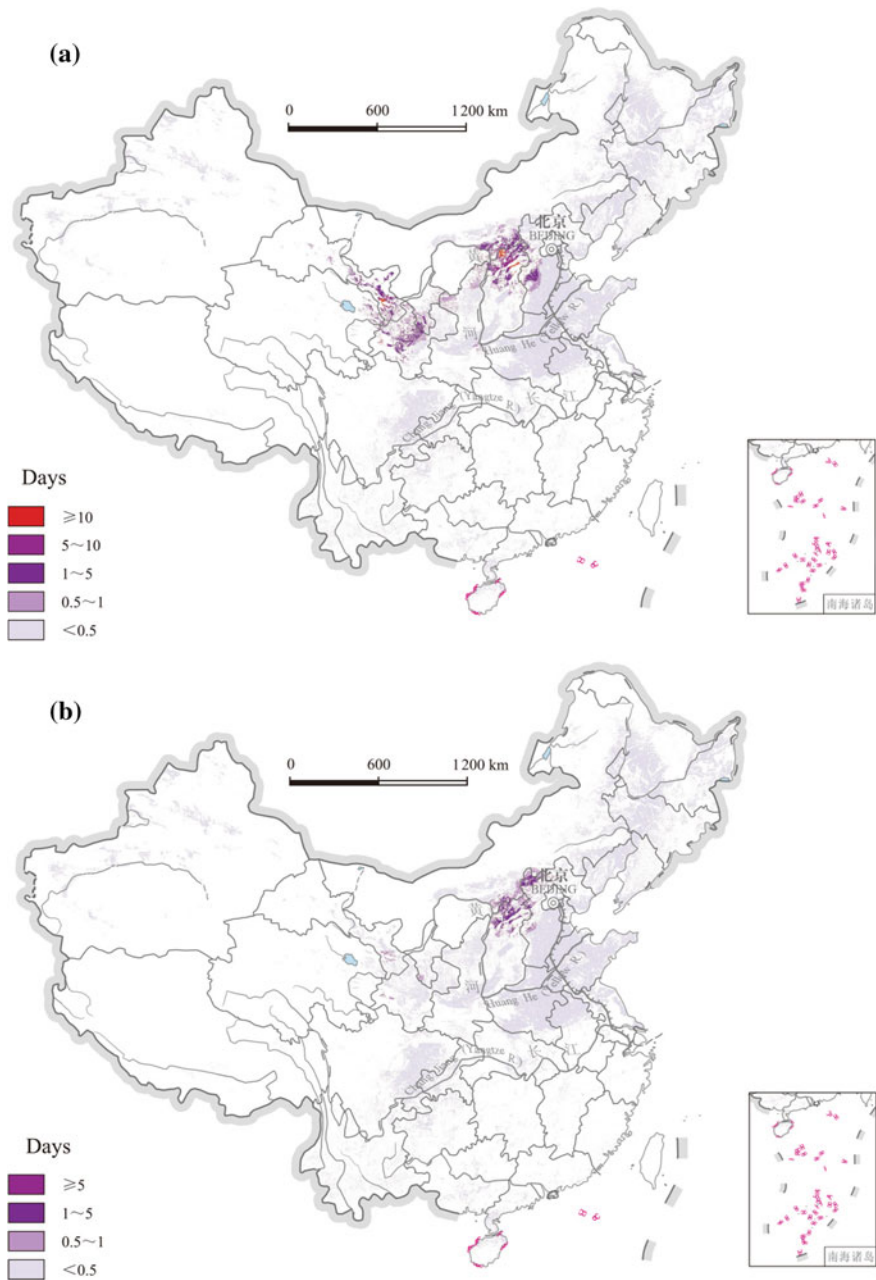


Fig. 4 Distribution of frost days in maize production areas: **a** Spring frost days in maize production areas; **b** Autumn frost days in maize production areas (Source Shi 2011, p. 112)

1.3 *Spatial Distribution of Hail*

Basic features of the spatial distribution of hail hazard in China are as follows: (1) From a broad regional perspective, hail occurrences in China generally differ between the eastern and the western areas. Areas east of the Greater Khingan Mountains–Yinshan Mountains-eastern edge of the Qinghai–Tibet Plateau line are where hails frequently occur. (2) Hails are widely distributed and scattered. There are 1,035 hail-stricken counties in China. (3) Under the general distribution pattern, that is, more hails in the central-eastern part and less hails in the western part, frequent hail hazards occur in one region, two belts, and eight centers (Fig. 5). The “one region” refers to the hail-prone areas north of the Yangtze River, south of the Yanshan Mountains, and east of the Qinghai–Tibet Plateau; the “two belts” refer to the hail-prone areas at the edge of the first topographic stage in China (especially areas to the east), and the hail-prone areas at the edge and to the east of the second topographic stage. (4) The eight high frequency centers of hail hazard include the Songnen Plain area between the Greater Khingan Mountains and the Lesser Khingan Range; areas in the eastern part of Inner Mongolia; the Chifeng-Liaoxi mountainous areas; Yanshan and piedmont plains; the contiguous areas of Shaanxi, Gansu, and Ningxia; Qinba Mountain areas; the contiguous areas of Yunnan, Guizhou, and Sichuan; and the Kashgar-Aksu areas of Xinjiang, details can be seen in Zhao et al. 2015.

2 **Formation and Assessment of Snow, Frost, and Hail Disasters**

2.1 *Snow Disasters*

Formation mechanism of snow disasters: Pastoral systems are particularly vulnerable to snow disasters. Snow disasters in pastoral areas are caused by heavy snowfall and other adverse natural conditions as well as the vulnerability of the animal production systems that do not have sufficient capacity to resist the impacts. In the winter, plants stop growing and the quality and quantity of forage grass on pastures gradually decline, thus it becomes increasingly difficult to meet the basal metabolic demand of livestock. Once heavy snow falls, especially when icy hard surface forms, pastures are covered by snow and ice and cannot be used by grazing animals. This will cause great difficulties for livestock and herding households who do not have sufficient forage grass reserves. Meanwhile, snowstorms are often accompanied by strong winds and temperature drop. Livestock that have poor sheltering facilities or no shelter die of coldness and hunger. When this takes place in a large area, the so-called “white disaster” occurs.

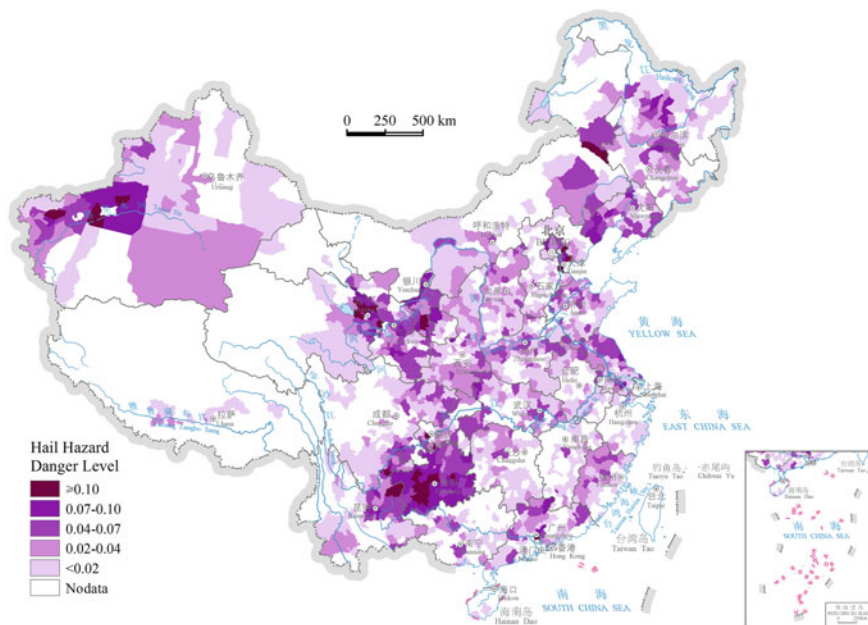


Fig. 5 Distribution of hail hazard in China

Likewise, early snow with strong wind and temperature decrease causes damage to crops, vegetables, and fruits. In snows, ground transportation is affected due to visibility decrease and accumulated snow coverage. Whether a snow becomes a disaster depends on the amount of snowfall, vulnerability of exposure units, and many other conditions.

In a regional snow disaster system, exposures refer to affected pastoral production systems, cities, and transportation systems; disaster-formative environment means regional nature and human environments; and natural hazard refers to the snowfall. Secondary hazards accompanying snows can be low temperature, strong wind, and low visibility, among others. Vulnerability of exposure units depends on their ability to resist the impacts; severity of hazard depends on the duration of snow, amount of snowfall, depth of accumulated snow, and other related natural factors; and stability of disaster-formative environment is mainly affected by conditions inductive to the occurrence of disasters. Interaction between the various components of regional snow disaster system affects and determines the magnitude of snow disaster risks.

Vulnerability of snow exposure units: In the case of snow disaster in pastoral systems, vulnerability curves can be calculated using the disaster-loss fitting method. Using snow disasters in the pastoral area of Qinghai Province as an example, the relationship between accumulated snow depth and livestock mortality during snow disasters is established. Based on the data from the snow disaster-case

database listed in Table 1, and using the least square method, the vulnerability curve (Fig. 6) can be described as follows:

$$R_L = 1 - 1/\exp(0.0064389 \times H) \tag{1}$$

where, R_L refers to livestock mortality during snow disasters, H refers to accumulated snow depth. The R^2 is 0.808 and passes the significance test.

Highways and airports, the two most fragile snow hazard-affected traffic systems, are examined for loss rates: highway loss rate (%) = stoppage time/snow duration; airport loss rate (%) = stoppage time/snow duration.

Similarly, data from the snow disaster-case database (listed in Table 1) and the least square method are used to establish the vulnerability models for highways (Eq. 2) and airports (Eq. 3) to snow disasters.

$$R_H = 1 - 1/\exp(0.596828 \times H) \tag{2}$$

$$R_A = 1 - 1/\exp(0.0613722 \times H) \tag{3}$$

where, R_H is highway loss rate during snow disasters, R_A is airport loss rate during snow disaster, and H is accumulated snow depth. The R^2 is 0.9301 and 0.9396, respectively and passes the significance tests.

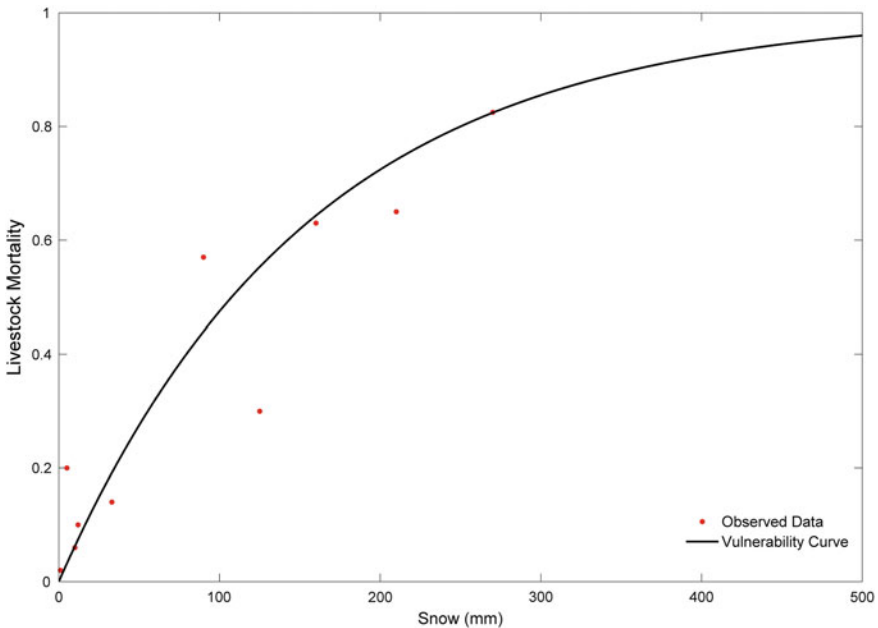


Fig. 6 Vulnerability curve of animal husbandry to snow disasters

Spatial distribution of snow disaster risks in China: With regard to the spatial pattern of snow disaster risks of animal husbandry, the spatial distribution of expected rate of livestock deaths from snow disasters is obtained using Eq. 1 and the spatial distribution of historical snow hazards (snow depth) (listed in Table 1)—this approach assumes that the future snow hazard distribution will largely remain the same as in the past decades. The loss rate is low in the eastern and southern parts and relatively high in the western and northern parts of the country. High-value areas of loss rate are relatively concentrated, mainly distributed in the eastern part of the Qinghai–Tibet Plateau, North Xinjiang area, and areas west of the Lesser Khingan Range. These regions are the areas with the highest risk of potential future snow disasters (Fig. 7).

For animal husbandry across the country, snow disaster risk and potential losses decrease from northwest to southeast, and this is primarily determined by the regional climatic conditions—with low temperature and rich moisture in the high risk areas. Areas with snow disaster risks for animal husbandry (loss rate values) between 0.01 and 0.1 (low loss rate) occupy a large part of the country. Taking the early winter period as an example, areas of low loss rate (0.01–0.1) accounted for 54.53, 28.10, 19.80, and 16.93 % of the grassland area nationwide at the 2, 5, 10, and 20-year return period risk levels, respectively.

For any return periods of the hazard, snow disaster-loss rates of the Qinghai–Tibet and the North Xinjiang areas are all above 0.1; loss rates of most areas are higher than 0.2. This is followed by the northeastern part of China, where maximum loss rate is also above 0.2. The percentage of high risk (0.1–0.2) areas on the grasslands of China increases with the increase of years of return period—taking the early winter period as an example, it increases to 6.41 % for the 20-year return period from 4.81 % for the 2-year return period, 5.43 % for the 5-year return period, and 5.81 % for the 10-year return period. Similarly, the percentage of areas with low loss risk (0–0.1) on the grasslands decreases with the increase of years of return period, from 83.27 % for the 2-year return period, 64.06 % for the 5-year return period, and 52.12 % for the 10-year return period to 41.58 % for the 20-year return period. With 2-year hazard return period, high loss rate areas are mainly concentrated in the Qinghai–Tibet and the North Xinjiang areas. This is consistent with their high snow hazard occurrence and intensity. However, although in the northeastern area of China the snow hazard occurrence and intensity are high, loss rate of animal husbandry in this area is low, which is below 0.1 in most places. The main reason is that the vulnerability and exposure of animal husbandry to snow disasters is low here. When the return period increases to 20 years, high-value area of loss risk also expands toward the southeastern part of the Qinghai–Tibet Plateau, areas north of Tianshan, and areas south of the Lesser Khingan Range.

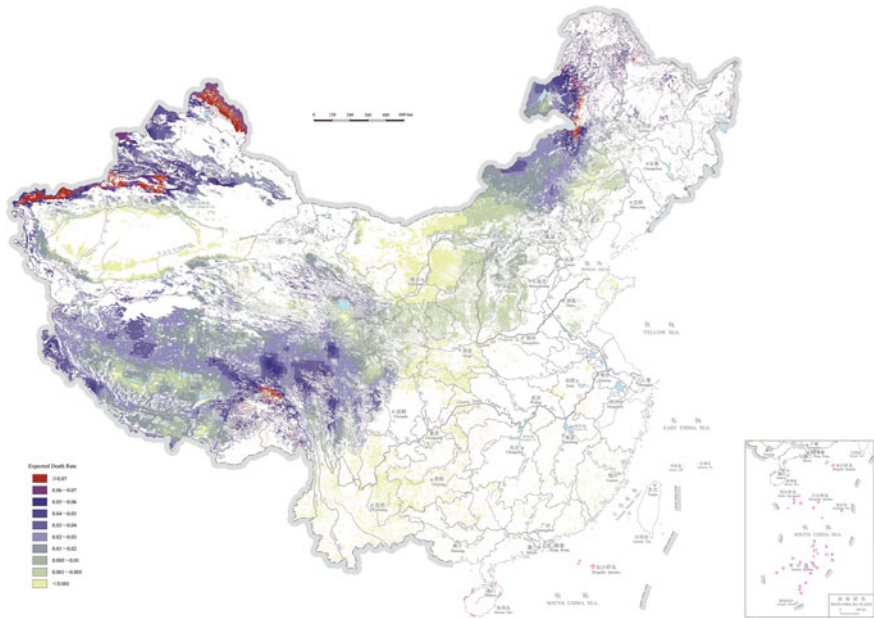


Fig. 7 Snow disaster risk for animal husbandry in China (Source Shi 2011, p. 106–107)

With regard to the spatial distribution of snow disaster risks for highway transportation, average loss rate of Chinese highways generally decreases from the north to the south. It is lower in southern China and higher in northwestern and northeastern areas. High-value areas of loss rate are relatively concentrated, mainly cover most roads of Heilongjiang Province, including important highways such as the Harbin–Dalian Highway, Harbin–Tongjiang Highway, Shenyang–Harbin Highway, as well as sections of highways in Jilin Province, including the Chang–Ji Highway and Chang–Ying Highway, and the Urumqi–kuitun section of Xinjiang Autonomous Region—all of these have the highest disaster risk. The areas with moderate and light loss rate are located in the Beijing–Tianjin region and most road sections of provinces such as Shanxi, Shaanxi, Liaoning, Gansu, Shandong, and so on. This shows that wide areas in northern China have relatively high snow disaster risks for highways (Fig. 8).

With regard to the spatial distribution of snow disaster risks for airports, average loss rate for airports in China generally decreases from the north to the south, and airport loss rates are lower in southern China and higher in northwestern and northeastern areas. High-value areas of loss risk are relatively concentrated, mainly distributed at nine airports: Mudanjiang Airport of Heilongjiang Province; Hulunbeier and Manzhouli Airports in the northern part of Inner Mongolia Autonomous Region; Altay, Urumchi, Nalati, and Yining Airports of Xinjiang; as well as Qamdo and Nyingchi Airports of Tibet Autonomous Region, and these airports have the highest disaster risk. The airports with moderate and light loss rate

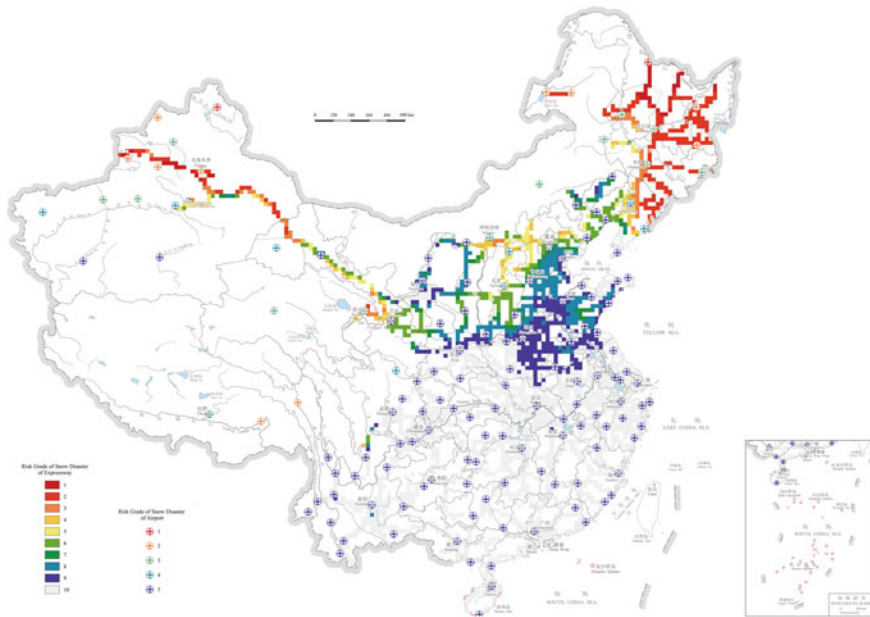


Fig. 8 Snow disaster risk for high transportation in China (Source Shi 2011, p. 110–111)

include Harbin Airport of Heilongjiang Province; Yanji and Changchun Airports of Jilin Province; Kuqa and Aksu Airports of Xinjiang; as well as Xining and Golmud Airports of Qinghai Province. Airports with low loss rates are located in the Beijing–Tianjin region and in provinces such as Shanxi, Shaanxi, Liaoning, Gansu, and so on. This shows that wide areas in northern China have relatively high snow disaster risk for airports.

With 2-year hazard return period, high loss rate for highways is mainly concentrated in Heilongjiang Province, Xinjiang Autonomous Region, and the Hexi Corridor. In the Lesser Khingan Range and the Qinghai–Tibet Plateau areas, although the snow hazard occurrence and intensity are high, given that highways are very few here so the regional snow disaster risk is low too—this is mainly determined by the vulnerability and exposure of highways. When the return period increases to 20 years, high loss rate areas also expand towards the west along the Hexi Corridor, and from Heilongjiang Province to Jilin and Liaoning Provinces.

Under 2-year hazard return period, airports with high loss rates include Qamdo Airport of Tibet and Kuqa Airport of Xinjiang. Under 5-year hazard return period, airports with high loss rate expand to Altay Airport of Xinjiang and Manzhouli Airport of Inner Mongolia. When the return period increases to 20 years, airports with high loss rate include Ulanhot Airport of Inner Mongolia, Harbin Airport of Heilongjiang Province, Golmud Airport of Qinghai Province, Urumchi Airport of Xinjiang, and Lhasa Airport of Tibet. This is consistent with their high snow hazard occurrence and intensity. However, although the snow hazard occurrence and

intensity are high in the northeastern areas of the Qinghai–Tibet Plateau, given that airports are very few here, so the snow disaster risk is low too. Again this is mainly determined by the vulnerability and exposure of airports.

2.2 Frost Disasters

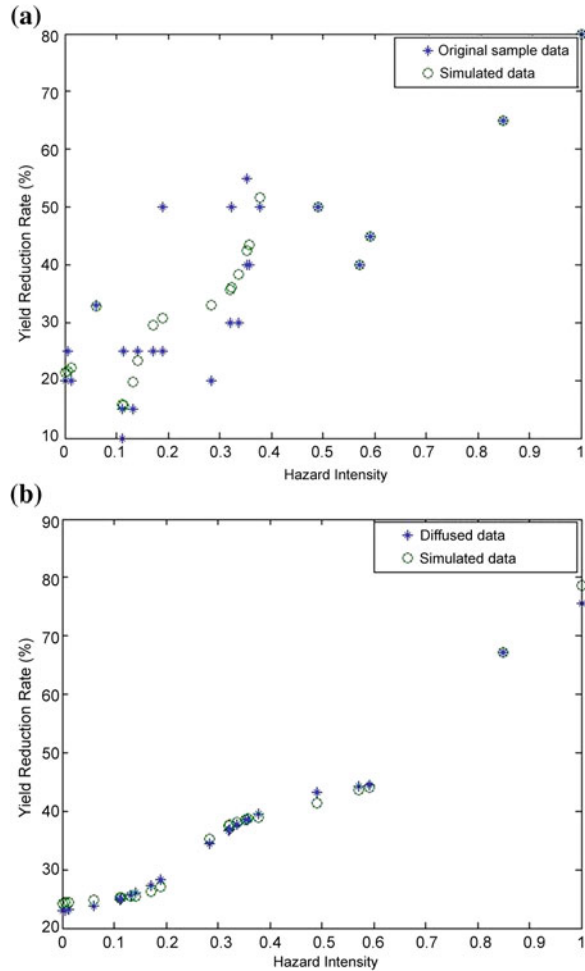
Formation mechanism of frost disasters: In the growth and development periods of crops, when the temperature drops below the lower limit of suitable temperature, the growth of crops will be delayed or stopped. When this happens at a large scale and causes serious damages a low temperature disaster occurs. Low temperature disasters can be divided into above freezing and below freezing low temperature disasters, in which below freezing low temperature disasters include freeze injury and frost disaster. Freeze injury refers to that the crops suffer below 0 °C low temperature or sharp temperature decrease during the winter while frost disaster mainly occurs in the turn of the winter and the spring as well as that of the autumn and the winter when cold air suddenly invades, or the earth surface suddenly undergoes radiation cooling, then surface temperature of soil and plant drops below 0 °C, causing the phytoplasm being damaged, thus the plants will be damaged or die.

Vulnerability of frost exposure units: For wheat crop that has the most complete disaster cases and data, a mixed fuzzy neural network model was used to derive the vulnerability equation of frost disaster for wheat and establish the relationship between hazard intensity and yield loss rate. For other important frost hazard-affected food crops and cash crops such as maize, rape, and apple, the vulnerability to frost disasters was determined by the different frost degree and yield reduction rate described in the meteorological standard *Degree of Crop Frost Damage* (QX/T 88-2008).

The study introduced an improved fuzzy mathematics theory based on information diffusion (assessment method for wheat vulnerability of mixed fuzzy neural network model based on information diffusion technology) for calculating wheat crop vulnerability to frost disaster. The process is as follows: generate causality fuzzy relationship from source sample, and then generate models without contradiction by approximate reasoning, and use these models to train neural network. Estimate the relation between daily minimum temperature and yield reduction rate of wheat, and the result is shown in Fig. 9.

Because the original sample data is discrete in distribution and incompatible, the resulting input–output is very unstable and disordered when simply simulated by Back Propagation (BP) neural network; therefore it cannot correctly show the vulnerability relation between minimum temperature and yield reduction rate (Fig. 9a). However, a favorable input–output relation can be derived from using the sample smoothed through information diffusion approximate reasoning and then BP network training (Fig. 9b).

Fig. 9 Relationship between minimum temperature and yield reduction rate of wheat simulated by Back Propagation (BP) neural network: the simulated result of **a** original sample, **b** sample after information diffusion



The vulnerability of maize, rape, and apple is determined according to the yield reduction rate of each during light frost, moderate frost, and heavy frost specified in *Degree of Crop Frost Damage* (QX/T 88-2008). The standard specifies that frost disasters of crops are divided into three degrees (light frost disaster, moderate frost disaster, and heavy frost disaster) according to the minimum temperature, low temperature intensity, and damage and yield reduction degree of the crop that suffered from frost disasters.

Light frost disaster refers to a situation where the minimum temperature drops obviously, but low temperature intensity is not large. The plant top, leaf apex, or few laminae are frostbite; frostbite rate is less than 30 %, and some frostbite part can be recovered. Generally, the yield reduction of food crop is less than 5 %.

Moderate frost disaster refers to a situation where the temperature decrease is obvious and frostbite rate is 30–70 %. Most lamina at the upper part of the plants is frostbite and cannot be recovered; part of the seedling is frozen to death. And the production of food crop decreases 5–15 %.

Heavy frost disaster refers to a situation where the temperature deduction and low temperature intensity are great, with a frostbite rate of more than 70 %. Most lamina at plant canopy and most seedlings are frozen to death. The production of food crop decreases more than 15 % or even reaches total crop failure.

According to the vulnerability value of each hazard-affected crop indicated in the *Degree of Crop Frost Damage*, we fit the vulnerability curve of maize, rape, and apple in the growing period using EXCEL (logarithmic function).

Spatial distribution of frost disaster risks in China: A series of frost disaster risk maps calculated using the vulnerability relations and historical frost/low temperature data show the spatial distribution of potential yield loss of wheat, maize, rape, and apple under 5-year hazard return period and 20-year hazard return period.

The moderate and high risk areas of wheat frost disaster in China are mainly concentrated in the areas north of 40° N. In regions south of 40° N, the moderate and high risk areas of wheat frost disaster mainly concentrated in Qinghai, Tibet, and part of Gansu Province. On the whole, wheat frost disaster risk is low in the south, and the area of moderate and high risk regions increase from 2-year return period to 20-year return period. Wheat frost disaster risk is relatively low in the Yellow River Basin, Liao River Basin, and Huai River Basin. The low risk area of wheat frost disaster is mainly concentrated in the Yangtze River Basin and the Pearl River Basin (Fig. 10).

Spring frost for maize is mainly light frost, which accounts for 91.93 % of the total frost area. Moderate and high risk areas are mainly concentrated in the border area between north Shanxi and south and east Inner Mongolia, and central Gansu Province (Fig. 11a). The autumn frost of maize growing areas in China is mainly light and moderate, which account for 98.77 % of the total frost area. The high and extremely high disaster risk areas of autumn frost of maize is very few, mainly concentrated in the northwest of Heilongjiang, northeast of Inner Mongolia, and some areas of North Xinjiang. In addition, large areas of south-central Inner Mongolia and north Shanxi have moderate frost disaster risk (Fig. 11b).

2.3 Hail Disasters

Formation mechanism of hail disasters: Hail disaster is a severe meteorological disaster caused by strong convective weather system (Zhou et al. 2014; Hu et al. 2015; Zhao et al. 2015; Wang et al. 2016). Even though the spatial range is small and duration is relatively short, it comes fast and with high strength, often accompanied by strong wind, heavy rain, sharp temperature reduction, and other paroxysmal and disastrous synoptic process. It causes mechanical injury to the fruits as well as branches and leaves of crops, leading to yield reduction or crop

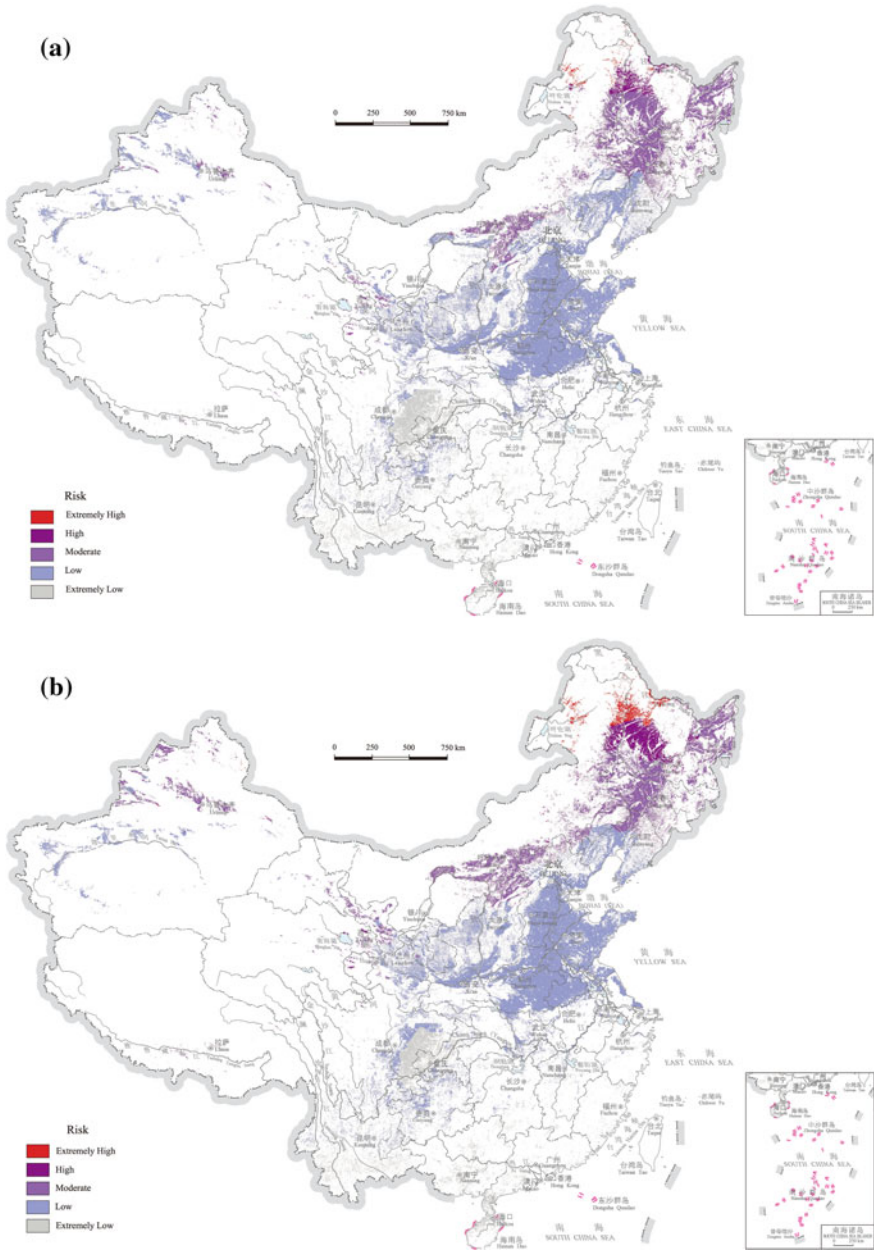


Fig. 10 Wheat yield reduction (risk) of frost disasters in China: **a** 5-year return period; **b** 20-year return period (Source Shi 2011, p. 114–115)

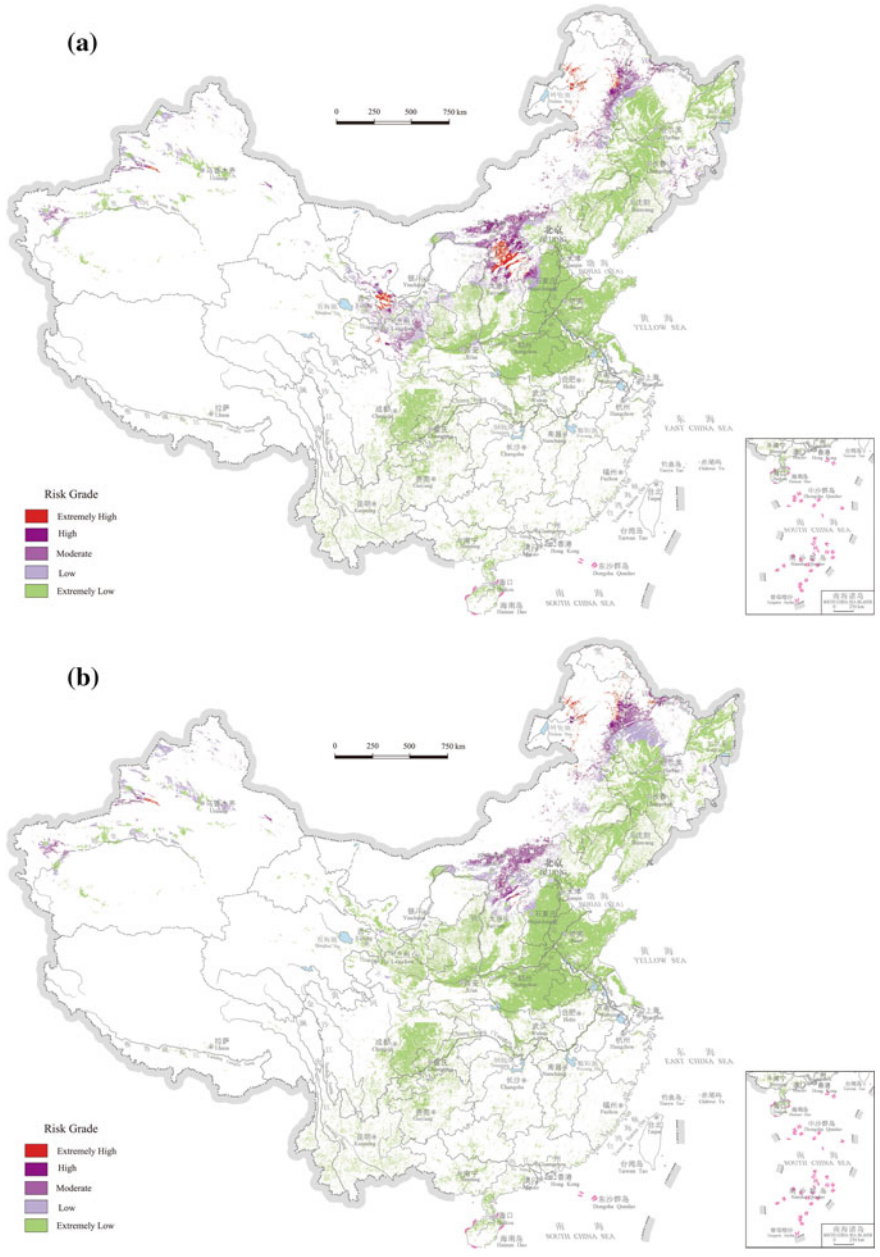


Fig. 11 a Spring frost risk for maize and b autumn frost risk for maize Source Shi 2011, p. 113)

failure (Zhou et al. 2014; Hu et al. 2015; Zhao et al. 2015; Wang et al. 2016). It also causes damages to vehicles, urban facilities (solar panel, street light, glass, and so on), and other non-agricultural objects.

Generally cumulonimbus may generate thunder shower, but only strongly developed cumulonimbus with tall and large cloud formation and strong uprising air as well as abundant moisture inside the cloud, can result in hail. Generally, there is a very strong updraft enters from the cloud base and exits from the upper cloud in front of the cloud. In addition, there is a downdraft flows in from the middle layer of the back side and flows out from the cloud base. Here is the precipitation area where hail is generated in general. These two organized updraft and downdraft are connected with the ambient airflow, so the air flow structure in strong hail clouds is continuous. The strong updraft not only supplies sufficient moisture to hail clouds, but also supports the hail particles to stay in the cloud. When the updraft cannot hold the hail any longer, it will drop from the cloud and precipitate.

Vulnerability of frost exposure units: Vulnerability of exposure unit is inseparable from the occurrence of a hail disaster. It plays an important role in aggravating or mitigating the disaster impact. Generally, exposure's vulnerability can be represented by the vulnerability curve between hazard intensity and disaster-loss rate. In this study, hazard intensity is represented by hail frequency only (moderate strength is assumed for all hail events). The capability of crops to resist the impact of hails varies in different growth periods. Therefore, the loss rate of a crop under the impact of moderate strength hail hazards in different growth periods is used as its vulnerability index (c_i). In addition to relating to the hail resistance ability (fragility) of the crop, the vulnerability of a crop to hail disasters is also related to per unit area yield level and planting scale of the crop. Under the same hail disaster-strength, the higher the level of per unit area yield, the higher the hail disaster-loss; and as an indicator of the degree of exposure, the larger the planting area of the crop, the higher the exposure level and the higher the disaster loss. Therefore, this study uses the product of per unit area yield of a crop (p), exposure of the crop (e), and fragility of the crop in different growth periods (c_i) to show the overall vulnerability of a crop in a particular area to hail disasters. The model of vulnerability of a crop in certain area to hail disasters is as follows:

$$v_i = p \times e \times c_i \quad (4)$$

where, v_i refers to the vulnerability of a crop to hail disasters at the i th growth period; p refers to per unit area yield of the crop; e refers to planting scale of the crop; and c_i refers to fragility of the crop at the i th growth period.

Hail disaster risk of the crop is the product of hazard intensity and vulnerability:

$$R_i = h_i + v_i \quad (5)$$

where, R_i refers to the hail disaster risk for a crop at the i th growth period; and h_i refers to hail hazard intensity at the i th growth period, wherein

$$h_i = b_i/d_i \quad (6)$$

b_i refers to hail frequency at the i th growth period; and d_i refers to the total number of days of the i th growth period.

Using cotton as an example, fragility of cotton crops under the impact of hail hazard ranks from high to low in the bud stage (t_3), boll stage (t_4), seedling stage (t_2), sowing and emergence stage (t_1), and boll opening stage (t_5). Vulnerability of crops at the t_1 and t_5 stages is relatively low nationwide, but is higher in the southern Xinjiang area. In addition to Xinjiang, the high vulnerability area in the t_2 stage is concentrated in southern Hebei and northern Henan areas. Fragility of cotton plant in the t_3 stage is particularly high when suffering from hails, therefore at t_3 the high vulnerability areas are expanded, covering the border area of northeast Henan, Shandong, and Hebei. High vulnerability area at the t_4 stage is concentrated in the border area of Henan and Shandong. On the whole, the high vulnerability area of cotton to hail disasters is concentrated in the Huang-Huai-Hai Plain, Jiangnan Plain, and Xinjiang areas. These areas are the major cotton producing areas in China, characterized by sufficient light and heat, high production output, and large planting area. Particular attention on hail disaster risk prevention is needed here.

Spatial distribution of hail disaster risks in China: The spatial distribution of hail disaster risks of cotton crops in five growth periods are analyzed below as the first example of hail disaster risks for agricultural production in China. Figure 12 shows the hail disaster risks of cotton in two different growth periods. Hail disaster risks of t_1 is relatively low, with relatively small high risk areas, concentrating in Aksu of Xinjiang and northern Anhui; high risk areas of t_2 are mainly concentrated in southern Xinjiang, the middle part of the north slope of the Tianshan Mountains, northern Anhui, eastern Henan, central Hubei, central Shaanxi, and northeastern Jiangsu Provinces. Compared to the t_2 stage, high risk areas of t_3 is expanded northward, connecting northern Anhui, eastern Henan, southern Hebei, and northwestern Shandong Provinces, and this is the main area for disaster-prevention in the bud stage. Compared to the t_2 and t_3 stages, high risk areas of t_4 is decreased and the distribution is more scattered, mainly concentrated in Xinjiang, the Weihe River valley, and the Huang-Huai-Hai Plain. The hail disaster risks in the boll opening stage are relatively low. During the whole growing period, hail disaster risks of cotton in western Liaoning, Sichuan Basin, and South China is relatively low, while that in inland areas of the northwest is relatively high (Fig. 12, Table 2). These results are well coincided with the research of Wang et al (2016).

Fragility of maize crops under the impact of hail hazard ranks from high to low in the heading stage (t_2), seedling stage (t_1), and grain stage (t_3), with the percentage area of high hail disaster risk of 12.14, 4.00, and 0.96 %, respectively. The heading stage is the high risk period for maize production with regard to hail disaster, so it needs focused attention on disaster-prevention. The spatial distribution of hail

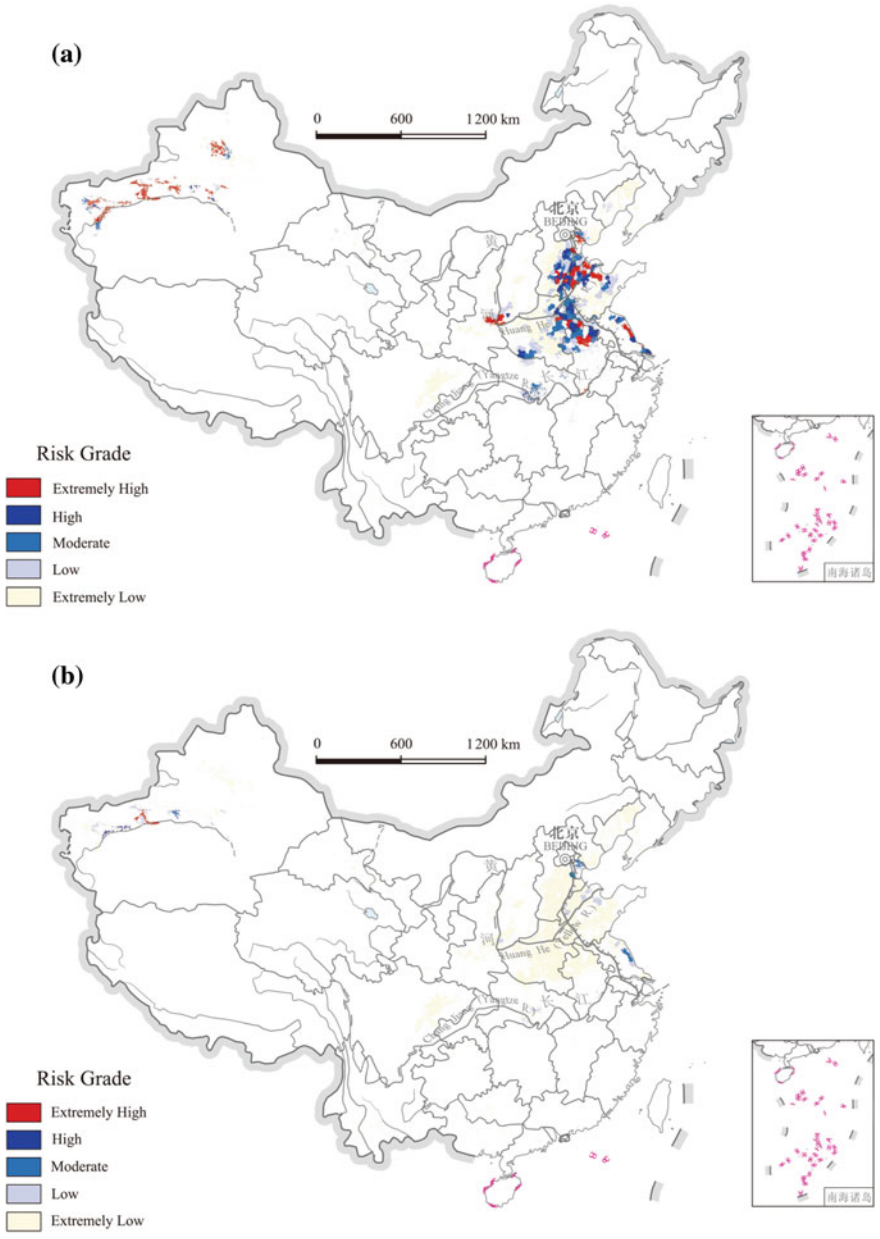


Fig. 12 Hail disaster risks of cotton in different growth periods. **a** Bud stage (t_3). **b** Boll opening stage (t_5) (Source Shi 2011, p. 96)

Table 2 Percentage area of different hail disaster risk levels of cotton in various growth periods in China

t	Percentage of cotton growing area (%)			
	High risk	Moderate risk	Low risk	Extremely low risk
t ₁	2.87	7.2	12.17	77.62
t ₂	13.08	21.11	28.92	36.89
t ₃	20.10	20.8	24.76	34.25
t ₄	7.65	16.58	24.12	7.66
t ₅	0.78	3.03	17.02	79.17

disaster risks of maize crops in three growth periods has the following features: In the t₁ stage, hail disaster risk is relatively low, with relatively small high risk areas, concentrating in some places of the Beijing-Tianjing-Hebei area. Compared to t₁, the highrisk area in t₂ is larger, mainly concentrated in the central part of Jilin, the Beijing-Tianjing-Hebei area, and southern Ningxia. There is almost no high risk area in t₃ (Fig. 13, Table 3).

Fragility of spring wheat crops under the impact of hail hazard ranks from high to low in the heading-maturity stage (t₃), jointing-heading stage (t₂), and seedling-jointing stage (t₁). On the whole, the high risk areas are relatively few. The heading-maturity stage needs focused attention on disaster-prevention. The high risk areas of hail disaster is mainly concentrated in western Shanxi, southern Ningxia, eastern Qinghai, and central Inner Mongolia, where should be also the focused disaster-prevention area at the heading-maturity stage (Fig. 14, Table 4).

Fragility of winter wheat crops under the impact of hail hazard ranks from high to low in the heading-maturity stage (t₃), jointing-heading stage (t₂), and seedling-jointing stage (t₁), with the percentage area of high hail disaster risk of 20.95, 4.15, and 0 %, respectively. The heading-maturity stage is the high risk period of winter wheat hail disaster, so it needs focused attention on disaster-prevention. The spatial distribution of hail disaster risks of winter wheat crops in the three growth periods in China has the following features: t₁ hail disaster risk is relatively low with most places belonging to the low risk and extremely low risk area; the moderate risk areas are few and there is no high risk area. The high risk area in t₂ is mainly concentrated in southern Henan, northern Anhui, and northern Jiangsu. Compared to t₂, the t₃ high risk area is expanded northward, connecting northern Anhui, eastern Henan, southern Hebei, and northern Jiangsu, as well as the northern and central areas of Shandong, Shanxi, and part of Shaanxi, where focused attention should be devoted to disaster-prevention during the heading-maturity stage (Fig. 15, Table 5).

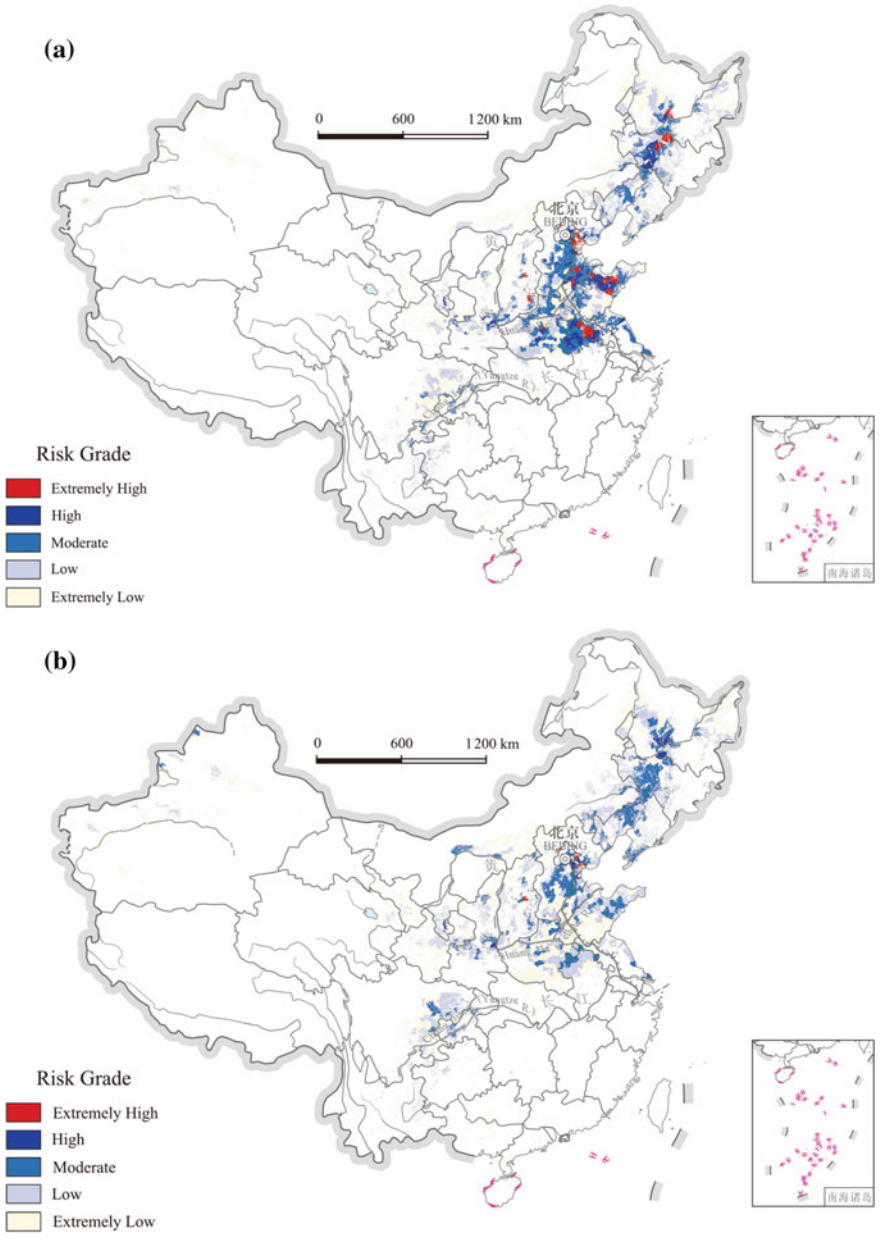


Fig. 13 Hail disaster risk of maize in different growth periods. **a** Seeding stage (t_1). **b** Grain stage (t_3) (Source Shi 2011, p. 97)

Table 3 Percentage area of different hail disaster risk levels of maize in various growth periods in China

t	Percentage of maize growing area (%)			
	High risk	Moderate risk	Low risk	Extremely low risk
t ₁	0.4	13.31	36.99	41.41
t ₂	12.14	21.91	36.31	29.64
t ₃	0.96	7.24	46.71	4.39

3 Responses to the Low-Temperature Freezing Rain and Snow Disaster in Southern China in 2008

3.1 Disaster Situation

Processes and characteristics of disastrous weather: From 10 January to 2 February 2008, five low-temperature freezing rain and snow weather processes struck most parts of China continuously, especially the southern areas. Based on its strength, this continuous extreme low-temperature freezing rain and snow weather reached the 50-year return period as a whole, and in several areas, it even reached the 100-year return period. Rainfall (snowfall) mainly concentrated in areas such as the middle- and lower-reaches of the Yangtze River, most southern parts of China, and the northwest of Yunnan. Accumulated precipitation of these areas reached 50–100 mm. For the southern parts of Jiangsu and Anhui Provinces, most regions south of the Yangtze River, and some parts of South China, the precipitation exceeded 100 mm. Compared to the same period of ordinary years, rainfall in places such as most areas north of the Yangtze River, the southern parts south of the Yangtze River, most parts of South China, western Yunnan, as well as southeastern and western Tibet was doubled or tripled and in some parts the precipitation was more than tripled. The average temperature in the northwest and central eastern regions of China was lower than in the same period of ordinary years by 1–4 °C, while the difference in regions such as the central eastern part of Hubei, most parts of Hunan, central eastern part of Guizhou, central north of Guangxi, most parts of Gansu, Ningxia, western part of Inner Mongolia, and southern part of South Xinjiang was greater than 4 °C. According to the observations, this extreme low-temperature freezing rain and snow weather can be divided mainly into the following five processes (Table 6) (EMEGSEO 2008; EC-SCNDM 2008).

As a whole, this low-temperature freezing rain and snow weather was rarely seen since the founding of the People's Republic of China in 1949, and was featured by wide spatial scope of influence, long duration, low average temperature, high average precipitation, and thick snow cover and icing.

Wide spatial scope of influence: The continuous low-temperature freezing rain and snow weather impacted 20 provinces, autonomous regions, and municipalities, including Shanghai, Jiangsu, Zhejiang, Anhui, Fujian, Jiangxi, Henan, Hubei, Hunan, Guangdong, Guangxi, Chongqing, Sichuan, Guizhou, Yunnan, Shaanxi,

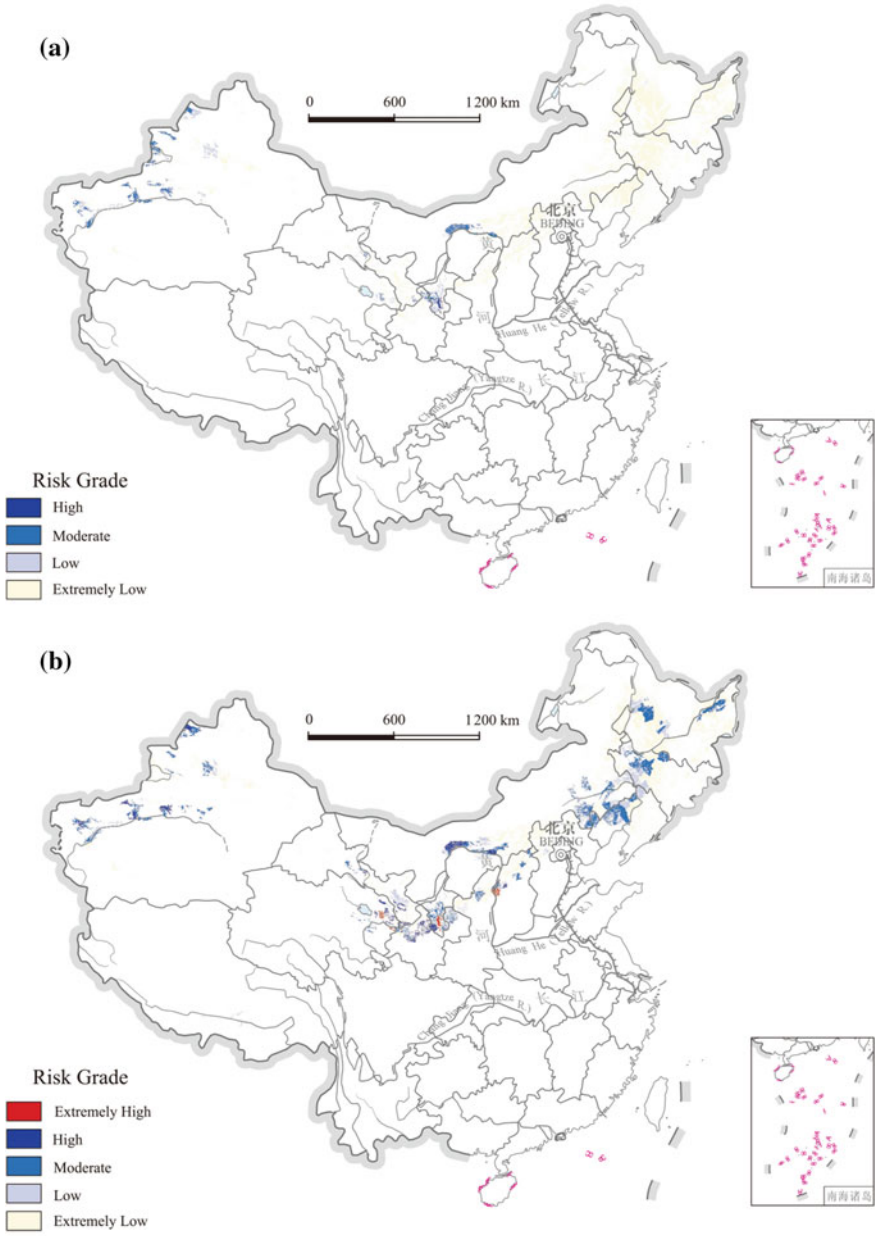


Fig. 14 Hail disaster risk of spring wheat in different growth periods. **a** Seedling-jointing stage (t_1). **b** Heading-maturity stage (t_3) (Source Shi 2011, p. 98)

Table 4 Percentage area of different hail disaster risk levels of spring wheat in various growth periods in China

t	Percentage of spring wheat growing area (%)			
	High risk	Moderate risk	Low risk	Extremely low risk
t ₁	0.58	9.52	21.9	68.81
t ₂	5.07	31.11	29.95	33.86
t ₃	6.6	29.13	27.66	36.61

Gansu, Qinghai, Ningxia, and Xinjiang. From the distribution of nationwide frozen days from 10 January to 3 February it can be seen that except South China, the northeast region, and Yunnan, freezing rain and snow weather struck most parts of China, among which Hunan, most parts of Hubei, northwestern Jiangxi, central south of Anhui, and central Guizhou experienced 10–20 frozen days.

Long duration: From December 1, 2007 to February 2, 2008, the second longest number of continuous days with average temperature below 1 °C occurred in the middle- and lower-reaches of the Yangtze River and Guizhou—it was only shorter than that in the winter of 1954/55; while the number of average frozen days in the middle- and lower-reaches of the Yangtze River and Guizhou exceeded that in the winter of 1954/55 and became the longest in the same time period in history. Within this area, Hunan Province experienced a year with the widest coverage and longest duration of frozen days since the records started, which surpassed that of 1954/55 and the number of stations that saw freeze was the highest since the records started, the duration of freeze ranked the second only after that in 1982/83 and 1954/55; the number of continuous low temperature days in most parts of Hubei Province reached 16–18, which was the longest since 1954/55, with 15–18 continuous rain and snow days—the longest compared to the same period in history; Anhui Province encountered a continuous snowfall for 24 days, which surpassed that of 1954/55 and 1968/69 (both were 16 days) with the longest duration since the founding of the People’s Republic of China, and the year saw the longest rainfall duration since the records started.

Low average temperature: The intensity of this continuous low-temperature freezing rain and snow weather was high. The average minimum temperature was clearly low (2–4 °C lower than that in ordinary years); average maximum temperature was also abnormally low (5–10 °C lower than that in ordinary years). In Guizhou, Hunan, Hubei, and Jiangxi, average maximum temperature reached the minimum value and rainfall and snowfall was the third highest in the same time period in history. Average maximum temperature in the middle- and lower-reaches of the Yangtze River and Guizhou was abnormally low, which surpassed that in 1976/77 by a large margin and became the lowest in the same time period in history; average temperature of Hubei and Hunan reached the minimum in the same time period in history while the low average maximum temperature at such large scale was a 100-year return period hazard event.

High average precipitation: Precipitation in six provinces and autonomous region, including Henan, Sichuan, Shaanxi, Gansu, Qinghai, and Ningxia was the highest in the same time period since 1951; the snowstorm in Zhejiang was the

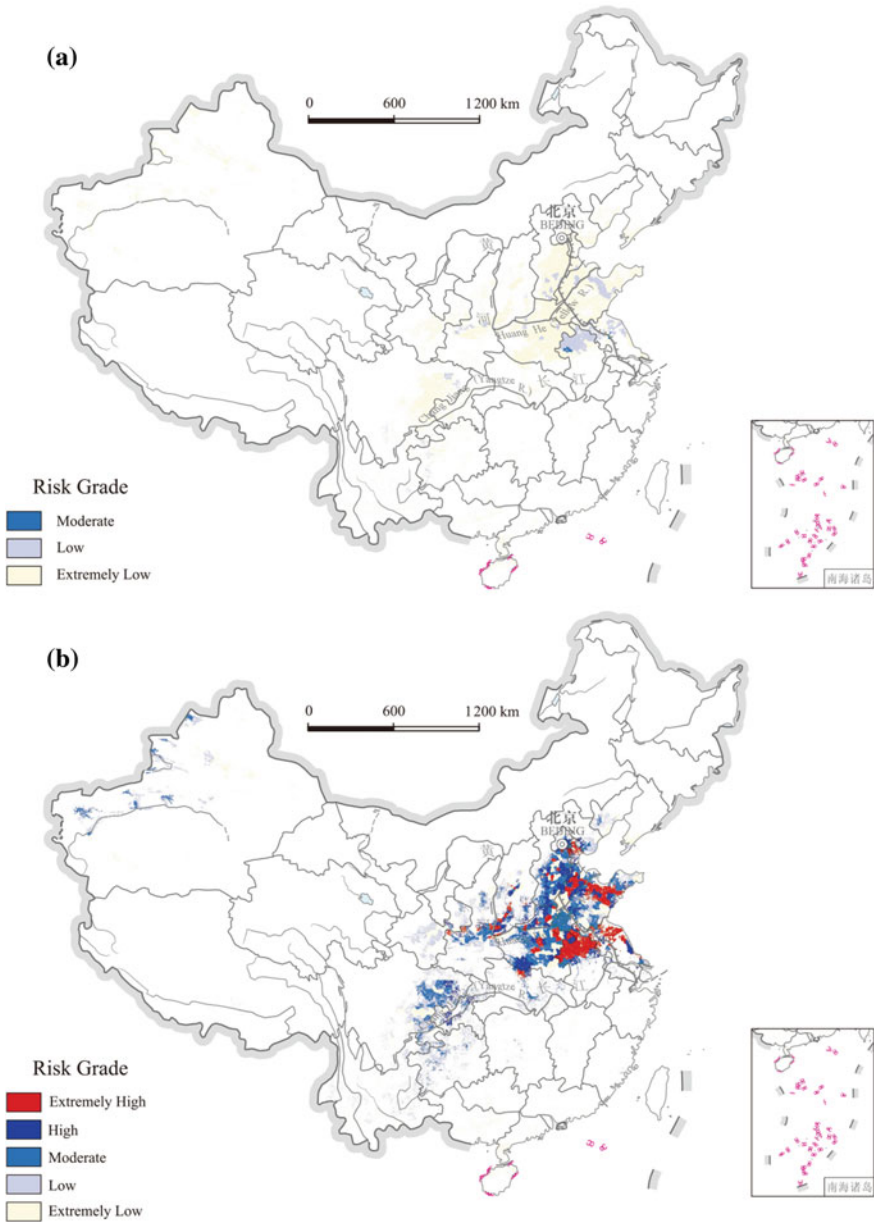


Fig. 15 Hail disaster risk of winter wheat in different growth periods. **a** Seedling-jointing stage (t₁). **b** Heading-maturity stage (t₃) (Source Shi 2011, p. 99)

strongest since 1984; precipitation in some parts of Jiangsu, Anhui, Jiangxi, Guangdong, Guangxi, and Yunnan was over 100 mm while that in Tongling of Anhui and Jiujiang of Jiangxi surpassed 150 mm; the depth of snow in some parts

Table 5 Percentage area of different hail disaster risk levels of winter wheat in various growth periods in China

t	Percentage of winter wheat growing area (%)			
	High risk	Moderate risk	Low risk	Extremely low risk
t ₁	0	0	4.99	95.01
t ₂	4.15	7.95	37.96	49.94
t ₃	20.95	11.4	33.93	33.63

Table 6 Conditions of the five low-temperature freezing rain and snow weather processes since 10 January 2008

Process	Heavy snow-snowstorm region	Freezing rain region
First process (10–16 Jan.)	Central Shaanxi, southern part of Shanxi, Henan, central north of Anhui, northern Jiangsu, Hubei, Hunan, and northwestern Jiangxi	Central south of Hunan, western and southern parts of Guizhou
The second process (18–22 Jan.)	Eastern Hubei, southern Henan, northern and central Anhui, northern Jiangsu, and northern Hunan	Southern Anhui, most parts of Hunan, Guizhou, and northeastern Guangxi
The third process (25–29 Jan.)	Southern Henan, eastern Hubei, Anhui, Jiangsu, and northern Zhejiang (with snow depth of 20–45 cm on 28 Jan.)	Most parts of Jiangxi and Guizhou, some parts of Hunan
The fourth process (31 Jan.–2 Feb.)	Central Hunan, northern Jiangxi, southern Anhui, southern Jiangsu, and northern Zhejiang (with snow depth in some areas reaching 20–35 cm on 2 Feb.)	Guizhou, Hunan, Jiangxi, Zhejiang, and Yunnan
The fifth process (4–6 Feb.)	Hunan, northern Jiangxi, western Guizhou, and eastern Yunnan	Eastern Yunnan and western Guizhou

Source EMGSEO (2008), EC-SCNDM (2008)

of Anhui and Jiangsu reached 30–50 cm, which was the highest in the past 50 years; the area covered by snow in Shanghai, Jiangsu, Anhui, Henan, Hubei, and Shaanxi took up more than 90 % of the total areas while Guizhou, Hunan, and Chongqing the snow covered area was 40–75 % of the total.

Thick snow cover and icing: The maximum snow depth in Wuhan of Hubei Province was 27 cm, which ranked the second only after that in 1954/55 (32 cm); the icing thickness of electric wires in Guizhou Province broke the record value since the meteorological records started and the freezing duration of 49 counties (cities) also broke the historical records; the duration, snow depth, and influences of regional snowstorms in Jiangsu were all at the top among the records, with the snow depth of 23 cities and counties (districts) surpassing the extreme values since 1961, among which the accumulated maximum snow depth of Nanjing was 37 cm—the maximum value since 1961. Moreover, because the wind speed on ground was clearly low and humidity of the atmosphere was high, the snow was difficult to be

blown away or evaporate, thus increasing the thickness of accumulated ice and snow. Average daily wind speed and maximum wind speed of Yizhang Weather Station in Chenzhou, Hunan (near the areas along the Beijing–Zhuhai Highway in Nanling) were lower than 1.8 and 3.5 m/s, respectively, and lower than the wind speed needed to blow away snow (5 m/s); average relative humidity of the atmosphere in Yizhang Weather Station was up to 75 % and even reached more than 80 % during the third and fourth weather processes.

Disaster losses: The losses incurred by this low-temperature freezing rain and snow disaster were extremely high, far exceeding that of similar disasters in ordinary years. The disaster spread to 20 provinces, autonomous regions, and municipalities (Table 7), caused 129 deaths, 4 people missing, and 1,660,000 people urgently transferred due to the disaster; the area of affected crops was 11,874,200 ha and the area experienced total crop failure was 1,690,600 ha; the number of collapsed houses was 485,000 and damaged houses amounted to 1,686,000; direct economic losses due to the disaster was RMB 151,650,000,000 Yuan. Hunan, Guizhou, Jiangxi, Anhui, Hubei, Guangxi, Sichuan, and Yunnan were the hardest hit provinces (EC-SCNDM 2008).

Compared to the previous serious nature disasters since 1998, the spatial scope of influence, number of deaths and missing people due to the disaster and urgently transferred population, quantity of collapsed houses, and direct economic losses due to this low-temperature freezing rain and snow disaster all belonged to the catastrophic category (Table 8), especially the spatial scope of influence and direct economic losses of the disaster equaled those of the 1998 great floods and the three-year severe drought in 1999–2001, while the number of deaths and missing people and urgently transferred population, as well as collapsed houses far exceeded the average level of low-temperature freezing and snow disasters in recent years. The scale of losses from one disaster was rarely seen (Shi et al. 2008).

Compared to the losses due to the low-temperature freezing and snow disasters in 2002–2007 (Table 9), this severe low-temperature freezing rain and snow disaster caused extremely serious losses, with the number of affected people, urgently transferred people, collapsed houses, and direct economic losses all surpassing the yearly average level in 2002–2007 and the number of urgently transferred people, collapsed houses and damaged houses, and direct economic losses were ten times more than the average level.

Economic and social impacts: This disaster led to serious economic and social impact, which was mainly on infrastructure such as transportation, electricity, and communication as well as on forest and other ecosystems.

The disaster had serious impacts on people's living. It resulted in a great number of collapsed and damaged houses, making the lives of the disaster victims, especially the low-income people, even more difficult. Owing to the rain and snow weather process, transportation such as highway and civil aviation, was restricted in a large scale; the transportation of agricultural products was difficult, which resulted in shortage in supply; prices of these products hiked in some areas; logistics supply such as food, clothing, drinking water, and candles as well as the supply of production materials such as agricultural materials and seeds for the affected people in

Table 7 Low-temperature freezing rain and snow disaster situations in various provinces (by 30 February 2008)

Provincial administrative area	Affected population 10 ⁴ people	Number of deaths due to the disaster Person	Missing population due to the disaster Person	Urgently transferred population 10 ⁴ people	Area of affected crops 10 ³ ha	Area with total crop failure 10 ³ ha	Number of collapsed houses 10 ⁴ houses	Number of damaged houses 10 ⁴ houses	Direct economic losses RMB 10 ⁸ Yuan
Total	20727.5	129	4	166.0	11874.2	1690.6	48.5	168.6	1516.5
Shanghai City	-	2	-	0.2	10.7	0.0	0.0	0.1	1.6
Jiangsu Province	245.3	7	-	2.1	232.4	12.0	0.9	1.7	27.8
Zhejiang Province	2381.9	9	-	13.6	832.9	40.8	0.4	0.0	174.3
Anhui Province	1342.3	12	-	13.1	695.3	63.6	9.1	17.3	132.3
Fujian Province	167.6	-	-	0.5	32.8	1.2	0.1	21.3	30.9
Jiangxi Province	2210.0	7	-	22.6	1468.0	353.0	4.2	23.1	272.0
Henan Province	94.1	-	-	0.8	139.4	2.7	0.3	0.6	6.8
Hubei Province	2279.8	13	-	21.7	1417.7	112.0	9.8	17.0	114.2
Hunan Province	3927.7	20	-	27.7	2500.1	458.7	6.7	30.0	172.0
Guangdong Province	419.0	-	-	29.0	414.7	21.2	0.2	0.1	33.6
Guangxi Zhuang Autonomous Region	1399.0	2	-	5.8	861.1	49.1	5.9	7.2	200.0
Chongqing City	548.6	2	-	0.6	246.3	27.7	0.3	1.4	9.6
Sichuan Province	1059.9	5	-	4.5	535.6	54.0	2.1	8.8	58.3
Guizhou Province	2654.8	27	-	11.2	1489.7	317.5	3.1	12.8	198.3
Yunnan Province	1139.6	22	4	11.0	590.9	110.7	3.9	19.7	50.8

(continued)

Table 7 (continued)

Provincial administrative area	Affected population 10 ⁴ people	Number of deaths due to the disaster Person	Missing population due to the disaster Person	Urgently transferred population 10 ⁴ people	Area of affected crops 10 ³ ha	Area with total crop failure 10 ³ ha	Number of collapsed houses 10 ⁴ houses	Number of damaged houses 10 ⁴ houses	Direct economic losses RMB 10 ⁸ Yuan
Shaanxi Province	185.0	–	–	1.0	253.3	20.0	0.4	0.9	4.6
Gansu Province	448.0	–	–	–	135.8	45.3	0.4	3.3	17.8
Qinghai Province	70.5	–	–	–	0.0	0.0	0.5	1.4	4.2
Ningxia Hui Autonomous Region	116.6	–	–	0.5	10.8	1.1	0.3	0.9	4.7
Xinjiang Uygur Autonomous Region	35.1	1	–	–	–	–	0.1	1.0	1.8
Xinjiang Production and Construction Corps	2.7	–	–	–	6.7	–	0.0	0.0	1.2

Source Shi et al. (2012)

Table 8 Loss comparison of catastrophic disasters since 1998

Catastrophe	Number of affected provinces	Number of deaths and missing people (person)	Urgently transferred population (10 ⁴ people)	Number of collapsed houses (10 ⁴ houses)	Direct economic losses (RMB 10 ⁸ Yuan)
Low-temperature freezing rain and snow disaster in 2008	20	133	166.0	48.5	1516.5
Floods in the Huaihe River Basin in 2007	3	39	144.1	13.3	195.9
No. 4 strong tropical storm Bilis in 2006	6	843	336.9	39.1	348.2
No. 8 ultra-strong typhoon Saomai in 2006	3	483	180.1	13.7	196.5
Heavy drought of Sichuan and Chongqing in 2006	2	–	–	–	222.7
No. 14 typhoon Ranim in 2004	6	183	66.0	7.22	198.9
Large-scale floods in the Huaihe River Basin in 2003	3	31	217.8	38.9	364.3
Great floods in 1998	29	2,291	1664.0	583.3	2104.4

Source Shi et al. (2012)

remote mountainous areas and other remote areas became tight; agricultural production and animal husbandry also were greatly affected. In addition, as this disaster occurred during the peak time of travel for Spring Festival, the transportation system was further stressed because some railways, highways, and civil aviation were forced to be closed, causing more than 870,000 passengers stranded, among which 80,000 people were stranded and need assistance in Hunan Province alone while 107,000 people were stranded during the peak time in Guizhou Province. During the emergency rescue and disaster-relief period, the number of disaster-affected people and people stranded on the railways and highways who needed assistance amounted to 6,555,000 in total.

Electric power facilities were greatly damaged. Affected by the disaster, among the power systems nationwide (including the system of the State Grid Corporation, the system of the South Grid Corporation, local power grids, and individual systems owned by power plants), in total 35,710 electric power lines were out of service;

Table 9 Comparison between the low-temperature freezing rain and snow disaster in 2008 and the yearly low-temperature freezing and snow disasters in 2002–2007

Year	Number of deaths and missing people	Urgently transferred population	Collapsed houses	Direct economic losses
	person	10 ⁴ people	10 ⁴ houses	RMB 10 ⁸ Yuan
Low-temperature freezing rain and snow disaster in 2008	133	166.0	48.5	1516.5
2002	102	0.1	0.16	108.91
2003	9	–	3.38	47.8
2004	24	2.7	5.9	96.6
2005	79	7.6	10.7	72.9
2006	10	1.6	7.7	169.0
2007	31	5.4	1.4	186.5
Mean value of yearly losses in 2002–2007	42	2.9	4.9	113.6

(Source Shi et al. 2012)

2,007 substations were closed; 8,501 towers for 110–500 kV lines collapsed; the working of electrical power system in 13 provinces, autonomous regions, and municipalities was affected and 170 cities and counties were out of electricity; during the peak time 42,000,000 KW capacity in power plants was shut down due to lack of coal, and there were 19 provinces, autonomous regions, and municipalities adopting power rationing.

Transportation was once seriously blocked. Owing to the outage of electric power system in Hunan, Jiangxi, and Guizhou, the Beijing–Guangzhou Railway, Beijing–Kowloon Railway, and Beijing–Shanghai Railway were suspended for a period of time; traction power supply network for the trunk lines of the Beijing–Guangzhou Railway and the Shanghai–Kunming Railway (two major railways) were damaged, the signal system of railway communication was out of electricity and the transportation of some sections was obstructed—at the worst point, the number of passenger cars stranded on the Beijing–Guangzhou Railway and the Shanghai–Kunming Railway were 387, with 1,800,000 passengers stranded at the main passenger depots. Facilities such as power supply devices for contact networks of railways, bridges/tunnels/culverts, communications signals, rolling stock, and houses for stations along the lines, were damaged to different extents. A total of 82,000 km roads nationwide was damaged due to the disaster, among which 6,869 km were highways and the damages mainly involved damaged pavements, safety fences, marking lines, and trees as well as collapsed subgrade and side slope of several sections; various main highways in the disaster areas were closed due to freezing; the national roads and provincial roads were seriously crowded and blocked; the sections of the Beijing–Zhuhai Highway in northern Guangdong and Hunan Provinces were once closed down totally, with more than 20,000 vehicles

and 100,000 passengers stranded during the peak time; 230,000 km highways in the country was closed for multiple times due to freezing with serious crowding and blocking, 700,000 stranded vehicles, and 2,160,000 trapped passengers, and causing the cancellation of 1,100,000 passenger buses that affected the travel of more than 34,000,000 persons. The rain and snow caused the cancellation of 3,840 flights across the country and delay of 9,550 flights and a large number of passengers remained at the airports; 14 airports along the middle- and lower-reaches of the Yangtze River were closed at some point, and some airport facilities such as runways, vehicle equipment, water, heating and electricity, as well as airport buildings in four provinces including Guizhou, Jiangxi, Hunan, and Hubei, were damaged.

The supply of coal for power generation and refined oil was threatened. Because the power was cut off and traffic was blocked, and some coal mines were on holiday ahead of the Spring Festival or closed for maintenance, the supply of coal was seriously affected. The inventory of coal at some power plants decreased sharply and the stored coal dropped from the normal 15 days' supply down to seven, which was less than half of the normal level. During the most difficult period, there were 86 power plants where the stored coal cannot last for three days; 42,000,000 KW of capacity were shut down due to lack of coal for fuel and 19 provinces, autonomous regions, and municipalities adopted power rationing. Transportation and distribution of refined oil and liquefied gas in disaster areas, especially delivery by vehicles on highways was greatly affected; accident potential of some oil transport equipment and pipelines increased while the supply of refined oil faced enormous pressure. The power failure in large areas of Guizhou affected transport of refined oil by pipelines in the southwest, which threatens market supply of refined oil in Guizhou and Yunnan; some areas once restricted or stopped the supply of gas for production.

Serious damage to crops occurred. The total area of affected crops nationwide was 11,874,200 ha, among which the disaster area was 5,842,600 ha and that experienced total crop failure was 1,690,600 ha. The disaster in six provinces and autonomous region including Hunan, Hubei, Jiangxi, Guangxi, Guizhou, and Yunnan was serious, accounting for 66 % of the disaster area nationwide. Cash crops and horticulture crops such as rape, vegetables, and oranges suffered greatly from the disaster. The area of affected rape accounted for 50 % of the areas where rape was planted in the autumn and winter while the output of rapeseed was expected to reduce by 1,700,000 tons; the area of affected vegetables accounted for about 35 % of the areas where vegetables were planted in the autumn and winter. A total of 6,060,000 livestock and 62,750,000 poultries were dead; fine stock breeding system was damaged heavily; facilities such as vinyl houses and buildings for livestock were damaged seriously; rural water supply facilities, irrigation and drainage canal systems and facilities, embankments, reservoirs, and sluice gates, and so on also were seriously damaged.

Great losses of forestry were severe. The area of affected forestry in the country was 22,666,700 ha, which accounted for 7.4 % of the land area of forestry nationwide; 2,140 state-owned farms of forestry, 1,158 state-owned nursery gardens, 663 nature reserves, and 29,127 other state-owned units were affected, with

serious damages to the infrastructure. The disaster caused destructive damage to income of forestry and agriculture. Forestry income accounted for more than 50 % of the gross income of forestry and agriculture, thus the disaster would greatly affect income of forestry and agriculture in the following 3–5 years, and also influence the reform of collective forest property right system. The disaster had great negative impacts on ecological improvement—the affected areas had the fastest development of forestry, the most prosperous vitality, and the best forest resources, accounted for 1/10 of the total forest area of China and the damaged area equaled to the increased forest area in one five-year plan period; the disaster of forestry would affect the attainment of the objective that the forest coverage of China would reach 20 % in 2010. The shutting down of forestry enterprises would affect the employment of nearly 1 million people and the supply of forest products in China in coming years. In addition to the hard task of planting and rebuilding the damaged forest, damage to forestry infrastructure placed even greater pressure on fully recovering the production.

Industrial enterprises were shut down in a large scale and public infrastructure was seriously damaged. Influenced by power failure and blockage of traffic, 1,794 coal mines were shut down in four provinces including Jiangxi, Hunan, Guizhou, and Yunnan; 83 % of the above designated size industrial enterprises in Hunan Province and 90 % of the industrial enterprises in Jiangxi Province were once shut down; the output of fertilizer in Guizhou Province was reduced by 300,000 ton and the enterprises of the Aluminum Group of China in Guizhou were all shut down with reduced industrial output value of RMB 1,000,000,000 Yuan per month. Water plants in some cities stopped working and 42,000 km water supply network was cracked due to frost; more than 1,800 km sewage network was damaged and the environmental impact was serious as waste and sewage water were not processed timely; 333,000 poles for fixed-line communication fell or broke, with 53,000 km damaged lines; 19,000 mobile base stations were damaged; 705 TV transmitting stations and 89,000 km cable TV transmission network were damaged, which caused disruption of urban and rural communication and information and TV network transmission; normal operation of 174 stock trading sites were affected; supply of gas for living and production was restricted or stopped in many cities; 133 gas stations of PetroChina and Sinopec collapsed and delivery line of refined oil in the southwest stopped transportation intermittently. About 36,000 primary and middle schools were affected, among which 23,000 classrooms and dorms collapsed, with about 1,420,000 km² construction area, and 4,080,000 m² buildings became unsafe.

Impacts on the ecosystem were profound. Owing to the influences of low-temperature freezing rain and snow disaster in vast disaster areas in the south, various ecosystems suffered from overall damage. Natural forest ecosystems were damaged; most parts of secondary forest ecosystems and planted forest ecosystems also suffered overall damage. Wild animals were affected widely as well. In some natural forests, some rare and endangered animals were affected to different extent, even several species died out tragically. Moreover, some aquatic ecosystems were also affected by melt water of polluted ice and snow, which caused poor water

quality and further led to pollution of the water area, thus affecting normal growth of aquatic organisms. The risks posed by the pollution may last for a long time.

Causes of the disaster: This low-temperature freezing rain and snow disaster mainly happened in the populated areas in southern China during the Spring Festival travel peak. The forceful meteorological hazard and mountains and hills in these regions resulted in grid damage and power failure, traffic disruption, and serious damages of agriculture and forestry, finally leading to this rare large-scale disaster. The formation of this large-scale disaster was due to the combined action of all factors in the complex disaster system (ADREM 2008). The specific causes are discussed as follows.

The special terrain of mountains and hills aggravated the disaster. The disaster was closely related to the topography, geomorphology, and characteristics of the weather in the disaster area. The disaster was mainly distributed in the low hill and plateau areas of China, especially the Yunnan–Guizhou Plateau and the Nanling Mountains. The altitude of most disaster areas was above 300–500 m and more than 2,000 m in some places. Since air temperature decreases progressively with increasing altitude (about 0.6 °C when the altitude increases for 100 m), air temperature in the mountainous area is lower than the plain area. The large-scale power supply and communication facilities often pass the high mountains, where the humidity was also high (nearly saturated) so ice and snow could not evaporate. In addition, the wind speed in the disaster area was low, sometimes near still. The sleet rapidly accumulated on the buildings; the pressure of accumulated ice and snow was in some places 10 times greater than the design standard, resulting in the damage of numerous power supply and communication facilities. In the worst stricken area—Chenzhou City of Hunan Province, the average altitude of most counties and districts is above 300 m; the altitude of about 30 % area of the city is above 500 m and in some areas this is more than 1,000 m. Along the Beijing–Zhuhai Highway from Chenzhou City to Shaoguan City of Guangdong Province, the altitude of 50 % road section is above 300 m, among which, the altitude of the section from Liangtian to Yizhang is more than 500 m; elevation on both sides of the highway is even above 1,000 m. During the entire process of the extreme low-temperature freezing rain and snow weather, the average temperature of most regions in Chenzhou City was between –2.0 and –8.0 °C, which intensified the severity of the disaster.

The main disaster areas were densely populated, and the socioeconomic impacts were further amplified by the Spring Festival travel. Extreme large-scale passenger flow and logistics transportation during the pre-holiday period already challenged the limits of the infrastructure, water and electricity supply, logistics, and social management systems even without the disaster. The main stricken areas of the disaster were in the southern regions of China; in these areas, the population density was very high (the average population density of Anhui, Jiangxi, Hubei, Hunan, Guangxi, Guizhou Provinces, and other serious disaster areas was above 200 people/square kilometer, which is far more than the national average of 133 people/square kilometer), transportation lines were dense, public infrastructure had low anti-freezing capacity, the importance of agriculture and forestry in the regional

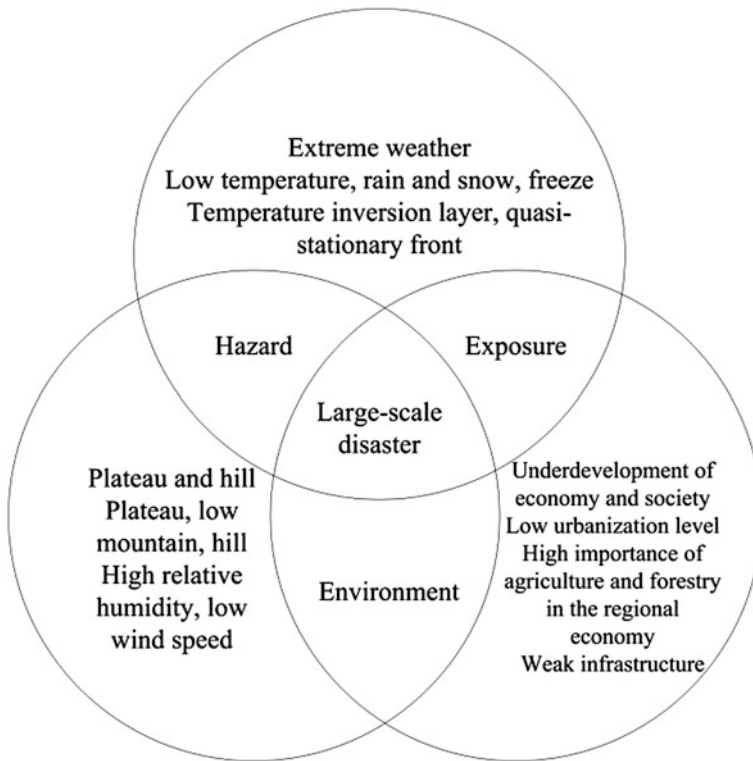


Fig. 16 Schematic diagram for the interaction between the main factors of the disaster system

economy was high, and the public had little means to prevent an ice and snow disaster. The combination of these factors triggered a series of problems, which amplified the social impact of the disaster and created great difficulties for emergency rescue and disaster relief (Fig. 16).

The chain characteristics of the disaster aggravated the situation: Under the interaction of the extreme meteorological conditions and the terrain factor, this rare low-temperature freezing rain and snow weather caused large snow and ice accumulation on buildings. Meanwhile, in the daytime and after each weather process, the temperature would rise slightly, resulting in the temporary melting of ice and snow that formed all kinds of icicle. The accumulated freezing layer formed during the four previous weather processes sometimes reached above 40 cm (Fig. 17). It imposed great load on the buildings, and thus resulted in the destruction or damage of large-scale grid infrastructure in the disaster area, leading to unprecedented power failure accident. Power failure—a secondary disaster—was the root cause of the service disruption of the railways, highways, communication, water supply, fuel gas, and other lifelines, and production systems in the disaster area. The flow of people, information, and materials and products was obstructed, and normal production and life order were severely affected. A chain of hazards and disasters was

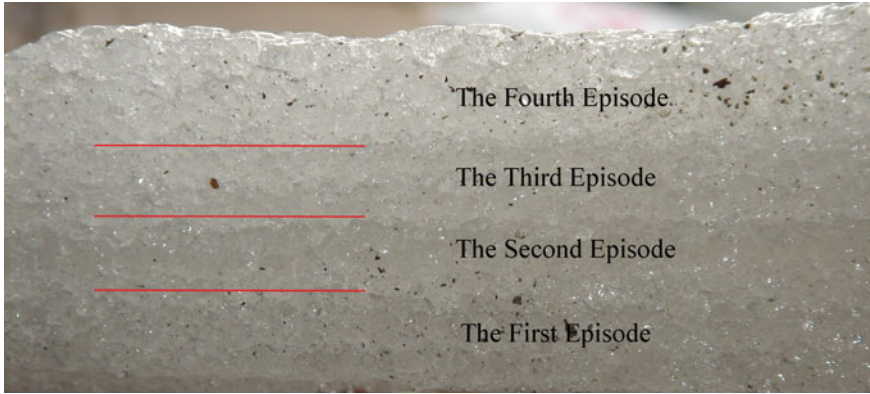


Fig. 17 The ice layer accumulated on the Yuxiang Flour Processing Plant in Chenzhou City of Hunan Province during the four episodes of snow and ice accumulation, 10 January–6 February 2008. (Photograph by Peijun Shi)

formed: low temperature—rain and snow—freezing—compression and pulling by snow and ice (natural hazard)—power failure—water shortage—road congestion—airport closure (production accident)—station congestion—passenger accumulation (public security incident)—damage of living environment—pollution of drinking water sources—impact on food quality (public health incident).

The main stricken areas of this low-temperature freezing rain and snow disaster were important passages of transportation for passengers, coal, and other materials and electricity transmission, as well as densely populated. The amplification effect caused by the overlaying of secondary and derivative disasters was prominent, which had an all-around impact on the economy and society. During this large-scale disaster, the central government, local governments, and the general public all took part in the disaster relief and emergency rescue efforts. The emergency response capability of the government and the society was tested and further understanding about large-scale disasters was gained. The experiences provided valuable lessons for the governance of catastrophic disasters and emergency response in the future (Shi 2008).

3.2 *Emergency Rescue Process*

Start state level II emergency plan and establish the Emergency Command Center for the transportation of coal, electricity, and oil as well as risk reduction and disaster relief (NDRC 2008): In order to organize and coordinate the responses to the freezing rain and snow disaster, on 28 January 2008, the State Council established the Emergency Command Center for the transportation of coal, electricity, and oil as well as risk reduction and disaster relief (hereinafter referred to as Emergency Command Center), which was responsible for coordinating the

responses to this large-scale disaster. A total of 29 units including the communist party, the government, and the army participated in this temporary organization. The office of the Emergency Command Center was located in the National Development and Reform Commission. On the night of January 29, the Emergency Command Center held the first plenary meeting to establish the working priorities of restarting road transportation, ensuring electricity supply, and reassuring the public according to the demand of the central government and the State Council based on the comprehensive analysis of the disaster situation. Meanwhile, six headquarters for ensuring the transportation of coal, electricity, and oil; reopening the road quickly; repairing the grids quickly; disaster relief and logistics supply; post-disaster reconstruction; and public information campaign were established with the aim of intensifying command and coordination of important working areas. The Emergency Command Center held a conference every night to command and dispatch the overall rescue and relief work as well as reported important information to the Central Committee of the Communist Party of China (CCCPC) and the State Council timely. The headquarters cooperated for information exchange and problem-solving. As of 13 February 2008, the No. 208 Executive Meeting of the State Council analyzed the progress of emergency rescue and relief work and made the decision to change the emphasis from emergency rescue to comprehensive restoration and reconstruction after the disaster. On February 15, the State Council approved and published the *Report on Rescue and Relief Work and Post-Disaster Reconstruction Arrangement* submitted by the Emergency Command Center. Within three weeks the Emergency Command Center as a temporary structure had accomplished its mission and was decommissioned.

Nationwide coordinated emergency response to the large-scale disaster:

According to the forecast of disastrous weather, leaders of the State Council made important instructions. The Emergency Command Center of the State Council issued disaster early warning on January 10, 15, 19, and 21, 2008 and asked related regions and departments to implement all measures to deal with the snowstorm attack. On 14 January, the National Development and Reform Commission started a cross-department economic operation coordination mechanism to arrange the work of increasing the production and transportation of coal for power generation. On January 18, the Ministry of Public Security initiated transportation emergency management; the railway system launched the Spring Festival travel special arrangements 5 days earlier than scheduled. On January 25, Premier Wen Jiabao went to Hebei Province and Beijing to inspect the Spring Festival travel special arrangements, held office meeting at the Beijing West Railway Station, and arranged Spring Festival travel, transportation of coal for power generation, as well as logistics transportation during the Spring Festival period. At the same time, policies for organizing passenger transportation, intensifying quick transportation of coal for power generation, and implementing prioritized transportation of fresh agricultural products were put forward. On January 25–27, damage to the Guizhou and Hunan grids caused power failure in many areas and subsequently, the transportation of some sections of Beijing, Guangzhou, Shanghai, Kunming, and other railway trunk lines was obstructed; Beijing–Zhuhai Highway was seriously

blocked. On January 26, the General Office of the State Council held emergency meeting to discuss the transportation of coal and oil and transmission of electricity and disaster relief work; on January 27, the State Council held video and telephone conference to carry out detailed deployment. On January 28 and February 1, the Executive Meetings of the Political Bureau of the Central Committee of the Communist Party of China and the State Council held a special meeting on emergency rescue and disaster relief work; during this time, President Hu Jintao and other key leaders of the central government went to the main coal-producing provinces and most serious stricken areas to command the production and quick transportation of coal as well as disaster relief work. On January 30, the State Council held the Office Meeting of National Committee for Disaster Reduction to analyze the disaster situation comprehensively and make arrangements for production and logistics supply for people in the disaster area. On the same day, China Meteorological Administration initiated a level II emergency plan; the Ministry of Civil Affairs and State Electricity Regulatory Commission (SERC) initiated a level II emergency plan for disaster relief and for large-scale power failure of the grids; the Ministry of Railways, Ministry of Communication, and Ministry of Public Security also initiated emergency plans. Moreover, all levels of the governments in the disaster area carried out emergency response mobilization; State Grid, telecommunications, and other state-owned enterprises took on their social responsibility. The People's Liberation Army and People's armed Police took on difficult tasks in emergency rescue and disaster relief. By 12 February, the dispatched personnel from the People's Liberation Army reached 319 thousand; armed police personnel reached 348 thousand, and organized people's police paramilitary officers reached 1,882 thousand. A total of 5,930 thousand police officers worked in the frontline to maintain order, control traffic, remove ice and snow, and rescue the disaster victims.

Nationwide mobilization to tackle difficult tasks in emergency rescue and disaster relief: According to the general requirements of ensuring transportation, power supply, and livelihood security of the disaster-affected people put forward by the CCCPC and the State Council to cope with the large-scale disaster, the Emergency Command Center of the State Council, governments at all levels, and relevant authorities in the disaster areas organized the operations to clear roads, transport coal for power generation, repair the damaged grids, and secure the living of people in the disaster areas and logistics supply.

Mobilize all forces to clear the roads. Securing transportation played a crucial role in ensuring power supply and people's living. The Emergency Command Center convened thematic meetings several times to discuss and adopt specific measures for clearing the roads; transportation, railway, and police departments strengthened the unified command and with joint efforts of governments at all levels and relevant authorities in the disaster areas, as well as strong support of the People's Liberation Army, armed police force, and police officers, mobilized all forces to remove snow and break ice, move stranded vehicles, transfer diesel locomotives and generators for the Beijing–Guangdong Railway and Shanghai–Kunming Railway; meanwhile, advised the migrant workers to stay and celebrate

the Spring Festival in cities where they worked to relieve transportation pressure during the Spring Festival; strengthened the unified command and traffic advisories to avoid new traffic jams; enhanced the support for the assessment of the disaster situation. With the joint efforts and comprehensive measures, the major airports affected by the disaster reopened on February 3; the Beijing–Zhuhai Highway reopened to traffic on February 4 and 3.5 million passengers stranded in Guangzhou were all transported on February 5.

Further improve the arrangements for the production and transportation of coal for power generation. All major coal-producing provinces and autonomous regions and important coal producers made great efforts to increase coal production. Railways and transportation departments organized to transport the coal quickly. Daily loading capacity of coal for power generation by the railway reached 43,000 vehicles on average, increased by 53.9 % compared to the same time period of a normal year, and daily transport volume of Datong–Qinhuangdao Railway reached 1 million tons on average, increased by 22 % compared to the same time period; and daily loading of the four ports in the north, including the Qinhuangdao Port, reached 1.3 million tons, increased by 24 % compared to the same time period. The Emergency Command Center connected the leading power plants in emergency with coal mines and railways in a “point-to-point” manner. Through the joint efforts of all parties, the coal directly supplied to the power plants reached 27.7 million tons on February 24 and the storage returned to the normal 14 days’ supply.

Concentrate strong forces to repair the damaged grids. The State Grid Corporation of China and China Southern Power Grid Corporation organized a large number of technical teams across the country to repair power supply facilities of railways and residential areas. The number of participants who took part in this work amounted to 420,000. Railway departments and transportation departments placed priority on the transportation of materials needed for repairing electric power facilities with the full support of local governments, the army, armed police, police, militia and reserve forces, and oil for power generation was supplied timely by the two leading suppliers—Sinopec and PetroChina. On February 6, the New Year Eve, 95 % of power lines and 99 % of substations that were in shutdown due to the disaster were recovered.

Implement policies and measures to secure the living of people in the disaster areas. According to the requirements of supplying food, ensuring protection against cold, providing temporary housing and medical treatment, the Emergency Command Center, relevant local governments and authorities organized timely to allocate and transfer relief supplies to the disaster areas, including grain, food oil, fast food, tents, padded clothes and blankets, flashlights, radios, generators, petroleum products and liquefied petroleum gas, and so on; arranged temporary shelters for people affected by collapsed and damaged houses and offered help to stranded travelers. Financial departments and civil affairs departments allocated RMB 1.824 billion Yuan as central government emergency assistance funds for disaster victims and an additional RMB 710 million Yuan to low-income residents in urban and rural areas of the worst-hit provinces as temporary subsidies. The health departments at all levels dispatched 25,000 medical teams and further

organized and implemented prevention and control measures for public health incidents resulted from secondary disasters and derivatives disasters, so as to prevent major epidemics after the disaster.

Strengthen organization and market supervision to ensure logistics supply in the disaster areas. The Emergency Command Center focused on disaster relief and at the same time ensured logistics supply in the disaster areas. Food-related authorities organized to process grain and distributed the processed grain and food oil timely to local reserves; commerce departments, financial departments, and other related authorities allocated reserved pork and other daily necessities; imported pork and soybean oil and other supplies. The agricultural departments organized farmers in the disaster area promptly to repair destroyed facilities, plant/replant fast-growing vegetables, as well as commanded the northern major producing area of off-season vegetables and production bases of winter vegetables in the south to expand production; meanwhile, enhanced advising and organized joint production and sales of fresh agricultural products between the disaster areas and non-disaster areas, and created wholesale markets of agricultural products in the disaster areas and provinces jointly to ensure the supply of fresh agricultural products. PetroChina and Sinopec prioritized oil supply for vehicles transporting grain and food, vegetables, and other fresh agricultural products, whose tolls were exempted by the traffic authorities. Authorities reduced fees charged to retailers of fresh agricultural products and implemented temporary price intervention policies for daily necessities and relief goods, and strengthened market supervision and price control in the disaster areas to ensure stability of major commodities prices and maintained the order of the market.

The nationwide actions in the five areas identified above achieved remarkable effects in coping with this large-scale disaster.

Strengthen information release by the government and guide public opinions: In order to enhance the authority, timeliness, correctness, and comprehensiveness of information about the large-scale disaster, the Emergency Command Center, the Publicity Department of the CCCPC, and the Information Office of the State Council strengthened information release and created a positive environment for the public opinions during emergency rescue and disaster relief.

First, enhance the information release of disaster relief. The Emergency Command Center successively issued 21st announcements to direct various regions and parties concerned in the following works: clearing the roads, repairing the grids, transporting coal for power generation, clearing stranded travelers, arranging migrant workers to celebrate the Spring Festival locally, stabilizing prices in the disaster areas; and guide them to strengthen the prevention of secondary disasters in geology, infrastructure, forestry, public health, animal and plant epidemic diseases, among others. Second, establish a press release mechanism and build a positive environment for public opinions. The Emergency Command Center has organized several press release conferences and media briefings and set up “authorized release” and other columns on major news media and key websites such as the People’s Daily and CCTV to release the progress of disaster relief throughout the country every day. The Publicity Department of the CCCPC organized the central

and local press media, key news websites to closely focus on the overall disaster relief; they published timely the important measures issued by the central government and parties concerned, as well as inspiring stories of people in disaster relief to boost the spirit of the public. Third, strive to obtain the understanding and support of the international community. The International Communication Office of the CCCPC strengthened the information release of disaster relief, actively guided public opinions on the internet, and invited foreign media to cover news in the disaster areas. The Ministry of Foreign Affairs notified the disaster situations to ambassadors of various countries stationed in China as well as international organizations, and arranged Chinese embassies to introduce the disaster situation and relief work to the foreign governments, international organizations, and overseas Chinese communities. The International community has positively evaluated the relief work of the Chinese government and people in the face of the freezing rain and snow disaster in the south.

Formulate post-disaster restoration and reconstruction plans and organize various forces to promote the post-disaster reconstruction work: In accordance with the requirements of the CCCPC, the Emergency Command Center quickly developed the *Guidelines for the Restoration and Reconstruction Planning of the Low-Temperature Freezing Rain and Snow Disaster* (the Guideline), which was issued by the State Council upon approval. The Guideline specified to focus on the grids and emergently repair damaged infrastructures; stress on the repair of irrigation facilities to recover agricultural production as soon as possible; and emphasize the repair of collapsed houses to recover normal life of people in the disaster areas. In addition, it also defined the objectives and tasks, main responsibilities, key priorities in work, time requirements, and policies and measures of post-disaster reconstruction, and proposed the principles of “planning in advance, coordinating arrangements, defining priorities, stressing key points, putting self-rescue in the first place, government supported, local based, centrally subsidized.” Raise funds through multiple channels, coordinately arrange various funds such as central government funds, investment within central budget, and relief funds from the civil affairs administration, and carry out a solid post-disaster restoration and reconstruction. Under the Guideline, the affected provinces and autonomous regions also developed own reconstruction plans.

In order to put the post-disaster reconstruction policies formulated by the central government into practice, the central budget arranged RMB 28.543 billion Yuan as restoration and reconstruction funds, of which the Ministry of Finance in conjunction with relevant departments arranged RMB 25.543 billion Yuan, and the Development and Reform Commission jointly with relevant departments arranged RMB 3.0 billion Yuan. In addition, according to the decision of the Executive Meetings of the State Council on March 26, 2008, the central government arranged RMB 562.5 billion Yuan to invest in the “Three Rural” program, added RMB 25.25 billion Yuan to the central budget on top of the infrastructure investment of RMB 73.9 billion Yuan and RMB 2 billion Yuan as infrastructure investment within the central budget, which was used for agriculture and food production in disaster-affected provinces and autonomous regions.

By the end of March 2008, the grid, communication network, and traffic facilities had nearly recovered to normal. The damaged public facilities, water sources in rural areas, collapsed houses, industries, and enterprises had basically completed the restoration and reconstruction at the end of June 2008. Since the forestry ecology was damaged severely and the period of forestry reconstruction is long, at the end of June 2008, the planning for damaged forestry recovery in 3–5 years had been completed, which was put into practice thereafter.

3.3 *Lessons Learned*

The Chinese government has achieved a great success in the disaster relief and post-disaster recovery of the freezing rain and snow disaster in southern China, and the model of coping with large-scale disaster by nationwide mobilization has been fully promoted. These are positively recognized by the Chinese society and the international communities. However, the sudden onset, great complexity, and extraordinary hazard severity of the large-scale disaster also revealed the vulnerability of lifeline systems, such as coal, electricity, oil, and transportation, of China in the process of rapid industrialization and urbanization, which indicates that the risk governance and coping ability of China in the face of large-scale disasters still need to be improved and strengthened in many aspects.

Lessons—main problems: Emergency management systems and mechanisms need to be further improved. First, the emergency management structures, particularly those at the city and county levels are generally lagged; second, the liaison between various authorities and information exchange mechanism are conspicuous. In the early stage of the disaster, poor information exchange occurred. For instance, along the highways and some major transportation hubs, the management parties only focused on reducing the pressure from traffic flow on their own systems but with little regard for the overall interests. This, together with information asymmetry, resulted in traffic congestion and increased retention on some roads, which delayed the relief operations.

Operability of the emergency plans and the effective coordination between various plans shall be improved. This large-scale disaster originated from the extreme weather that was rarely seen in the history. Although various authorities and regions had developed a number of related plans, there was a lack of specialized plan for coping with major weather disasters. Meanwhile, the disaster also exposed problems such as lack of connection between some existing plans, poor coverage of the contents, and poor operability. In particular, some basic plans did not define core contents such as how to initiate actions and responsibilities of various divisions, which resulted in their inoperability in emergency response practice. Moreover, training following the plans was far from adequate.

Disaster forecast and early warning capabilities need to be improved. During the five episodes of freezing rain and snow weather, the meteorological department had issued accurate forecasts. However, due to the limited monitoring methods and

technology, as well as insufficient research on the formation mechanism of major meteorological disasters, especially in many places people mistakenly considered the disastrous weather as meteorological disaster forecast, an overall consideration of disastrous weather, landform, and climatic conditions of the disaster-affected areas was missing. The forecast focused on the short-term weather process and underestimated the duration and intensity of the disastrous weather processes, especially the extremely severe impact of four overlapping weather processes in the Nanling Mountainous area. Meanwhile, due to the lack of historical data and relevant information in professional meteorological monitoring of power grid and traffic systems, appropriate assessment of hazard impact brought to the power grid, traffic system, and economy and society at large by the disastrous weather, as well as corresponding disaster early warning, were non-existent.

Emergency rescue equipment and materials are insufficient. During the process of coping with the disaster, professional relief and rescue equipment, technological methods, and material reserves in some places were apparently insufficient and even the numbers were unclear—examples are snow removal vehicles, tyre chains, earth levelers, forklift, gunnysacks, industrial salt, and individual protection devices; some places even without a satellite phone. In parts of those areas, the emergency reserves for logistics were too low to ensure the basic living of disaster victims, such as providing food, candles, kerosene, and so on.

Infrastructure could not meet the demand of disaster prevention. First, the extensive damage of power lines and facilities exposes the vulnerability of these systems. The disaster caused power failure in several cities and counties in Hunan, Guizhou, and Jiangxi Provinces; some local grids suffered devastating damage, indicating that China has many deficiencies in power distribution, power grid design standards, emergency ice-melting technology, and so on. Second, the overall traffic capacity of roads and railways was limited. The Beijing–Zhuhai highway was always congested in northern Guangdong and southern Hunan, and this time traffic congestion was more seriously. In the years preceding the disaster, the upgrading of the national and provincial highways by the local governments progressed rather slowly, therefore the traffic capacity of those highways was too low for traffic diversion. Railway transportation capacity shortage was always serious during the Spring Festival period and for the transport of bulk goods. Third, the design standards of water supply and drainage systems and other urban public facilities were too low to adapt to climate change and the demand of the development of a modern society. Some facilities had long passed the retirement age, so their ability to withstand natural disasters was rather weak.

Societal risk awareness needs to be further improved. First, some places and authorities lacked the sense of potential dangers. The snow changed from a scenery—heavy snow—snowstorm—snow disaster and authorities lacked the ability to identify, report, control, and solve the problems in a very timely manner. Some leaders lacked the ability to appropriately handle the emergency situation according to the regulation and make decision based on scientific knowledge. Second, the capacity of the public in disaster prevention, mitigation, and avoidance was weak and there was a lack of self-aid and mutual aid emergency response capabilities. Urban and rural

residents were generally poorly prepared for disasters and did not keep candles, flashlights, and so on at home. When in some places disaster information had been released, a large number of vehicles still moved into the crowded highways; some drivers even seized the emergency lane, resulting in complete blockage of the local road network. Third, disaster insurance coverage was low. The amount of compensation in the disaster accounted for only about 4 % of the total losses. The vast majority of businesses, farmers, and infrastructure were not covered by insurance. Forest insurance system had not been established.

The serious damage to forestry revealed many of its problems such as focusing too heavily on plantation and neglecting forest management, inadequate investment in forestry, among others. Over the years, governments at all levels attached much importance to the forest coverage indicators and neglected factors such as unit stock volume of the forested land, which reflects the quality of forest. Forestry investment only included afforestation costs and forest management costs were not included, resulting in key problems such as low forest productivity, poor forest structure, slender trees, and weak disaster resilience. In some forest areas in southern China the result of decades of investment in forestry development was severely damaged by the disaster and the risk of continuous aggravation of losses was evident. This includes the increased risk of forest fire, decline of tree growth, increase of plant diseases and infestation of insect pests, rotting of broken branches. Moreover, the recovery period of forestry is long, therefore many forestry holders and workers face major production and livelihood challenges.

Suggestion—further improving policy measures to cope with large-scale disasters: Continue to improve the national and local emergency management systems. First, improve the national and local emergency plan systems, and designate the meteorological disaster emergency plan as a national specific plan. Second, further promote the development of national and local government emergency management institutions and strengthen the comprehensive coordination and unified command capabilities of governments at all levels. Third, further improve emergency response mechanisms such as emergency response coordination and information sharing to ensure that when an emergency situation has occurred, the upper and lower levels of authorities, various departments, as well as military and local government forces can keep close communication, develop rapid actions, and join forces. Fourth, strengthen the public education and implementation of the *Law of the People's Republic of China on Emergency Response*. Local governments and departments shall formulate corresponding regulations as soon as possible.

Effectively improve the early warning capability for large-scale disasters. Weather forecasting is different from meteorological disaster forecasting and disaster early warning. Strengthen the research on early warning and forecasting technologies for extreme weather and natural disasters under the background of global climate change, thus to provide scientific support for the prevention and mitigation of disasters. Improve the ability of disaster information service provision and dissemination.

Strengthen the development of emergency response support capacities. First, we must further improve various emergency material reserves. Second, strengthen the

development of emergency response teams and equipment, establish comprehensive emergency rescue teams based on the existing fire departments, improve the emergency rescue volunteer system, and adopt advanced technologies and equipment. Third, improve transportation support, especially the overall transport coordination ability in coping with large-scale disasters. Fourth, accelerate the development of emergency response platforms, ensure smooth and speedy emergency information transmission, and support decision making and command under emergencies.

Further improve the disaster prevention ability and resilience of electric power facilities and urban public infrastructure. The state shall re-evaluate the electric power sources of urban grids with respect to source layout and planning, and add or adjust emergency power supply points. Strengthen the construction of distribution network in urban and rural areas to improve their self-protection capability in case of power failure of main regional networks and enhance the independence of local grids under emergency. Improve the design standards for disaster prevention of electric power grids and urban public infrastructure.

Enhance the overall societal disaster risk governance awareness and capability. First, strengthen the ability of leaders at all levels of government in dealing with disaster events. Second, strengthen awareness-raising and education of the society in risk governance, improve the risk awareness of the public, and effectively improve their ability in disaster prevention, self-aid, and mutual aid. Third, enhance the awareness of disaster insurance of the public and continuously improve the national large-scale disaster insurance system. The state shall provide policy support for establishing national large-scale disaster insurance funds and reinsurance arrangements.

Implement supportive policy for the post-disaster restoration and reconstruction of forestry. With careful consideration and thorough planning, post-disaster reconstruction can be turned into a great opportunity for developing a forest ecosystem and reconstructing a forestry management system in the disaster areas. Further emphasize the principles of properly selecting forest types and trees, optimize the selection of tree species, and comprehensively improve the disaster resilience of forest ecosystems. Increase the policy support for forest restoration and reconstruction and establish large-scale disaster policy insurance system for forestry.

References

- ADREM (Academy of Disaster Reduction and Emergency Management), Ministry of Civil Affairs and Ministry of Education, Beijing Normal University. 2008. Compilation of consultation material for coping with freezing rain and snow disaster in the south (internal document). April 2008 (in Chinese).
- An, Y.X., W.P. Jin, et al. 2004. The study on growth differences of different types of cotton plants attacked by hail in cotton cotyledon stage. *China Cotton* 31(10): 12–13 (in Chinese).
- CMA (China Meteorological Administration). 2008. *China meteorological disasters yearbook*. Beijing: Meteorology Press (in Chinese).

- Dong, A.X., and Q. Zhang. 2004. New development of hail research in China and main scientific problem. *Arid Meteorology* 22(3): 68–76 (in Chinese).
- EC-SCNDM (Experts Committee of the State Committee for Natural Disaster Mitigation). 2008. Integrated assessment of the freezing rain and snow disaster in southern China (internal report). May 2008 (in Chinese).
- EMEGSEO (Emergency Management Expert Group of the State Emergency Office). 2008. Investigation report on prevention and relief of low-temperature freezing rain and snow disaster (internal document). April 2008 (in Chinese).
- Feng, Y.X., and W.X. He. 2000. The temporal and spatial distribution of maize frost damages in China. *Chinese Journal of Agrometeorology* 21(3): 6–10 (in Chinese).
- Feng, Y.X., W.X. He, Z.F. Sun, et al. 1999. Climatological study on frost damage of winter wheat in China. *Acta Agronomica Sinica* 25(3): 333–340 (in Chinese).
- Feng, Y.X., W.X. He, and M.J. Rao. 2000. Relationship between frost damage and leaf temperature with winter wheat after jointing stage. *Acta Agronomica Sinica* 26(6): 707–712 (in Chinese).
- Hu, G. F., M.M. Qiu, L. Zhou, et al. 2015. Experimental study on cotton vulnerability to hail hazard: The effect of simulated hailfall on cotton damages. *J. Nat. Dis* 24, 139–148. (In Chinese)
- Li, M.S., D.L. Wang, X.L. Zhong, et al. 2005. Current situation and prospect of research on frost of winter wheat. *Journal of Natural Disasters* 14(4): 72–78 (in Chinese).
- NDRC (National Development and Reform Commission). 2008. Report on fighting with low-temperature freezing rain and snow disaster and post-disaster reconstruction (internal document). April 2008 (in Chinese).
- Shi, P.J. 2008. Establish large-scale disaster governance system. *Seeking Truth* 8: 47–49 (in Chinese).
- Shi, P.J. 2011. *Atlas of natural disaster risk of China*. Beijing: Science Press (in Chinese and English).
- Shi, P.J., D. Tang, W.H. Fang, W. Xu, W.J. Dong, and B. Chen. 2008. Seeing large-scale risk governance measures of China from coping with the low-temperature freezing rain and snow large-scale disaster in 2008. *Insurance Studies* 5: 5–12 (in Chinese).
- Shi, P.J., C. Jeager, and Q. Ye. 2012. *Integrated risk governance: Science plan and case studies of large-scale disasters*. Beijing: Beijing Normal University Publishing Group and Berlin Heidelberg: Springer.
- Wang, L., G.F. Hu, Y.J. Yue, et al. 2016. GIS-Based Risk Assessment of Hail Disasters Affecting Cotton and Its Spatiotemporal Evolution in China. *Sustainability* 8(3): 218; doi:10.3390/su8030218.
- Yue, Y.J., J. Li, G.F. Hu, et al. 2015. Equipment and methodology for experimental research of cotton vulnerability to hail hazard. *J. Catastrophol* 30, 102–107. (In Chinese)
- Zhang, Y.C., W.X. He, and S.K. Li. 1991. *Introduction to agro-meteorological disasters in China*. Beijing: China Meteorological Press (in Chinese).
- Zhao, J.T., Y.J. Yue, J. A. Wang, et al. 2015. Study on Spatio-temporal Pattern of Hail Disaster in China Mainland from 1950 to 2009. *Chin. J. Agrometeorol.* 36, 83–92. (In Chinese).
- Zhou, L., Y.J. Yue, Li, J., M.M. Qiu, et al. 2014. Review of research on vulnerability assessment of hail hazard bearing body. *Chin. J. Agrometeorol.* 35, 330–337. (In Chinese)

Blown Sand Disasters in China

Lianyou Liu, Yanli Lyu, Wei Xu, Jing'ai Wang and Peijun Shi

Abstract Blown sand disasters are caused by sand activity. It can lead to casualties of people and livestock, declining productivity of farmland and pasture, damage to buildings, roads, communication and other facilities, as well as deterioration of air quality (Gao et al. 2000). In northern China, due to the dry and windy climate and large land areas that are covered with sparse vegetation, sand activity is intense and blown sand disasters occur frequently with serious damages. Depending on the severity, sand and dust storm (SDS) weathers can be divided into floating dust, sand-blowing, and sand and dust storm types. Among these, strong and extremely strong sand and dust storms are the main types of SDS weather that causes blown sand disasters (CMA 2006). Sandstorm and dust storm have been a notable natural phenomenon in northern China historically (Zhang 1982). Due to the constantly growing human activities, the coupling effect of land desertification and climatic aridification has been strengthened and thus increases the risk of blown sand disasters. This chapter discusses sand and dust storm and blown sand disasters in northern China, including the spatiotemporal distribution characteristics of sand and dust storms, formation process of blown sand disasters and influences, blown sand disaster risk, and a case of blown sand disasters in China in 2000.

Keywords Sand and dust storm (SDS) · Blow sand hazard · Blown sand disaster exposure · Blown sand disaster risk

L. Liu · Y. Lyu · W. Xu

Key Laboratory of Environmental Change and Natural Disasters of Ministry of Education,
Beijing Normal University, Beijing 100875, China

J. Wang

School of Geography, Beijing Normal University, Beijing 100875, China

P. Shi (✉)

State Key Laboratory of Earth Surface Processes and Resource Ecology,
Beijing Normal University, Beijing 100875, China
e-mail: spj@bnu.edu.cn

1 Spatial and Temporal Patterns of Sand and Dust Storms

1.1 Spatial Distribution of Sand and Dust Storms

Northern China suffers from sand and dust storms every year. The Northwest region stands in the hinterland of the Eurasian continent, which has an arid climate, sparse vegetation cover on the land surface, loose soil, and abundant sand sources. With the breakout of cold waves in the winter and spring, strong wind and sand and dust storm weathers occur frequently. Figure 1 shows the spatial distribution of annual average frequency of sand and dust storm in northern China from 1951 to 2005 based on the observed data of weather stations and surface data produced by weighted interpolation of data from the stations. As can be seen from the map, two main areas witness frequent sand and dust storms: the Tarim Basin and vicinity in southern Xinjiang; and the Alxa Plateau, Hexi Corridor and Ordos Plateau in mid-western Inner Mongolia and their surrounding areas (Wang et al. 2003). Qaidam Basin and Sanjiangyuan region in western Qinghai as well as northeastern Inner Mongolia are also regions where sand and dust storms occur frequently.

The areas with annual average sand and dust storm frequency over 10 times were mainly sited in the arid and extreme arid regions. Ruoqiang and Minfeng in Xinjiang experienced the highest sand and dust storm frequency of more than 20 times yearly; while sand and dust storm frequency in Anxi and Minqin in Gansu, Yanchi in Ningxia, and Jurh in Inner Mongolia, among others, were around 15 times per annum. These areas formed the center of sand and dust storm occurrence. While the occurrence of sand and dust storm has close relationship with the distribution of desert and sand, exposed farmland is also the main source. These areas provide the main underlying surface condition that determines the pattern of spatial distribution of sand and dust storms in China. The spatial pattern of mean duration

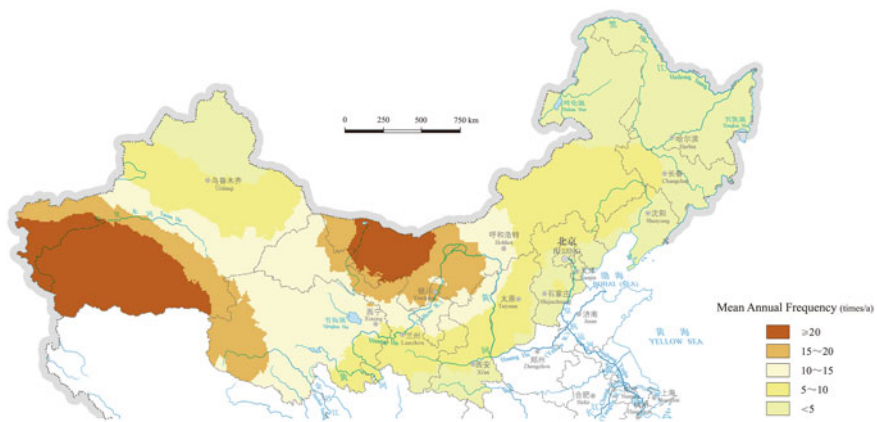


Fig. 1 Spatial distribution of annual average frequency of sand and dust storm (SDS) in northern China, 1951–2005 (Source Shi 2011, p. 80)

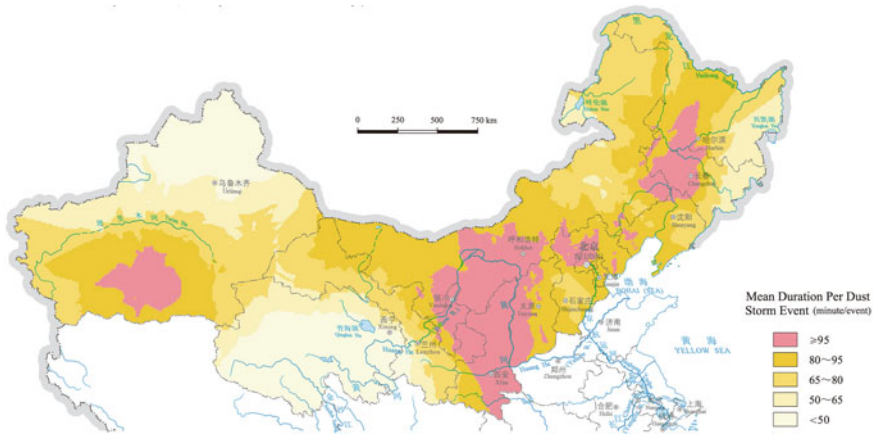


Fig. 2 Average annual duration of sand and dust storm in northern China (Source Shi 2011, p. 81)

per sand and dust storm in northern China is shown in Fig. 2. The main areas with average duration of more than 95 min per event are in Northeast China Plain, Hetao Plain, central taklamakan desert and North of North China Plain.

Overall, the spatial distribution of sand and dust storms in northern China shows the following characteristics: (1) The affected area is large—vast areas from Xinjiang in the west to coastal regions in the east are affected by sand and dust storms. Thirteen provinces in northern China are influenced to various degrees; even the Yangtze River Basin may be affected. (2) The sand and dust storm prone areas are centered on mainly two areas—the Tarim Basin and the Alxa Plateau. (3) The source areas have a close relationship with desertification and human activities. Large tract of desert, sandy area, and farmland surfaces provide extremely rich sand and dust materials for the formation and development of sand and dust storms.

Using sand and dust storm data of weather stations, the spatial distribution of sand and dust storms in every decade from 1954 was analyzed. Data from 1954–1959 were used for statistics of the 1950s. Spatial interpolation was used to generate the spatial distribution of annual average sand and dust storm days of 13 provinces in northern China for every decade since the 1950s.

In the past six decades, the frequency of sand and dust storms in northern China showed a declining trend generally with decreasing spatial scopes of hazard occurrence. The Three North Shelterbelt Development Program beginning in 1978 and the Project for Blown Sand Source Area Control around Beijing and Tianjin implemented in 2000, as well as the Grain for Green Project and the Return Pasture to Grassland Project contributed to the increased coverage of forest and grassland year by year, and may have played some role in controlling sand and dust storms. In the 1950s, the annual average frequency of sand and dust storms in northern China was close to 10 days with the prone areas distributed in the Tarim Basin and

surrounding areas, Hexi Corridor, eastern Qinghai, Alxa Plateau, Ordos Plateau, and eastern Inner Mongolia. In the 1960s, the annual average frequency of sand and dust storms in northern China was 8 days and the spatial scope of the affected areas reduced significantly, mainly distributed in the Tarim Basin and surrounding areas, Alxa Plateau, and Ordos Plateau, and sparsely distributed in western Qinghai and eastern Inner Mongolia. In the 1970s, the frequency of sand and dust storms in northern China was again 8 days, wherein sand and dust storms in Ordos Plateau witnessed a decrease while western Qinghai experienced an increase in frequency. In the 1980s, the sand and dust storm frequency in northern China was 7 days, with no clear change in the center of affected areas but continuous decline in spatial scope. In the 1990s, sand and dust storm frequency in most high frequency areas reduced to about 5 days, with the affected areas mainly in the Tarim Basin, western Qinghai, areas near the Qinghai Lake, Alxa Plateau, among others. During the first decade of this century, areas where annual average sand and dust storms exceeded 20 days appeared only in the Tarim Basin, while the average sand and dust storm frequency in northern China reduced to about 4 days.

1.2 Temporal Distribution of Sand and Dust Storms

Based on sand and dust storm records of 150 weather stations in northern China during 1954–2010, statistics of year-to-year changes of sand and dust storm days are generated and shown in Fig. 3.

In the past six decades, annual sand and dust storm days in northern China have shown a general decreasing trend with some fluctuations (Qian et al. 2002; Zhou 2001). In the 1950s, sand and dust storm occurrence was most frequency, with an annual average of almost 10 days; in the 1960s, it decreased in the early years, increased in the middle of the decade, and then decreased again; in the 1970s, it first increased then began to decrease in later years; in the 1980s, the decrease was obvious; since the later years of the 1990s, especially after 1997, sand and dust storm

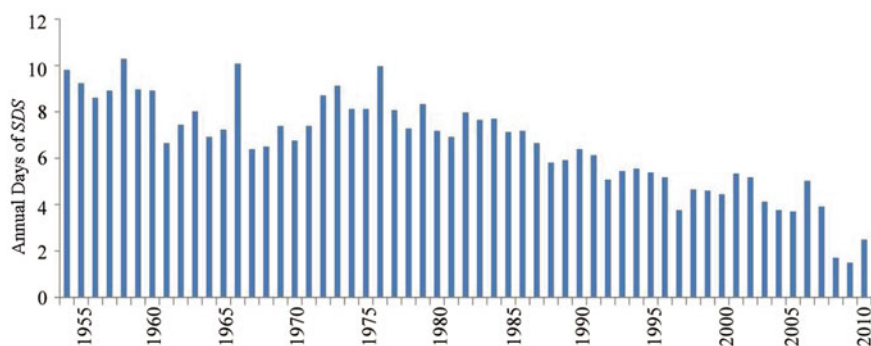


Fig. 3 Annual days of sand and dust storms (SDS) in northern China, 1954–2010

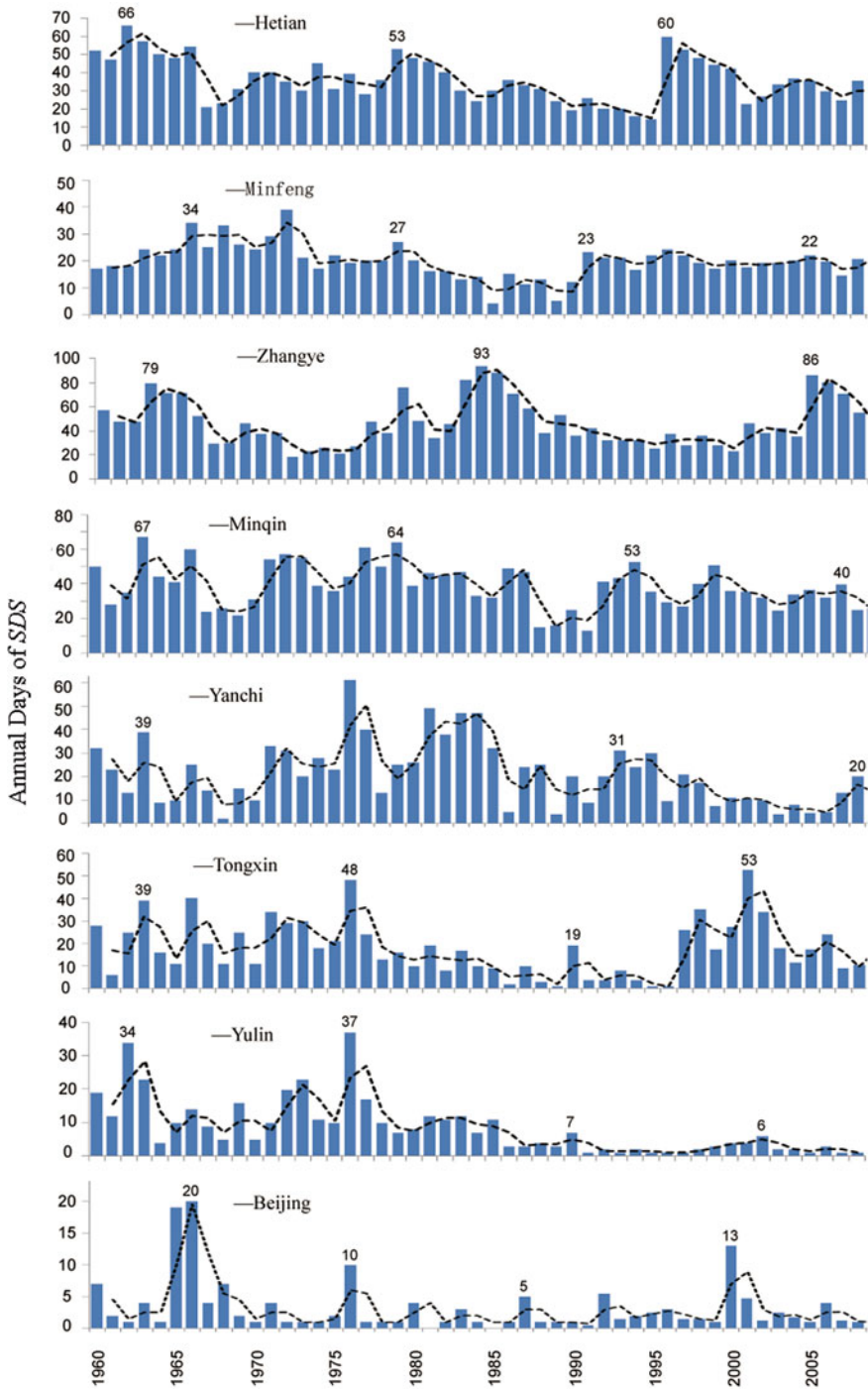


Fig. 4 Number of sand and dust storm (SDS) days at typical weather stations of northern China, 1960–2009

occurrence increased again; after 2000, it clearly decreased for three consecutive years and increased again in 2006, but not exceeding the long-term annual average value.

Sand and dust storm frequency in northern China have shown an overall decreasing trend (Fig. 4); however, there has been clear regional differences due to the variations in regional climatic conditions. Hetian, Minfeng, Minqin, Zhangye, Yanchi, Tongxin, Yulin, and Beijing from West to East were selected to represent extreme arid, arid, semiarid, and semi-humid regions, respectively, and sand and dust storm frequency at these stations are shown in Fig. 4. By analyzing changes of annual sand and dust storm days at these stations, it can be seen that in 1960–2009, sand and dust storm frequency reduced significantly as aridity decreased across the region and the fluctuation period shortened as well.

Hetian and Minfeng are located in the extreme arid region with almost 40 sand and dust storm days annually and a 23-year fluctuation cycle, on average; Minqin and Zhangye belong to the arid region and their average sand and dust storm days and cycle of fluctuation were around 30 days and 19 years, respectively; Yanchi, Tongxin, and Yulin lie in the semiarid region, with an average sand and dust storm days and cycle of fluctuation of around 15 days and 15 years; Beijing lies in the semi-humid region, and the average sand and dust storm days and cycle of fluctuation were around 5 days and 10 years. The number of sand and dust storm days in extreme arid and arid regions are relatively stable over the years while in semiarid and semi-humid regions this number was considerably lower.

2 Formation and Assessment of Sand and Dust Storms

2.1 Formation Process of Blown Sand Hazard

The relationship between climate and sand and dust storms: A correlation analysis was conducted to examine the relationships between the number of sand and dust storm days and rainfall, temperature, and wind speed and the resulting correlation matrix is shown in Table 1. The variables include sand and dust storm days in the spring and in the whole year; spring rainfall in the current year, summer, autumn, and winter rainfall in the previous year; spring temperature in the current year, summer, autumn, and winter temperature in the previous year; average wind speed in the spring and the whole year.

It can be seen from Table 1 that the number of sand and dust storm days are negatively correlated with rainfall and positively correlated with temperature and wind speed.

(1) Spring and yearly sand and dust storm days have a clear negative correlation with precipitation in the current spring and previous summer and autumn but weaker correlation with rainfall of previous winter. Sand and dust storm days decrease as rainfall increases and increase as aridity increases. The amount of precipitation in previous autumn and the current spring impose the strongest influence on sand and dust storm occurrences (Prospero and Lamb 2003).

Table 1 Result of correlation analysis between dust storm (SDS) days and climatic variables (r)

Rainfall (mm)	Spring SDS (day)	Yearly SDS (day)	Temperature (°C)	Spring SDS (day)	Yearly SDS (day)	Wind speed (m/s)	Spring SDS (day)	Yearly SDS (day)
The spring	-0.097	-0.127	The spring	0.653	0.699	Average in spring	0.717	0.644
Last summer	-0.017	-0.004	Last summer	0.179	0.188	Annual mean	0.497	0.626
Last autumn	-0.124	-0.180	Last autumn	0.232	0.179			
Last winter	-0.001	-0.002	Last winter	0.356	0.247			

Data source China Meteorological Administration

(2) Spring and yearly sand and dust storm days have a clear positive correlation with temperature of the current spring and previous summer, autumn, and winter, with highest correlation with temperature of the current spring. This indicates that the increase in temperature of the current spring is an important meteorological condition that affects the occurrence of sand and dust storms. The impact of temperature on land surface in the spring is mainly embodied in evapotranspiration of moisture that leads to instability of local heat flux as well as generates updraft, which is the power factor that forms much strong wind in the spring and leads to large scale sand and dust storms in the northern areas of China.

The relationship between land surface and sand and dust storms: Underlying land surface conditions (vegetation coverage, roughness, soil structure and humidity, and so on) poses important impact on sand entrainment and dust emission. Because sand and dust storms result from the interaction between strong wind and underlying land surface, the relationship between strong wind days and sand and dust storm days of different underlying surfaces can reflect regional susceptibility to sand and dust storms (Song et al. 2005).

Considering the natural environment and land use, there are mainly nine types of underlying land surfaces in northern China: forest (8.3 %), farmland (18.6 %), grassland (20.7 %), desert and sand (19.2 %), gobi (18.3 %), salt playa (3.4 %), glacier (8.5 %), lakes (2.1 %), and other (0.9 %). Farmland, grassland, desert and sand, gobi, and salt playa are the potential source areas of sand and dust storms. These five land surface types cover 80.2 % of the total arid and semiarid areas in China. Forests with high vegetation cover, glaciers covered by snow and ice, and lake water are not considered as potential dust source areas.

Farmlands are mainly distributed in plain areas, with rainfed farmland mainly in the East and irrigated farmland in the west. Grasslands are distributed in the northeast region, Inner Mongolia, and mountains of the desert area in the northwest. Deserts are distributed both in the semiarid areas in the East and arid areas in the west. Annual rainfall is less than 200 mm in the West arid desert areas, where vast mobile sand dunes are found, and between 200–450 mm in the East semiarid regions, where semi-fixed and fixed dunes dominate. Gravel Gobi are distributed

widely in piedmont pluvial fans and diluvial plains northwest of the Ondor Temple-Bailingmiao Temple-Etuoke Banner-Yanchi line. Salt playas mainly exist in the Qaidam Basin in Qinghai and near the terminal lakes of inland rivers, for example, Lop Nor at the downstream of the Tarim River and Juyanhai at the downstream of the Heihe River.

Figure 5 shows annual change of strong wind days and sand and dust storm days in various underlying surface type areas, with data from three representative weather stations in each area. Between 1961 and 2000, average annual strong wind

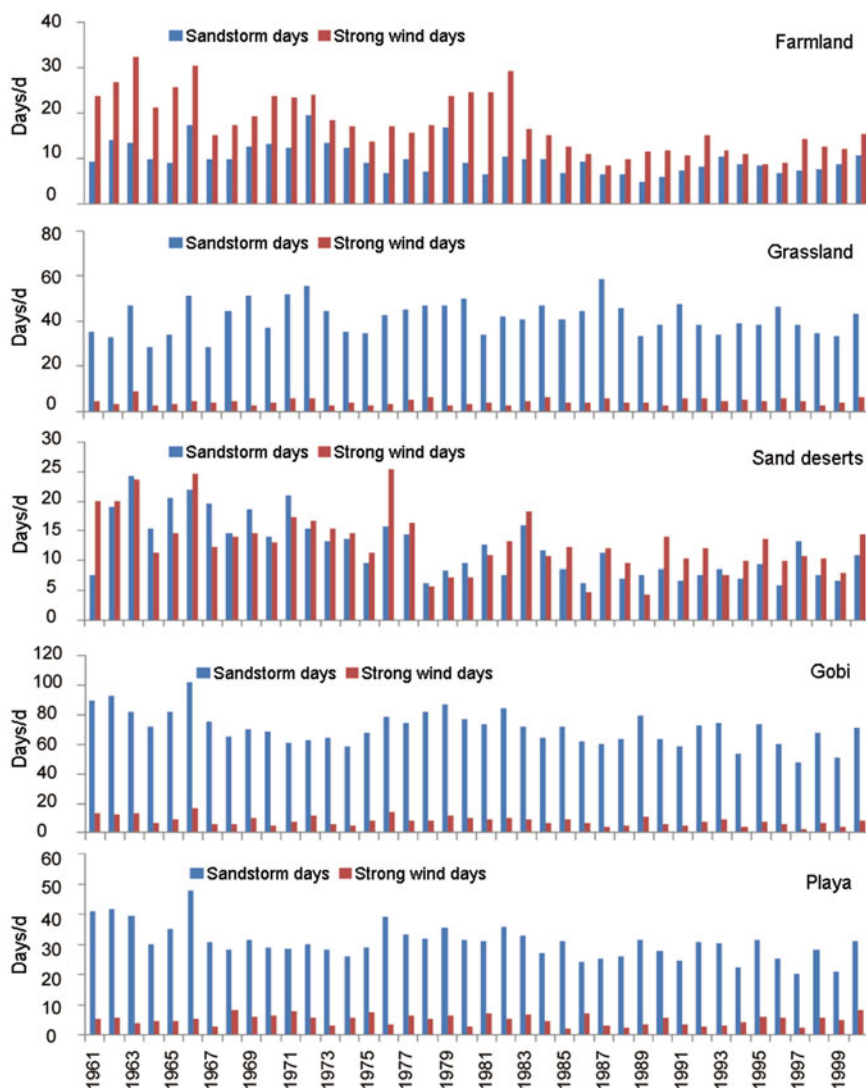


Fig. 5 Strong wind days and sand and dust storm days for five land surface types, 1961–2000

days of the grassland, gobi, and salt playa areas were 41, 71, and 56 days, respectively, while in farmland and desert areas these were 10 and 12 days. Annual average sand and dust storm frequency of farmland and desert areas was 18 and 13 days while in the grassland, gobi, and salt playa areas this was 5, 8, and 5 days. Sand and dust storm days in the grassland, gobi, and salt playa areas were considerably fewer than the strong wind days. These areas can be classified as underlying surface types with high wind energy and low breakout of sand and dust storms. Sand and dust storm days of farmland and desert areas were close to or even more than strong wind days. These areas can be classified as underlying surface types with low wind energy and high breakout of sand and dust storms.

2.2 *The Impact of Sand and Dust Storms*

Impact on agriculture and animal husbandry: Wind erosion of soil is the main manifestation of agricultural blown sand disaster, which can cause the loss of organic matter and fine particulate matter in soil and lead to coarsening of surface soil, and reducing soil fertility. On the other hand, sand dunes encroaching into farmland can cause desertification of farmland soil and sand burial of farmland in large areas. More than 30 km² of oases in the northern part of Linze County in Hexi Corridor has being buried by sand due to invasion of sand dunes (Fig. 6).

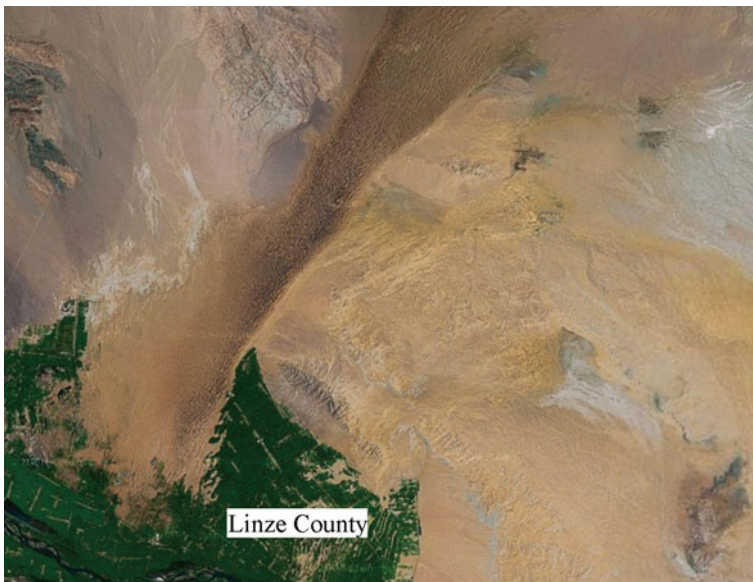


Fig. 6 Sand dune encroaching into oases of Linze in Hexi Corridor, Gansu Province, China (Source Image from Google Earth)

Table 2 Estimates of Soil fertility loss at different stages of desertification in Naiman Banner, Inner Mongolia

Degree of desertification	Vegetation coverage (%)	Organic matter (%)	Total nitrogen (%)	Total phosphorus (%)
Potential desertification	>40	0.5–1.0	0.02–0.07	0.02–0.06
Mild desertification	26–40	0.2–0.5	0.01–0.06	0.01–0.04
Moderate desertification	16–25	0.1–0.3	0.009–0.02	0.01–0.03
Severe desertification	6–15	0.06–0.2	0.005–0.013	0.01–0.02
Extremely severe desertification	0–15	0.04–0.08	0.002–0.014	0.008–0.015

Source Zhu and Chen (1994)

According to field investigations, the depth of farmland soil eroded by a single strong sand and dust storm could reach 10 cm (Huang and Niu 1998). The content of organic matter, total nitrogen, and total phosphorus decreases as desertification progresses (Zhu and Chen 1994) (Table 2).

Dong (2002) estimated that in China the annual loss of soil organic matter, nitrogen, and phosphorus element due to wind erosion is about 559,000,000 t, equivalent to 268,000,000 t fertilizer, with a value of nearly RMB 17 billion Yuan (Table 3).

Wind and blown sand activity is strong in the spring. Once young seedlings suffer from abrasion and cutting by blown sand, they will wither and die, leading to loss of harvest (Fig. 7). Wind erosion and desertification may intensify grassland degradation and reduce yield of forage. Sand and dust sticking to stem and leaves of grass can lead to the increase of livestock mortality.

Impact on traffic and communication: About 1,500 km railways, 30,000 km highways, and 50,000 km irrigation ditches are affected by blown sand in northern China. Blown sand disasters mainly occur in moving sand areas with strong wind. Strong wind can cause not only the corrosion of subgrade, but also damage to infrastructure such as electric power and communication lines. Strong wind can even overturn trains and lead to severe accidents. The Hundred-mile Windy Area and the Thirty-mile Wind Gap of the Lanzhou–Xinjiang Railway and the South Xinjiang Railway are the famous hazard zones. On 28 February 2007, a passenger train was caught in a strong sand and dust storm in Turpan of Xinjiang in northwest China, where the momentary wind speed reached 45.1 m/s (Level 14). A total of 11 carriages were overturned by fierce wind, four people died on the spot and more than 30 people were injured (Fig. 8). Sand and dust storm can reduce visibility by a large margin, which leads to traffic accidents. For example, the sand and dust storm occurred in Gansu on 5 May 1993 turned daytime into complete dark, caused total stop of operation of the Hexi Highway and suspension of the Lanzhou–Xinjiang Railway for 31 h. The sand and dust storm on April 5 1998 led to forced closing of seven airports and canceling of about 70 flights.

Table 3 Soil fertility loss from desertification in China

Type of desertification	Area (10,000 km ²)	Fertility loss (10,000 t)					
		Organic matter	Barnyard manure	Nitrogen element	Urea	Phosphorus element	Superphosphate
Potential	15.8	2948.28	14711.92	255.1	553.37	205.87	1029.35
Developing	8.10	788.86	3936.41	45.68	99.13	163.86	819.3
Strongly developing	3.48	753.35	3759.22	58.76	127.51	362.62	1813.1
Total	27.38	4490.49	22407.55	367.84	780.01	732.35	3661.75

Source Dong (2002)



Fig. 7 Abrasion and cutting of young seedlings of crops and grass by blown sand (Photos at upper and lower right, courtesy of E. Skidmore) (Photograph by Lianyou Liu)



Fig. 8 Impact of wind and blown sand on traffic and communication (Photo at right, courtesy of Shadati) (Photograph by Lianyou Liu)

Impact on atmospheric environment: Sand and dust storm is one of the main factors affecting air quality in China. According to an analysis of total suspended particulate (TSP) nationwide during 1981–2007, annual average concentration of 93 cities was $402 \mu\text{g m}^{-3}$, with the maximum value of $628 \mu\text{g m}^{-3}$ in Lanzhou and minimum value of $82 \mu\text{g m}^{-3}$ in Haikou (Zhang et al. 2010). Annual average concentration showed a clear decreasing trend from North to South and from inland to coastal areas. Annual average concentration of 11 northern coastal cities was $463 \mu\text{g m}^{-3}$, 38 northern inland cities was $497 \mu\text{g m}^{-3}$, 15 southern coastal cities was $235 \mu\text{g m}^{-3}$, and 29 southern inland cities was $309 \mu\text{g m}^{-3}$ (Zhang et al.

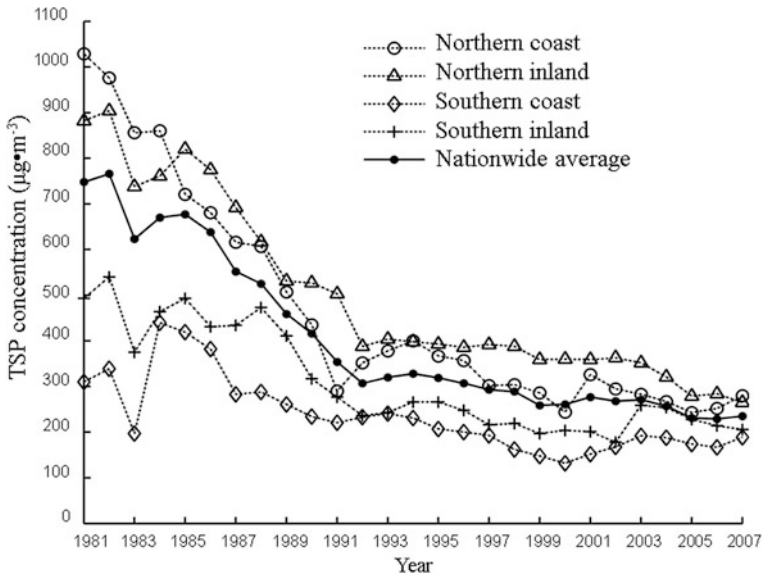


Fig. 9 Nationwide annual average TSP concentration, 1981–2007 (Source Zhang et al. 2010)

2010). Sand and dust storm-induced air pollution is an adverse factor for human health.

Annual average TSP concentration of major cities in the whole country decreased from 1981 to 2007, which showed the same trend as the decreasing sand and dust storm frequency in the North (Fig. 9).

The correlation coefficient R^2 between sand and dust storm frequency and TSP concentration is 0.97. Annual dustfall ($t\ km^{-2}\ a^{-1}$) in the major cities of China is positively correlated to sand and dust storm frequency, as well as the TSP concentration, and the correlation coefficient R^2 is 0.94 and 0.92, respectively. Therefore, sand and dust storm are the main factor influencing the spatiotemporal distribution of TSP content and dustfall in China (Fig. 10).

Impact on lakes and reservoirs: Lake area in sandy areas of northern China is nearly $2 \times 10^4\ km^2$, which accounts for about 25 % of the total lake area and 30 % of water storage nationwide (Wang and Dou 1998). Lakes and reservoirs in sandy areas are extremely important for maintaining agricultural and industrial production, people's living, and ecological security in an arid environment. These surface water bodies also face the threat of blown sand disaster. For example, the blown sand intruding into the Qinghai Lake is $8.87 \times 10^6\ t/a$ and the isolated gulfs formed by sand reduce the lake surface area (Zhao et al. 1993). Drift sand flowing into the Longyangxia Reservoir from upwind is $1.23\text{--}2.84 \times 10^7\ m^3$ per year, which reduces the volume of water in the reservoir and hydroelectric generation (Dong et al. 1993) (Fig. 11).

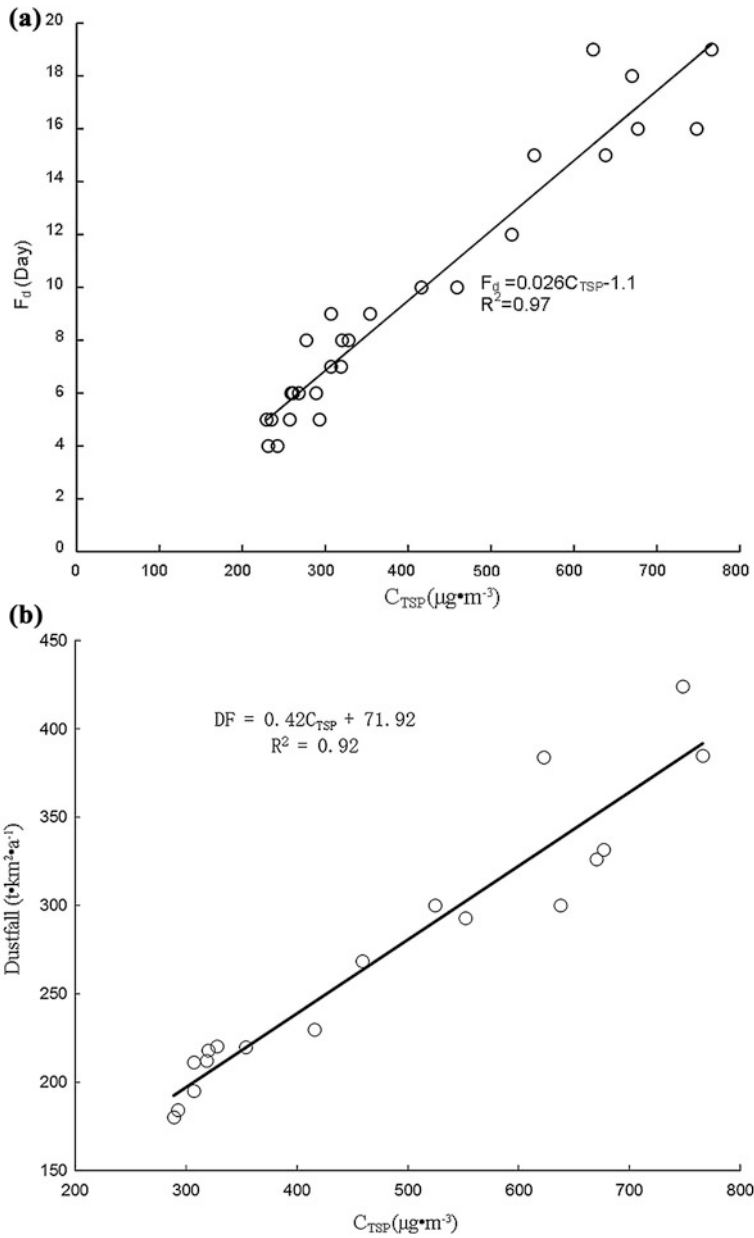


Fig. 10 Relationships of annual average TSP concentration (C_{TSP}) with **a** annual average sand and dust storm frequency (F_d), and with **b** dustfall in major cities of China (Source MEPC 1981–2007)

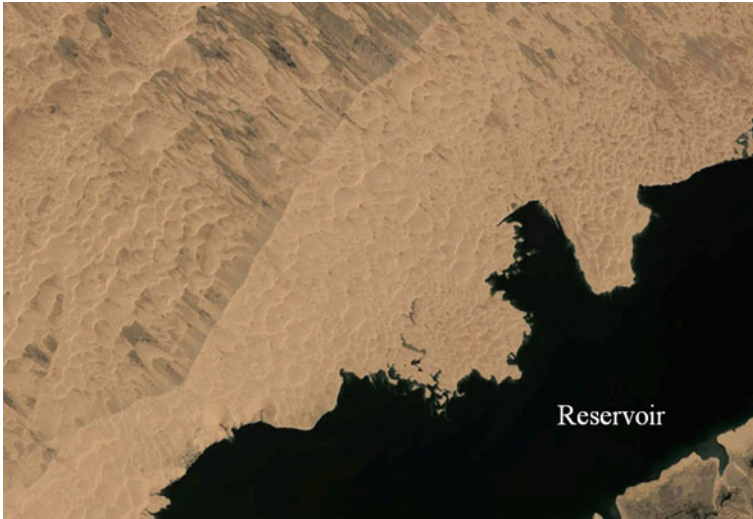


Fig. 11 Migrating dunes intruding into the Longyangxia Reservoir in the Gonghe Basin of Qinghai Province (Source Image from Google Earth)

2.3 Sand and Dust Storm Disaster Risk

Trend analysis of sand and dust storm days: Based on the records of sand and dust storm days, it can be established that in most stations the number of sand and dust storm days exhibited periodical fluctuation over the recent 50 years in China. According to the return period of peak years of sand and dust storm days, 58 stations in northern China that have relatively complete records of sand and dust storm days were selected to establish an empirical equation for estimating annual average occurrence days of sand and dust storm in the coming 10 years. The equation is established as follows:

$$SS_t = \frac{SS_{t-1} + SS_{t-2}}{2} \quad (1)$$

where, SS_t is the sand and dust storm days of the estimated year t , SS_{t-1} and SS_{t-2} is the values of the previous cycle and before the previous cycle, respectively.

Based on this formula, the predicted value of sand and dust storm days at each station was calculated (Fig. 12). The spatial distribution map of annual average sand and dust storm days in northern China from 2011 to 2020 was compiled using the reverse distance weighted interpolation method.

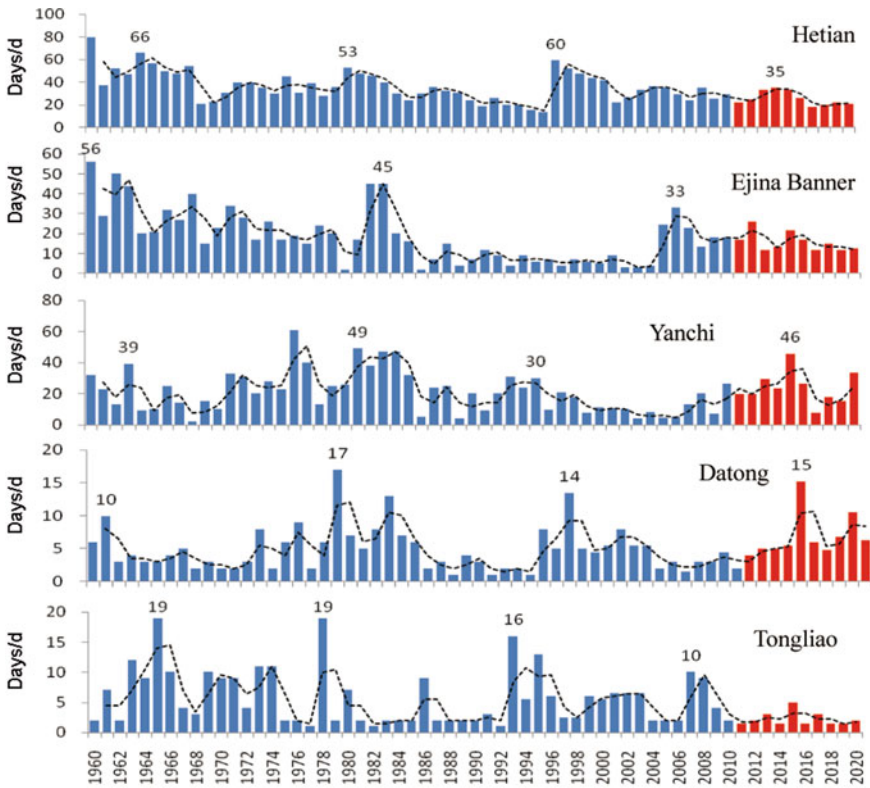


Fig. 12 Predicted values of sand and dust storm days at typical stations, 2011–2020

2.3.1 Hazard Intensity

Figure 13 presented the intensity of blown sand hazard in northern China by return periods of 10 years, 20 years, and 30 years. It can be seen that the main areas with long average duration of blown sand are in South Heilong–North Liaoning, North Shannxi–western Shanxi, northern-Gansu, and mid-southern Xiinjiang. These areas with long average duration spread with the return period increase. This result is useful to understand the future spatiotemporal characteristics of sand and dust storms in northern China.

Risk estimation of blown sand disasters: Risk of sand and dust storms that affect regional population and cultivated land is assessed based on the estimated annual average sand and dust storm days in the coming 10 years, the cultivated land area, and population density for 13 provinces of northern China at the county level. The 2002 population and 2002 cultivated land area data were used in the analysis. Risk index maps are created using the spatial analysis module of GIS. The calculation method is as follows:

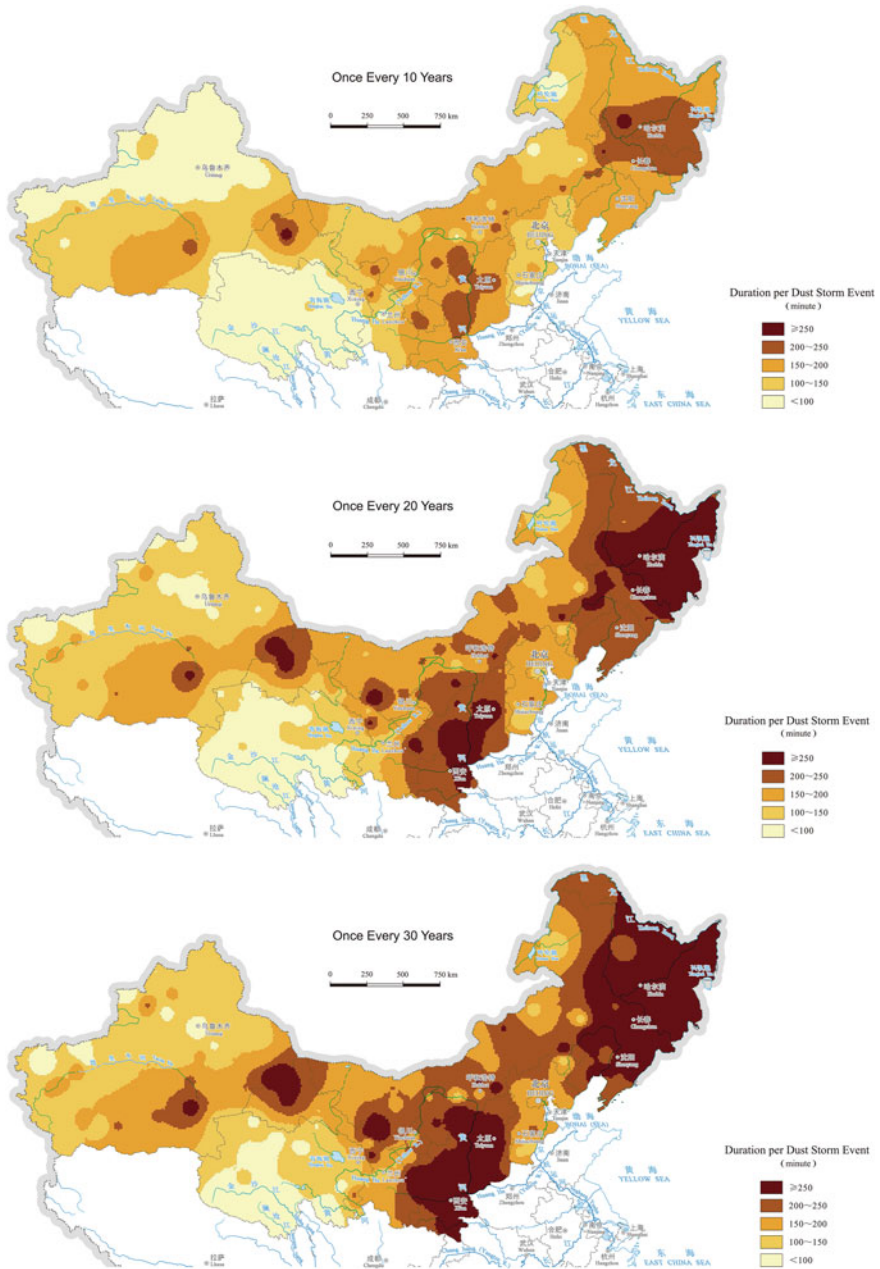


Fig. 13 Intensity of blown sand hazard in northern China (Source Shi 2011, p. 82)

$$R_f = a \times c \tag{2}$$

$$R_p = a \times b \tag{3}$$

$$R_{ss} = mR_f \times nR_p \tag{4}$$

where, R_f is the risk level of farmland of sand and dust storm disaster, R_p is the risk level of population of sand and dust storm disaster, R_{ss} is the integrated risk level of sand and dust storm disaster, a is the average annual number of sand and dust storm, c is the normalized regional cultivation index of farmland, b is the normalized regional population density; m and n are parameters obtained by AHP.

Based on the above equations, blown sand disaster risk map of farmland and population in northern China is obtained (Figs. 14 and 15). Blown sand disaster risk of farmland is affected by annual average sand and dust storm days and distribution of farmland. Areas of highest blown sand disaster risk of cultivated land mainly distribute in the surrounding areas of the Tarim Basin, Hexi Corridor, and the transitional zone between the farming and pastoral areas. Blown sand disaster risk of population is higher in the East, due to the high population density of the eastern area of northern China. The spatial pattern of integrated blown sand disaster risk in northern China is very similar to the one of farmland (Fig. 16).

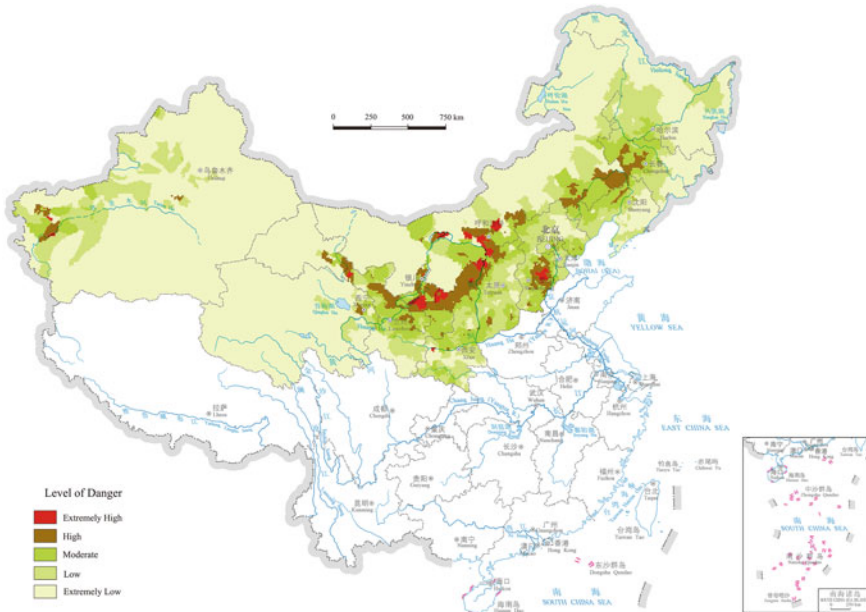


Fig. 14 Blown sand disaster risk of farmland in northern China (Source Shi 2011, p. 83)

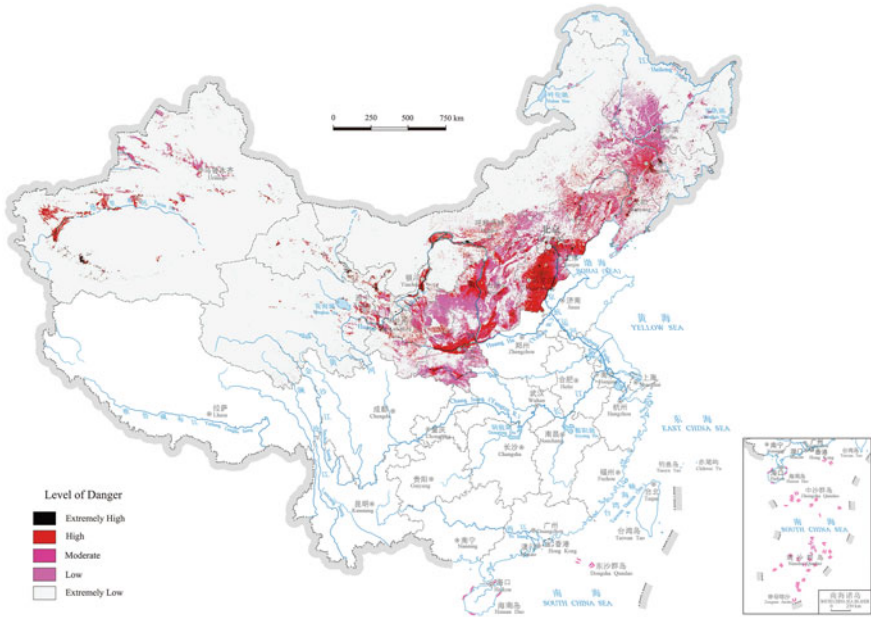


Fig. 15 Blown sand disaster risk of population in northern China (Source Shi 2011, p. 83)

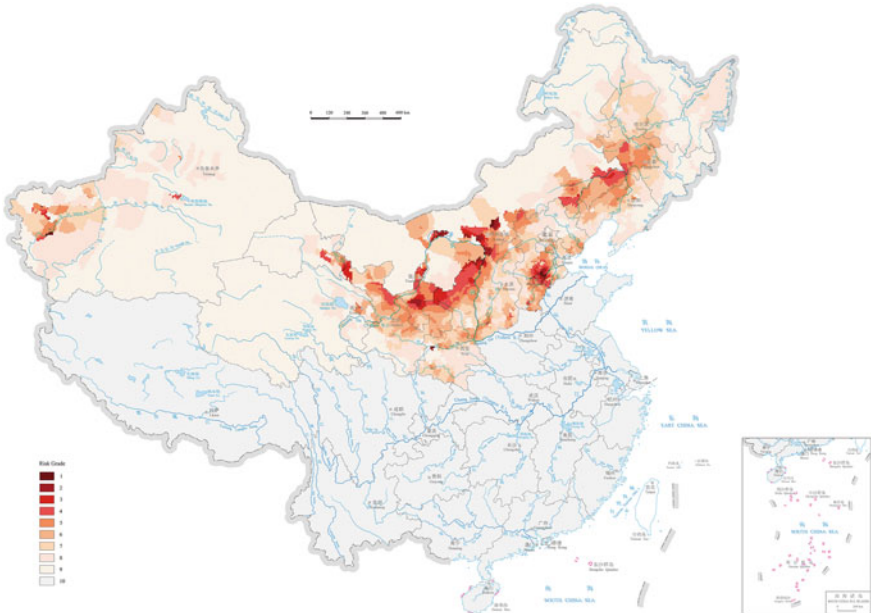


Fig. 16 Integrated blown sand disaster risk grade in northern China (Source Shi 2011, p. 84–85)

3 The Blown Sand Disasters in Northern China in 2000

In the past decades, frequent sand and dust storms have caused great losses in economy, agricultural production, and life in the affected areas. Shi et al. (2000b) collected 10 typical sand and dust storm cases in China from 1949 to 1998, and analyzed their affected areas and losses (Table 4). The sand and dust storms in 2000, however, received much broader public attention compared to the other cases.

3.1 Blown Sand Disasters of 2000

From March to June 2000, 13 sand and dust storm events occurred successively in northern China. The bad weathers were rare in the past century and featured by early occurrence in the year, high frequency, wide impact, and extensive damages and exerted heavy impacts on the economic and social development, transportation, atmospheric environment, as well as the life, property, and health of people in the affected areas, especially in Beijing and its surrounding area. Thus these events attracted unprecedented attention of the government, academics, and the public. Based on reports released by some provincial-level newspapers and journals, Wang and colleagues (2001) established the spatiotemporal patterns of these blown sand disasters and conducted a systematic assessment on the risk of blown sand disasters.

The 13 blown sand disasters occurred in 2000 struck 18 provinces, autonomous regions, and municipalities and 1,061 banners and counties with a total affected area of 3.259 million km² (Table 5). Among these, the sand and dust storm during April 5–7 affected the largest area (2 million km²), struck 16 provinces, autonomous regions, and municipalities and 892 counties and banners. Ye et al. (2000) estimated that the affected area by eight sand and dust storms was about 2 million km².

In 2000, the first blown sand disaster occurred in the beginning of March, 15–20 days earlier than usual. There were six sand and dust storms in April, once per 5 days on average, which was 1–2 days shorter than an average year. Meanwhile, the average duration of these sand and dust storms was 3 days, with a maximum of 5 days, which was also rare in the history of this region. The affected area of farmland reached about 416,000 km² and the affected population was 560 million, accounting for 43 % of the total population of the country. The affected area and spatial extent varied between these sand and dust storms (Wang et al. 2001) (Fig. 17).

Table 4 Typical sand and dust storm cases in China, 1949–1998

Time	Spatial scope	Sand and dust storm disaster situation
1949	Hami in Xinjiang	At 8:00 a.m. on March 18, a sudden change of weather occurred in Hami City, with fierce wind and heavy sandstorm, the sky turned dark in the storm. The storm died out by midnight, and three people were killed
1952	23 counties in Hexi of Gansu Province	On April 9, severe sand and dust storm occurred in 23 counties, including Jiuquan, Dunhuang, Linze, Zhangye, Shandan, Yongchang, Wuwei, and Huan County. More than 400 ha farmland was buried by sand in Yongchang County. According to the records of the Zhangye Meteorological Station, the storm occurred at 15:00 p.m. in April 9 and lasted until the morning of April 10. At the peak of the storm, the visibility level dropped to grade 0 and wind strength reached grade 9
1961	Turpan in Xinjiang	From May 31 to June 1, a strong wind with grade 12 strength occurred. Many portions of the Lanzhou–Xinjiang Railway in the Turpan Basin were buried by sand, resulting in a severe derailing accident of the No. 91 train. More than 10 carriages were derailed, among which one was thrown in the air and crushed; several hundred electric power utility poles were broken; traffic were shut down for 36 h; more than 40 Karezes were buried in Xiamaya and other places; and more than 20 people died or were injured
1979	Central Xinjiang	Wind strength was more than grade 12 at the Hami to Urumchi section of the Lanzhou–Xinjiang Railway on April 10. The railway line was shut down for nearly 38 h. South Xinjiang Railway was shut down for 167 h. In addition, 21 thousand m ² houses were damaged, 7,800 m ² door and window glass were broken, 3 elementary school students were killed. Materials worth of RMB 16.984 million Yuan in an army warehouse were damaged, and 2 soldiers were killed. From April 10 to 11, the grade 12 severe wind lasted for 8 h, and 30 thousand ha crops were damaged, 5,758 trees were broken,

(continued)

Table 4 (continued)

Time	Spatial scope	Sand and dust storm disaster situation
		108 Karezes and 402 large and small sized canals were buried by sand, 62.5 t wheat straw and 2.5 t fertilizer were lost, 16 houses collapsed, 26 houses were on fire, 10 people were killed, and 40 people were injured. In addition, communication was shut down. The total loss was RMB 1.439 million Yuan
1983	Turpan, Toksun, Yuepuhu, Yengisar, Karashahr etc. in Xinjiang	According to incomplete statistics, due to a grade 8 severe wind from April 25 to 28, more than 24 thousand ha crops were lost, 51 thousand trees were damaged, 9.2 km canal was filled by sand, 843 livestock were killed, 242 houses collapsed or were burned down by fire, and four people were killed. On April 26, more than 4,800 ha crops in the Turpan region were affected, 1,400 ha grape plants were damaged, and nearly 10 thousand trees and several hundred utility poles for power supply and communication were broken. In addition, 90 karezes were filled by sand, 108 houses collapsed and nine were on fire, 18 families were affected by the disaster, seven people were killed, and 155 livestock died. Railway transport facilities encountered damage of different degrees and more than 600 pieces of glass in doors and windows of the No. 69 passenger train and stations were crushed
1983	Central and western Inner Mongolia; Yulin in Shaanxi Province	From April 27 to 29, in the affected area the observed wind strength was grade 8 to grade 9 and maximum instantaneous wind speed was 38 m/s, which is rare for the area. During this period, sand and dust storm weather occurred in Yijinhuole League and visibility dropped to below 200 m. According to incomplete statistics, during this disaster, 33 people were killed and 46 were injured, 98 thousand livestock died, part of the pasture and animal pens were covered with sand, 78 wells in Otog Banner were buried by drift sand and 15 animal pens collapsed. In Yulin Prefecture, 25 people were killed and 62 thousand livestock were died or missing

(continued)

Table 4 (continued)

Time	Spatial scope	Sand and dust storm disaster situation
1986	Anxi and Dunhuang in Gansu Province	A sand and dust storm occurred in 17 h from May 18 to 20 and visibility dropped to grade 0. According to the local meteorological station, in terms of visibility and duration of sand and dust storm, this was the worst case ever since the record started in 1938. During this disaster, 14.9 thousand ha crops were affected, 2,020 ha of which were destroyed and 1,200 ha were heavily damaged. Also, 140 ha vegetables were completely damaged, 235 t fruits fell down, 16.4 thousand grafts of fruit plants were damaged, and 25 thousand trees were broken. Additionally, 14 large stock and 659 sheep were died or missing, two small dams were flooded, 29.4 km canal was buried by sand, and 24.5 km electrical wire were destroyed. This disaster also caused three fires, and 57 houses, 105 animal pens, and fence of 384 m collapsed, more than 1,800 t coal and 1.5 t mirabilite were blown away. The total loss was more than RMB 12 million Yuan
1986	Hetian region in Xinjiang	From May 18 to 19 of May, a severe sand and dust storm occurred, which caused 25 thousand tons output reduction of wheat, 120 to 150 thousand dan output reduction of cotton. Also, local corns, fruit trees, grapes, melons, and vegetables were heavily affected by this disaster. During this sand and dust storm, 10 people were killed, 9 were missing, 4,128 livestock were missing or died, 218 houses and 125 animal pens collapsed, and 736 utility poles were blown down. The direct losses were more than RMB 50 million Yuan
1993	Turpan and Hami in Xinjiang; Hexi region in Gansu Province; Zhongwei in Ningxia; western Inner Mongolia	From 14:00 to 19:00 on May 5, a black storm resulted in 85 deaths and 264 people were injured. Also, 10–30 cm top layer soil was blown away and 373 thousand ha crops were affected by this storm. During this disaster, 120 thousand livestock died, more than 1000 km canals were buried by sand, 6,012 utility poles were blown down. The Lanzhou–Xinjiang Railway

(continued)

Table 4 (continued)

Time	Spatial scope	Sand and dust storm disaster situation
		was shut down for 37 h, 4,412 houses were destroyed, and dustfall content was up to 161–256 t per km ² . The direct losses were RMB 560 million Yuan
1998	12 districts and prefectures in the northwest	From April 17 to 19, this sand and dust storm damaged 30.7 thousand ha crops, 110.9 thousand livestock died, and 1.56 million people were affected. The direct losses were RMB 800 million Yuan

Source Shi et al. (2000b)

3.2 Impact of the Blown Sand Disasters in 2000

Affected regions: 18 provinces, autonomous regions, and municipalities were affected by the sand and dust storms in 2000 (Table 6). The disaster frequency in Inner Mongolia was the highest, up to 13 times, followed by Ningxia, Shanxi, Gansu, Shaanxi, Hebei (10–12 times). Beijing and Tianjin were hit eight times. The disaster impact was severe.

Coverage area index of hazards, I_{ca} , is defined as the total area affected by all hazard events divided by total land area in a region. In Ningxia, I_{ca} was the highest, up to 9.18, which means the total affected area by the 11 blown sand disasters was 9.18 times of its regional land area. In Beijing, Tianjin, Hebei, Shanxi, and Inner Mongolia, I_{ca} was 6–8; in Gansu, Shaanxi, Liaoning, Henan, Shandong, Jiangsu, Anhui, Shanghai, I_{ca} was 2–5. Compared with other disasters, the I_{ca} of blown sand disasters in 2000 was tens of hundreds of times higher than that of other disasters.

Regional differentiation in blown sand hazard frequency: Z_C represents the number of blown sand hazards occurred in a certain period. Figure 18 shows the regional distribution of blown sand hazard frequency in 2000 by county unit. There were 29 counties that experienced more than 12 extreme blown sand hazard events, 44 counties witnessed 10–11 events, 8–9 events occurred in 63 counties, 6–7 events occurred in 250 counties, 4–5 events occurred in 355 counties, and 1–3 events occurred in 317 counties. The regional differentiation of blown sand hazard frequency in 2000 has four characteristics: (1) The high value center of disaster frequency was located in Alxa and Xilin Gol Leagues, mid-western Inner Mongolia, which experienced more than 10 sand and dust storm events. This spatial distribution pattern is largely consistent with the high frequency sand and dust storm areas identified by Xu and Hu (1996), but the area was more to the East. (2) The frequency of sand and dust storms decreased southward and eastward from Alxa and Xilin Gol Leagues. (3) Areas with more than eight disaster events, that is, Alxa and Xilin Gol Leagues, northern Hebei, Shanxi, Shaanxi, and Ningxia, were the main source areas of sand and dust storms. Meanwhile, Beijing, Tianjin, and most other areas of northern China were mainly affected by blowing sand and

Table 5 Affected areas of the 13 blown sand disasters in 2000, China

ID	Time of occurrence	Affected area (10 ⁴ km ²)	Number of affected counties	Affected provinces
1	Mar 2–Mar 3	65.7	226	Inner Mongolia, Shaanxi, Shanxi, Hebei, Beijing, Tianjin, etc.
2	Mar 17–Mar 18	41.2	106	Inner Mongolia, Gansu, Ningxia, Shaanxi, Shanxi, Hebei, Beijing, Tianjin, etc.
3	Mar 21–Mar 23	189.9	589	Inner Mongolia, Gansu, Ningxia, Shaanxi, Shanxi, Hebei, Beijing, Tianjin, Henan, Liaoning, Jilin, etc.
4	Mar 25–Mar 29	205.9	912	Inner Mongolia, Gansu, Ningxia, Shaanxi, Shanxi, Hebei, Beijing, Tianjin, Henan, Anhui, Shandong, Jiangsu, Shanghai, Liaoning, etc.
5	Apr 05–Apr 07	220.3	892	Inner Mongolia, Gansu, Ningxia, Shaanxi, Shanxi, Hebei, Beijing, Tianjin, Henan, Liaoning, Jilin, Qinghai, Anhui, Jiangsu, Shanghai, etc.
6	Apr 09–Apr 12	162.6	572	Inner Mongolia, Gansu, Ningxia, Shaanxi, Shanxi, Hebei, Beijing, Tianjin, Henan, Liaoning, etc.
7	Apr 12–Apr 13	146.5	218	Inner Mongolia, Gansu, Ningxia, Qinghai, Xinjiang, etc.
8	Apr 18–Apr 19	34.8	90	Mongolia, Gansu, Ningxia, Shaanxi, Hebei, etc.
9	Apr 22–Apr 23	59.5	68	Mongolia, Gansu, Ningxia, Shaanxi, Shanxi, etc.
10	Apr 24–Apr 29	162.9	607	Inner Mongolia, Gansu, Ningxia, Shaanxi, Shanxi, Hebei, Beijing, Tianjin, Henan, Anhui, Shandong, Jiangsu, Liaoning, etc.
11	May 07–May 10	91.0	106	Inner Mongolia, Gansu, Ningxia, Shaanxi, Shanxi, Hebei, etc.
12	May 11–May 12	147.9	786	Mongolia, Gansu, Ningxia, Shaanxi, Shanxi, Hebei, Beijing, Tianjin, Henan, Anhui, Jiangsu, Shanghai, Zhejiang, etc.
13	May 17–May 18	53.9	60	Inner Mongolia, Ningxia
Total	Mar 02–May 18	325.9	1061	18 provinces, autonomous, and municipalities

Source Wang et al. (2001)

floating dust from sources outside these areas. This is largely consistent with the view that sand and dust storms were originated from mid-western Inner Mongolia and northwest of Hebei Province (Ye et al. 2000). (4) The south boundary of blown sand hazards was in northern Zhejiang, in the form of mud rain and strong wind

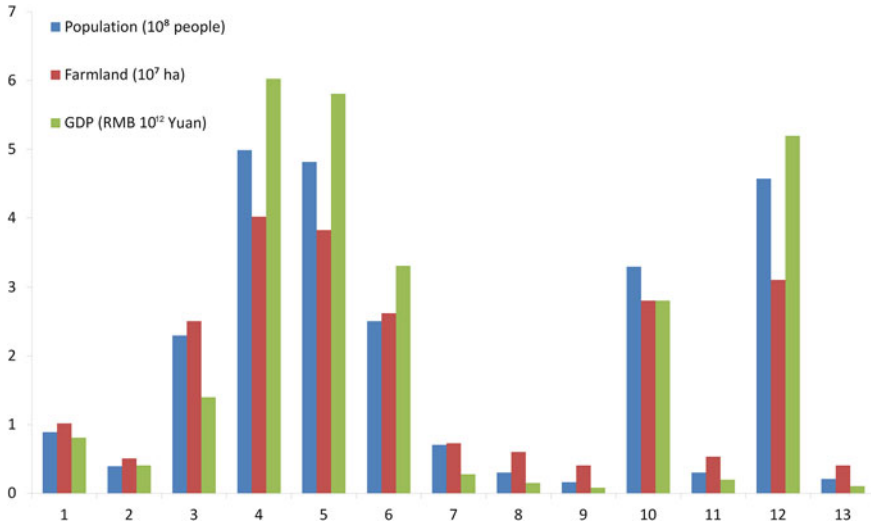


Fig. 17 Affected population, farmland, and GDP by the 13 blown sand disasters in 2000, China (Source Wang et al. 2001)

Table 6 Hazard influencing conditions of sand and dust storms in 2000, China

Provinces, autonomous regions, municipalities	Hazard occurrences (Z_c , times)	Coverage area index of hazards ^a (I_{ca})
Inner Mongolia	13	6.68
Ningxia	11	9.18
Hebei	10	7.23
Shanxi	11	7.22
Beijing	8	7.62
Tianjin	8	6.81
Shaanxi	12	4.69
Gansu	10	3.67
Liaoning	5	3.57
Henan	6	3.31
Shandong	3	4.65
Jiangsu	4	3.68
Anhui	4	2.52
Shanghai	2	2.00
Qinghai	2	0.43
Zhejiang	1	0.31
Xinjiang	1	0.17
Jilin	1	0.15

^a I_{ca} Accumulative area affected by blown sand disasters/provincial (municipality, autonomous region) area

Source Wang et al. (2001)

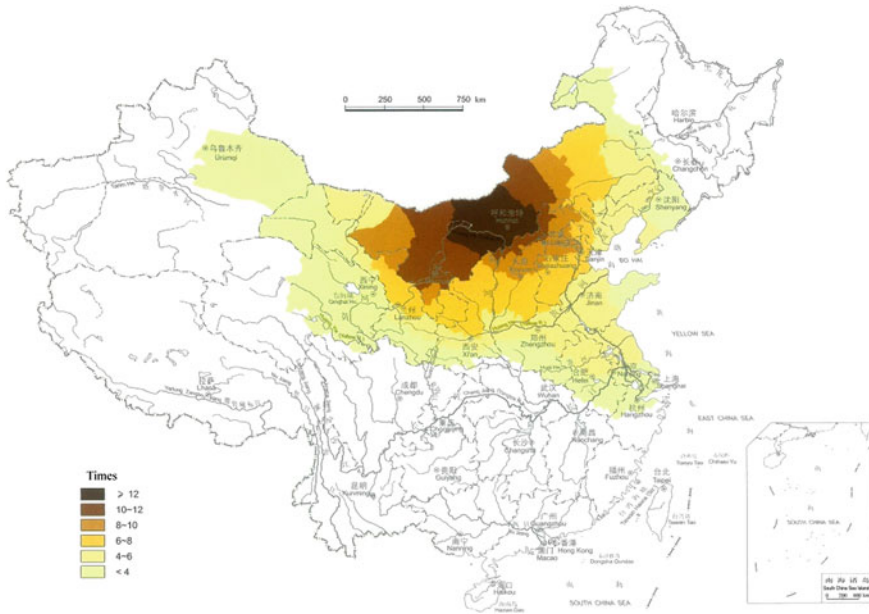


Fig. 18 Blown sand hazard frequency (Z_C) in 2000, China (Source Shi 2003, p. 174)

caused by blown sand weather. This was near the 28° N south boundary of dustfall record in historical period (Zhang and Sun 2001).

Regional blown sand disaster exposure in 2000: Blown sand disaster exposure index, C_H , is an composite index of population density (person/km²), farmland ratio (%), and GDP per unit area (ten thousand Yuan/km²). The higher this value, the greater the potential risk of the concerned socioeconomic system.

$$C_H = (a + b + c)/3 \tag{5}$$

where, a is the score of population density, b is the score of percentage of farmland, and c is the score of GDP per unit area (scores of a , b , and c are between 1–6). Classification of the three parameters and corresponding score of each class are shown in Table 7.

Regional differentiation of blown sand disaster exposure index C_H for 2000 shows the following characteristics: (1) Areas of high C_H values (above 12) cover large cities, especially the municipalities and provincial capitals. These areas have high population density and high GDP per unit area. (2) Areas with C_H values from 6 to 9 were distributed in the North China Plain and Fenwei Plain and were closely linked with areas of high population density and high percentage of farmland. (3) Areas with C_H value from 4 to 6 were distributed extensively in the transitional zone between farming and pastoral areas in northern China and the Hexi Corridor, while areas with C_H value lower than 4 were concentrated in the grassland and

Table 7 Classification and scores of population density, percentage of farmland, and GDP per unit area

Scores of Classes	Population density (1,000 person/km ²)	Percentage of farmland (%)	GDP per unit area (100,000 Yuan/km ²)
6	≥ 0.16	≥ 80	≥ 800
5	0.08–0.16	40–80	400–800
4	0.04–0.08	20–40	200–400
3	0.02–0.04	10–20	100–200
2	0.01–0.02	1–10	50–100
1	<0.01	<1	<50

Source Wang et al. (2001)

desert zones. (4) C_H values generally decreased from southeast to northwest, from the farming areas to the pastoral areas, manifesting a converse trend with the blown sand hazard frequency (Fig. 19).

Impact level of blown sand disasters in 2000: Blown sand hazards and impacts are influenced by many factors. The occurrence and impact of blown sand disasters are not only related to blown sand weather, but also the natural and socioeconomic conditions of the affected areas. In this particular case of blown sand disasters, the disaster impact (W_X) is expressed as the mean of disaster frequency Z_C and exposure C_H , namely $W_X = (Z_c + C_H)/2$. The blown sand disaster impact for each

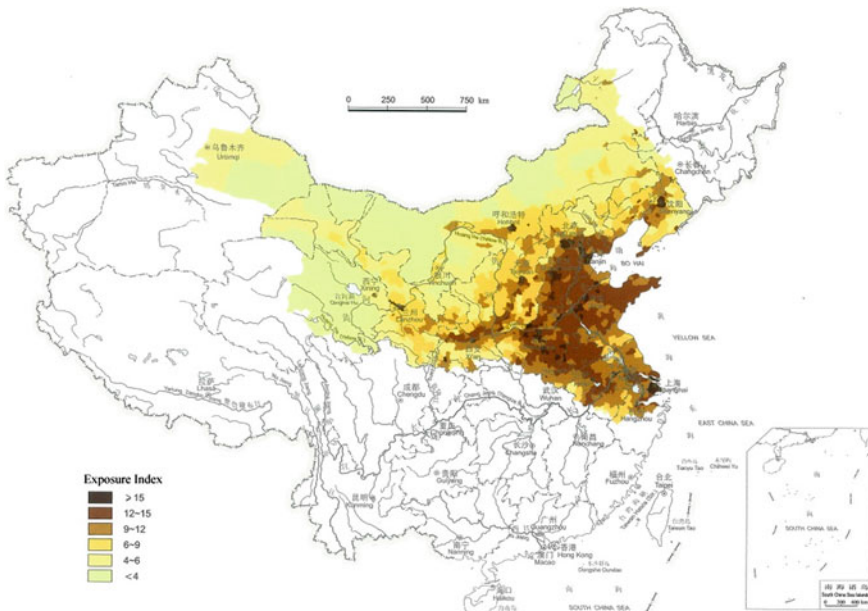


Fig. 19 Blown sand disaster exposure index (C_H) in 2000, China (Source Shi 2003, p. 175)

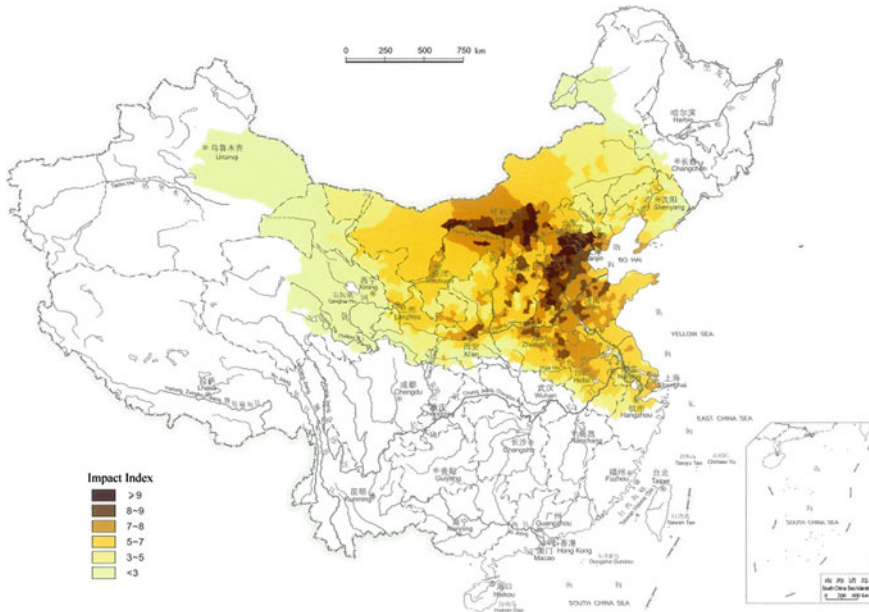


Fig. 20 Blown sand disaster impact in 2000, China (Source Shi 2003, p. 176)

county unit in the affected regions is shown in Fig. 20. The assessment result shows that: (1) There were 19 counties with $W_x > 9$, scattered from east to west in Beijing, Tianjin, Datong in Shanxi Province, and Shangdu County, Hu-bao Plain, and Houtao in Inner Mongolia. These areas were affected to the highest extent by the blown sand disasters. (2) There were 332 counties with W_x between 8–9 in Ulan Qab, Hetao Plain, and Ordos Plateau in Inner Mongolia, northern Shanxi, Beijing, Tianjin, most areas of Hebei Province, northwestern Shandong Province, and northern Henan Province. The rainfed farming area to the north of the Yinshan Mountain where desertification was most severe, Otindag Sandy Land, and Kubuqi Desert were all within this category, with high Z_C value. (3) There were 508 county units with W_x values between 5 and 8, which were linked to the above mentioned high value areas and formed a large triangular region. To the north of the triangle is the border of Mogolia. The southwest boundary extended from Alxa Zuo Banner in western Inner Mongolia to Hangzhou of Zhejiang Province via Dingxi County in the eastern part of Gansu Province. The northeast boundary stretched from Xilinhot City of Xilin Gol League in central Inner Mongolia to Qinhuangdao City via Duolun County and Fengning County of Chengde City in northern Hebei Province. This triangular area is the key area of blown sand disaster risk reduction in China. (4) There were 203 counties with W_x values lower than 5, which are located in eastern Inner Mongolia and western Liaoning Province and extended eastward to the forest steppe zone; in Badain Jaran Desert, Tenger Desert, Dongjiang Gobi, the wind erosion area of eastern Qaidam Basin, Horqin Sandy Land, and Hulun Buir

Sandy Land; as well as in eastern Xinjiang, western Inner Mongolia, Gansu, and eastern Qinghai Province.

3.3 *Lessons Learned*

In light of the severe blown sand disasters in northern China in 2000, public awareness of blown sand disaster increased, and the Chinese government adopted a series of new measures to combat land degradation and desertification.

Scientific analysis on the formation of sand and dust storms: In 2000 after the occurrence of the severe blown sand disasters, the Ministry of Science and Technology (MOST) organized multidisciplinary expert teams to conduct an investigation and comprehensive analysis of typical hazard areas, and released a research report on blown sand disaster formation and scientific and technological measures for preventing its occurrence in China (Shi et al. 2000a). On 17 May 2000, the expert group submitted a report to the State Council leader in the form of science and technology lectures, which indicated that the main reasons for the severe blown sand disasters in 2000 was climate warming and drying, and land use and land cover change induced by human activities (Shi et al. 2001). The report proposed four functional zones, namely, the capital-circle, the transitional zone between farming and pastoral areas, the plain zone, and the desert and oasis zone, and suggested that different vegetation recovery measures should be adopted to reduce surface exposure and increase the capacity to prevent the formation of and damage from sandstorms (Zhu and Chen 1994). Meanwhile, the State Forestry Bureau also made an investigation on the blown sand disasters and proposed measures to strengthen the Grain for Green Project in plain areas and to implement the Project for Wind and Sand Source Area Control around Beijing and Tianjin.

Project for Wind and Sand Source Area Control around Beijing and Tianjin: *Project Planning for Wind and Sand Source Area Control around Beijing and Tianjin* was approved by the State Council in March 2002 and implemented comprehensively after a 2-year pilot project. This plan aimed to control land desertification through significant ecological improvements in Beijing, Tianjin and surrounding areas, by using various biological and engineering measures to increase forest coverage, rehabilitate land of desertification, and reduce blown sand disaster and the impact of sand and dust storm weather, within a total project area of 458,000 km² in the next 10 years.

Main measures of the project included: (1) Enclose and protect existing forests and prohibit all commercial logging activities. (2) Implement the Grain for Green Project in steep slope cropland areas in river basins and cropland on slopes around reservoirs. (3) Speed up the comprehensive control of water and soil erosion and reduce sediment yield. (4) Plant multilayered forests integrating trees, shrubs, and grasses for the conservation of water supply. (5) Construct wind-breaking and sand-fixing forests in large scale to form a windbreak and sand-fixation system. (6) Adjust the structure of livestock herds and transform animal husbandry from

grazing to captive breeding. (7) Construct windbreak network of farmland and pastures. (8) Carry out ecological emigration in the northern area of Martin North.

Project for Wind and Sand Source Area Control around Beijing and Tianjin was divided into two stages: the first stage was in 2001–2005 and the second was in 2006–2010. By 2010, the project shall return 2,630,000 ha of grain plots to forests, plant 4,940,000 ha of forests, improve 10,630,000 ha of grasses, and construct 113,889 supporting facilities for water conservancy; integrated improvement of small watersheds shall reach 2,340,000 ha, and ecological emigration should move 180,000 people out of the control area.

Grain for Green Project in plain areas: Due to deforestation, steep slope cultivation, and grassland reclamation, China has suffered from severe water and soil erosion and blown sand disasters for many decades. Natural disasters such as floods, droughts, and sand and dust storms occurred frequently and severely affected people's life and production, as well as the national ecological security. In 2000, *Some Opinions of the State Council on Further Implementation of Pilot Work for Grain for Green Project* (GF [2000] No. 24) was released. On 10 Jan 10, 2002, Western Region Development Office of the State Council held a video conference on the Grain for Green Project, which determined to fully launch the project and formed *Some Opinions of the State Council on the Further Improvement of Grain for Green Policy Measures* (GF [2002] No. 10) and *Regulations for Grain for Green Project*. On the basis of further investigation and research and extensive consultation with provinces (autonomous regions, municipalities) and relevant departments and experts, the State Forestry Bureau, jointly with the National Development and Reform Commission, Ministry of Finance, Western Region Development Office of the State Council, and the State Grain Administration, compiled the *Planning for Grain for Green Project* (2001–2010).

The scope of the Grain for Green Project covers 25 provinces (autonomous regions, municipalities), including Beijing, Tianjin, Hebei, Shanxi, Inner Mongolia, Liaoning, Jilin, Heilongjiang, Anhui, Jiangxi, Henan, Hubei, Hunan, Guangxi, Hainan, Chongqing, Sichuan, Guizhou, Yunnan, Xizang, Shaanxi, Gansu, Qinghai, Ningxia, Xinjiang, and Xinjiang Production and Construction Corps, and a total of 1,897 counties (including cities, districts, and banners). In line with the principle of “setting protection according to damage” and in accordance with the intensity of hazards of water and soil erosion and wind erosion and desertification, water and climatic conditions, and topography and landforms, the project areas are divided into 10 categories: (1) high mountain and canyon areas in the southwest; (2) mountainous and hilly areas in Sichuan, Chongqing, Hubei, and Hunan Provinces; (3) low mountain and hilly areas in the middle and lower reaches of the Yangtze River; (4) Yunnan–Guizhou Plateau areas; (5) mountainous and hilly areas in Hainan and Guangxi Provinces; (6) alpine grassland and meadow areas at the source areas of the Yangtze River and Yellow River; (7) arid desert areas in Xinjiang; (8) loess hilly-gully areas; (9) arid and semiarid areas in northern China; (10) mountainous and sandy areas in the northeast. In line with the principle of “highlighting the key issues and key areas; prioritizing most pressing issues, and emphasizing effectiveness,” 856 counties in the upper reaches of the Yangtze River,

the middle and upper reaches of the Yellow River, sand and dust source areas in Beijing and Tianjin, and important catchment areas by lakes and reservoirs, the Hongshui River Basin, Heihe River Basin, and Tarim River Basin were selected as key areas in project implementation. The objectives and tasks of the project implementation are to return 14,670,000 ha of reclaimed farmland to forests, afforest 17,330,000 ha of hilly wasteland and uncultivated lands, return nearly all steep slope farmlands to forests, and improve all farmlands of severe desertification by 2010; the forest and grass coverage of the project areas will be increased by 4.5 %, and the ecological condition of the project areas will be greatly improved.

Research on sand and dust storm disaster early warning system: In light of the aggravated blown sand disasters in northern China, China Meteorological Administration organized various forces to carry out the construction of sand and dust storm disaster early warning system through cooperation with the State Forestry Bureau, under the support of the Ministry of Science and Technology. In the winter of 2004, system in-service testing was initiated. In 2005, the system was officially operating and started monitoring and early warning services. Through painstaking efforts over several years, this system is now able to monitor and perform early warning of sand and dust storms national-wide and make assessments on the scope, affected population, and macroeconomic losses of sand and dust storms.

References

- CMA (China Meteorological Administration). 2006. Grade of sand and dust storm weather (GB/T 20480-2006).
- Dong, G.R. 2002. *Formation and evolution of Chinese desert climate change and desertification research*. Beijing: Ocean Press (in Chinese).
- Dong, G.R., S.Y. Gao, J. Jin, et al. 1993. *Land desertification of Gonghe Basin in Qinghai Province and prevention methods*. Beijing: Science Press (in Chinese).
- Gao, S.Y., P.J. Shi, S. Ha, et al. 2000. Causes of rapid expansion of blown-sand disaster and long-term trend of desertification in northern China. *Journal of Natural Disasters* 9(3): 31–37 (in Chinese).
- Huang, W., and Y. Niu. 1998. The sand and dust storm damage and its countermeasure in northwest China. *Journal of Arid Land Resources and Environment* 12(3): 83–88 (in Chinese).
- MEPC (Ministry of Environmental Protection of the People's Republic of China). 1981–2007. *China environment yearbook*. Beijing: China Environment Yearbook Press (in Chinese).
- Prospero, J.M., and P.J. Lamb. 2003. African droughts and dust transport to the Caribbean: Climate change implications. *Science* 302(5647): 1024–1027.
- Qian, Z.A., M.H. Song, and W.Y. Li. 2002. Analyses on distributive variation and forecast of sand-dust storms in recent 50 years in North China. *Journal of Desert Research* 22(2): 106–111 (in Chinese).
- Shi, P.J. 2011. *Atlas of natural disaster risk of China*. Beijing: Science Press (in Chinese and English).
- Shi, P.J., et al. 2000a. Chinese sandstorm disasters and scientific and technological countermeasures. Expert Group of Desertification Governance of the Ministry of Science and Technology of the People's Republic of China (in Chinese).

- Shi, P.J., P. Yan, S.Y. Gao, et al. 2000b. The sandstorm disasters in China and its research progress. *Journal of Natural Disasters* 9(3): 71–77 (in Chinese).
- Shi, P.J., P. Yan, and Y. Yuan. 2001. The driving force of the blown-sand activity in northern China. *Quaternary Research* 21(1): 41–47 (in Chinese).
- Shi, P.J. 2003. *Atlas of natural disaster system of china*. Beijing: Science Press (in Chinese and English).
- Song, Y., Z.J. Quan, L.Y. Liu, et al. 2005. The influence of different underlying surface on sand-dust storm in northern China. *Journal of Geographical Sciences* 15(4): 431–438.
- Wang, S.M., and H.S. Dou. 1998. *Lakes' record in China*. Beijing: Science Press (in Chinese).
- Wang, J.A., W. Xu, P.J. Shi, et al. 2001. Spatiotemporal pattern and risk assessment of wind sand disaster in China in 2000. *Journal of Natural Disasters* 10(4): 1–7 (in Chinese).
- Wang, S.G., J.Y. Wang, and Z.J. Zhou. 2003. Regional characteristics of dust events in China. *Geographical Journal* 58(2): 193–200 (in Chinese).
- Xu, Q.Y., and J.S. Hu. 1996. Analysis on spatiotemporal features of sandstorm in Northwest China. *Disaster reduction in China* 6(3): 42–45 (in Chinese).
- Ye, D.Z., J.F. Chou, J.Y. Liu, et al. 2000. Causes of sand-stormy weather in northern China and control measures. *Acta Geographica Sinica* 55(5): 513–521 (in Chinese).
- Zhang, D.E. 1982. Analysis on “dust rain” phenomenon in historical period. *Science Bulletin* 27 (5): 294–297.
- Zhang, D.R., and X. Sun. 2001. Variation of the southern limits of dustfall records and the inferred historical climate drought in northern China. *Quaternary Research* 21(1): 1–7 (in Chinese).
- Zhang, X.X., P.J. Shi, L.Y. Liu, et al. 2010. Ambient TSP concentration and dustfall in major cities of China: Spatial distribution and temporal variability. *Atmospheric Environment* 44: 1641–1648.
- Zhao, H.B., D.N. He, D.S. Zhang, et al. 1993. The calculation of sand discharge entering Qinghai Lake and formation of submerged barriers. *Journal of Lake Sciences* 5(30): 40–46 (in Chinese).
- Zhou, Z.J. 2001. Blowing-sand and sandstorm in China in recent 45 years. *Quaternary Research* 21(1): 9–17 (in Chinese).
- Zhu, Z.D., and G.T. Chen. 1994. *Sandy desertification in China*. Beijing: Science Press (in Chinese).

Storm Surge Disasters in China

Weihua Fang, Fujiang Yu, Jianxi Dong and Xianwu Shi

Abstract Storm surge is the main marine hazard in the coastal areas of China. Located in the west of the North Pacific Ocean, the land of China crosses three climatic zones—temperate, subtropical, and tropical—with more than 18 thousand km coastal lines, making it one of the very few countries in the world that are affected not only by tropical but also extra-tropical storm surges. Based on the historical storm surge records and observed tidal station data, this chapter analyzes the spatial and temporal characteristics of storm surges, including the interannual variation of frequency, hazards, vulnerability, and risk levels, in the coastal areas of China. Typhoon Saomai storm surge disaster, one of the most serious in China since 1949, is taken as an example to examine the emergency response mechanism and experiences of the Chinese government in the face of such disasters.

Keywords Storm surge · Spatiotemporal pattern · Emergency response · Saomai

Storm surge is a coastal flood where water is pushed toward the shore by the force of the winds swirling around a storm. This advancing surge combines with the normal tides to create the hurricane storm tide, which can increase the mean water level to heights impacting roads, homes, and other critical infrastructure (FEMA2010). In addition, wind driven waves are superimposed on the storm tide. This rise in water level can cause severe flooding in coastal areas, particularly when the storm tide coincides with the normal high tides, causing storm surge disaster (FEMA2010). Storm surge can be divided into two types according to the nature of the storm, that is, tropical cyclone storm surge and extra-tropical storm surge.

W. Fang (✉)

Key Laboratory of Environmental Change and Natural Disasters,
Ministry of Education of Beijing Normal University, Beijing 100875, China
e-mail: weihua.fang@bnu.edu.cn

F. Yu · J. Dong

National Marine Environmental Forecasting Center, Beijing 100081, China

X. Shi

National Marine Hazard Mitigation Service, Beijing 100194, China

Storm surge disaster is the main marine disaster in China. The hazard is consisted of the astronomical tide, storm surge, and waves (Galagan 2008), usually simplifying by the term storm tide. China is located in the west of the North Pacific Ocean and crosses three climatic zones—temperate, subtropical, and tropical, which makes it one of the very few countries in the world that are affected by both typhoon storm surges and extra-tropical storm surges. Typhoon storm surge happens at all seasons and is most common in the summer. It usually hits South China Sea and East China Sea coast with the characteristics of fierce oncoming force, fast speed, high intensity, and strong destructive power. Many of the extra-tropical storm surges, on the other hand, usually occur in the Yellow Sea and the Bohai Sea coast in the spring and the autumn, with the characteristics of relatively gentle water-rising process and a lower height of storm tide than typhoon storm surges (Ye and Yu 2002; Hu and Zhang 2006).

Based on the data from the *Data Compilation of China's Marine Disasters in Forty Years (1949–1990)* (Yang et al. 1991) and *China's Marine Disaster Bulletin (1989–2010)* (State Oceanic Administration 1989–2010) both by the National Marine Environmental Forecasting Center (NMEFC) of China, this chapter analyzes the spatiotemporal variability of storm surge hazard intensity. It also assesses the storm surge vulnerability and summarizes the spatiotemporal distribution of storm surge risk along the coast of China by combining the coastal population and GDP data of 2002, at a spatial resolution of 1 km. Finally, this chapter examines disaster responses through a case analysis of storm surge disaster caused by Typhoon Saomai.

1 Spatial and Temporal Patterns of Storm Surge Disasters

As the leading marine hazard in China, storm surges occur from the south to the north, covering nearly the entire coastline of China, especially in coastal regions of Zhejiang, Fujian, and Guangdong Provinces. It happens every year with high occurrences, resulting in considerable damage to human life and the economy. Storm surge disasters have been a serious threat in China. Tens of thousands, even millions of people in coastal areas have to evacuate in such event and many houses, farmlands, aquaculture farms, and seawall dikes are flooded or damaged, with direct economic losses up to RMB tens of billions. From 2001 to 2005, 27 storm surges hit China, resulting in 377 deaths (including those missing), which accounts for 32 % of the total number of deaths in marine disasters during this time period, also causing direct economic losses of RMB 61.082 billion Yuan, which is 96 % of the total direct economic losses from all types of marine disasters.

1.1 *Spatial Distribution of Storm Surge Disasters*

Storm tide disasters have occurred almost every year in China since 1949. In every 2 years on average, there was a severe disaster. Multiple severe storm surge disasters also happened in some years. For example, a total of eight storm tide disasters occurred in 1989. Severe storm surges usually cause damages simultaneously in several provinces. In the cases of the No. 9216 and No. 9711 storm surge disasters in 1992 and 1997, from Fujian Province in the south to Liaoning Province in the north, six provinces and two direct-controlled municipalities in east China were affected. According to incomplete statistics, 217 typhoon storm surges above yellow warning grade and 118 above orange warning grade, as well as 63 extra-tropical storm surges above yellow warning grade and 12 above orange warning grade, had occurred in 1949–2007.

According to the collected data on historical calamities and tide observation records, the following five coastal sections are identified as high frequency regions of storm surge (Ye and Yu 2002): (1) Bohai Bay to Laizhou Bay coast; (2) the Yangtze estuary and Hangzhou Bay from southern Jiangsu coast to northern Zhejiang Province; (3) Wenzhou of Zhejiang Province to the Min River estuary in Fujian Province; (4) Shantou to Pearl River estuary in Guangdong Province; and (5) East bank of Leizhou Peninsula to northeast Hainan Province.

If a storm surge coincides with an astronomical high tide, especially when maximum storm surge tides overlay with the high tide of an astronomical tide, catastrophic disaster can occur. Even without astronomical tide or high tide, high water rising of big storm surge could still lead to severe tide disasters. Because the coastline of China is long, tidal difference of various sea zones is large. With the largest of 7–8 m and smallest of 1–2 m, tidal difference of astronomical tide at a specific location plays a key role in causing a disaster during a storm surge (Song et al. 2005). The tidal difference in China's coastline gradually increases from the north, the Yellow Sea, to the south, the East China Sea, then decreases from the East China Sea to the South China Sea. In the South China Sea, it increases from east to west in Guangdong Province. On the whole, the tidal difference in East China Sea is the largest and that in the Hangzhou Bay is about 7–8 m. The next largest is found in the Yellow Sea, where tidal difference on the coast of Jiangsu Province reaches 5–6 m. The Bohai Sea ranks the third in tidal difference, at 3–4 m in the coastal area of Tianjin. The tidal difference in the South Sea is only about 2–4 m in the coast of Guangdong Province. Moreover, in Qinhuangdao of Hebei Province and the Yellow River estuary, the tidal difference is 1–2 m, which is the smallest because they are located at amphidromic points (Song et al. 2005).

Coastline in some provinces and cities of China is tortuous and many harbors go deep into the inland area. Since storm surges are very sensitive to complicated micro-terrains, they are more severe in coastal zones of horn shape and estuaries, such as the Bohai Bay, Laizhou Bay, Yangtze estuary, Hangzhou Bay, Pearl River

Estuary, and Leizhou Peninsula. As stipulated in the *Emergency Plan of Storm Surge, Tsunami and Sea Ice* (State Oceanic Administration 2009) issued by the State Council of China, early warning of storm surges is given at four grades—grade I, II, III, and IV, meaning particularly severe, severe, relatively severe, and mild, with the designated color code of red, orange, yellow, and blue respectively, based on the intensity of storm surge hazards. In order to highlight the severity of grade I and grade II storm surge disaster, the concept of storm surge disaster degree is introduced (which focuses solely on the hazard and does not take into consideration human casualties and property losses as well as other secondary disasters). To highlight the importance of hazard intensity of orange grade (III) and above in causing disasters, each hazard grade is assigned a different weight. Disaster degree is calculated by multiplying the number of occurrences of each grade of hazard intensity (I, II, and III, that is, red, orange, and yellow, respectively) by the weight of the hazard grade (Eq. 1). Hazard intensity is determined by how much a high tide level in a single storm surge process exceeds local warning tide level.

$$Dg = W_R \times 10 + W_O \times 5 + W_Y \times 1 \quad (1)$$

where Dg represents disaster degree of a place; W_R , W_O , and W_Y are the number of occurrences of red, orange, and yellow grade storm surges, respectively.

Using Eq. 1, disaster degree of each tidal station is calculated based on the frequency of occurrence and weight of each hazard grade. Then the overall storm surge hazard severity of the place (that is, disaster degree) is categorized into four classes according to the disaster degree value. By normalizing the disaster degrees from all tidal stations, the disaster degree classes are defined as follows: blue class, $0 \leq Dg < 0.25$; yellow class, $0.25 \leq Dg < 0.5$; orange class, $0.5 \leq Dg < 0.75$; and red class, $0.75 \leq Dg \leq 1$. The disaster degree map of a region depicts its overall storm surge hazard severity. Figure 1 shows storm surge disaster degree in China's coastal area.

With red, orange, yellow, and green representing class 4, 3, 2, and 1 of overall storm surge hazard severity respectively, it can be seen that from north to south, Liaoning and northern Hebei Provinces belong to the class 1 area, Tianjin and southern Hebei Province are class 3 areas, the Laizhou Bay coast in Shandong Province is a class 3 area, the southeast coast of Shandong Peninsula and Jiangsu coast are class 1 areas, the Yangtze River estuary is a class 3 area, the Hangzhou Bay, Taizhou coast, Wenzhou, and the southern part of Zhejiang Province are class 4 areas, northern Fujian is a class 3 area, the Min River estuary in Fujian Province is a class 4 area, central Fujian Province is a class 2 area, southern Fujian Province is a class 1 area, the eastern part of Guangdong Province, Pearl River estuary, and east coast of Leizhou Peninsula are class 3 areas, the western part of Guangdong Province is a class 2 area, the northeast and southwest parts of Hainan Island are class 3 and 1 areas respectively, and the Guangxi coast is a class 1 area.

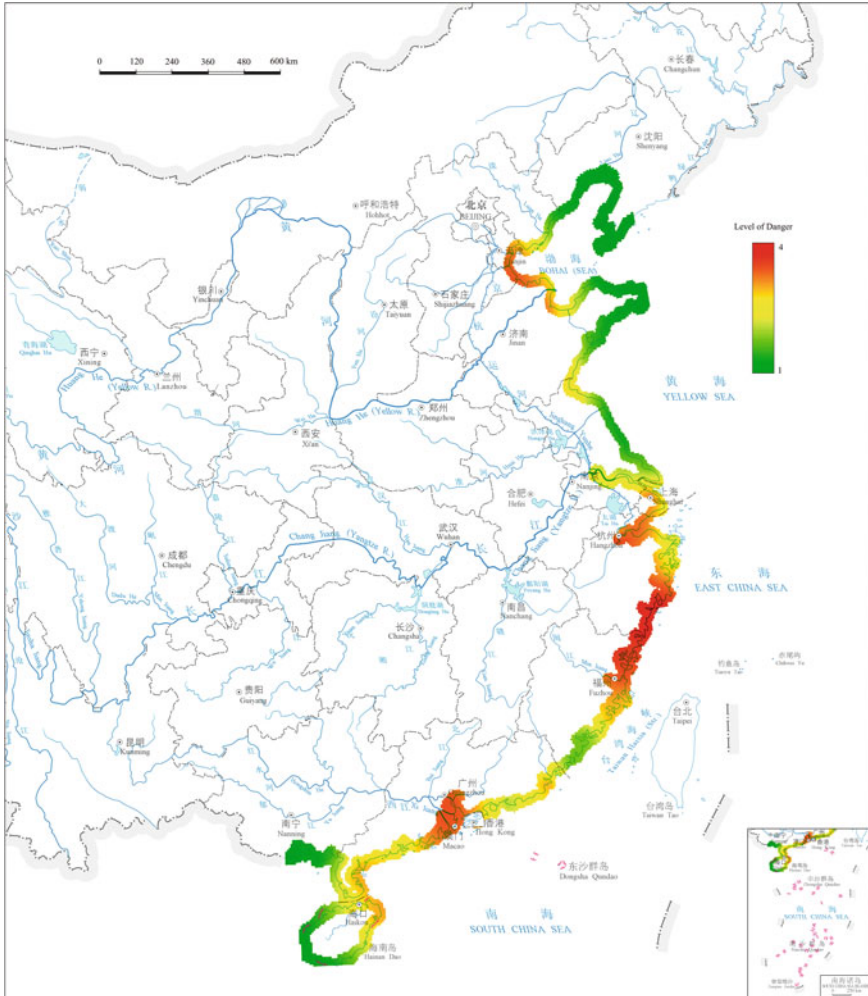


Fig. 1 Storm surge overall hazard severity in China's coastal regions (Source Shi 2011, p. 86)

1.2 Temporal Distribution of Storm Surge Disasters

From 1949 to 2012, the frequency of typhoons and storm surges had shown an overall tendency of increase (Fig. 2). A total of 440 typhoon storm surges were recorded between 1949 and 2012, with an annual average of 6.88 storm surges. The highest annual occurrences were in 2007 and 2012, with 13 storm surges reported in each year. The lowest annual occurrences was two, which occurred in 1949, 1952, 1955, and 1957. With the growth of population and rapid socioeconomic development in coastal areas, the degree of losses caused by marine disasters in

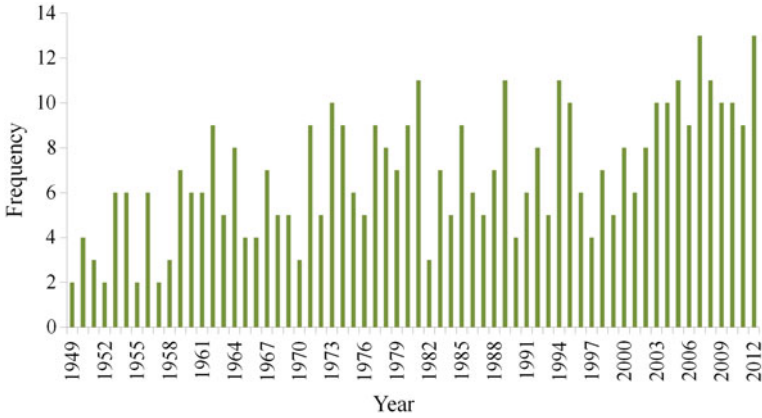


Fig. 2 Number of typhoon-induced storm surges in China, 1949–2012

China will continue to increase and marine disasters may cause direct economic losses in the order of tens of billions Yuan.

Interannual variability of extra-tropical storm surges in China during 1951–2012 is shown in Fig. 3. A total of 440 extra-tropical storm surges were recorded, with an annual average occurrences of 6.98. There was no extra-tropical storm surge recorded in 1953, 1956, 2000, 2001, and 2002. Temperate storm surge happened less frequently in the 1950s but more frequently in the 1960s, 1970s, 2000s. The peak appeared in 2009, with 22 storm surges recorded. It should be pointed out that although extra-tropical storm surges happened more frequently than typhoon storm surges in 1960–1990 in general, their intensity were lower than that of typhoon storm surges. As a result, the losses were smaller. In China, most of the extremely severe storm surge disasters were caused by typhoon storm surges.

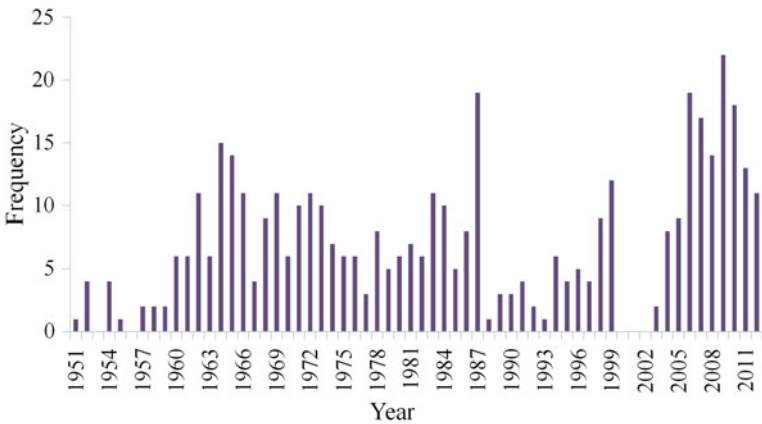
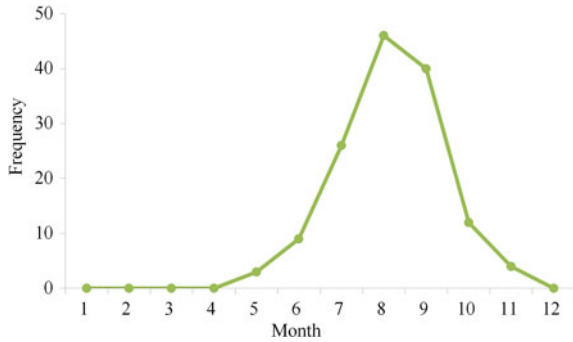


Fig. 3 Interannual variability of extra-tropical storm surges in China, 1951–2012

Fig. 4 Seasonal distribution of typhoon storm surges in China, 1949–1997



According to incomplete statistics, from the Han Dynasty (206 BC) to 1946, 576 extremely severe tide disasters hit the coastal regions of China. Since the establishment of the Peoples' Republic of China, in the 49 years by 1997 there were 150 typhoon storm surges, among which 64 were severe. There were 59 extra-tropical storm surges in the same time period and seven of them were severe storm surges. From 1949 to 1990, there were 12 extremely severe storm surge disasters [*Data Compilation of China's Marine Disasters in Forty Years (1949–1990)* (Yang et al. 1991)]. In China, storm surge disasters mainly happen in the summer and autumn, most of which are caused by typhoons. There was a smaller number of extra-tropical storm surges in the Bohai Bay area (Ye and Yu 2002). Figure 4 shows the seasonal distribution of the 150 typhoon storm surges of category I or higher that occurred in 1949–1997 in China. Storm surges that happened in August and September account for 57 % (86 times) of the total storm surges. This is the same period as the peak typhoon season in coastal regions. August to October is also an astronomical high tide period. So, when typhoon arrives during the astronomical high tide period, severe or extremely severe storm tide disaster could happen. From December to March, there was no storm surge. There were only 16 storm surges in October and November, which also coincide with typhoon occurrences.

Table 1 shows the statistics of seasonal storm surge frequency in different coastal plains in China during 1949–1990. In January to March, storm surges only took place in mid-latitude coastal areas such as plains in the west coast of the Bohai Sea and the Yellow River Delta and all of these were extra-tropical storm surges. These storm surge disasters were mainly caused by overlying extra-tropical cyclone storm surges and astronomical high tides. From April to June, since there is almost no typhoon, there was almost no typhoon storm surge, particularly in the Min River Delta in the coastal region of Fujian Province where the number of storm surge was zero, but many extra-tropical storm surges happened in the Bohai Bay and the Yellow River Delta region. From July to September, typhoon happened frequently and storm surges were very frequent in the Pearl River Delta, Yangtze River Delta Plain, and North Jiangsu coastal plain. These storm tide disasters were mainly due to the overlying inland water rise caused by typhoon and astronomical high tide. In

Table 1 Frequency of storm surges in different seasons in the coastal plains of China, 1949–1990

Coastal plain	January– March	April– June	July– September	October– December	Total
Littoral Plain in northern Hainan	0	3	9	3	15
Littoral Plain in Guangxi Province	0	1	5	0	6
Pearl River Delta	0	2	16	3	21
Han River Delta	0	1	3	1	5
Min River Delta	0	0	8	0	8
Yangtze River Delta	0	1	18	1	20
Northern Jiangsu Coastal Plain	0	1(1)	15	0	16
Yellow River Delta	20(20)	19(19)	22(9)	35(35)	96
Bohai West Coast Plain	15(15)	12(12)	9(4)	32(32)	68
Lower Liao River Delta	0	0	4(1)	0	4

Note Numbers in brackets are the frequency of occurrence of extra-tropical storm surges *Data source* Yang (2000)

the transitional autumn season from October to December, cold and warm air flows are active over the sea in the north, resulting in frequent extra-tropical storm surges. Storm surge monitoring and forecasting therefore shall be strengthened in this season.

2 Formation and Assessment of Storm Surge Disaster Risks

Many storm surge numerical models were established in Europe from the 1950s, such as the SLOSH, DELFT3D, MIKE12, GCOM2D/3D, and TAOS models (Song et al. 2005), and these models have been applied in many fields. The National Marine Environmental Forecasting Center (NMEFC) of China also developed numerical storm surge prediction models and carried out risk assessment of storm surge disasters in China.

Storm surge disaster risk assessment methods include statistical methods based on historical observations (Xu and Tang 1998) and methods that combine probabilistic statistical models and numerical method (Kleinosky et al. 2006), as well as methods that combine stochastic events and numerical modeling (Wood et al. 2011). The first method, that is, extreme value analysis based on historical data, is used in this chapter. Population and GDP data at 1 km grid were used as exposure for vulnerability assessment. Storm surge disaster risk in China was evaluated semi-quantitatively.

2.1 Formation Mechanism of Storm Surge Disasters

Storm surge disaster is caused by water rise along banks resulting from the combination of storm surge, astronomical tide, and waves in near shore (State Oceanic Administration, People's Republic of China 2009). Four conditions contribute to the formation of storm surge disaster: (1) abnormal weather system, that is, regional strong wind and abnormal (low) atmospheric pressure; (2) astronomical high tide; (3) geographic environment where the land flattens out in the coast; and (4) coast sections that are economically developed and densely settled. Severe storm surge disasters that are highly destructive could occur when all four conditions are met concurrently at the same coastal locations (Chen 1994).

2.2 Vulnerability to Storm Surge Disasters

Storm surge disaster risk mainly depends on the interaction between the hazard and vulnerability of the society at risk.

Population and economic activities are major considerations in storm surge vulnerability assessment. Although the disaster prevention capacity of coastal communities is an important factor of vulnerability, given that reliable data is not easily accessible and the local warning tide level has already considered such capacity, storm surge disaster risk assessment in this chapter is mainly based on vulnerability of population and economy (GDP).

In this assessment, GDP and population data in 2002 at each 1 km grid are applied. In vulnerability calculation, the population and economy variables are given different weights, that is, 0.6 for population and 0.4 for GDP. Figure 5 shows the distribution of vulnerability to storm surge in coastal regions of China. The Bohai Bay, Laizhou Bay, Haizhou Bay, Yangtze estuary, Min River estuary, Pearl River estuary, and Hangzhou Bay that have a smooth terrain are greatly affected by storm surges. The assessment area is 20 km from the coastline in these regions, while for other coast sections the buffer zone is 10 km from coastline. The figure shows that because the Yangtze Delta estuary, Zhejiang coastal region, and Guangdong coastal region are the economically most developed and densely populated regions, they have the highest vulnerability to storm surges. Even mild storm surges may result in great losses. Therefore, these regions are key targets of engineering defensive measures for storm surge disaster in China. The vulnerability of Shandong Peninsula is also high, partly due to great economic losses and casualties caused by strong typhoons heading north that reach this area, but also because the region around the Bohai Sea is frequently hit by extra-tropical storm surges that cause smaller losses. Eastern Guangdong Province, northern Hainan Province, and Guangxi Littoral Plain are areas with medium vulnerability and are also key coastal regions where storm surge disaster prevention measures should be taken.

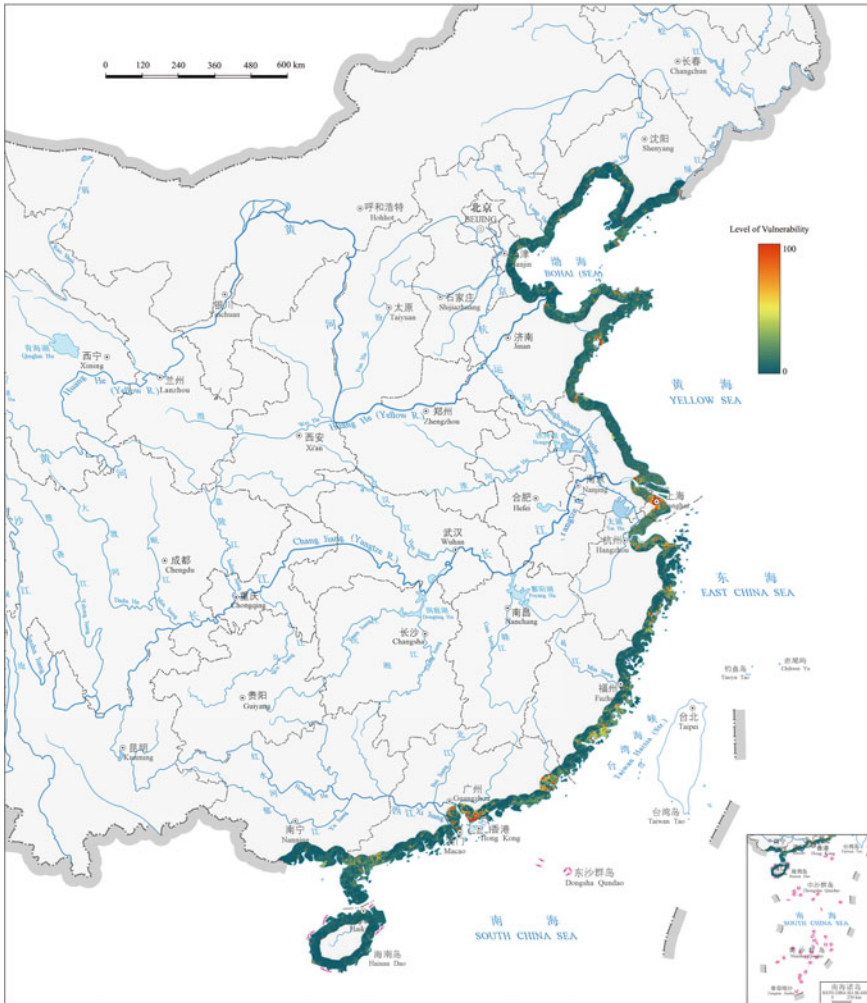


Fig. 5 Vulnerability to storm surges in coastal regions of China (Source Shi 2011, p. 87)

2.3 Storm Surge Disaster Risk

The National Marine Environmental Forecasting Center has issued the *National Marine Calamities Bulletin* annually at the end of each year since 1989, providing a general evaluation on marine disasters such as storm surge, sea wave, and sea ice happened in the year. After more than 20 years, a procedure for identifying data source and content and information verification of various disasters for statistical analysis as well as loss evaluations of different disaster types has been formed.



Fig. 6 Storm surge disaster risks in China (Source Shi 2011, p. 88–89)

A reliable database for understanding marine disasters, especially for storm surge risk assessment has been developed.

Figure 6 shows storm surge disaster risk profile of China’s coastal areas. By taking storm surge hazard and vulnerability of the exposure units, especially potential human casualties and economic losses resulting from storm surge catastrophes into consideration, this map shows that the high-risk regions are along the coast of the Bohai Bay and Haizhou Bay, Yangtze estuary in Shanghai, Hangzhou Bay, Taizhou and Wenzhou coast in Zhejiang Province, Ningde and the Min River estuary coast in Fujian Province, Shantou coast, Pearl River estuary, eastern Leizhou Peninsula in eastern Guangdong Province, and the northeast coast of Hainan Province. Distribution of high-risk regions basically corresponds to the severe hazard areas. The flat and open terrain in estuary areas can easily result in storm surge disaster, and all severe storm surges in history mainly happened in these regions. Because of their favorable geographic locations, these regions are highly developed economically, with many important lifeline projects and large enterprises and public institutions, and are heavily populated. Although in these regions the construction of tide-resisting facilities with high standard reduces the frequency of disasters to some extent, with very high population density and highly developed economy, losses would be significant once a disaster happens.

Losses resulting from storm surges are closely related to storm surge hazard intensity, affected areas, and other natural factors. Meanwhile, conditions of disaster prevention facilities, terrain, and landforms in a disaster area, as well as

implementation of disaster prevention and reduction measures also play major roles in affecting disaster losses. Storm surges occurring in different geological environments, for example bedrock and loose sedimentary coasts, will result in different damages and impacts. Bedrock coast is usually made of hard rocks and the distance of intrusion into inland is short when storm surge hits. Loose sedimentary coast is usually flat. Especially in the case of mudflat coast, the beach is very broad and flat, with slope gradient of only about 0.5 %. When a storm surge occurs, the land area submerged by sea water is large, making the risk of storm surge disaster in these areas relatively high. Storm surge disaster risk usually to a large extent depends on the sediment and soil types in the area of impact. Sediments and soils at the Yangtze River estuary are generally loose because of the confluence flowing into the sea. Thus the impact of storm surge on the Yangtze Delta and the downstream area is high and storm surge of the same intensity may result in greater losses, effectively making the risk of storm surge disaster here higher than in other areas. An accurate storm surge warning and effective disaster prevention measures will reduce losses to a great extent when such hazard occurs. In storm surge disaster risk assessment, the two important elements, that is, hazard assessment and assessment of vulnerability of exposure units, are not equally reliable. At present, research on vulnerability and coping capacity of coastal communities is very few because of the complexity of such assessments, which involve a large number of factors such as social, economic, disaster prevention engineering facility, and non-structural measure. These factors have great influence on the vulnerability of the exposure units.

3 Response to Typhoon Saomai (No. 0608) in 2006

3.1 Disaster Situation

The details about the super typhoon Saomai (No. 0608) in 2006 are found in the chapter *Typhoons in China* in this book. Only storm surges associated with Saomai are discussed in this chapter.

Saomai's landing resulted in violent storm surges, which can be divided into three stages: (1) Initial vibration stage. The typhoon arrived at shore and water rise occurred slowly for 12 h; (2) Strong vibration stage. The typhoon moved to the continental shelf and water rise occurred very rapidly within a short period of time as the typhoon approached the ports. It lasted for 3 h after the typhoon landed; (3) After-vibration stage. Water rise reached the peak and started to drop at a higher rate for about 8 h (Lu and Ma 2007).

Typhoon Saomai landed within the astronomical high tide period of mid-July of the lunar calendar. As a result, tide level in each coastal observation station reached astronomical high water level soon after the landing of the typhoon. Strong wind and rainstorm brought by the typhoon as well as astronomical high tide caused the intrusion of a large amount of sea water. The combination of the three further enhanced the destructive force of Typhoon Saomai (Table 2).

Table 2 Water levels at coastal tidal stations during Typhoon Saomai (cm)

Site name	Warning water level (cm)	Above warning water level (cm)
Jiantiao	66	–
Haimen	53	–
Kanmen	79	–
Longwan	133	34
Wenzhou	131	44
Ruian	255	62
Aojiang	401	48
Shacheng	178	26
Sansha	117	32
Guantou	87	24
Baiyantian	66	4
Meihua	112	14
Pingtian	142	–

Note “–” indicates water level did not exceed the warning water level

Data source State Oceanic Administration (1989–2010)

Typhoon Saomai resulted in an extremely severe storm surge disaster in the coastal areas of Zhejiang and Fujian Provinces, with an economic loss of RMB 7.017 billion Yuan. A total of 230 people died and 96 were missing from the storm surge impacts (Fig. 7). In Zhejiang Province, the affected population in Taizhou, Wenzhou, and Lishui reached 3.456 million, with two persons killed. 103,200 ha of farmland were flooded, and 674 dikes breached with a total length of 81.1 km; 5,180 dikes were damaged with a total length of 396.4 km; and 1,833 shore revetments broke down. Moreover, 678 embankments were destroyed and 10,600 ha of marine aquaculture area were affected, and 20,000 tons of aquatic products were lost. A total of 1,003 fishing vessels (899 boats) were sunk while 1,153 ships were damaged. The direct economic loss of damaged aquaculture and fishing vessels was RMB 630 million Yuan.

In Fujian Province, the disaster hit 14 counties and cities and 164 towns, with 1,455,200 people affected, among which, 228 people died and 96 were missing; 68,800 ha of crops were affected while 44,230 ha were damaged, leading to a direct economic loss of RMB 6.387 billion Yuan (State Oceanic Administration 1989–2010). Early warning for this storm surge was accurate and boats at sea were informed to return to ports in advance. However, despite the warning some fishermen stayed in havens to protect the boats and sea farms. This resulted in severe casualties.

3.2 Storm Surge Disaster Response

Storm early warning: Super typhoon Saomai occurred during the astronomical high tide period. Before its landing, marine forecasting station of all levels had



Fig. 7 Storm surge disaster after Typhoon Saomai (*Source* Photograph from State Oceanic Administration 1989–2010)

released storm surge warning and sea wave warning as well as emergency warning, and the National Marine Environmental Forecasting Center had made an accurate forecast of the typhoon track. In Zhejiang Province, the provincial Flood Control and Drought Prevention Headquarters, Meteorological Bureau, and Ocean and

Piscatorial Bureau carried out deployments related to typhoon disaster prevention and protection and disaster response before its landing. Three hours before the arrival of Typhoon Saomai, 1.001 million people were evacuated and 34,313 boats returned to the ports. Evacuation was particularly focused on people living by rivers, along the coast, and in low-lying areas, as well as those living in temporal houses and buildings of poor condition. Public facilities such as schools, theaters, and stadiums were open to the evacuees. In Fujian Province, beginning from 8 August—2 days before the landfall, marine vessels, aquaculture workers, and people in dangerous areas on land had started to be evacuated. More than 36,000 vessels at sea in the whole province had returned to haven by 12:00 on 10 August. Meanwhile, aquaculture workers had been shifted ashore and about 570,000 people had been evacuated. The Shanghai Flood Control Headquarters released an astronomical high tide flood warning and a blue warning for storm tide, which was unprecedented in history.

Emergency rescue: After Typhoon Saomai landed, Fuding City of Fujian Province that was severely affected by the storm surge disaster immediately established a salvage and search and rescue leading group. Working groups including marine salvage team, marine search and rescue team, rehabilitation team, external affairs team, and publicity team for search and rescue work were set up so as to actively carry out disaster emergency response activities. Three provincial medicine aid teams from the Fujian Provincial Hospital, Fujian Xiehe Hospital, and the First Affiliated Hospital of Fujian Medical University as well as the epidemic prevention team from Fujian Provincial Center for Disease Control and Prevention went to the disaster areas and undertook disaster relief and prevention work to control the occurrence and spread of communicable disease. They mainly focused on the monitoring and analysis of the epidemic situation of major communicable diseases like cholera, and paid close attention to the development of the situation and projection and early warning. Ministry of Civil Affairs and Ministry of Finance allocated RMB 30 million Yuan to Zhejiang and Fujian Provinces on 16 August to support the active response to Typhoon Saomai and storm surge disaster.

3.3 Lessons Learned

Successful early warning of storm surge and active disaster relief greatly reduced the losses resulted from Typhoon Saomai and storm surge. However, many problems emerged during the disaster emergency response process, especially in the relocation before the disaster. These pose new challenges to emergency management and disaster risk reduction work. The lack of relevant relocation standards, obstacles in evacuation and relocation regulations, and insufficiency awareness of the general public on laws concerning disaster prevention and risk reduction as well as the general lack of self-care knowledge counteract part of the efforts made by various parties concerned. Although storm surge early warning had been sent out by relevant government departments, detailed implementation plans for evacuation and

relocation were not provided. There was no comprehensive disaster response plans that can be applied in the implementation. Existing laws and regulations were not applicable to such emergency situation as typhoons and storm surges. In addition, risk communication by relevant government departments to make the general public realize the urgency of the disaster and the safety benefit of disaster prevention was far from adequate. The lack of awareness of relevant laws and disaster risks on the part of the public in the disaster areas became a great obstacle for emergency rescue and relief.

References

- Chen, K.X. 1994. Storm surge disaster and formation mechanism in Tianjin. *Ocean Development and Management* 11(3): 41–43 (in Chinese).
- FEMA (Federal Emergency Management Agency). 2010. Hurricane hazards: Storm surge.405 Accessed on 8 Sept 2014.
- Galagan, C. 2008. Storm surge inundation analysis and visualization, EBC 3rd annual ocean management conference, Duxbury, Massachusetts. 11 July 2008. <http://www.ebcne.org/fileadmin/pres/Galagan.pdf>. Accessed 8 Sept 2014.
- Kleinosky, L.R., B. Yarnal, and A. Fisher. 2006. Vulnerability of Hampton Roads, Virginia to storm-surge flooding and sea-level rise. *Natural Hazards* 40(1): 43–70.
- Hu, G.K., and Q.T. Zhang. 2006. Influence of storm surge on coastal areas of China and its protective measures. *Marine Information* 4: 20–21 (in Chinese).
- Lu, B.Y., and L.F. Ma. 2007. The main character of super typhoon No. 0608 (SAOMAI) and characteristics analysis of its storm surge affecting. *Marine Forecasts* 24(4): 92–96 (in Chinese).
- Shi, P.J. 2011. *Atlas of natural disaster risk of China*. Beijing: Science Press (in Chinese and English).
- Song, X.J., Q.Z. Liu, and Z.G. Wang. 2005. Key scientific problems in marine environmental forecasting. *Marine Forecasts* 22(supplement): 7–16 (in Chinese).
- State Oceanic Administration, People's Republic of China. 1989–2010. China Marine Disaster Bulletin 1989—2010 (in Chinese).
- State Oceanic Administration, People's Republic of China. 2009. Emergency plan for storm surge, sea waves, tsunami and sea ice disasters (in Chinese).
- Wood, R.M., M. Drayton, A. Berger, P. Burgess, and T. Wright. 2011. Catastrophe loss modeling of storm-surge flood risk in eastern England. *Philosophical Transactions of the Royal Society A: Mathematical, Physical and Engineering Sciences* 363(1831): 1407–1422.
- Xu, Q.W., and S.D. Tang. 1998. Research on the method of evaluating the economic loss caused by storm surge disaster. *Marine Science Bulletin* 17(1): 1–12 (in Chinese).
- Yang, G.S. 2000. History change and future trends of storm surge disaster in china's coastal areas. *Journal of Natural Disasters* 9(3): 23–30 (in Chinese).
- Yang, H.T., S.Z. Tian, L. Ye, et al. 1991. *Chinese marine disasters four decades compilation*, 4–7. Beijing: China Ocean Press (in Chinese).
- Ye, L., and F.J. Yu. 2002. The long-term change and forecast of storm surge disasters in China. *Marine Forecasts* 19(1): 89–96 (in Chinese).